UNIVERSIDAD DE MURCIA

ESCUELA INTERNACIONAL DE DOCTORADO

TESIS DOCTORAL

SYSTEMIC ALTERATIONS AND BRAIN CHANGES IN PHYSIOLOGY AND PATHOLOGY. THE *OCTODON DEGUS* AS A MODEL OF AGING AND MULTIMORBIDITY.

ALTERACIONES SISTÉMICAS Y CAMBIOS CEREBRALES EN FISIOLOGÍA Y PATOLOGÍA. EL *OCTODON DEGUS* COMO MODELO DE ENVEJECIMIENTO Y MULTIMORBILIDAD.

D.ª Lorena Cuenca Bermejo

2023

UNIVERSITÀ DEGLI STUDI DI MILANO

Dipartimento di Biotecnologie Mediche e Medicina Traslazionale

Dottorato in Medicina Traslazionale – Ciclo XXXIV – BIO/10

SYSTEMIC ALTERATIONS AND BRAIN CHANGES

IN PHYSIOLOGY AND PATHOLOGY.

THE *OCTODON DEGUS* AS A MODEL

OF AGING AND MULTIMORBIDITY.

Docenti guida:
Prof. Alessandro Prinetti
Prof. María Trinidad Herrero Ezquerro

Direttore del corso di dottorato: Prof. Chiarella Sforza

Tesi di Dottorato di:
LORENA CUENCA BERMEJO

Matricola n. R12463

Anno Accademico 2022/2023

Systemic alterations and brain changes in physiology and pathology. The *Octodon degus* as a model of aging and multimorbidity

Alteraciones sistémicas y cambios cerebrales en fisiología y patología. El *Octodon degus* como modelo de envejecimiento y multimorbilidad.

To obtain the Degree of Doctor at the University of Murcia and the University of Milan, with "International Doctorate" mention (2023).

Memoria presentada para optar al Grado de Doctor por la Universidad de Murcia y la Universidad de Milán, con mención "Doctorado Internacional" (2023).

By/*Por*

Ms./Dña. Lorena Cuenca Bermejo

This thesis has been directed by

Prof. María Trinidad Herrero Ezquerro

Human Anatomy and Psychobiology

University of Murcia

Prof. Alessandro Prinetti

Department of Medical Biotechnology and Translational Medicine

University of Milan

A la belleza

CONTENTS

ACKNOWLEDGEMENTS

Escribir esta tesis ha sido un proceso muy emocionante ya que, a medida que construía las diferentes secciones de este manuscrito, me asaltaban todos los momentos asociados a ellas y las personas con las que he recorrido el camino estos años. Por eso, este documento no podría empezar sin que expresara lo enormemente agradecida que estoy por todo lo que me ha acompañado en esta aventura.

Agradezco al Ministerio de Ciencia, Innovación y Universidades por la financiación de este doctorado. Gracias a la Universidad de Murcia, a la Federación Europea de Neurociencia y a la Sociedad Internacional de Neuroquímica por las ayudas de movilidad que me han brindado durante mis estancias de investigación y congresos.

A mi directora, la profesora Doña María Trinidad Herrero Ezquerro, gracias por haberme acogido en tu grupo y por todas las oportunidades que me has ofrecido, que me han ayudado a crecer personal y profesionalmente.

Al mio co-direttore, il Prof. Alessandro Prinetti, per essere sempre un grande sostegno e per avermi aperto le porte del suo laboratorio. Grazie tantissime per tutto.

Quiero dar las gracias a todo el personal del servicio de experimentación animal de la Universidad de Murcia. Yolanda Martínez Verdú y Francisco Zapata Nicolás, os estoy enormemente agradecida por vuestra amabilidad permanente y por toda vuestra ayuda con los animales. Francisco Javier Pardo Fernández, muchísimas gracias por dejarme contar contigo y por alegrarme esos días de horas infinitas en el animalario. Especial agradecimiento también a María Fermina Ros Romero, por hacer siempre todo lo posible para facilitarnos el transporte de los animales.

A la Profesora Dña. María Josefa Fernández Del Palacio, por todo lo que me has enseñado "de corazón" y por transmitirme tu entusiasmo para estudiarlo.

Al Profesor D. José Joaquín Cerón Madrigal y a la Dra. Camila Peres Rubio, por vuestra valiosísima colaboración en los estudios y por todo el tiempo que me habéis dedicado.

A Miguel Ángel Gallego Mompeán, eres una de las mejores personas que he conocido. Gracias por tu energía y ayuda en todo momento. A Mari Carmen Izquierdo Guillén, por toda la asistencia administrativa que me has aportado estos años.

Al Dr. Carlos Manuel Martínez Cáceres, por tu inmensa profesionalidad, por tranquilizarme siempre con tus consejos científicos y tu ayuda cuando me encontraba perdida, me has enseñado muchísimo. Y, cómo no, gracias por tu particular sentido del humor.

A mi queridísima Ana Luisa Gil Martínez, porque desde que te conocí te convertiste en un referente para mí, dentro y fuera del laboratorio. Aunque dejamos de trabajar juntas en mi primer año de doctorado, he sentido que me acompañabas en todos los que han venido después. Gracias por tu luz.

A mi compañera Consuelo Sánchez Rodrigo, por tu dedicación y por todos esos momentos que compartimos al comienzo de este viaje y que no han dejado de hacerme sonreír cada vez que los recordaba. A mis compañeros Fillipe Mendes, Elisa Pizzichini, Valeria Gonçalves, Jacopo Marongiu y Pablo Gallo Soljancic. Gracias por todas las horas de trabajo que hemos compartido y por las risas, soy muy afortunada por haber podido trabajar con amigos. No podría concebir este grupo sin pensar en vosotros.

Ai miei colleghi dell'Università degli studi di Milano, Sara, Simona e Chiara. Già sapete quali sono le mie parole di ringraziamento e tutto quello che significate per me. Grazie per tutto quello che mi avete fatto imparare e per avermi fatto sentire sempre a casa. Siete nel mio cuore. Al Prof. Massimo Aureli, grazie per condividere con me la tua sapienza scientifica e della vita, e grazie anche per venire a "disturbarmi" mentre stavo lavorando.

A todos los alumnos que habéis pasado por el laboratorio en estos años. Nombraros a todos extendería demasiado esta sección, pero quiero que sepáis que os agradezco a cada uno de vosotros la ilusión y las ganas de aprender, que me ayudaban tanto en esos días en los que estábamos desbordados. Gracias por haberme comprendido y haberme hecho el camino un poco más fácil. Yo también he aprendido mucho de vosotros.

A mi "hermanico" Losa, gracias de corazón, por estar siempre, por tantas conversaciones y consejos, por todo lo que sabes que hemos compartido. A Mari Carmen, gracias por cuidarme tanto, incluso las veces en las que necesitabas que fuera al revés, eres maravillosa. Gracias a mis amigos Irene, Paula, Alfredo, Iván, Javi, Pilar, Elena y África, que habéis sido siempre un hombro en el que apoyarme, en lo bueno y en lo menos bueno. Por muchos años que pasen y muchos kilómetros de por medio, os siento tan cerca como cuando estábamos en la misma clase. A Lorena Cano, me siento afortunada por haber coincidido contigo dentro del laboratorio y más feliz aún por poder llamarte "amiga". Gracias de todo corazón a todos, tengo mucha suerte de poder contar con vosotros.

A los que no habéis nacido dentro de mi familia, pero que ya sois parte de ella. A Esperanza, gracias por todo tu amor, por tu apoyo y por ese intercambio de fuerzas tan bonito que tenemos. Mil gracias por cuidarme tanto. A Juan, por tener siempre una

solución para todo y por hacernos saber que podemos contar contigo siempre, has traído paz a mi vida.

A mis tíos, Juani y Antonio, y a mi primo Álvaro, gracias por tantísimo cariño independientemente de la distancia y del tiempo. Sois un pilar fundamental, un hogar para mí. A mi abuela Lolina, que has estado presente en todas mis etapas, desde que me llevabas al cole cogida de la mano hasta ver tu casa invadida por todos mis apuntes para estudiar estos años. Gracias porque siempre me has acompañado llenándome con tus mejores palabras para tener siempre una autoestima bien alta.

A mis padres, no podría ser yo sin vosotros. Gracias, porque tengo en vosotros lo más importante: el apoyo incondicional para hacer lo que me hace feliz, sin ningún tipo de cuestión. Gracias por tranquilizarme cuando las cosas no son tan fáciles, ayudándome a confiar en mí misma. A mi hermana, por ser tan *beautiful in your way*, mi estrella. Qué bonito ir de la mano en esta etapa también, estamos juntas hasta el final.

A Fernando. Gracias por todo y por tantísimo. Gracias por las horas y el cariño invertidos directamente en este manuscrito. Pero, sobre todo, gracias por todo lo que hay fuera de él, compañero. Gracias por hacerme sentir que estás siempre a mi lado, acompañándome en cada paso, enseñándome algo nuevo cada día. Gracias por hacer nuestro camino tan especial y por mejorarlo siempre, eres un regalo.

Y, por último, muchas gracias a ti. Porque gracias a ti hemos llegado hasta aquí, y esto también es tuyo.

SUMMARY

SUMMARY

The worldwide life expectancy has experienced a dramatic rise in the last century, resulting in an increase in the proportion of people aged over 65 years old. Unfortunately, this increase in longevity has not been accompanied by an increase in the years of "disease-free life". Rather, the incidence and impact (social and economic) of age-associated diseases have increased in parallel. Thus, the study of the mechanisms associated with aging is an area of vital importance to identify which characteristics of aging are related to the appearance of age-associated pathologies, such as cardiovascular diseases, cancer and neurodegenerative disorders. In addition, the aging of the population is represented by the emergence of specific concomitant conditions, including loss of cognitive and physical function, polypharmacy or multimorbidity. In this sense, it is key to consider the extensive communication that exists between different tissues and organ systems. That is, changes that occur at the systemic level can have an effect at the central nervous system level, and *vice versa*.

Several evidence have pointed out that aging manifests at the clinical level when there is an imbalance between cell damage and compensatory mechanisms. However, it is evident that this process, as well as the susceptibility to multimorbidity, affects individuals in a heterogeneous manner. This individual variability can be explained by the interaction among different biological factors, such as genetics or biological sex, and external factors, such as the environment, diet or socioeconomic determinants. In particular, the role of biological sex and gender in different pathologies, prognosis and response to treatments has been increasingly recognized. However, the inclusion of sex (and gender) as a variable still represents a need in clinical and preclinical research.

Performing aging studies in human patients presents several obstacles. In this sense, the use of experimental models is very useful in pre-clinical phases and can help to understand the nature of the mechanisms underlying aging and how their interactions may predispose to pathology. In recent years, the *Octodon degus* (*O. degus*) has been proposed as a relevant tool in biomedical research. Unlike traditional rodents, the *O. degus* is diurnal and shows several biological characteristics similar to humans, including the development of some pathological traits associated with human aging. Among them, it has been evidenced the spontaneous appearance of pathological features such as β-amyloid plaques and phosphorylated tau protein deposits, as well as postsynaptic dysfunction. Likewise, there is a high degree of homology with the most frequent neurodegenerative disease-related proteins (β-amyloid, tau, α-synuclein and APOE). In addition, some age-related changes have been described in this model, such as astrocytic activation and

oxidative stress markers, neuronal apoptosis, white matter changes similar to those of human aging, cognitive and behavioral dysfunction, type II diabetes, cataracts, retinal alterations and circadian rhythm changes. For all these reasons, this model represents a promising alternative to reproduce the multimorbidity scenario found in human aging. However, several aspects of the *O. degus* biology have not been characterized yet.

With this in mind, the main objective of this thesis was the characterization of the *O. degus* as a natural model of aging by exploring systemic and brain changes along aging, as well as their interaction, including sex as an experimental variable. For this purpose, studies were performed on a total of 110 animals aged from 6 months old to 7 years old, which were divided according to age, sex or treatments. The data presented in this thesis are the result of the combination of *in vivo* analyses (plasma analytes, cardiac function and behavior), with the *post mortem* evaluation in different brain areas of neuroinflammatory processes, changes in lipid composition, lipid peroxidation and neuronal death.

The first block of results of this work provides the sex-specific values of the biochemical profile in the blood of *O. degus* during aging. The analytes determined allowed us to examine the general metabolism, hepatic, renal and pancreatic functions, oxidation and inflammatory status. We found that most parameters were significantly altered in aged animals, with differences between males and females. The analytes analyzed indicated that these animals develop hepatic, renal and pancreatic dysfunction associated with aging. Also, plasma oxidation and inflammation levels were significantly increased in older animals compared to younger animals. Differences between males and females were also found along aging, specially in the analytes related to general and liver, muscle, and kidney metabolism, to redox-status or to inflammatory status. The biggest differences were related to oxidative status, suggesting higher oxidation in males versus females. Due to the high inter-individual variability of the data, especially accentuated in the older groups, the statistical analyses did not show significant differences in some parameters, such as glucose levels or inflammation indicators. This situation is of great interest since, taking into account that the animals in this study are not genetically identical and that they have been maintained in the same environmental conditions, only some of them are susceptible to develop sub-clinical pathological states that may predispose to the development of chronic diseases associated with aging.

The second block of results shows the study of *in vivo* cardiac function evaluated by electrocardiography. In this section, the normal ranges for the heart rate, duration and voltage of the electrocardiogram waves and intervals, as well as electrical axis deviation, were determined. The statistical analysis revealed that the parameters that showed the

greatest differences according to sex were the higher incidence of arrhythmias and greater deviation of the electrical axis of the heart in males than in females. Likewise, some electrocardiogram modifications were detected when comparing the different ages. Heart rate decreased significantly at older ages, with males being more affected than females. QRS complex duration was significantly increased in females as they aged, but not in males. Finally, the QT interval duration of younger females was significantly shorter than that of males of the same age, while in the senile stage this situation was reversed. Therefore, the data obtained showed that *O. degus* develop spontaneous cardiac alterations associated with aging that differ between males and females, adding value to this model for use as a natural model for investigations of the cardiovascular system.

Thirdly, we analyzed the cognitive impairment associated with aging with a sex perspective, and its possible relationship with the neuroinflammatory status (microglia and astrocytes) in the dorsal hippocampus. Considering the effect of age, aged *O. degus* (>4 years) showed a very significant cognitive impairment when they were compared to young animals. Interestingly, when possible differences associated with the sex were investigated, we found that they were significant in the aged animals: during the training sessions, the aged females showed a better performance than the aged males, which was reversed on the day of the final test. *Post mortem* studies revealed that, in all dorsal hippocampal subareas analyzed, neuroinflammation was significantly increased in older animals, being the basal immunolabeling levels for microglia and astrocytes higher in males than in females. Correlation analyses indicated that increased neuroinflammation is related to worse cognitive performance, especially in the dentate gyrus and *Cornu Ammonis* subfield 1. The information derived from these studies characterizes for the first time age-associated cognitive decline in *O. degus* and its relationship to neuroinflammation in the dorsal hippocampus, with a component of inter-individual variability.

The fourth block of results corresponds to the analysis of the lipid composition in the brain of *O. degus* during aging, in both males and females. For this purpose, four brain areas were analyzed: prefrontal cortex (PFC), striatum, cortex and cerebellum. Analysis of total lipid extracts showed that changes in lipid species in the PFC, striatum and cortex were more influenced by the age of the animals than by their sex, while in cerebellum both variables influenced more significantly the lipid composition. The changes observed during aging were region-specific, those in glycosphingolipids being common to all regions. The greatest sex-associated differences were found in gangliosides at all ages, while sphingomyelin and sulfatides were significantly different when comparing males and females of senile age. Finally, given its key role in spatial memory circuits, lipid

peroxidation (POL) was analyzed in the PFC. We found that it was significantly increased along aging, males showing significant higher levels of POL than females. In addition, higher POL significantly correlated with worse cognitive performance. On the one hand, these results represent a first piece of information in the brain lipid characterization of this model. On the other hand, these data support the inclusion of sex as a variable to understand differential age-associated neurodegeneration, as well as the higher prevalence of certain diseases such as Alzheimer's disease.

Finally, we validated the use of *O. degus* as a model of experimental Parkinsonism based on 1-methyl-4-phenyl-1,2,3,6-tetrahydro-pyridine (MPTP) intoxication. MPTP intoxicated animals showed dysregulation of blood glucose levels, together with motor and cognitive alterations. Post-mortem analysis revealed a very significant loss of dopaminergic neurons in the Substantia Nigra pars compacta (SNpc) and in the ventral tegmental area (VTA), although dopaminergic terminals were not altered. Similarly, a highly significant reduction of noradrenergic neurons in the locus coeruleus (LC) was detected in MPTP-intoxicated animals. These findings were accompanied by a significant increase in microglial and astroglial response in the ventral midbrain (SNpc and VTA), striatum, dorsal hippocampus and LC of parkinsonized animals. These results demonstrate, for the first time, that *O. degus* is sensitive to MPTP-induced neurotoxicity, and therefore it is proposed as a suitable model for the study of experimental Parkinsonism beyond the motor circuits.

In summary, this research represents a reasonable contribution to the scientific community in different aspects. On the one hand, a longitudinal study of the present dimensons considering both males and females in the *O. degus* had never been done before. First place, it provides validation of different experimental procedures and protocols in this species. Second place, the results presented in this thesis contribute to a better characterization of the *O. degus*, providing a starting point for future studies in the field of physiopathology and guidelines for veterinary care to early diagnosis and monitorization. On the other hand, the findings obtained support the validity of this species as a unique tool for aging research in the context of multimorbidity, possesing similarities with humans that are not present in other preclinical models. In additionally, the sex-related differences found increase the value of this model, since it offers the possibility of approaching different scientific questions from the sex perspective. Finally, the results derived from the present project set the basis for future studies that focus both in the better characterization of the model and in the individual susceptibility to different age-associated disorders considering the sex differences.

RESUMEN

La esperanza de vida a nivel mundial ha experimentado un ascenso dramático en el último siglo, resultando en un aumento de la proporción de personas mayores de 65 años. Lamentablemente, este aumento en la longevidad no ha estado acompañado por un incremento en los años de "vida libre de enfermedades", sino que la incidencia y el impacto (social y económico) de las enfermedades asociadas a la edad se han visto aumentados en paralelo. Por todo ello, el estudio de los mecanismos asociados al envejecimiento es un área de vital importancia para identificar qué características propias del envejecimiento se relacionan con la aparición de patologías asociadas a la edad, tales como las enfermedades cardiovasculares, el cáncer y los trastornos neurodegenerativos. Además, el envejecimiento de la población está representado por la aparición de condiciones concomitantes específicas, incluyendo la pérdida de funciones cognitiva y física, la polifarmacia o la multimorbilidad. En este sentido, es clave considerar la extensa comunicación que existe entre los diferentes tejidos y sistemas de órganos. Es decir, los cambios que se producen a nivel sistémico pueden tener un efecto a nivel del sistema nervioso central, y *viceversa.*

Diversas evidencias han señalado que el envejecimiento se manifiesta a nivel clínico cuando existe un desbalance entre daños celulares y mecanismos compensatorios. Sin embargo, resulta evidente que este proceso, así como la susceptibilidad a la multimorbilidad, se manifiestan de una forma heterogénea entre individuos. Esta variabilidad individual aparece como resultado de la interacción entre diferentes factores biológicos, como la genética o el sexo biológico, y externos, como el ambiente, la dieta o los condicionantes socioeconómicos. En particular, el papel del sexo biológico y el género en la aparición de diferentes patologías, pronóstico y respuesta a tratamientos ha sido reconocido de forma creciente. A pesar de ello, la inclusión del sexo (y el género) como variable todavía representa una necesidad en las investigaciones clínica y preclínica.

La investigación del envejecimiento en pacientes humanos presenta obstáculos. En este sentido, el uso de modelos de experimentación es muy útil en fases pre-clínicas y puede ayudar a comprender la naturaleza de los mecanismos que subyacen al envejecimiento, y cómo sus interacciones pueden predisponer a la patología. En los últimos años, el *Octodon degus* (*O. degus*) se ha propuesto como una herramienta relevante en la investigación biomédica. A diferencia de los roedores tradicionales, el *O. degus* es diurno y muestra diversas características biológicas similares a los humanos, incluyendo el desarrollo de rasgos patológicos asociados al envejecimiento humano. Entre ellos, se ha descrito la aparición espontánea de placas β-amiloides y depósitos de proteína tau fosforilada, así como la disfunción postsináptica. Asimismo, existe un alto

grado de homología con las proteínas relacionadas con enfermedades neurodegenerativas más frecuentes (β-amiloide, tau, α-sinucleína y APOE). Además, se han descrito algunos cambios relacionados con la edad en este modelo, como activación astrocítica y marcadores de estrés oxidativo, apoptosis neuronal, cambios en la sustancia blanca similares a aquéllos de envejecimiento humano, disfunción cognitiva y comportamiento, diabetes tipo II, cataratas, alteraciones retinianas y cambios del ritmo circadiano. Por todo ello, este modelo representa una alternativa prometedora para reproducir el escenario de multimorbilidad que se encuentra en el envejecimiento humano. Sin embargo, diversos aspectos de la biología del *O. degus* no se han caracterizado aún.

Teniendo esto en cuenta, el principal objetivo de esta tesis fue caracterizar el *O. degus* como modelo de envejecimiento natural explorando cambios sistémicos y cerebrales con la edad, así como su interacción, incluyendo el sexo biológico como variable experimental. Para ello, los estudios se realizaron en un total de 110 animales con edades comprendidas entre los 6 meses y los 7 años, que fueron divididos según su edad, sexo o tratamientos. Los datos presentados en esta tesis son el resultado de la combinación de análisis *in vivo* (analitos plasmáticos, función cardíaca y comportamiento), con la evaluación *post mortem* en distintas áreas cerebrales para determinar procesos neuroinflamatorios, cambios en composición lipídica, peroxidación lipídica y muerte neuronal.

El primer bloque de resultados de este trabajo recoge los valores del perfil bioquímico en sangre del *O. degus* específicos de sexo durante el envejecimiento. Los analitos estudiados permitieron examinar el metabolismo general, las funciones hepática, renal y pancreática, los estados oxidativo e inflamatorio. Encontramos que la mayoría de parámetros estaban significativamente alterados en los animales añosos, con diferencias entre machos y hembras. Los analitos analizados indicaron que estos animales desarrollaban disfunción hepática, renal y pancreática asociada al envejecimiento. Asimismo, los niveles de oxidación e inflamación plasmáticos estaban significativamente aumentados en los animales añosos en comparación a los jóvenes. A lo largo del envejecimiento se encontraron diferencias entre machos y hembras, especialmente en los marcadores de metabolismo de hígado, músculo y riñón, y a los estados redox e inflamatorio. Las mayores diferencias se encontraron en el estado oxidativo, con niveles más elevados en machos que en hembras. Debido a la elevada variabilidad inter-individual que presentaron los datos, especialmente acentuada en los grupos de mayor edad, los análisis estadísticos no mostraron diferencias significativas en algunos parámetros, como es el caso de los niveles de glucosa o indicadores de inflamación. Esta situación es de gran interés ya que, teniendo en cuenta que los animales de este estudio

no son genéticamente idénticos y que han sido mantenidos en idénticas condiciones ambientales, sólo algunos de ellos fueron susceptibles de desarrollar estados patológicos sub-clínicos que pueden predisponer al desarrollo de enfermedades crónicas asociadas al envejecimiento.

El segundo bloque de resultados corresponde al estudio de la función cardíaca *in vivo*, evaluada mediante electrocardiografía. En esta sección se determinaron los rangos de valores para frecuencia cardíaca, duración y voltaje de los diferentes componentes del electrocardiograma, así como la desviación del eje eléctrico. El análisis estadístico reveló que los parámetros que mostraron mayores diferencias según el sexo fue la incidencia de arritmias y desviación del eje eléctrico del corazón, ambos superiores en machos. Asimismo, se detectaron algunas modificaciones del electrocardiograma al comparar las diferentes edades. La frecuencia cardíaca disminuyó significativamente en las edades más avanzadas, mostrándose los machos más afectados que las hembras. La duración del complejo QRS se vio significativamente aumentada en hembras a medida que envejecían, pero no en machos. Por último, la duración del intervalo QT de las hembras más jóvenes era significativamente inferior a la de los machos de la misma edad, mientras que en la etapa senil esta situación se vio invertida. Por todo ello, los datos obtenidos muestran que el *O. degus* desarrolla alteraciones cardíacas espontáneas asociadas al envejecimiento que difieren entre machos y hembras, lo que añade valor a este modelo para su uso como modelo natural para investigaciones del sistema cardiovascular.

En tercer lugar, analizamos el deterioro cognitivo asociado al envejecimiento con perspectiva de sexo, y su posible relación con el estado neuroinflamatorio en el hipocampo dorsal. A lo largo de todo el proceso experimental, los *O. degus* envejecidos (>4 años) mostraron un deterioro cognitivo muy significativo al compararlos con los animales jóvenes. Interesantemente, al investigar las posibles diferencias asociadas al sexo, encontramos que éstas, si bien no se encontraron en los animales más jóvenes, fueron significativas en los animales añosos. De esta forma, durante las sesiones de entrenamiento, las hembras añosas mostraron un mejor rendimiento que los machos que se vio invertido el día del test final. Los estudios *post mortem* revelaron que, en todas las subáreas del hipocampo dorsal analizadas, la neuroinflamación estaba significativamente aumentada en los animales de mayor edad, siendo los niveles basales de inmunomarcaje para microglía y astrocitos superiores en los machos. Los análisis de correlaciones indicaron que el aumento de neuroinflamación se relaciona con un peor rendimiento cognitivo, especialmente en las áreas de giro dentado y *Cornu Ammonis 1*. La información derivada de estos estudios caracteriza por primera vez el deterioro cognitivo asociado a

la edad en el *O. degus* y su relación con la neuroinflamación en hipocampo dorsal, con una componente de variabilidad inter-individual.

El cuarto bloque de resultados corresponde a los análisis de la composición lipídica en el cerebro del *O. degus* durante el envejecimiento, con perspectiva de sexo. Para ello, se analizaron cuatro áreas cerebrales: corteza prefrontal (CPF), estriado, corteza y cerebelo. El análisis de los extractos lipídicos totales mostró que los cambios en las especies lipídicas en la CPF, estriado y corteza se vieron más influidos por la edad de los animales que por el sexo, mientras que en cerebelo ambas variables influyeron en la composición lipídica. Los cambios observados durante el envejecimiento fueron específicos de cada región, aunque los glicoesfingolípidos aparecieron alterados en todas ellas. Las mayores diferencias asociadas al sexo de los animales se encontraron en los gangliósidos en todas las edades, mientras que la esfingomielina y las sulfatidas fueron significativamente diferentes al comparar machos y hembras de edades seniles. Por último, dado su papel clave en los circuitos de memoria espacial, se analizó la peroxidación lipídica (POL) en CPF. En relación a esta última, se encontró significativamente aumentada durante el envejecimiento, mostrando los machos niveles significativamente superiores de POL que las hembras. Además, una mayor POL correlacionó de manera significativa con un peor rendimiento cognitivo. Por un lado, estos resultados suponen una primera pieza de información en la caracterización lipídica cerebral de este modelo. Por otro, estos datos apoyan la inclusión del sexo como variable para entender la neurodegeneración diferencial asociada a la edad, así como la mayor prevalencia de patologías como la enfermedad de Alzheimer.

Finalmente, se validó uso del *O. degus* como modelo de Parkinsonismo experimental basado en la intoxicación con 1-metil-4-fenil-1,2,3,6-tetrahidro-piridina (MPTP). Los animales intoxicados con MPTP mostraron una desregulación de los niveles de glucosa en sangre, junto con alteraciones motoras y cognitivas. El análisis *post mortem* reveló una pérdida muy significativa de neuronas dopaminérgicas en la *Sustancia Negra pars compacta* (SNpc) y en el área tegmental ventral (ATV), aunque las terminales dopaminérgicas no se vieron alteradas. Del mismo modo, se detectó una reducción muy significativa de las neuronas noradrenérgicas del *locus coeruleus* (LC) en los animales intoxicados con MPTP. Estos hallazgos fueron acompañados de un aumento significativo de la respuesta microglial y astroglial en el mesencéfalo ventral (SNpc y ATV), en el estriado, en el hipocampo dorsal y en el LC de los animales parkinsonizados. Estos hallazgos demostraron, por primera vez, que el *O. degus* es sensible a la neurotoxicidad inducida por MPTP, por lo que apoyan a esta especie como un modelo adecuado para el

estudio de Parkinsonismo experimental más allá de la afectación motora y en un contexto de multimorbilidad.

Por todo ello, esta investigación supone una contribución razonable para la comunidad científica en diferentes aspectos. Por un lado, nunca antes se había realizado un estudio longitudinal de esta envergadura que considerase machos y hembras en el *O. degus*. En primer lugar, aporta la validación de protocolos que antes no se habían empleado en esta especie. En segundo lugar, los resultados presentados en esta tesis contribuyen a una mayor caracterización del *O. degus*, aportando un punto de partida para estudios futuros de fisiopatología y guías a nivel veterinario para diagnóstico precoz y monitorización de alteraciones. Por otro lado, los hallazgos obtenidos apoyan que esta especie es una herramienta única para investigación en envejecimiento en el contexto de multimorbilidad, con similitudes a los humanos que no están presentes en otros modelos preclínicos. Además, las diferencias asociadas al sexo encontradas incrementan el valor de este modelo, ya que ofrece la posibilidad de abordar futuros estudios desde una perspectiva de sexo en fisiología y patología. Por último, los resultados presentados en esta tesis asientan la base para futuros estudios que se enfoquen tanto en una mayor caracterización del modelo como de la susceptibilidad individual al desarrollo de enfermedades asociadas a la edad con la posibilidad de estudiar diferencias de sexo.

RIASSUNTO

L'aspettativa di vita a livello globale è aumentata drasticamente nell'ultimo secolo, con il conseguente aumento della percentuale di persone con più di 65 anni. Purtroppo, l'aumento della longevità non è stato accompagnato da un aumento degli anni di "vita libera dalla malattia". Al contrario, l'incidenza e l'impatto (sociale ed economico) delle malattie legate all'età sono aumentati in parallelo. Per tutti questi motivi, lo studio dei meccanismi associati all'invecchiamento è un'area di vitale importanza per identificare quali caratteristiche dell'invecchiamento sono correlate alla comparsa di patologie associate all'età, come le malattie cardiovascolari, il cancro e i disturbi neurodegenerativi. Inoltre, l'invecchiamento della popolazione è caratterizzato dall'insorgenza di specifiche condizioni concomitanti, tra cui la perdita di funzioni cognitive e fisiche, la politerapia o la multimorbilità. A questo proposito, è fondamentale considerare l'ampia comunicazione che esiste tra diversi tessuti e sistemi di organi. In altre parole, i cambiamenti che si verificano a livello sistemico possono avere un effetto a livello del sistema nervoso centrale e *vice versa*.

È dimostrato che l'invecchiamento si manifesta a livello clinico quando c'è uno squilibrio tra il danno cellulare e i meccanismi di compensazione. È evidente, però, che questo processo e la predisposizione alla multimorbilità si manifestano in modo eterogeneo tra diversi individui. Questa variabilità individuale appare come il risultato dell'interazione tra diversi fattori biologici, come la genetica o il sesso biologico, e fattori esterni, come l'ambiente, la dieta o i fattori di condizionamento socioeconomici. In particolare, negli ultimi decenni è stato sempre più riconosciuto il ruolo del sesso biologico e del genere nella comparsa di diverse patologie, nella prognosi e nella risposta ai trattamenti. Nonostante ciò, l'inclusione del sesso (e del genere) come variabile rappresenta ancora una necessità nella ricerca clinica e preclinica.

La ricerca sull'invecchiamento nei pazienti umani presenta degli ostacoli. In questo senso, l'uso di modelli sperimentali è molto utile nelle fasi precliniche e può aiutare a comprendere la natura dei meccanismi alla base dell'invecchiamento e come le sue interazioni possano predisporre alla patologia. Negli ultimi anni, l'*Octodon degus* (*O. degus*) è stato proposto come modello importante per la ricerca biomedica. A differenza dei roditori tradizionali, l'*O. degus* è diurno e presenta svariate caratteristiche biologiche simili all'uomo, compreso lo sviluppo di alcuni tratti patologici associati all'invecchiamento umano; tra questi, sono stati descritti la comparsa spontanea di placche di β-amiloide e depositi di proteina tau fosforilata e disfunzioni postsinaptiche. Esiste anche un elevato grado di omologia con le più comuni proteine associate alle malattie neurodegenerative

(β-amiloide, tau, α-sinucleina e APOE). Inoltre, in questo modello sono stati descritti alcuni cambiamenti legati all'età, come attivazione astrocitaria e marcatori dello stress ossidativo, apoptosi neuronale, alterazioni della materia bianca simili a quelle dell'invecchiamento umano, disfunzioni cognitive e comportamentali, diabete di tipo II, cataratta, alterazioni della retina e cambiamenti del ritmo circadiano. Pertanto, questo modello rappresenta un'alternativa promettente per riprodurre lo scenario di multimorbilità che si riscontra nell'invecchiamento umano. Tuttavia, diversi aspetti della biologia dell'O. *degus* non sono stati caratterizzati ancora.

Con queste premesse, l'obiettivo principale di questa tesi è stato quello di utilizzare il modello di invecchiamento naturale *O. degus* per esplorare i cambiamenti sistemici e cerebrali che si verificano con l'età, nonché la loro interazione, tenendo conto dell'influenza del sesso. A tal fine, sono stati condotti studi su un totale di 110 animali di età compresa tra i 6 mesi e i 7 anni, suddivisi per età, sesso o trattamento. I dati presentati in questa tesi sono il risultato della combinazione dell'analisi *in vivo* (analiti plasmatici, funzione cardiaca e comportamento), con la valutazione *post mortem* in diverse aree cerebrali dei processi neuroinfiammatori, cambiamenti nella composizione lipidica, perossidazione lipidica e morte neuronale.

La prima parte dei risultati di questo lavoro comprende l'analisi del profilo biochimico specifico del sesso nel sangue di *O. degus* durante l'invecchiamento. Gli analiti studiati ci hanno permesso di esaminare il metabolismo generale, le funzioni epatiche, renali e pancreatiche, lo stato ossidativo e infiammatorio. Abbiamo riscontrato che la maggior parte dei parametri era significativamente alterata negli animali invecchiati, con differenze tra machi e femmine. In particolare, i livelli di proteine totali, colesterolo e calcio sono risultati significativamente più elevati negli *O. degus* anziani rispetto a quelli più giovani. Gli analiti analizzati hanno indicato che questi animali sviluppano disfunzioni epatiche, renali e pancreatiche associate all'invecchiamento. Inoltre, i livelli di ossidazione e infiammazione plasmatica sono risultati significativamente più elevati negli animali anziani rispetto a quelli giovani. Nell'invecchiamento, differenze legate al sesso sono state trovate, soprattutto nei marcatori del metabolismo epatico, muscolare e renale, negli stati redox e infiammatori. Le differenze maggiori sono state riscontrate nello stato ossidativo, con livelli più elevati nei maschi rispetto alle femmine. A causa dell'elevata variabilità interindividuale dei dati, soprattutto nei gruppi più anziani, le analisi statistiche non hanno mostrato differenze significative in alcuni parametri, tra cui i livelli di glucosio o gli indicatori di infiammazione. Questa situazione è di grande interesse poiché, tenendo conto che gli animali di questo studio non sono geneticamente identici e che sono stati tenuti in condizioni ambientali identiche, solo alcuni di essi sono suscettibili allo sviluppo di stati

patologici sub-clinici che possono predisporre all'insorgenza di malattie croniche associate all'invecchiamento.

Il secondo blocco di risultati è relativo allo studio della funzione cardiaca *in vivo,* valutata mediante elettrocardiografia. In questa sezione sono stati determinati gli intervalli di normalità per la frequenza cardiaca, la durata e il voltaggio delle onde e degli intervalli dell'elettrocardiogramma, nonché la deviazione dell'asse elettrico. L'analisi statistica ha rivelato che i parametri che mostravano le maggiori differenze in base al sesso sono stati la maggiore incidenza di aritmie e la maggiore deviazione dell'asse elettrico del cuore nei maschi rispetto alle femmine. Inoltre, sono state rilevate alcune modifiche dell'elettrocardiogramma nel confronto tra le diverse età. La frequenza cardiaca è diminuita in modo significativo negli animali di età più avanzata, con i maschi più colpiti delle femmine. La durata del complesso QRS è aumentata significativamente nelle femmine con l'avanzare dell'età, ma non nei maschi. Infine, la durata dell'intervallo QT delle femmine più giovani era significativamente più breve rispetto a quello dei maschi della stessa età, mentre nella fase senescente la situazione era invertita. Pertanto, i dati ottenuti mostrano che *O. degus* sviluppa alterazioni cardiache spontanee associate all'invecchiamento che differiscono tra maschi e femmine, il che aggiunge valore al suo potenziale utilizzo come modello naturale per le indagini sul sistema cardiovascolare.

In terzo luogo, abbiamo analizzato il deterioramento cognitivo associato all'invecchiamento in modo genere-dipendente e la sua possibile relazione con lo stato neuroinfiammatorio (microglia e astrociti) nell'ippocampo dorsale. Durante tutte le fasi sperimentali gli *O. degus* anziani (>4 anni) hanno mostrato un declino cognitivo molto significativo rispetto agli animali giovani. È interessante notare che, indagando le possibili differenze associate al sesso degli animali, abbiamo riscontrato che queste, pur non essendo state riscontrate negli animali più giovani, erano significative in quelli più anziani. Pertanto, nelle varie sessioni di allenamento, le femmine hanno mostrato una performance migliore rispetto ai maschi; la situazione si è invertita nel giorno del test finale. Gli studi *post mortem* hanno rivelato che, in tutte le sotto-aree dell'ippocampo dorsale analizzate, la neuroinfiammazione aumentava significativamente negli animali più anziani, con livelli di immunomarcatura basale per microglia e astrociti più elevati nei maschi rispetto alle femmine. Le analisi di correlazione hanno indicato che l'aumento della neuroinfiammazione è correlato a prestazioni cognitive peggiori, soprattutto nelle aree del giro dentato e del *Cornu Ammonis* (regione 1). Le informazioni derivate da questi studi dimostrano per la prima volta il declino cognitivo associato all'età in *O. degus* e la sua relazione con la neuroinfiammazione nell'ippocampo dorsale, con una componente di variabilità interindividuale.

Il quarto blocco di risultati corrisponde all'analisi della composizione lipidica nel cervello di *O. degus* durante l'invecchiamento, in relazione al sesso. A tal fine, sono state analizzate quattro aree cerebrali: corteccia prefrontale (CPF), striato, corteccia e cervelletto. L'analisi degli estratti lipidici totali ha mostrato che le variazioni delle specie lipidiche nella CPF, nello striato e nella corteccia erano più influenzate dall'età degli animali che dal sesso, mentre nel cervelletto entrambe le variabili influenzavano la composizione lipidica. I cambiamenti osservati durante l'invecchiamento sono specifici per ogni regione, mentre quelli dei glicosfingolipidi sono comuni a tutte le regioni. Le maggiori differenze legate al sesso sono state riscontrate nei gangliosidi, a tutte le età, mentre la sfingomielina e i solfatidi sono risultati significativamente diversi nel confronto tra maschi e femmine in età senile. Infine, dato il suo ruolo chiave nei circuiti della memoria spaziale, nella CPF è stata analizzata la perossidazione lipidica (POL), di cui ne è stato riscontrato un aumento significativo durante l'invecchiamento e nel confronto tra maschi e femmine. Inoltre, una POL più elevata correlava in modo significativo con prestazioni cognitive peggiori. Questi risultati, da un lato rappresentano una prima informazione nella caratterizzazione dei lipidi cerebrali di questo modello, dall'altro confermano che il sesso costituisce un'ulteriore variabile per comprendere il diverso grado di neurodegenerazione associata all'età, nonché la diversa incidenza di alcune malattie, come il morbo di Alzheimer, in maschi e femmine.

Infine, *O. degus* è stato validato come modello di parkinsonismo sperimentale basato sull'intossicazione da 1-metil-4-fenil-1,2,3,6-tetraidropiridina (MPTP). Gli animali intossicati da MPTP hanno mostrato una disregolazione dei livelli di glucosio nel sangue, oltre a disturbi motori e cognitivi. L'analisi *post mortem* ha rivelato una perdita notevolmente significativa di neuroni dopaminergici nella Substantia Nigra pars compacta (SNpc) e nell'area tegmentale ventrale (ATV), sebbene i terminali dopaminergici non fossero alterati. Analogamente, negli animali intossicati da MPTP è stata rilevata una riduzione altamente significativa dei neuroni noradrenergici nel locus coeruleus (LC). Questi risultati sono stati accompagnati da un aumento significativo delle risposte microgliali e astrogliali nel mesencefalo ventrale (SNpc e ATV), nello striato, nell'ippocampo dorsale e nel LC degli animali "parkinsonizzati". Questi risultati dimostrano, per la prima volta, che *O. degus* è sensibile alla neurotossicità indotta dall'MPTP, rendendolo un modello adatto per lo studio del parkinsonismo sperimentale, al di là della compromissione motoria.

In conclusione, questa ricerca offre un contributo ragionevole alla comunità scientifica sotto diversi aspetti. Da un lato, uno studio longitudinale di questa portata che considera maschi e femmine in *O. degus* non è mai stato condotto prima. In primo luogo,

fornisce la convalida di protocolli che non erano stati utilizzati in precedenza in questa specie. In secondo luogo, i risultati presentati in questa tesi contribuiscono a una migliore caratterizzazione di *O. degus*, fornendo un punto di partenza per futuri studi sulla fisiopatologia e linee guida veterinarie per la diagnosi precoce e il monitoraggio delle alterazioni. D'altra parte, i risultati ottenuti confermano che questa specie è uno strumento unico per la ricerca sull'invecchiamento nel contesto della multimorbilità, con somiglianze con l'uomo che non sono presenti in altri modelli preclinici. Inoltre, le differenze associate al sesso riscontrate aumentano il valore di questo modello, in quanto offre la possibilità di affrontare studi futuri da una prospettiva sessuale in fisiologia e patologia. Infine, i risultati presentati in questa tesi pongono le basi per studi futuri che si concentrano sia sull'ulteriore caratterizzazione del modello sia sulla suscettibilità individuale allo sviluppo di malattie associate all'età, con la possibilità di studiare le differenze di sesso.

SUMMARY REFERENCES

Barrientos, R. M., Kitt, M. M., Watkins, L. R., & Maier, S. F. (2015). Neuroinflammation in the normal aging hippocampus. Neuroscience, 309, 84–99. https://doi.org/10.1016/j.neuroscience.2015.03.007

Cao, W., & Zheng, H. (2018). Peripheral immune system in aging and Alzheimer's disease. Molecular neurodegeneration, 13(1), 51. https://doi.org/10.1186/s13024-018-0284-2

Chang, L. Y., Ardiles, A. O., Tapia-Rojas, C., Araya, J., Inestrosa, N. C., Palacios, A. G., & Acosta, M. L. (2020). Evidence of Synaptic and Neurochemical Remodeling in the Retina of Aging Degus. Frontiers in neuroscience, 14, 161. https://doi.org/10.3389/fnins.2020.00161

Cuenca-Bermejo, L., Pizzichini, E., Gonzalez-Cuello, A. M., De Stefano, M. E., Fernandez-Villalba, E., & Herrero, M. T. (2020). *Octodon degus*: a natural model of multimorbidity for ageing research. Ageing research reviews, 64, 101204. https://doi.org/10.1016/j.arr.2020.101204

Estrada, C., López, D., Conesa, A., Fernández-Gómez, F. J., Gonzalez-Cuello, A., Toledo, F., Tunez, I., Blin, O., Bordet, R., Richardson, J. C., Fernandez-Villalba, E., & Herrero, M. T. (2015). Cognitive Impairment After Sleep Deprivation Rescued by Transcranial Magnetic Stimulation Application in *Octodon degus*. Neurotoxicity research, 28(4), 361–371. https://doi.org/10.1007/s12640-015-9544-x

Ferrucci, L., Gonzalez-Freire, M., Fabbri, E., Simonsick, E., Tanaka, T., Moore, Z., Salimi, S., Sierra, F., & de Cabo, R. (2020). Measuring biological aging in humans: A quest. Aging cell, 19(2), e13080. https://doi.org/10.1111/acel.13080

van Groen, T., Kadish, I., Popović, N., Popović, M., Caballero-Bleda, M., Baño-Otálora, B., Vivanco, P., Rol, M. Á., & Madrid, J. A. (2011). Age-related brain pathology in *Octodon degus*: blood vessel, white matter and Alzheimer-like pathology. Neurobiology of aging, 32(9), 1651–1661. https://doi.org/10.1016/j.neurobiolaging.2009.10.008.

Hurley, M. J., Deacon, R. M. J., Beyer, K., Ioannou, E., Ibáñez, A., Teeling, J. L., & Cogram, P. (2018). The long-lived *Octodon degus* as a rodent drug discovery model for Alzheimer's and other age-related diseases. Pharmacology & therapeutics, 188, 36–44. https://doi.org/10.1016/j.pharmthera.2018.03.001

Inestrosa, N. C., Reyes, A. E., Chacón, M. A., Cerpa, W., Villalón, A., Montiel, J., Merabachvili, G., Aldunate, R., Bozinovic, F., & Aboitiz, F. (2005). Human-like rodent amyloid-beta-peptide determines Alzheimer pathology in aged wild-type *Octodon degus*. Neurobiology of aging, 26(7), 1023–1028. https://doi.org/10.1016/j.neurobiolaging.2004.09.016

Inestrosa, N. C., Ríos, J. A., Cisternas, P., Tapia-Rojas, C., Rivera, D. S., Braidy, N., Zolezzi, J. M., Godoy, J. A., Carvajal, F. J., Ardiles, A. O., Bozinovic, F., Palacios, A. G., & Sachdev, P. S. (2015). Age Progression of Neuropathological Markers in the Brain of the Chilean Rodent *Octodon degus*, a Natural Model of Alzheimer's Disease. Brain pathology (Zurich, Switzerland), 25(6), 679–691. https://doi.org/10.1111/bpa.12226

Krishnaswami, A., Beavers, C., Dorsch, M. P., Dodson, J. A., Masterson Creber, R., Kitsiou, S., Goyal, P., Maurer, M. S., Wenger, N. K., Croy, D. S., Alexander, K. P., Batsis, J. A., Turakhia, M. P., Forman, D. E., Bernacki, G. M., Kirkpatrick, J. N., Orr, N. M., Peterson, E. D., Rich, M. W., Freeman, A. M., Bhavnani, S. P., & Innovations, Cardiovascular Team and the Geriatric Cardiology Councils, American College of Cardiology (2020). Gerotechnology for Older Adults With Cardiovascular Diseases: JACC State-of-the-Art

Review. Journal of the American College of Cardiology, 76(22), 2650–2670. https://doi.org/10.1016/j.jacc.2020.09.606

de Lange, A. G., Barth, C., Kaufmann, T., Maximov, I. I., van der Meer, D., Agartz, I., & Westlye, L. T. (2020). Women's brain aging: Effects of sex-hormone exposure, pregnancies, and genetic risk for Alzheimer's disease. Human brain mapping, 41(18), 5141–5150. https://doi.org/10.1002/hbm.25180

Mayne, K., White, J. A., McMurran, C. E., Rivera, F. J., & de la Fuente, A. G. (2020). Aging and Neurodegenerative Disease: Is the Adaptive Immune System a Friend or Foe?. Frontiers in aging neuroscience, 12, 572090. https://doi.org/10.3389/fnagi.2020.572090

Otalora, B. B., Hagenauer, M. H., Rol, M. A., Madrid, J. A., & Lee, T. M. (2013). Period gene expression in the brain of a dual-phasing rodent, the *Octodon degus*. Journal of biological rhythms, 28(4), 249–261. https://doi.org/10.1177/0748730413495521

Szabadfi, K., Estrada, C., Fernandez-Villalba, E., Tarragon, E., Setalo, G., Jr, Izura, V., Reglodi, D., Tamas, A., Gabriel, R., & Herrero, M. T. (2015). Retinal aging in the diurnal Chilean rodent (*Octodon degus*): histological, ultrastructural and neurochemical alterations of the vertical information processing pathway. Frontiers in cellular neuroscience, 9, 126. https://doi.org/10.3389/fncel.2015.00126

Tarragon, E., Lopez, D., Estrada, C., Ana, G. C., Schenker, E., Pifferi, F., Bordet, R., Richardson, J. C., & Herrero, M. T. (2013). *Octodon degus*: a model for the cognitive impairment associated with Alzheimer's disease. *CNS neuroscience & therapeutics*, *19*(9), 643–648. https://doi.org/10.1111/cns.12125

Tarragon, E., Lopez, D., Estrada, C., Gonzalez-Cuello, A., Ros, C. M., Lamberty, Y., Pifferi, F., Cella, M., Canovi, M., Guiso, G., Gobbi, M., Fernández-Villalba, E., Blin, O., Bordet, R., Richardson, J. C., & Herrero, M. T. (2014). Memantine prevents reference and working memory impairment caused by sleep deprivation in both young and aged *Octodon degus*. *Neuropharmacology*, *85*, 206–214. https://doi.org/10.1016/j.neuropharm.2014.05.023

Teissier, T., Boulanger, E., & Deramecourt, V. (2020). Normal ageing of the brain: Histological and biological aspects. Revue neurologique, 176(9), 649–660. https://doi.org/10.1016/j.neurol.2020.03.017

World health statistics 2022: monitoring health for the SDGs, sustainable development goals. Geneva: World Health Organization; 2022. Licence: CC BY-NC-SA 3.0 IGO.

Yarnoz, M. J., & Curtis, A. B. (2008). More reasons why men and women are not the same (gender differences in electrophysiology and arrhythmias). The American journal of cardiology, 101(9), 1291–1296. https://doi.org/10.1016/j.amjcard.2007.12.027.

Zampino, M., Polidori, M. C., Ferrucci, L., O'Neill, D., Pilotto, A., Gogol, M., & Rubenstein, L. (2022). Biomarkers of aging in real life: three questions on aging and the comprehensive geriatric assessment. GeroScience, 44(6), 2611–2622. https://doi.org/10.1007/s11357-022-00613-4

Zucker, I., Prendergast, B. J., & Beery, A. K. (2022). Pervasive Neglect of Sex Differences in Biomedical Research. Cold Spring Harbor perspectives in biology, 14(4), a039156. https://doi.org/10.1101/cshperspect.a039156

SCIENTIFIC PRODUCTION

JOURNAL PUBLICATIONS

A. Directly related to the content of this thesis

Cuenca-Bermejo L, Peres-Rubio C, Cerón JJ, Sánchez-Rodrigo C, Kublickiene K, Raparelli V, Kautzky-Willer A, Norris CM, Pilote L, Herrero MT and the GOING-FWD Consortium. Influence of age and sex in the blood biochemical profile in the *O. degus*. *(Under review in Lab Animal, Chapter IV. 1 of this thesis)*.

Cuenca-Bermejo L, Fernández-Del Palacio MJ, Gonçalves VC, Bautista-Hernández V, Sánchez-Rodrigo C, Kublickiene K, Raparelli V, Kautzky-Willer A, Norris CM, Pilote L, Herrero MT and the GOING-FWD Consortium. Age and sex determine the electrocardiogram parameters in the *Octodon degus*. Bas Res Cardiology (Under Review in Laboratory Animals, *Chapter IV. 2 of this thesis*).

Cuenca-Bermejo L, Prinetti A, Kublickiene K, Raparelli V, Kautzky-Willer A, Norris CM, Pilote L, Herrero MT and the GOING-FWD Consortium. Old brain stories: how do age and sex influence the neurodegeneration-associated lipid changes? (Under Review in The Journal of Neurochemistry).

Cuenca-Bermejo, L., Pizzichini, E., Gonçalves, V. C., Guillén-Díaz, M., Aguilar-Moñino, E., Sánchez-Rodrigo, C., González-Cuello, A. M., Fernández-Villalba, E., & Herrero, M. T. (2021). A New Tool to Study Parkinsonism in the Context of Aging: MPTP Intoxication in a Natural Model of Multimorbidity. International journal of molecular sciences, 22(9), 4341. https://doi.org/10.3390/ijms22094341. *(Chapter IV. 5 of this thesis)*.

Cuenca-Bermejo, L., Pizzichini, E., Gonzalez-Cuello, A. M., De Stefano, M. E., Fernandez-Villalba, E., & Herrero, M. T. (2020). Octodon degus: a natural model of multimorbidity for ageing research. Ageing research reviews, 64, 101204. https://doi.org/10.1016/j.arr.2020.101204. *(Chapter I of this thesis)*.

Cuenca, L., Gil-Martinez, A. L., Cano-Fernandez, L., Sanchez-Rodrigo, C., Estrada, C., Fernandez-Villalba, E., & Herrero, M. T. (2019). Parkinson's disease: a short story of 200 years. Histology and histopathology, 34(6), 573–591. https://doi.org/10.14670/HH-18-073 *(Chapter I of this thesis)*.

B. Derived from participation in other research projects of the group

B.1. Aging

Fuentes, P., Amador, S., Lucas-Ochoa, A. M., **Cuenca-Bermejo, L.**, Fernández-Villalba, E., Raparelli, V., Norris, C., Kautzky-Willer, A., Kublickiene, K., Pilote, L., Herrero, M. T., & GOING-FWD Consortium (2021). Sex, rurality and socioeconomical status in Spanish centennial population (2017). Aging, 13(18), 22059–22077. https://doi.org/10.18632/aging.203563.

B.2. *Octodon degus*

Estrada, C., **Cuenca, L.**, Cano-Fernandez, L., Gil-Martinez, A. L., Sanchez-Rodrigo, C., González-Cuello, A. M., Fernandez-Villalba, E., & Herrero, M. T. (2019). Voluntary

exercise reduces plasma cortisol levels and improves transitory memory impairment in young and aged Octodon degus. Behavioural brain research, 373, 112066. https://doi.org/10.1016/j.bbr.2019.112066.

B.3. Parkinson's disease and systemic alterations

Romo-Vaquero, M., Fernández-Villalba, E., Gil-Martinez, A. L., **Cuenca-Bermejo, L.**, Espín, J. C., Herrero, M. T., & Selma, M. V. (2022). Urolithins: potential biomarkers of gut dysbiosis and disease stage in Parkinson's patients. Food & function, 13(11), 6306–6316. https://doi.org/10.1039/d2fo00552b

Cuenca-Bermejo, L., Almela, P., Navarro-Zaragoza, J., Fernández Villalba, E., González-Cuello, A. M., Laorden, M. L., & Herrero, M. T. (2021). Cardiac Changes in Parkinson's Disease: Lessons from Clinical and Experimental Evidence. International journal of molecular sciences, 22(24), 13488. https://doi.org/10.3390/ijms222413488

Navarro-Zaragoza, J., **Cuenca-Bermejo, L.**, Almela, P., Laorden, M. L., & Herrero, M. T. (2021). Could Small Heat Shock Protein HSP27 Be a First-Line Target for Preventing Protein Aggregation in Parkinson's Disease?. International journal of molecular sciences, 22(6), 3038. https://doi.org/10.3390/ijms22063038

Cuenca-Bermejo, L., Almela, P., Gallo-Soljancic, P., Yuste, J. E., de Pablos, V., Bautista-Hernández, V., Fernández-Villalba, E., Laorden, M. L., & Herrero, M. T. (2021). Cardiac tyrosine hydroxylase activation and MB-COMT in dyskinetic monkeys. Scientific reports, 11(1), 19871. https://doi.org/10.1038/s41598-021-99237-5

Gonçalves, V. C., **Cuenca-Bermejo, L.**, Fernandez-Villalba, E., Martin-Balbuena, S., da Silva Fernandes, M. J., Scorza, C. A., & Herrero, M. T. (2022). Heart Matters: Cardiac Dysfunction and Other Autonomic Changes in Parkinson's Disease. The Neuroscientist : a review journal bringing neurobiology, neurology and psychiatry, 28(6), 530–542. https://doi.org/10.1177/1073858421990000

Gil-Martinez, A. L., **Cuenca-Bermejo, L.**, Gonzalez-Cuello, A. M., Sanchez-Rodrigo, C., Parrado, A., Vyas, S., Fernandez-Villalba, E., & Herrero, M. T. (2020). Identification of differentially expressed genes profiles in a combined mouse model of Parkinsonism and colitis. Scientific reports, 10(1), 13147. https://doi.org/10.1038/s41598-020-69695-4

Almela, P., **Cuenca-Bermejo, L.**, Yuste, J. E., Estrada, C., de Pablos, V., Bautista-Hernández, V., Fernández-Villalba, E., Laorden, M. L., & Herrero, M. T. (2020). Cardiac Noradrenaline Turnover and Heat Shock Protein 27 Phosphorylation in Dyskinetic Monkeys. Movement disorders : official journal of the Movement Disorder Society, 35(4), 698–703. https://doi.org/10.1002/mds.27958

Melo-Thomas, L., Gil-Martínez, A. L., **Cuenca, L.**, Estrada, C., Gonzalez-Cuello, A., Schwarting, R. K., & Herrero, M. T. (2018). Electrical stimulation or MK-801 in the inferior colliculus improve motor deficits in MPTP-treated mice. Neurotoxicology, 65, 38–43. https://doi.org/10.1016/j.neuro.2018.01.004

Gil-Martínez, A. L., Estrada, C., **Cuenca, L.**, Cano, J. A., Valiente, M., Martínez-Cáceres, C. M., Fernández-Villalba, E., & Herrero, M. T. (2019). Local Gastrointestinal Injury Exacerbates Inflammation and Dopaminergic Cell Death in Parkinsonian Mice. Neurotoxicity research, 35(4), 918–930. https://doi.org/10.1007/s12640-019-0010-z

B.4. Parkinson's disease and neuroinflammatory processes

De Araújo, F. M., Frota, A. F., de Jesus, L. B., Macedo, T. C., **Cuenca-Bermejo, L.**, Sanchez-Rodrigo, C., Ferreira, K. M. S., de Oliveira, J. V. R., de Fatima Dias Costa, M., Segura-Aguilar, J., Costa, S. L., Herrero, M. T., & Silva, V. D. A. (2022). Aminochrome Induces Neuroinflammation and Dopaminergic Neuronal Loss: A New Preclinical Model to Find Anti-inflammatory and Neuroprotective Drugs for Parkinson's Disease. Cellular and molecular neurobiology, 10.1007/s10571-021-01173-5. Advance online publication. https://doi.org/10.1007/s10571-021-01173-5

de Araújo, F. M., **Cuenca-Bermejo, L.**, Fernández-Villalba, E., Costa, S. L., Silva, V. D. A., & Herrero, M. T. (2022). Role of Microgliosis and NLRP3 Inflammasome in Parkinson's Disease Pathogenesis and Therapy. Cellular and molecular neurobiology, 42(5), 1283–1300. https://doi.org/10.1007/s10571-020-01027-6

Gil-Martinez, A. L., **Cuenca-Bermejo, L.**, Gallo-Soljancic, P., Sanchez-Rodrigo, C., Izura, V., Steinbusch, H. W. M., Fernandez-Villalba, E., & Herrero, M. T. (2020). Study of the Link Between Neuronal Death, Glial Response, and MAPK Pathway in Old Parkinsonian Mice. Frontiers in aging neuroscience, 12, 214. https://doi.org/10.3389/fnagi.2020.00214

Gil-Martínez, A. L., **Cuenca, L.**, Estrada, C., Sánchez-Rodrigo, C., Fernández-Villalba, E., & Herrero, M. T. (2018). Unexpected Exacerbation of Neuroinflammatory Response After a Combined Therapy in Old Parkinsonian Mice. Frontiers in cellular neuroscience, 12, 451. https://doi.org/10.3389/fncel.2018.00451

Gil-Martínez, A. L., **Cuenca, L.**, Sánchez, C., Estrada, C., Fernández-Villalba, E., & Herrero, M. T. (2018). Effect of NAC treatment and physical activity on neuroinflammation in subchronic Parkinsonism; is physical activity essential?. Journal of neuroinflammation, 15(1), 328. https://doi.org/10.1186/s12974-018-1357-4

BOOK CHAPTERS

Carta, A; Pisanu, A; Palmas, M; Barcia, C; **Cuenca-Bermejo, L**; Herrero, MT. 2021. MPTP: Advances from an Evergreen Neurotoxin Handbook of Neurotoxicity.

CONGRESSES AND SCIENTIFIC MEETINGS

Lorena Cuenca-Bermejo, Simona Prioni, Sara Grassi, Ana María González-Cuello, Emiliano Fernández-Villalba, María Trinidad Herrero, Alessandro Prinetti. "Differential brain lipid composition in the Octodon degus, a matter of age and sex". Oral communication at the ISN-APSN Biennal Meeting. (Honolulu, United States, 2022).

Lorena Cuenca-Bermejo, Lucía Soriano-Moreno, Elisa Pizzichini, Valeria C. Gonçalves, María Guillén-Díaz, Elena Aguilar-Moñino, Consuelo Sánchez-Rodrigo, Ana-María González-Cuello, Emiliano Fernández-Villalba, and María Trinidad Herrero. "MPTP intoxication in the *Octodon degus*: effects on the nigrostriatal pathway and related areas" Oral communication at the NTS Virtual Meeting for Trainees (Online, 2021).

Lorena Cuenca-Bermejo, Elisa Pizzichini, Pablo Gallo-Soljancic, Consuelo Sánchez-Rodrigo, Ana-María González-Cuello, Emiliano Fernández-Villalba, María-Trinidad Herrero. "Octodon degus: a new rodent model to study Parkinson's disease". Poster presentation at the International Conference on Alzheimer's And Parkinson's Diseases (AD/PD21) (Online, 2021).

Lorena Cuenca-Bermejo, Lucía Soriano-Moreno, Elisa Pizzichini, Valeria C. Gonçalves, María Guillén-Díaz , Elena Aguilar-Moñino , Consuelo Sánchez-Rodrigo, Ana-María González-Cuello, Emiliano Fernández-Villalba, and María Trinidad Herrero. "The Octodon degus as a model for experimental Parkinsonism, beyond the motor system". Oral presentation at the LXXII Anual Meeting of the Spanish Society for Neurology (Online, 2020).

Lorena Cuenca-Bermejo, Consuelo Sánchez-Rodrig, Pablo Gallo-Soljancic, Emiliano Fernández-Villalba, María-Trinidad Herrero. "Validation of the MPTP model of Parkinsonism in the *Octodon degus*". Poster presentation at the FENS (Online, 2022).

Lorena Cuenca-Bermejo, Ana Luisa Gil-Martínez, Consuelo Sánchez-Rodrigo, Cristina Estrada-Esteban, María-Trinidad Herrero. "Acute Intoxication With Mptp In Experimental Parkinsonism: Age Matters?" Oral communication at III MENEDPRO (FENS satellite / NTS) (Berlin, Germany, 2018).

Lorena Cuenca-Bermejo, Ana Luisa Gil-Martínez, Cristina Estrada-Esteban, María-Trinidad Herrero. "Aging, MPTP and drug interaction: a key role of C-Jun N-terminal kinase subcellular localization?". Poster presentation at the European Glia Meeting (Edinburgh, United Kindgom, 2017).

LIST OF ABBREVIATIONS

4-HNE, 4-hydroxynoneal

AD, Alzheimer's disease

ALP, alkaline phosphatase

AST, aspartate aminotransferase alanine aminotransferase

AV, atrioventricular

Aβ, amyloid beta

BChE, butyrylcholinesterase

BM, Barnes Maze

bpm, beats per minute

CA, *Cornu Ammonis*

CA1, *Cornu Ammonis* subfield 1

CA2, *Cornu Ammonis* subfield 2

CA3, *Cornu Ammonis* subfield 3

CK, creatine kinase

CNS, central nervous system

CUPRAC, cupric reducing antioxidant capacity

CVD, cardiovascular diseases

DG, dentate gyrus

ECG, electrocardiogram

FRAP, ferric reducing ability of the plasma

GalCer, galactosylceramide

GFAP, glial fibrillary acidic protein

gGT, gamma-glutamyl transferase

GlcCer, glucosylceramide

GlcSph, glucosylphingosine

HR, heart rate

Iba1, ionized calcium binding adaptor molecule 1

LAD, left axis deviation

LC, *locus coeruleus*

LPO, lipid peroxidation

MEA, mean electrical axis

MPTP, 1-methyl-4-phenyl-1,2,3,6-tetrahydro-pyridine

NCD, noncommunicable disease

NFT, neurofibrillary tangles

O. degus, *Octodon degus*

PA, phosphatidic acid

PC, phosphatidylcholine

PD, Parkinson's disease

PE, phosphatidylethanolamine

PI, phosphatidylinositol

PON1, paraoxonase-1

PS, phosphatidylserine

RAD, right axis deviation

RME, reference memory errors

RNS, reactive nitrogen species

ROS, reactive oxygen species

RU, relative units

SA, sinoatrial

SAA, serum A-amyloid

SLM, stratum lacunosum-moleculare

SM, sphingomyelin

SNpc, *Substantia Nigra pars compacta*

SO, *stratum oriens*

r, Spearman's coefficient

SR, *stratum radiatum*

TEAC, trolox equivalent antioxidant capacity

THIOL, total thiol concentrations

TLC, thin layer chromatography

TLE, total lipid extract

TOS, total oxidant status

UIBC, unsaturated iron-binding capacity

VPC, ventricular premature complex

VTA, ventral tegmental area

WME, working memory errors

OVERVIEW OF THE THESIS' CONTENT

This thesis is built in the context of the current aging society, in which the increase in the life expectancy is in parallel with the increment in the burden of the age-related diseases. Most of these age-associated disorders, such as cardiovascular and neurodegenerative diseases, have largely been investigated, and big steps forward have been made to understand them. However, early detection tools or effective preventive and therapeutical strategies are not available for most of them, thus indicating that our knowledge about the aging phenotypes that can lead to pathological situations have not been completely defined yet. In this sense, our capacity to understand biological processes is strongly supported by the availability of pre-clinical models that can answer particular scientific questions.

Taking this background as a starting point, the conducting research line of this thesis is focused on the characterization of the *O. degus* as a model for physiological aging and experimental Parkinsonism, considering systemic and brain alterations. For this purpose, this manuscript is organized into six main chapters: Introduction, Hypothesis and Objectives, Materials and Methods, Results, Conclusions and Future perspectives.

The **first chapter** of this thesis concerns the **introduction** of relevant concepts to contextualize the following chapters. Firstly, **section I.1** compiles information relative to the aging population. Next (**section I.2**), concepts regarding the cardiac function and its alterations along aging are gathered. In **section I.3**, the central nervous system from the aging perspective is addressed, with special attention to the memory processes, brain lipids and age-related neurodegenerative disorders. Finally, the last part of this introductory chapter is dedicated to present the experimental model used in this thesis, the *Octodon degus* (**section I.4**).

In the **second chapter**, the **hypothesis and objectives** of this research project are formulated. Briefly, the objectives aim to investigate the effect of sex along aging on: i) the plasmatic biochemical profile, ii) the cardiac function, iii) the cognitive performance together with neuroinflammation in the dorsal hippocampus and iii) the brain lipid composition. A fourth objective proposes the validation of the *O. degus* as an experimental model for Parkinsonism based on the MPTP-neurotoxicity.

The **third chapter** contains the **materials and methodology** used in this doctoral thesis. This chapter describes details concerning the animals, the *in vivo* procedures and the behavioral tests performed, as well as the end point method followed by the samples' processing and *post mortem* studies.

The **fourth chapter** corresponds to the **results** and it is subdivided into five sections according to the research questions proposed in the objectives' section. All the sections follow the same scheme: firstly, a brief introduction (state of the art) is presented; secondly, the results obtained are presented; and thirdly, the discussion and conclusions. **Section IV. 1** is dedicated to the study of the influence of age and sex in the biochemical profile of plasma. Next, results regarding the cardiac evaluation by electrocardiography are covered in **section IV. 2**. The study of cognition and neuroinflammatory processes in the dorsal hippocampus considering both age and sex as experimental variables is included in **section IV. 3**. Then, **section IV. 4** is dedicated to the analysis concerning the lipid composition of different brain areas along aging taking into account sex differences. The last results' section (**section IV. 5**) shows the findings obtained in relation to the MPTP-induced experimental Parkinsonism in the *O. degus*, exploring the *in vivo* alterations (motor and non-motor), as well as *post mortem* studies to analyze brain-related areas (dopaminergic system, dorsal hippocampus and *locus coeruleus*).

The **conclusions** obtained along this research project are listed in the **fifth chapter**.

Since each results' section includes its own discussion, the final chapter is dedicated to integrate the results obtained in this thesis, as well as to the **discussion of the main findings** in relation to future perspectives.

CHAPTER I

INTRODUCTION

I.1. Aging

Aging is a natural biological process that occurs with time and is associated with physiological decline. Therefore, aging can be understood as a loss of robustness and flexibility in a biological system, ranging from cells, to tissues, organs and organisms (Bettio et al., 2017; Zampino et al., 2022). The aging phenotype can manifest as a series of physical and cognitive impairment as a result of time-dependent failure of cellular and molecular mechanisms, that were not restored by the mechanisms of repair. This is because as we age, the ability of cell repair is reduced, transcriptomic and translational alterations appear, together with impaired removal of damaged organelles and proteins, among others. Altogether, the appearance of these processes is translated in the accumulation of cellular defects that accumulate over the time and leads to age-associated disability, frailty and vulnerability to develop several disorders (**Figure I.1**) (Kirkwood, 2008; Lakatta, 2016).

I.1.1. Global aging of the population and burden of age-associated diseases

In the last decades, the worldwide aged population (>65 years old) and the life expectancy have unprecedently increased (Krishnaswami et al., 2020). From 2000 to 2019, the global life expectancy at birth increased from 66.8 years to 73.3 years (WHO, 2022). This demographic change towards to an increased longevity is associated with profound changes in the world's political and economic landscape, and represents a challenge to health and social care systems (Fabbri et al., 2015).

Noncommunicable diseases (NCDs), comprise the group of disorders that have a chronical nature and are the result of the interplay among physiology, genetics, environment and behavior. Although people of all groups of age are susceptible of being affected by NCDs, advanced age is the main risk factor for their development. In the last two decades, 87.8% of deaths in high income countries were attributed to NCDs, with heart disease, dementia and stroke as the leading causes (Global Health Observatory, 2022).

We cannot ignore the negative effect that the COVID-19 pandemic has exerted in several aspects of the health systems around the world, including the life expectancy. Current data suggest that the pandemic has slowed this rising trend for life expectancy that was seen in the precedent years (WHO, 2022). However, according to the World Health Organization report of 2022, the trend of deaths associated to NCDs continued to increase worldwide because the COVID-19 pandemic aggravated the illness and increased the risk of death, as well as promoted the disruption of NCDs-associated services (World Health Organization, 2020, 2022).

I.1.2. Aging and multimorbidity

As stated in the World Health Statistics (2022), "*in an ideal world, an increase in life expectancy would be driven primarily by increases in years lived in good health, with a shrinking proportion of years lived in disability. This would mean that people are both living longer and remaining in good health for longer periods and for greater proportions of their lives*" (WHO, 2022). Unfortunately, the increase in the life expectancy of the population is associated to the higher impact and prevalence of the age-associated disorders. In this sense, a high proportion of older individuals are affected by multiple chronic diseases. The simultaneous presence of two or more diseases in the same patient is known as multimorbidity (Van Den Akker et al., 1996; Yancik et al., 2007).
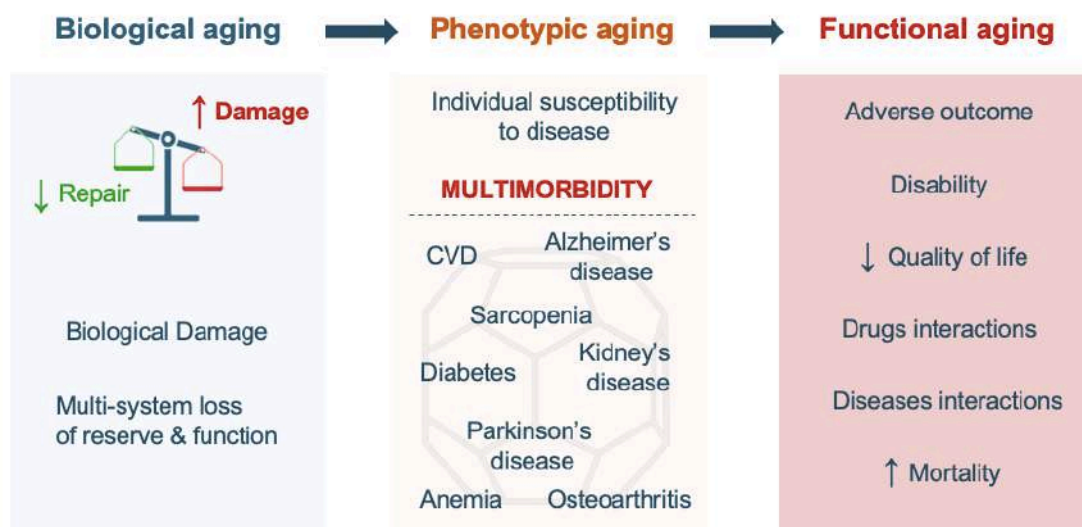
Figure I.1. **Age related-changes are contributors to functional aging**. Biological aging is the result of the imbalance among damage and repair mechanisms, leading to biological damage and multi-system loss of reserve and function. Phenotyping aging refers to the manifestation of the individual susceptibility to disease, which can give rise to multimorbidity. As a result of the progression of phenotypic aging, different adverse outcomes can be presented (functional aging), ranging from disability to increased risk of mortality. Adapted from Fabbri et al. (2015) and Zampino et al. (2022).

In the recent years, it has been proposed that the underlying biological changes that occur during aging can also drive the multiple age-related chronic diseases (**Figure I.1**) (Ferrucci et al., 2020). Thus, addressing those mechanisms will contribute not only to understand the biology of aging but also to develop strategies to prevent or delay multimorbidity (Fabbri et al., 2015). In this line, it is crucial to consider the extensive communication that exist among the different tissues and organs (Barrientos et al., 2015). Several works have demonstrated that changes at the systemic level can have an effect in the central nervous system, and *vice versa* (Cao and Zheng, 2018; Mayne et al., 2020). For example, a chronic immune peripheral challenge can promote the release of pro-

inflammatory cytokines by glial cells that can result in neuronal alterations (Maier and Watkins, 1998; Turrin et al., 2001; Gil-Martínez et al., 2019). Another illustrating fact is that although Parkinson's disease (PD) is a neurodegenerative disorder, the pathology goes beyond the brain and other systems such as the gut and the cardiovascular system are affected even in the prodromal phase (Cuenca-Bermejo et al., 2021a; Kakoty et al., 2021).

I.1.3. Aging and sex

A large proportion of the knowledge regarding age-related disorders derives from studies performed in pathological conditions, both in humans and in experimental models. Undoubtful, these sources of information have been extremely useful for the general understanding of the diseases, establishment of diagnostic criteria and therapeutical designs. While some authors propose that age-associated diseases must be considered as an isolated pathological condition, others support the idea that age-related disorders cannot be studied isolated from their main risk factor (i.e., the age). In this line, it is crucial to understand how the shared cellular and molecular mechanisms between physiological and pathological aging finally predispose to the outcome of age-related disorders. For example, the presence of protein aggregates has been considered the gold standard for histopathological diagnose of Alzheimer's disease (AD), but evidence from the last decades has demonstrated that these aggregates also appear in aged non-demented subjects (Paz Gavilán et al., 2006; Fjell et al., 2014; McCann et al., 2021).

In this line, some factors acting in the vulnerability scenario of aging, such as genetics, environmental factors or sex differences, are key to understand the individual susceptibility of developing pathologies (Teissier et al., 2020). There is a growing concern that sex influences the outcome of different pathologies, prognosis and response to treatments. Some examples include the incidence of different types of arrhythmias in men and women, or the fact that women are at significant higher risk of developing several types of dementia than men (Yarnoz and Curtis, 2008; de Lange et al., 2020). However, from a historical perspective, females have been underrepresented in preclinical and clinical approaches which might explain, for example, why women do not show the expected response to treatments (Zucker et al., 2021). Importantly, not only biological differences between sexes are responsible of the clinical outcomes, but also the socioeconomic factors play a role in healthy aging (Fuentes et al., 2021; Raparelli et al., 2021).

Therefore, exploring the concomitant effect of age and sex in the underlying mechanisms of age-related diseases might be the key for their understanding, providing further improved diagnosis and development of efficient therapies.

I.2. Aging and heart function

The cardiovascular system is responsible of delivering oxygen, nutrients and metabolites to the whole body. This function is possible thanks to the continuous pumping of the blood by the heart and its distribution by the vasculature (arterial, venous and capillary vessels) (Lammert and Zeeb, 2014).

I.2.1. General anatomy of the heart

The heart is a complex organ, composed of four distinct chambers: two atria and two ventricles, separated by the septum (interatrial and interventricular) (Litviňuková et al., 2020) (**Figure I.2**). According to its functionality, the heart has been classically divided into right and left sides. In the "right heart", unoxygenated blood enters via the inferior vena cava and the superior vena cava and it is sent to the lungs to get oxygenated via the pulmonary artery. The "left heart" receives the oxygenated blood coming from the lungs via the pulmonary veins and pumps it to the rest of tissues and organs via the aorta (Oberman and Bhardwaj, 2022). The unidirectional blood flow is ensured by the inlet valves that separate atria from the ventricles (mitral valve in the right side and tricuspid valve in the left side), and the outlet valves that separate the ventricles from the aorta (aortic valve) and the pulmonary artery (pulmonary valve) (Lammert and Zeeb, 2014) (**Figure I.2**).

I.2.2. Cardiac cycle

The main cardiovascular event to ensure and maintain the blood flow throughout the body is the cardiac output (output of the heart per minute), which is determined by the blood volume, the contractile strength and the heart cycle (Becker, 2015). The normal cardiac cycle is characterized by the regular contraction (systole) and relaxation (diastole) of the atria and ventricles. Ventricles are filled with blood during the diastolic phase, while the systolic phase consists of the ejection of the blood due to the ventricles' contraction (Oberman et al., 2022).

The flow of blood through both the left and the right side of the heart is enabled by pressure gradients: pressure in one cavity must be higher than the pressure in the

subsequent cavity to move from one to the other. Starting with the right heart, the atrium is passively filled with blood (diastole), which increases its pressure overcoming the one in the ventricle. This situation promotes the opening of the tricuspid valve which, in turn, enables the ventricle to start being filled. Subsequently, the ventricle must overcome the pressure on the other side of the pulmonary valve with an isovolumetric contraction (systole), while the tricuspid and the pulmonary valves are closed. The increase in the ventricle's pressure above the pressure coming from the pulmonary artery, induces the pulmonary valve to open and the blood to be pumped to the lungs to be oxygenated. Then, oxygenated blood returns and enters in a passive way the left atrium, which then contracts to overcome the pressure in the left ventricle. The mitral valve opens and the left ventricle starts to fill. With mitral and aortic valves closed, the ventricle undergoes an isovolumetric contraction to overcome the pressure from the other side of the aortic valve, thus promoting the aortic valve opening and blood exit to the body (Oberman et al., 2022). To accomplish their function, the left side of the heart generates a high-pressure system, whereas the right heart is characterized by a low-pressure gradient (Lammert and Zeeb, 2014).

HEART ANATOMY

Superior vena cava
Pulmonary artery
Pulmonary veins
Aortic valve
Atrial septum
Tricuspid valve
Inferior vena cava

Brachiocephalic trunk
Carotid artery
Subclavian artery
Aortic arch
Pulmonary arteries
Pulmonary veins
Pulmonary valve
Mitral valve
Ventricular septum
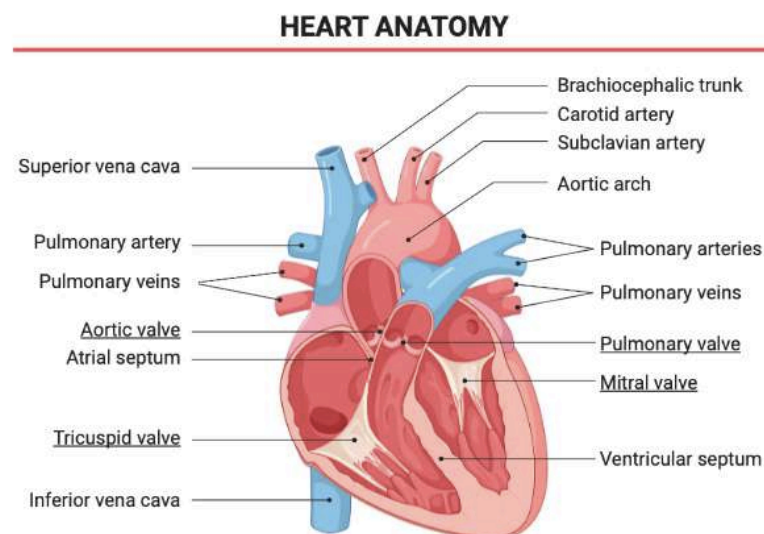
Figure I.2. Anatomy of the heart. Created in BioRender.com, adapted from Berry J.F (2020).

I.2.3. Electrophysiological considerations

The functional complexity of the heart is the result of a heterogeneous cellular composition with specialized properties, which is mainly represented by cardiomyocytes, endothelial cells and fibroblasts (Lammert and Zeeb, 2014; Litviňuková et al., 2020). The cardiac cycle is produced because the heart possesses its own intrinsic electrophysiological system. In this regard, the cellular composition of the heart's

conduction system can be categorized into two main groups: working cells and specialized neural-like conductive cells (Becker, 2015). The working cells refer to the muscular cells (myocardium) forming the atria and the ventricles, whereas the specialized cells comprise the sinoatrial (SA) node, the atrioventricular (AV) node, the bundle of His and the Purkinje fibers (**Figure I.3**). These cells have two unique features: i) they possess automaticity, i.e., the ability to initiate electrical impulses spontaneously; and ii) their action potential can directly initiate the depolarization of the cardiac muscle. Since cardiac muscle cells are intimately connected one to each other by the intercalated discs, they simultaneously function in a syncytium (Becker, 2015). Each cardiac cycle is determined by a series of ordered and complex electrophysiological events. The electrical circuit starts at the SA node, located in the right atrium and known as the pacemaker of the heart, which initiates the depolarization of the atrial muscle. The current travels to the left atrium via the bundle of cells called Bachman's bundle. This electrical signal generated in the SA node is transmitted down to the AV node. At this point, a pause in the electrical circuit is generated because a layer of connective tissue separates the atrial syncytium from the ventricles' one (Becker, 2015). This pause ensures the correct flow of blood through the heart, because its absence would originate the simultaneous contraction of the atria and the ventricles. The electrical impulse travels from the AV node to the Bundle of His, in the interventricular septum, which divides into two branches that transmits the current throughout the two ventricles (right and left bundle branches). Finally, the Purkinje fibers are the continuation of these two branches, supplying the ventricular space with the electrical output (Oberman and Bhardwaj, 2021; Chandler et al., 2009).
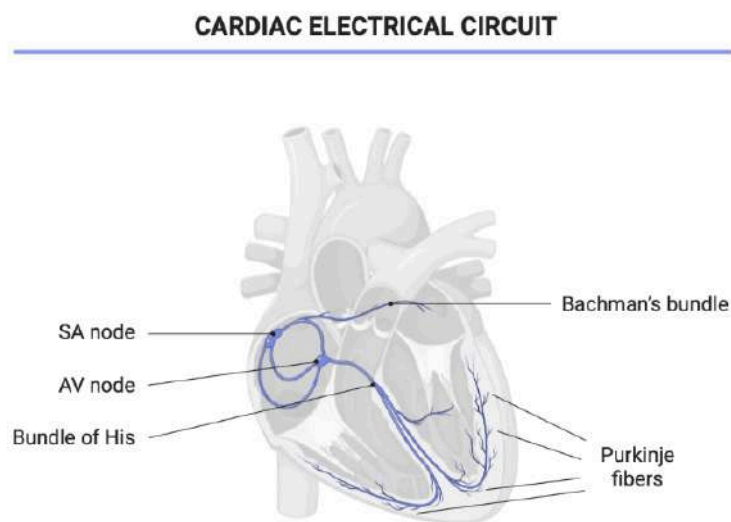
Figure I.3. Electrical circuit of the heart. SA = sinoatrial, AV = atrioventricular. Created in BioRender.com

I.2.4. Evaluation of the electrical activity of the heart: the electrocardiogram

In 1901, Willem Einthoven developed a galvanometer to record the cardiac electrical activity with a non-invasive method, the electrocardiography (ECG). He also established a uniform procedure for its registration based on the use of negatively and positively charged electrodes, between which the action potentials can spread. A third electrode serves to ground the current (Becker, 2015). The tracings obtained vary depending on the localization of these electrodes forming a triangle with the heart in the middle. William Einthoven described 3 electrodes' arrangements, which is known as the Einthoven's triangle and configure the primary limb leads I, II and III (**Figure I.4A**). Later research on this field proposed additional arrangements for the clinical use of the ECG tracing, up to a total of 12 leads.

Since it was developed, the ECG has been widely applied for clinical evaluation of the cardiac state (diagnosis and prognosis) and it is considered as a crucial tool for cardiovascular research (Yang et al., 2015; Konopelski and Ufnal, 2016).
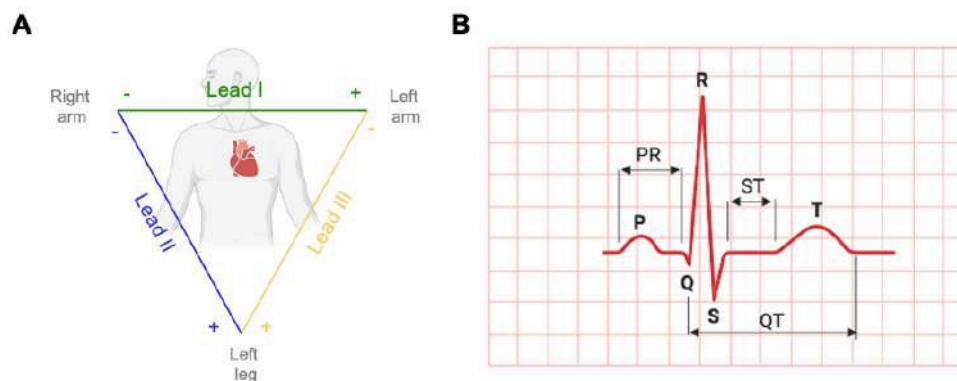
Figure I.4. **Technical aspects of the electrocardiogram. A)** Einthoven's triangle. **B)** Normal ECG tracing. Created in BioRender.com

The ECG tracing and parameters

The sequence of electrical events that occur in the cardiac cycle can be manifested by the ECG. Importantly, the voltages generated by the specialized cells of the conduction system are too small to be recorded by ECG and what the ECG tracing evidences is the action potentials of the muscle cells from the atria and the ventricles (Becker, 2015). The ECG tracing baseline (isoelectric line) represents the resting membrane potentials. Deflections from the baseline correspond to the different electrical events, which are usually measured and provide useful information regarding pathology of the

cardiovascular system, such as arrhythmia, infarction or ischemia. The ECG has a vertical axis that shows the voltage direction and a horizontal axis that denotes the time and sequence of events (Becker, 2015).

Figure I.4B shows a normal ECG tracing (i.e., healthy heart) (Konopelski and Ufnal, 2016), which is composed by the following elements:

P wave. The first deflection that can be identified is the P wave, which represents the depolarization of the atrial muscle cells. In human's and rodents' ECG recording, the P wave has a positive deflection in limb the lead II, a negative deflection in the lead aVR and the it is followed by a QRS complex. The lack of P wave and alterations in its shape have been related to arrhythmia (Konopelski and Ufnal, 2016).

PR interval. It is measured as the time from the beginning of P wave to the start of the QRS complex and it reflects the spread of the atrial depolarization to the ventricles depolarization (Beinfield and Lehr, 1968).

QRS complex. Located between waves Q and S it represents the ventricles depolarization. Important information derives from the analysis of its length (duration); for example, wide QRS complexes reflect alterations in the ventricular conduction and ventricular rhythms, while narrow QRS complexes are found in the supraventricular arrhythmias (Konopelski and Ufnal, 2016).

ST segment. This parameters describes the time in which the ventricles are depolarized, and it is measured from the end of the QRS complex to the start of the T wave (Konopelski and Ufnal, 2016). Alterations of the ST segment is crucial for the identification of myocardial infarction, myocardial ischemia diagnosis and intraventricular conduction blocks, among others (Wagner et al., 2009).

T wave. This deflection corresponds to the repolarization of the ventricles. In general, T wave appears as positive in the majority of the leads. Both high and low voltage T wave have been related to a series of pathological conditions (Konopelski and Ufnal, 2016).

QT interval. It represents the time comprised from the Q wave to the end of the T wave, and it shows the depolarization and repolarization of ventricular cardiomyocytes (Konopelski and Ufnal, 2016). Measuring the QT interval is widely recognized as a good indicator of drug toxicity in the heart (Hanada et al., 1999; Roden, 2004).

Heart rate (HR). Heart rate is the number of contractions of the heart in a specific period of time, usually 1 minute (beats per minute, bpm). Depending on the species, HR can be calculated using different strategies. For example, in humans, HR can be

calculated by measuring the time between two consecutive Q waves under physiological conditions. In rodents, because they commonly lack the Q wave, HR is determined from the RR interval.

I.2.5. The aging heart

A large body of evidence has shown that cardiac changes occur with aging, at the structural, functional and molecular levels. Some of these age-associated alterations, such as the increase in the thickness of the left ventricle, have been interpreted as adaptive changes (Lakatta, 2016). However, the vast majority of the changes identified in the heart of elderly people are considered to be deleterious for the cardiovascular capacity, such as the reduction of cardiac muscarinic receptors function (Brodde et al., 1998), impaired heart rate acceleration (Liu et al., 2014), reduction of cellular protein synthesis and RNA concentration (Meerson et al., 1978), cardiac hypertrophy, fibrosis or contractile dysfunction (Lakatta, 1993).

Age is the main risk factor to develop cardiovascular diseases. For this reason, more and more authors and cardiologists support the idea that age-associated changes cannot be dissociated from the pathology since they might be the key to understand it. Unfortunately, most of the cardiovascular research does not include the "age" variable and, therefore, the age-related modifications are underestimated. This scenario highlights the urgent need to incorporate the implications of cardiac alterations that occur with advancing age into research studies in order to understand which changes can be considered as physiological or pathological, and how physiological heart aging could, together with other factors, predispose to the pathological condition.

I.3. Aging and the central nervous system

The nervous system is one of the most important and complex systems of our body. Its main function is the reception and integration of internal and external environmental changes, and the production of signals to the rest of the body to regulate the response to these changes. Additionally, superior functions of the nervous system include learning, memory, cognition and language, among others. According to its function, the nervous system can be classified into autonomous and somatic, which can be both of them subdivided into: i) Central Nervous System (CNS), including encephalon and spinal cord; and ii) Peripheral Nervous System, integrated by cranial nerves, nerves, ganglia and peripheral fibers.

The nervous system is mainly composed by neurons and glial cells. In the CNS, glial cells are oligodendrocytes, astrocytes, microglia and ependymal cells (Crossman and Neary, 2007).

I.3.1. Brain aging

Similar to other organs and systems, the brain is susceptible to the effects of aging to molecules, cells, vasculature, morphology and, uniquely for this organ, cognition (Teissier et al., 2020). Some authors support the idea that some age-related processes are mechanisms of plasticity to adapt to the negative outcome of other alterations that occur with aging (Gray and Barnes, 2015). Whether these age-associated changes are considered as normal aging or as a primary pathology, it is clear that they represent a series of vulnerabilities that compromise brain functions. Thus, although "aged brain" is not a synonym of "pathological brain", the age-related changes that occur in the brain microenvironment are considered the main risk factor to develop age-associated neurodegenerative diseases (Azam et al., 2021).

At macroscopic level, the gradual loss of tissue mass has been identified when examining atrophy maps in normal aging (Scahill et al., 2003; Ezekiel et al., 2004; Enzinger et al., 2005; Fotenos et al., 2005; Hedman et al., 2012; Fjell et al., 2014). In this sense, brain regions especially vulnerable to normal age-changes are the frontal lobes (West, 1996; Rabbitt, 2005), the entire cerebral cortex (Driscoll et al., 2009; Fjell et al., 2009b) and medial and lateral temporal regions, such as the entorhinal cortex (Du et al., 2003; Ezekiel et al., 2004; Raz et al., 2005; Fjell et al., 2009a) and the hippocampus (Driscoll et al., 2003; Raz et al., 2004; Persson et al., 2012). Discrepancies exist regarding the age-related reduction of the hippocampal volume, since other authors have not found significant changes (Sullivan et al., 1995; Du et al., 2006; Bettio et al., 2017). This controversy is not fully understood; however, the suggestions reported in literature include the differences in the species used (mouse, rats and humans) (Von Bohlen und Halbach and Unsicker, 2002; Driscoll et al., 2003; Maheswaran et al., 2009), the range of ages examined (Driscoll et al., 2006) and the portion of the hippocampus studied (Driscoll et al., 2003; Gordon et al., 2013).

In the recent years, the molecular hallmarks of brain aging have been regarded as primary, antagonistic and integrative (López-Otín et al., 2013; Hou et al., 2019; Azam et al., 2021). The primary hallmarks refer to epigenetic alterations (Hwang et al., 2017), genomic instability (Lombard et al., 2005; Winner et al., 2011), telomeric attrition (López-Otín et al., 2013; Fang et al., 2017) and the loss of proteostasis (López-Otín et al., 2013).

The antagonistic hallmarks comprise compensatory mechanisms that occur in response to age-associated primary damage, including downregulation of nutrient sensing (Babbar and Saeed Sheikh, 2013), mitochondrial impairment (Ritz and Berrut, 2005; Jensen and Jasper, 2014) and cellular senescence (Fielder et al., 2017). Finally, the integrative hallmarks appear as a result of the cumulative damage of the primary and the antagonistic hallmarks (Azam et al., 2021), and they include altered intercellular communications (Frasca and Blomberg, 2016; Hammond et al., 2019) and stem cell exhaustion (Oh et al., 2014) (**Figure I.5**).
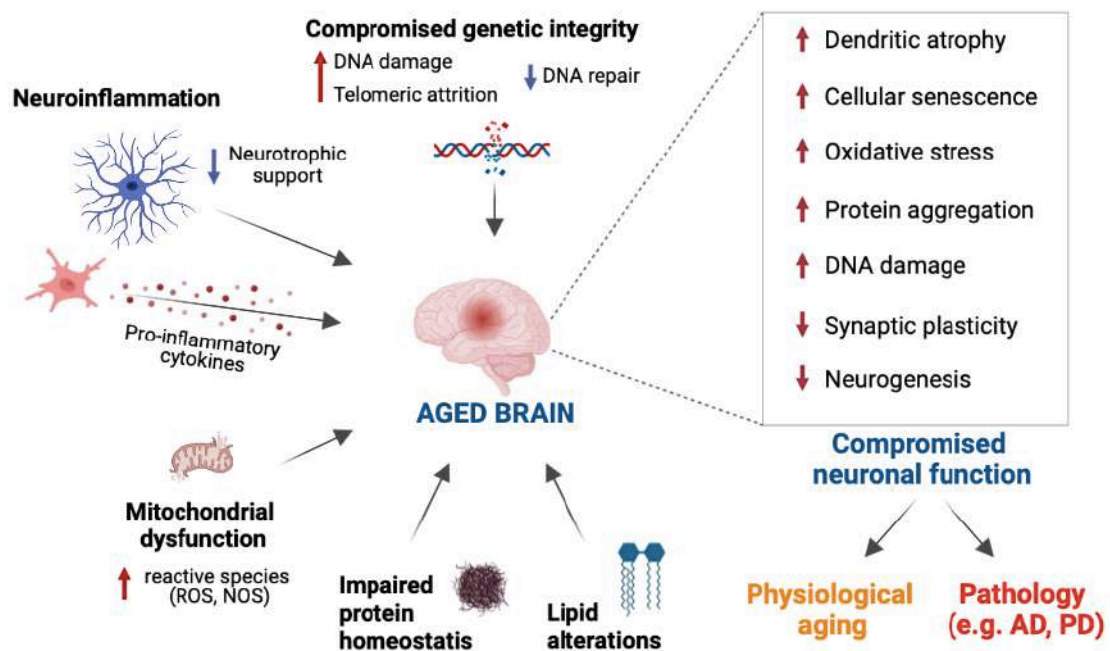
Figure I.5. **Features of brain aging features that lead to compromised neuronal function and may predispose to age-related neurodegenerative disorders.** The main hallmarks of the aged brain are the compromised genetic integrity, increased neuroinflammation, mitochondrial dysfunction and impaired protein homeostasis. Along aging, accumulation of cell damage leads to compromised neuronal function, which can promote adaptive changes and physiological aging, or can increase the risk to develop age-associated neurodegenerative diseases (such as Alzheimer's and Parkinson's disease). Inspired by Bettio et al. (2017) and Azam et al. (2021). Created in BioRender.com.

I.3.2. Oxidative stress

While reactive species are essential components in diverse signaling pathways, the accumulation of oxidative stress is a well-accepted characteristic of the aging process. Denham Harman proposed in 1954 the free radical theory of aging, in which he stated that free radicals "may be involved in production of the aging changes associated with the

environment, disease and an intrinsic aging process" (Harman, 1992; Ionescu-Tucker and Cotman, 2021). His theory is supported by a large body of evidence showing that there is an increment in the oxidative status concomitant with a reduction in the endogenous antioxidant mechanisms (both enzymatic and non-enzymatic) during the aging process (Moor et al., 2006; Calabrese et al., 2008; Venkateshappa et al., 2012; Bettio et al., 2017). The imbalance in the redox status with aging triggers the accumulation of reactive oxygen and nitrogen species (ROS and RNS, respectively), disruption of the lipids' and proteins' metabolism and DNA damage, which contributes to mitochondrial impairment and the amplification of the oxidative stress cycle (Balaban et al., 2005), finally causing cell injury.

The free radicals theory of aging is especially relevant to the CNS and it is considered as one of the main leading mechanisms of neurodegeneration. Neurons are particularly vulnerable to the oxidative stress since they are exposed to several oxidant insults, such as high calcium levels, mitochondrial dysfunction, genomic instability, glutamate-induced excitotoxicity, protein aggregation and the accumulation of reactive species (Wang and Michaelis, 2010). Additionally, neurons are non-dividing and post-mitotic cells, which means that they cannot be replaced in case of damage (Grimm and Eckert, 2017).

In the aged brain of humans and experimental models, several markers of oxidative stress have been detected to contribute, such as the increased lipid peroxidation (LPO) (Cini and Moretti, 1995), protein oxidation (Nicolle et al., 2001; Venkateshappa et al., 2012), toxic levels of metals (Jomova et al., 2010), as well as higher levels of the enzymes involved in the energy production (Yang et al., 2008). Importantly, several studies have pointed out that the neuronal response and susceptibility to oxidative stress during aging is not uniform in the different brain areas and neuronal populations. For example, neurons in the hippocampal *Cornu Ammonis* (CA) 1 region and cerebellar granule cell layer, are especially vulnerable to oxidative stress (Wilde et al., 1997; Wang et al., 2005, 2007, 2009). The increase of oxidative stress and the presence of several oxidative stress markers have been extensively demonstrated in neurodegenerative diseases, such as AD (Zhu et al., 2004), PD (Fahn and Cohen, 1992; Van Muiswinkel et al., 2004), or amyotrophic lateral sclerosis (Carrì et al., 2003). In summary, the CNS accumulates oxidative-induced damage during lifespan, which increases its susceptibility to neurodegeneration and to develop neurodegenerative diseases.

I.3.3. Neuroinflammaging

<u>Introduction to neuroinflammation</u>

Neuroinflammation is the inflammatory response that occurs in the nervous system to overcome insults (both endogenous and exogenous). Inflammatory mediators such as cytokines, ROS and secondary messengers, are produced by the resident CNS glial cells (microglia and astroglia), endothelial cells, and peripheral-derived immune cells (DiSabato et al., 2016). An acute neuroinflammatory response promotes defense, repair and adaptation of the tissue to harmful events. On the contrary, chronic and low-grade inflammation results to be detrimental for normal tissue function, and is characterized by persistent glial activation, high levels of proinflammatory cytokines and increased levels of oxidative stress (Calder, 2017; Azam et al., 2021).

The activation of brain immune cells, such as microglia and astrocytes, is a key step for neuroinflammation (Benjamin Chun-Kit Tong, 2017). Microglia are the main players of the innate immune system in the nervous system and they can be ubiquitously found in the brain. Microglial cells are characterized by a soma and highly motile processes which allow the continuous surveillance of the environment, the detection of pathogens and cellular debris (Nimmerjahn et al., 2005; Perkins et al., 2020). Microglia synthesize factors that contribute to tissue maintenance and also participate in the maintenance of the plasticity of neuronal circuits by protecting and remodeling the synapses (**Figure I.6**) (Guzman-Martinez et al., 2019; Kettenmann et al., 2011). Astrocytes' main function is to maintain neuronal function (**Figure I.7A**). Along with microglia, astrocytes also contribute to inflammatory responses in the brain by amplifying the microglial inflammatory signals and propagating the cytokine cycle, thus contributing to generate higher amounts of cytokines and oxidative signals (Farina et al., 2007; Benjamin Chun-Kit Tong, 2017).

Therefore, due to their key role in brain homeostasis, plasticity and defense, alterations in microglial and astroglial function have been related to pathological events and their progression.

<u>Neuroinflammation in aging and pathological implications</u>

Alterations in the immune system have been described in non-pathological aging, both in humans and in preclinical models (Ostan et al., 2008; Norden and Godbout, 2013; Franceschi and Campisi, 2014; Barrientos et al., 2015; Perkins et al., 2020). Additionally, uncontrolled neuroinflammation has become a hallmark of age-related neurodegenerative disorders and it is directed related with cognitive decline (Guzman-Martinez et al., 2019).

For example, inflammation has been demonstrated to exacerbate the amyloid beta (Aβ) peptide deposition in AD and α-synuclein truncation and aggregation in PD (Wang et al., 2016, 2022; Azam et al., 2021).

Large body of evidence points out that low-grade chronic inflammatory responses occur in normal aging and neurodegenerative diseases, which is supported by the maintenance of continuous positive feedback loops between microglia and astrocytes (Benjamin Chun-Kit Tong, 2017). The uncontrolled inflammatory cycle becomes neurotoxic, damaging healthy neurons, which can further activate immune cells and contribute to the ongoing inflammatory processes.
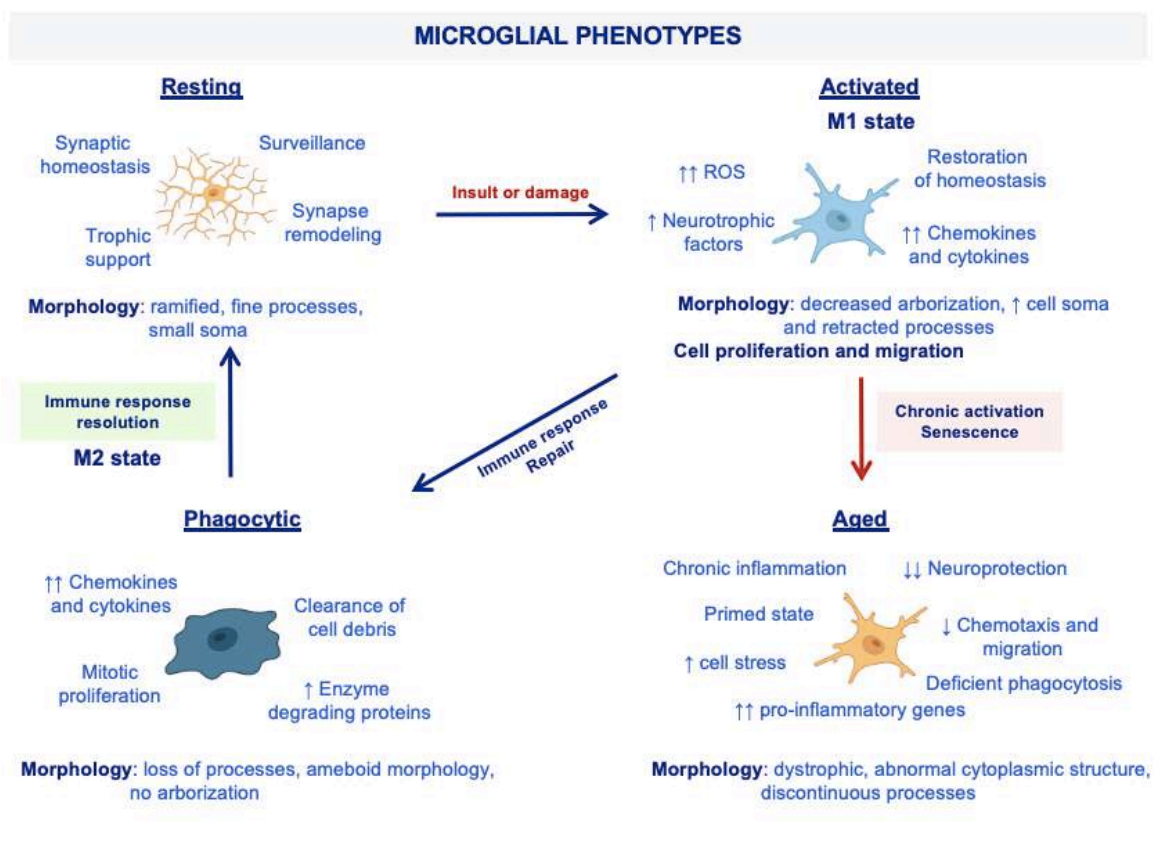
Figure I.6. Changes in microglia at phenotypic, molecular and functional levels. The physiological function of microglia is the continuous monitorization of the environment. When an insult or damage are detected, microglia activate and promotes inflammatory response, that can advance to its phagocytic state (M1 state), and promote its defense function. Once the damage is resolved, the homeostatic state is recovered by the balance towards anti-inflammatory microglia (M2 state). However, during the aging process, a chronic inflammatory state promotes the primed state of the microglia, thus contributing to a pro-inflammatory environment and reduced neuroprotective role. ↓ indicates decreased, ↑ indicates increased. Adapted from (Edler et al., 2021). Created in Biorender.com.

Together with the increase in pro-inflammatory cytokines and gene expression arrangement, changes in morphology are indicators of microglial activation (**Figure I.6**). In response to an acute challenge, microglia increase the expression of genes related to neuroinflammation and initiates morphological modifications, including the retraction of the cytoskeletal processes and the transition from ramified to ameboid shape (Kettenmann et al., 2011). These changes are typically visualized with antibodies directed against ionized calcium binding adaptor molecule 1 (Iba1), which results highly useful to study the maintained inflammatory state (i.e., in aging or neurodegeneration) (Perkins et al., 2020). Several authors proposed that the maintained pro-inflammatory state of microglia with advancing age occurs because these cells are sensitized or primed, i.e., with increased transcriptomic profile towards pro-inflammatory mediators and decreased anti-inflammatory mediators, reduced time and threshold for activation and exacerbated inflammatory response when activated (**Figure I.6**) (Henry et al., 2009; Norden and Godbout, 2013).
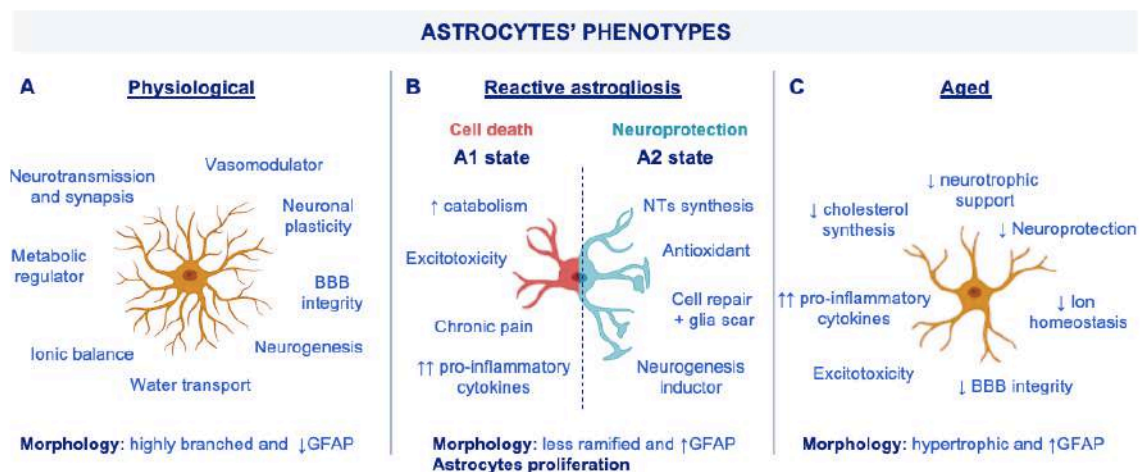
Figure I.7. **Astrocytic changes dependent on the environment. A)** Functions and morphology of astrocytes in physiological conditions, favoring the CNS homeostasis. **B)** Reactive astrogliosis can lead to neuroprotection or cell death depending on the environmental conditions. Historically, the pro-inflammatory state of astrocytes has been known as A1, while the anti-inflammatory one is the A2 state. **C)** Aging induces molecular and functional changes in the astrocytes. NTs = neurotransmitter, BBB = blood brain barrier, ↓ indicates decreased, ↑ indicates increased. Inspired by (Becerra-Calixto and Cardona-Gómez, 2017; Verkerke et al., 2021). Created in Biorender.com.

Reactive astrogliosis refers to the activation of astrocytes via biochemical, transcriptional, metabolic and morphological changes (**Figure I.7B**). On the one hand, reactive astrogliosis can result beneficial and produce neuroprotective effects by contributing to the formation of glial scar to isolate the damaged area, providing blood-

brain barrier reconstruction and trophic support of stressed neurons (Rodríguez-Arellano et al., 2016; Escartin et al., 2021). However, under certain circumstances (such as aging or neurodegenerative processes), maintained reactive astrogliosis can contribute to neurotoxicity (**Figure I.7C**) (Heneka et al., 2010; Valero et al., 2017). The glial fibrillary acidic protein (GFAP) is one of the astroglial genes that is up-regulated in reactive astrocytes and immunostaining against GFAP can manifest morphological changes in astrocytes (such as hypertrophic morphology) (Verkerke et al., 2021). Increased expression of GFAP, both at mRNA and protein levels, have been reported with aging and also in neurodegeneration, with a region-specificity (Nichols et al., 1993; David et al., 1997; Jyothi et al., 2015). Attending to GFAP immunoreactivity pattern, younger individuals' astrocytes are long and thin processed, while hypertrophic astrocytes (short and stubby processes) have been detected in older individuals (Cruz-Sánchez et al., 1998; Jyothi et al., 2015; Verkerke et al., 2021).

I.3.4. Cognitive decline and the hippocampus

Cognition can be broadly defined as the ability to perform processes such as memory, language, attention, association, problem solving and concept formation (Solari and Hangya, 2018). The changes in mental abilities that occur with increasing age are known as cognitive aging (Ownby, 2010). Importantly, aging affects selectively different cognitive functions: while some are potentiated along the lifespan (i.e., semantic abilities), others do significantly decline, such as the learning memory (Park et al., 2002; Oberauer et al., 2003; Hedden and Gabrieli, 2004; Fan et al., 2017). Indeed, memory is one of the earliest cognitive abilities that decline with aging, being the hippocampus-dependent spatial and episodic learning particularly vulnerable.

Learning and memory

As stated by Dr. Eric Kandel "learning is the process by which we acquire knowledge about the world and memory is the process by which that knowledge of the world is encoded, stored, and later retrieved" (Kandel et al., 2012). Memory can be divided into three groups, which are inter-communicated (Deiana et al., 2011):

a. Sensorial memory. Information coming from the external environment (images, sounds, odors, flavors) is captured for a very short period of time (seconds) and transmitted to the short-term memory.

b. Short-term memory. It is defined as a capacity to store a limited amount of information for a short period of time (seconds to a minute).

c. Long-term memory. This kind of memory can store larger quantities of information for unlimited duration. Long-term memory can be divided into declarative (explicit) or non-declarative (implicit) (Sharma et al., 2010). <u>Declarative memory</u> refers to the knowledge about facts and their meaning, including places, things and people, and can be classified as episodic memory and semantic memory (Anderson, 2013). The episodic memory includes personal events that occurred in a particular context (such as time and place), while the semantic memory refers to the knowledge of the facts independently of the context in which they were learned (Tulving, 1972; Miller and O'Callaghan, 2005). Particularly, spatial memory is considered episodic memory because it refers to the information stored within the spatio-temporal context (O'Keefe and Black, 1977). The major structures participating in declarative memory are the hippocampus and other medial temporal lobe structures, together with the neocortex (Knowlton et al., 1996). <u>Non-declarative memory</u> involves the acquisition of skills (motor) and habits, and answers the question "how". This kind of memory is mainly mediated by the neostriatum and cerebellum (Salmon and Butters, 1995; Knowlton et al., 1996).

The hippocampus. Generalities.

The hippocampus has a critical role in the learning and memory processes, and it is crucial for the age-associated and pathological cognitive decline, especially the long-term episodic-spatial memory (Pigott and Milner, 1993; Feigenbaum et al., 1996; Stefanacci et al., 2000; Astur et al., 2002; Corkin, 2002). This brain region is located in the medial temporal lobe, is part of the limbic system and is essential for learning tasks, memory consolidation, the spatial navigation and the regulation of emotional behaviors (El-Falougy and Benuska, 2006). The hippocampus is present across all the mammalian orders and has a long, curved form (C-shaped), and it is placed along the posterior-to-anterior axis in humans and in the dorsal-ventral axis in rodents (**Figure I.8A**) (Strange et al., 2014). Regarding functionality, the "dorsal-ventral dichotomy view" supports that the more dorsal parts are related to cognitive functions (in particular, spatial memory), while the ventral portion of the hippocampus mediate emotional responses (Moser et al., 1993, 1995). This segregated hippocampal functionality across the axis is also observed in its differential connectivity with multiple cortical and subcortical areas (Strange et al., 2014).
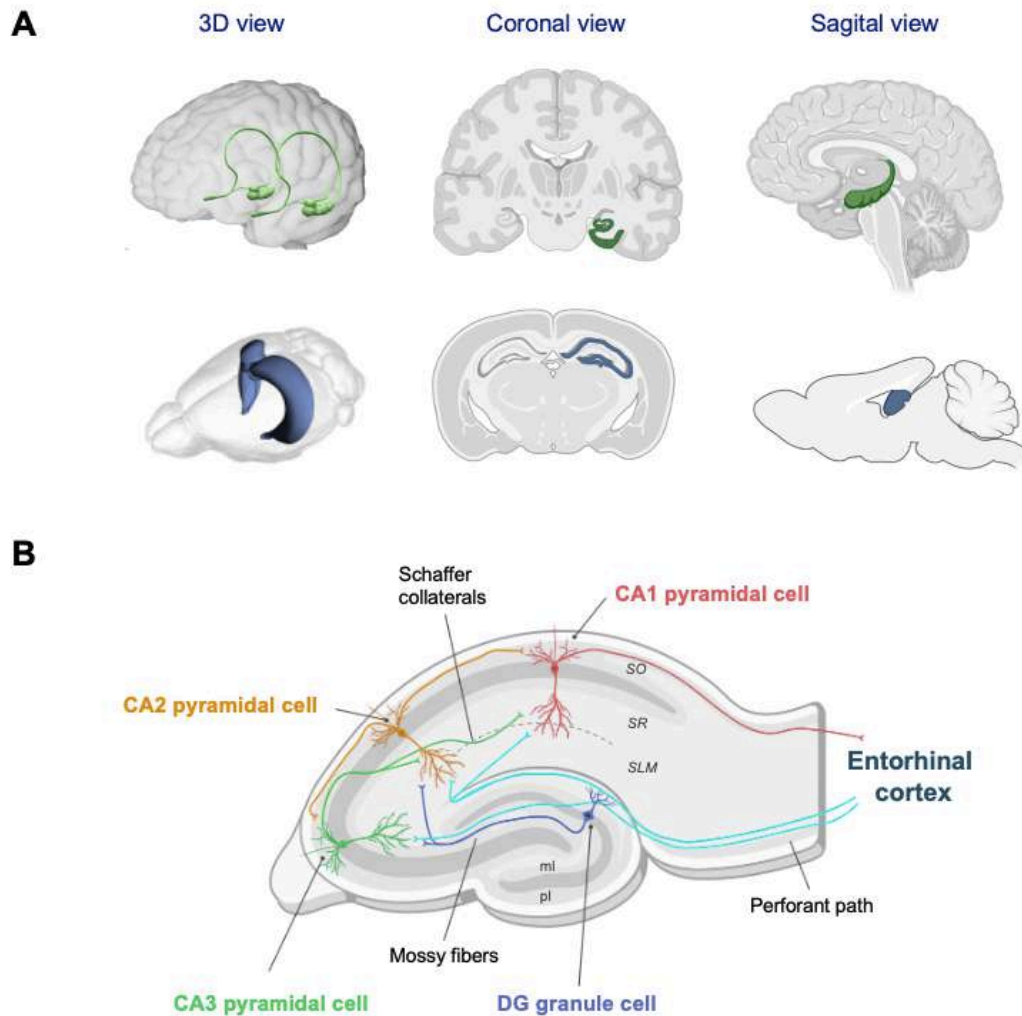
Figure I.8. The human and rodent hippocampus. A) Schematic representation of the anatomical position of the human (first row) and mouse (second row), from 3D view and coronal (dorsal level) and sagittal sections; **B)** Schematic representation of the neuronal connections in the rodent dorsal hippocampus and its subareas. Abbreviations: ml = molecular layer, pl = polymorph layer, SLM = *stratum lacunosum-moleculare*, SO = *stratum oriens,* SR = *stratum radiatum.* Inspired by (Strange et al., 2014; Chevaleyre and Piskorowski, 2016). Created in BioRender.com.

Due to its relevance in the research conducted in this thesis, the anatomy of the rodent dorsal hippocampus is described in the following lines (**Figure I.8B**), although the basic intrinsic hippocampal circuitry is well conserved across species. The hippocampus is formed by two main fields, the dentate gyrus (DG) and the *Cornu ammonis*, with its subregions CA1, CA2 and CA3 (Insausti and Amaral, 2012). All of the fields of the hippocampus have a similar laminar organization. In the DG, the principal cellular layer is constituted by the soma of the granular cells, whereas in the CA it is formed by the pyramidal cells (Hammond, 2015; Cappaert et al., 2015). Several types of interneurons innervate this principal cell layers, such as the basket cells, bistratified cells, the *oriens-lacunosum moleculare* cells and the axo-axonic cells (Hammond, 2015). From the cell

body, dendrites and axons emerge and are distributed in different layers. In the DG, the dendrites of the neurons form the molecular layer, whereas the projections of this neurons towards the CA3 subfield form the polymorphic layer. In the CA subregions, the narrow layer containing the basal dendrites with numerous spines forms the *stratum oriens* (SO). In the CA3 region, but not in the CA1 nor CA2, a thin area located just above the pyramidal cell layer called the *stratum lucidum* contains the mossy fiber axons coming from the DG. At the distal end of the *stratum lucidum*, a slight thickening of the cell layer can be found, which corresponds to the bend of the mossy fibers and the CA3-CA2 border (Cappaert et al., 2015). Mossy fibers connect both the CA3 and the CA2 fibers (**Figure I.8B**). Then, superficial to the stratum lucidum in the CA3 and just above the cell layer in CA1 and CA2, is the stratum radiatum (SR). In the SR, the CA3-CA2 and CA3-CA1 (Schaffer collaterals) connections are located. That is, apical dendrites from all the pyramidal cells which organize with a radial aspect forming the SR, which finally arborize in the stratum lacunosum moleculare (SLM) (Schultz and Engelhardt, 2014). The SLM is the most superficial portion of the hippocampus and it contains the fibers from the perforant pathway (coming from the entorhinal cortex) (Hammond, 2015; Cappaert et al., 2015) (**Figure I.8B**).

Circuitry organization of the hippocampus is complex, including intra- and extra-hippocampal connections, and even auto-associative networks (e.g., CA3-CA3 neuronal connections). Principal hippocampal inputs come from superficial layers of the entorhinal cortex, whereas the CA1-deeper entorhinal cortex layers connection represents the main output from the hippocampus (Roux et al., 2021). In the *stratum lucidum*, the apical dendrites of neurons of the CA3 and CA2 receive projections from rostrocaudal areas and cholinergic (septal nuclei) and histaminergic (supramammilary regions) inputs. Projections from the CA3 and the CA2 neurons, known as Schaffer collaterals, terminate in the SR and in the SO of the CA1. The CA2 pyramidal cell layer is relatively compact and narrow, located between the CA1 and the CA3. Compared to humans and nonhuman primates, the CA1 is thicker in rodents (Schultz and Engelhardt, 2014). Projections from the entorhinal cortex to the DG travels in the SLM and in the synapses with the distal apical dendrites of the pyramidal neurons. The information is transmitted in the hippocampus mostly unidirectionally via the tri-synaptic circuit and three hippocampal subregions participate: the DG, the CA1 and the CA3 (Soltesz et al., 2018). The hippocampus receives information from a variety of cortical regions, mainly the entorhinal cortex (**Figure I.8B**). Projections from the entorhinal cortex enter the DG is known as perforant path, which gives rise to the mossy fibers that terminate in the DG and in the CA3. CA3 innervates the CA1 via the Schaffer collaterals and then, CA1 outputs to the subiculum and the entorhinal cortex (Eichenbaum, 2004; Fan et al., 2017). Little is known regarding

the CA2 field, but several studies point out its relationship with social memory and processing of sensory information. Although less involved in the hippocampal circuit of spatial information, a recent study has shown that the CA2 pyramidal neurons are involved in the network of spatial information during physical immobility (Chao et al., 2020). The interactions between the ventral part of the rodent hippocampus (anterior in humans) and the medial prefrontal cortex (mPFC), are fundamental for episodic memory retrieval and consolidation (Preston and Eichenbaum, 2013; Chao et al., 2020).

The aged hippocampus

The hippocampus is known to be a brain area highly affected by aging. Different works of the last years have agreed that aging does not induce significant neuronal death in the hippocampus of humans, monkeys and rodents. Rather, several research groups have found some molecular and cellular processes that do characterize that aging hippocampus (Fan et al., 2017), including synaptic dysfunction, increase in the oxidative stress state, altered transcriptional and epigenetic regulation, microglial changes and detrimental neuroinflammatory processes, among others (Moor et al., 2006; Calabrese et al., 2008; Venkateshappa et al., 2012; de Diego et al., 2019; Singh et al., 2019). In addition, together with the subventricular zone, the GD is the major neurogenesis area in the adult brain (Bettio et al., 2017). In the aged brain, down-regulation of the neurogenesis has been described (Lazarov et al., 2010), which is translated into a loss of neuronal plasticity and is considered as a critical event in the early stages of AD (Fjell et al., 2014). All these features of the aged hippocampus contribute to impaired hippocampal function and plasticity, thus inducing hippocampal dependent cognitive deficits.

I.3.5. Lipids and neurodegeneration

Overview of lipids' biochemistry

Lipids are defined as organic compounds that are not soluble in water but soluble in organic solvents (Anon, 2000). Chemically, lipids are considered small hydrophobic or amphiphilic molecules that originate from two different building blocks: isoprene and ketoacyl groups (**Figure I.9A**) (Fahy et al., 2011; Naudí et al., 2015). Based on their complexity, lipids have been proposed to be classified as simple and complex. Simple lipids are compounds that can be separated into two distinct entities upon hydrolysis, such as acylglycerols (fatty acids + glycerol), while complex lipids include those that yield three or more products upon hydrolysis, such as glycerophospholipids (fatty acids + glycerol + headgroup) (Naudí et al., 2015).

A) LIPID BUILDING BLOCKS

Ketoacyl group

Isoprene group

Acetyl Propionyl

B) FATTY ACIDS

Saturated

Unsaturated
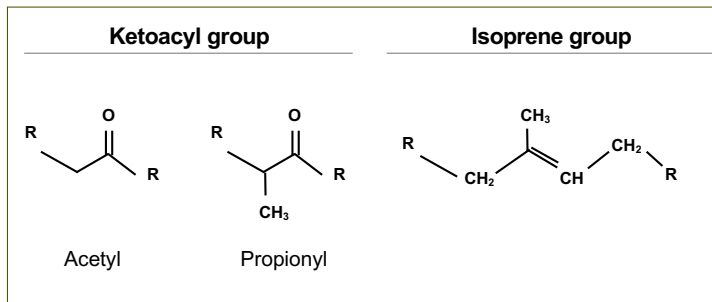
C) MOST COMMON BRAIN LIPIDS

TRIACYLGLYCERIDE

GLYCEROPHOSPHOLIPIDS

CHOLESTEROL

GLYCOSPHINGOLIPIDS

Sphingomyelin

Gangliosides

Cerebrosides

Sulfosphingolipids
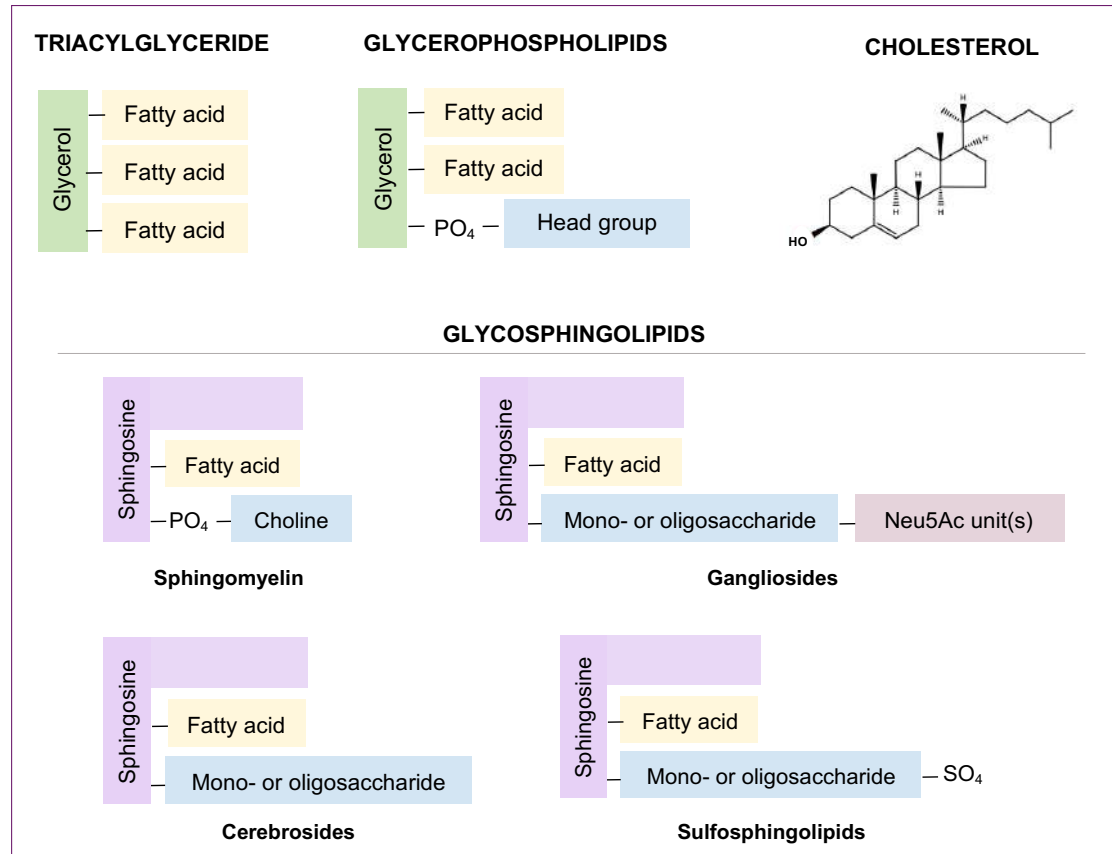
Figure I.9. Schematic representation of the general structures of different lipids classes. A) Ketoacyl and isoprene groups are the lipid building blocks. **B)** Fatty acids are formed by a carboxylic acid attached to hydrocarbonated chains **C)** The most common lipids found in the brain include triacylglycerides, glycerophospholipids, glycosphingolipids and cholesterol. Inspired by Naudí et al., 2015 and Nelson and Cox, 2017.

The LIPID MAPS Consortium developed in 2005 a classification system and nomenclature for lipids based on well-established chemical and biochemical properties and following the existing the International Union of Pure and Applied Chemists and the International Union of Biochemistry and Molecular Biology (IUPAC-IUBMB) guidelines (Fahy et al., 2009). According to this classification, lipids are divided into eight groups: i)

fatty acids, ii) glycerolipids, ii) glycerophospholipids, iv) sphingolipids, v) saccharolipids, vi) polyketides (derived from the condensation of ketoacyl groups), vii) sterols, and viii) prenol lipids (derived from the condensation of isoprene subunits). Among them, the categories found in the human brain are fatty acids, glycerolipids, glycerophospholipids, sphingolipids and sterols.

1) **Fatty acids** are carboxylic acids with hydrocarbonated chains (from 4 to 36 carbon atoms). This chain can be saturated (no double bonds) or unsaturated (one or more double bonds). Fatty acids are the basic building blocks of more complex lipids and via β-oxidation serve as source of energy (Nelson and Cox, 2017) (**Figure I.9B**).

2) **Glycerolipids** contain long-chain hydrocarbons attached to a glycerol molecule via ester linkages. Each carbon atom of glycerol (three in total) can be linked to a fatty acid, which is named as "acyl". If all three carbons of glycerol have a fatty acid attached, the compound is named triacylglycerol (triglyceride) (Fantini and Yahi, 2015) (**Figure I.9C**). Some glycerolipids found in the brain are 2-arachidonoyl-sn-glycerol and the 1-stearolyl-2-arachidonoyl-sn-glycerol (Naudí et al., 2015).

3) **Glycerophospholipids** are composed by two fatty acids linked by an ester bond to the first and second carbon of glycerol, and a polar head group attached to the third carbon by phosphodiester bond (**Figure I.9C and Figure I.10A**). The simplest glycerophospholipid is phosphatidic acid (PA), while other most complex glycerophospholipids include phosphatidylethanolamine (PE), phosphatidylcholine (PC), phosphatidylserine (PS), phosphatidylglycerol, phosphatidylinositol (PI) and cardiolipin (**Figure I.10B**). A special species of glycerophospholipids are plasmalogens, which are ether-linked alkenyl species with doble bond between C1 and C2. Although they are ubiquitous from all cell membranes, ethanolamine plasmalogens (Pls-Etn) are highly enriched in the nervous system (Dorninger et al., 2020; Kao et al., 2020).

4) **Sphingolipids** are composed by a polar head and two nonpolar chains. Differently to glycerophospholipids, sphingolipids do not contain glycerol. The basic component of sphingolipids is the sphingosine (**Figure I.9C**). The C1, C2 and C3 carbons in the sphingosine are structural analogs to the three carbons in the glycerol of the glycerophospholipids. A fatty acid linked by amide bond to the NH_2 group of the C2, is the fundamental common unit of all sphingolipids and it is known as ceramide (**Figure I.11A**). Sphingolipids can be divided into sphingomyelin (SM), cerebrosides, sulfatides and gangliosides (Nelson and Cox, 2017). Cerebrosides, sulfatides and gangliosides are glycosphingolipids, since they have one or more sugar residues.

- SM (N-acylsphingosine-1-phosphocholine) contain PC as polar head group, so it can also be considered as phospholipid together with glycerophospholipids (**Figure I.11B**).

- Cerebrosides are usually found in the external layer of the cell membrane and they have one or more sugars as polar head group, which are attached to the primary hydroxyl of sphingosine by a β-glycosidic linkage (**Figure I.11B**). The main cerebroside in the brain is galactosylceramide (GalCer). Cerebrosides containing two or more sugars (usually a combination of D-glucose, D-galactose or N-acetyl-D-galactosamine) are named globosides (**Figure I.11B**). Cerebrosides and globosides are also known as neutral glycosphingolipids.

- Sulfatides are lipids belonging to the subclass of sulfosphingolipids, which are esters of galactocerebrosides in which a sulfate group is placed at the C3. Sulfatide is the only sulfosphingolipid present in the brain (**Figure I.11B**) (Naudí et al., 2015).

- Gangliosides are the most complex sphingolipids. Their polar head groups contain oligosaccharides and one or more terminal residues of N-acetylneuraminic acid (Neu5Ac), also known as sialic acid (**Figure I.9C and Figure I.11B**). Gangliosides with one sialic acid residue are gangliosides from GM series (e.g., GM1, GM2, GM3); gangliosides with two sialic acid residues are gangliosides from GD series (e.g., GD1a, GD1b); gangliosides from the series GT have three sialic acid residues (e.g., GT1b) and the ones from the GQ series, four (e.g., GQ1b) (Nelson and Cox, 2017).

5) **Sterols** have a steroid nucleus as characteristic basic structure, consisting in four joint rings, three of them with six carbons and the other with five (**Figure I.9C**). The major sterol found in the brain is cholesterol, which accounts for 20-25% of the total cholesterol in the body (Egawa et al., 2016).

Relevant techniques for the lipid analyses include liquid chromatography (e.g., thin layer chromatography), gas chromatography-mass spectrometry and mass spectrometry imaging (Kao et al., 2020).

A   **Glycerophospholipids (general structure)**

B
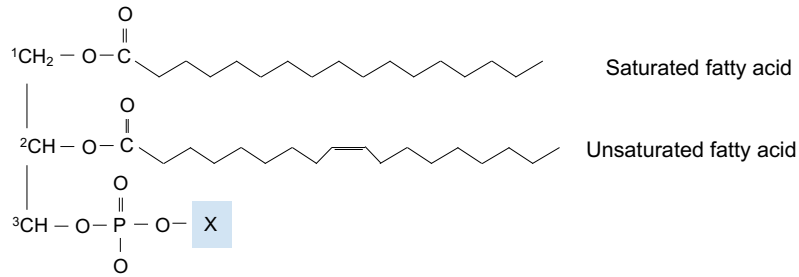
Glycerophospholipid name	X group	X group formula
Phosphatidic acid	——	— H
Phosphatidylethanolamine	Ethanolamine	— CH_2 — CH_2 — $\overset{+}{N}H_3$
Phosphatidylcholine	Choline	— CH_2 — CH_2 — $\overset{+}{N}(CH_3)_3$
Phosphatidylserine	Serine	— CH_2 — CH — $\overset{+}{N}H_3$; COO^-
Phosphatidylglycerol	Glycerol	— CH_2 — CH — CH_2 — OH; OH
Phosphatidylinositol 4, 5-biphosphate	*myo*-inositol 4,5-biphosphate	
Cardiolipin	Phosphatidylglycerol	

Figure I.10. Glycerophospholipids. A) The common glycerophospholipids are diacyilglycerols linked to alcohols by phosphodiester bond. **B)** Glycerophospholipids. A) The common glycerophospholipids are diacyilglycerols linked to alcohols by phosphodiester bond. **B)** Phosphatidic acid is the reference compound. Each glycerophospholipid derivate is named according to the alcohol in the polar head group (X), with the prefix "phosphatidyl-". In cardiolipin, a single glycerol is shared by two phosphatidic acids. Adapted from Nelson and Cox, 2017.

A   **Sphingolipid (general structure)**

Sphingosine

$OH - {}^3CH - CH = CH - (CH_2)_{12} - CH_3$

$^2CH_2 - N$

O

$^1CH - O - X$

H

Fatty acid chain
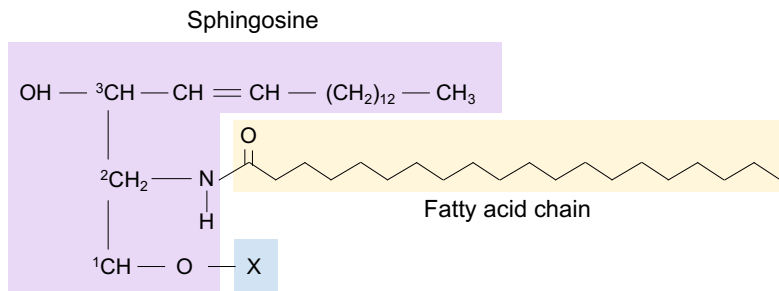
B

Sphingolipid name	X group	X group formula
Ceramide	———	— H
Sphingomyelin	Phosphocholin	$-P(=O)(O^-) - O - CH_2 - CH_2 - N^+(CH_3)_3$
Neutral glycolipids (glucosylcerebroside)	Glucose	
Lactosylceramide (globoside)	>1 sugar residue	
GM1 (ganglioside)	(-) charged oligosaccharides with one or more sialic acid residues	Neu5Ac / Glc — Gal — GalNac — Gal

Figure I.11. Sphingolipids. A) General structure of a sphingolipid. The three carbons in the polar side of the sphingosine are analogous to the three carbons in the glycerol of glycerophospholipids. The amino group in the C-2 is linked to a fatty acid by amide bond. This fatty acid, which is usually saturated or monosaturated and contains 16, 18, 22 or 24 carbon atoms. **B)** Different sphingolipids depending on the group with polar head linked to the C-1. Ceramide is the reference compound of the sphingolipids. Gangliosides are the most complex sphingolipids, with complex oligosaccharides as polar head groups. Abbreviations: Gal = galactose; GalNac = N-acetyl-galactosamine; Glc = glucose; Neu5Ac = N-acetylneuraminic acid. Adapted from Nelson and Cox, 2017.

Overview of brain lipids

The brain is the most lipid-rich organ and lipids account for at least 50% of its dry weight (O'Brien and Sampson, 1965; Sastry, 1985; Kao et al., 2020). The lipid composition of the human brain has been extensively reviewed by different authors (Naudí et al., 2015). In simplistic terms, lipids in the brain comprise around 50% phospholipids, below 40% glycolipids, 10% cholesterol (including cholesterol ester and traces of triglycerides). In addition, brain has a very high content of n-3 and n-6 polyunsaturated fatty acids, such as docosahexaenoic acid (DHA) and arachidonic acid (AA) (Skowronska-Krawczyk and Budin, 2020).

Although other macromolecules and associated proteins are also active components of biological membranes, the lipids that are present on them determine its basic structure and functions, drive the formation of highly organized multimolecular structures, and lead to the creation of multiple and multidimensional levels of order (Sonnino et al., 2014). This concept becomes particularly evident in the nervous system, which possesses a unique lipid composition that allows the high degree of specialized cellular and tissue functions (Aureli et al., 2015). Indeed, the lipid composition of biological membranes determines a series of properties, which are crucial for neuronal and glial cell physiology.

In several types of cells, especially neurons and glia, the composition of the two plasma membrane monolayers is known to be asymmetric: the inner leaflet is enriched in PS, PE and PI, while the outer leaflet is enriched in PC and SM (Nelson and Cox, 2017). In addition to this heterogeneous composition, the lipids in neuronal and glial cell membranes continuously undergo rapid changes (e.g., removal and replacement, deacylation and reacylation cycles), which is termed as "membrane remodeling" and that ensures the adjustments in the chemical structure and molecular shape of the cell membranes (Naudí et al., 2015).

Specific nervous system's functions are known to be dependent on the dynamic and the biomechanical properties of the cell membranes (e.g., membrane curvature), such as signaling by membrane-bound networks, synaptic vesicle trafficking, neurotransmitter release and reception, ion channel activation and activity, and action potential propagation (Skowronska-Krawczyk and Budin, 2020).

Importantly, the intrinsic features of some membrane lipids lead to the formation of small membrane domains known as lipid rafts. In other words, even in membrane regions with undistinguishable morphology and architecture, their components do not undergo free lateral diffusion but are transiently confined to the lipid rafts, thus giving rise to a sort of

lateral order within biological membranes (Aureli et al., 2015; Grassi et al., 2020). This micro- or nano-entities serve as signaling platforms in which proteins can organize multiprotein complexed at membrane level (Sonnino and Prinetti, 2012).

In addition to key structural components, lipids are also known to be mediators (messengers) in several cell pathways. For example, glycerophospholipids are known to participate in cell differentiation, calcium homeostasis, inflammation, neural cell migration or gene expression, among others; phospholipids (e.g., ceramide and sphingosine) regulate cell growth, neurite retraction, vascular dynamics or cell survival; different forms of cholesterol have role in neurogenesis as well as in apoptosis (Piomelli et al., 2007; Farooqui, 2009; Naudí et al., 2015; Doyle et al., 2018).

Thus, lipids are essential elements in the brain and they play a role in both health and disease.

Brain lipids relevant to the aging process

Evidence regarding the role of lipid alterations as key contributing factors to both brain aging and neuropathologies have gained attention (Hallett et al., 2019; Grassi et al., 2020; Moll et al., 2020, 2021). Indeed, lipid disruption has been related to compromised brain function (Yoon et al., 2022). For example, it has been demonstrated that sphingolipids, in particular gangliosides, and cholesterol are crucial players in the neurodegeneration associated with different forms of dementia, AD and PD (Wong et al., 2017; McFarlane and Kędziora-Kornatowska, 2019; Kao et al., 2020; Chiurchiù et al., 2022; Cuenca-Bermejo et al., *Under Review*).

The aim of most conventional studies was to determine changes in lipidic composition and to establish relationships with aging-related processes and neurodegeneration. The amount of cerebral lipids increases and then begin to gradually decrease after the age of 50 (Kao et al., 2020). In general, the study of brain lipid changes has been done from the perspective of pathological conditions (e.g., Alzheimer's disease) (Phillips et al., 2022). However, a current of thoughts support the idea that aging is a condition of vulnerability that might predispose to age-related pathologies; therefore, it is essential to understand the changes associated to physiological aging. Some authors have reviewed the age-associated changes in the brain lipid composition (Svennerholm et al., 1989, 1991, 1994; Naudí et al., 2015b; Skowronska-Krawczyk, Dorota; Budin, 2020; Ooi et al., 2021). **Table I.1** collects general lipid changes associated to aging.

In the last years, due to the emerging role of oxidative stress as one of the key mechanisms leading to aging-related phenotypes, the research focus has also been directed to the study of LPO as a potential harmful event for the membranes structure and the CNS function (Spiteller, 2002) LPO refers to the presence of lipid-associated oxidative stress. Lipids can be easily oxidized because of their reaction with ROS or by enzymes like lipoxygenases, cyclooxygenases and cytochrome P450 (Li et al., 2022). LPO in cellular membranes elevate the endogenous production of reactive aldehydes and their derivatives such as glyoxal, methylglyoxal (MG), malondialdehyde (MDA), and 4-hydroxy-2-nonenal (4- HNE) (Li et al., 2022). 4-HNE is the most toxic byproduct and its primary mechanism of toxicity is its ability to bind to proteins, inactivating some antioxidant enzymes and, therefore aggravating the oxidative stress scenario (Zarrouk et al., 2014; Sottero et al., 2017). Moreover, the 4-HNE-protein complex can cause autoimmune reactions, thus contributing to neurodegenerative processes (De Virgilio et al., 2016). The 4-HNE and the 4-HNE complex have been found in AD, PD, Huntington disease and amyotrophic lateral sclerosis patients (Shibata et al., 2011; Di Domenico et al., 2017).

I.3.6. Pathological brain aging

As previously mentioned, aging is associated with some debilitating neurodegenerative diseases, being AD and PD the most common and prevalent ones. The following lines the overview of the pathological aspects of these disorders is presented.

The elaboration of this part of the Introduction chapter is based on the published reference: Cuenca et al., 2019. Agreement documents for its use from all the co-authors and permission rights obtained from the journal can be found in the Annex I.

Table I.1. **Changes in the lipid brains along aging**. ↑ indicates increase, while ↓ indicates decrease. PE=phosphatidylethanolamine, PC=phosphatidylcholine, PI=phosphatidylinositol, PlsCho=choline plasmalogens, Pls-Etn=ethanolamine plasmalogens. Inspired by Naudí et al., 2015 and Sipione et al. 2020.

KIND OF LIPID	VARIATION	SPECIES	SAMPLE	REFERENCES
FATTY ACIDS				
Polyunsatured Fatty Acids	↓	Human	Cortex and hippocampus	Bourre, 2009; Naudí et al., 2015; Rider et al. 2008; Cutuli 2017
			Plasma	Ajith, 2018; Cole et al., 2009
			Orbitofrontal cortex (grey matter)	Parasa et al. 2016
			Brain	Pottala et al. 2014.
		Rat	Hippocampus	McNamara et al., 2008; Terracina et al., 1992a, 1992b
GLYCEROPHOSPHOLIPIDS				
PE	↓	Human	Brain (region not specified)	Bourre, 2009 Farooqui et al. 1988
PC	↓		Brain (region not specified)	Farooqui et al. 1988
PI	↓		Brain (region not specified)	Farooqui et al. 1988
Plasmalogens				
Plasmalogen PlsCho	↑	Human	Plasma	Dorninger et al. 2018
	↑	Mouse	Brain (region not specified)	Torello et al. 1986
Plasmalogen PlsEtn	↓	Mouse	Brain (region not specified)	Torello et al. 1986
Cardiolipin	↓	Rat	Brain (not specified region)	Petrosillo et al. 2008
SPHINGOLIPIDS				
Ceramide	↑	Human	Striatum and hippocampus	Jazvinšćak Jembrek et al., 2015; Naudí et al., 2015
			Brain (region not specified) Frontotemporal area	Soreghan et al. 2003 He et al. 2010
Sphingomyelin	↓	Human	Brain (region not specified)	Soreghan et al. 2003
Gangliosides	↓	Human	Frontal and temporal lobe	Svennerholm et al. 1994; Kracun et al. 1992
		Human	Brain (region not specified)	Svennerholm et al. 1991; Segler-Stahl et al., 1983; Palestini et al., 1990; Kracun et al., 1992b; Mo et al., 2005
		Mouse	Brain (region not specified)	Ohsawa 1989;
			Frontal and temporal lobe	Svennerholm et al. 1994
		Rat	Frontal and temporal lobe	Kracun et al. 1992
Sulfatide	↓	Human	Frontal gyrus (superior)	Cheng et al. 2013
CHOLESTEROL				
	↓	Human	Frontotemporal cortex, HPC, caudate nucleus and cerebellum	Söderberg et al. 1990; Svennerhol et al. 1991.
		Rat	Hippocampus	Frank et al. 2008

Alzheimer's disease. General aspects.

AD is the most common age-associated neurodegenerative disorder in the world and the main form of dementia. It has a progressive and chronic nature and clinical signs include cognitive dysfunction, memory loss and behavioral alterations (Scheltens et al., 2022). Its main histopathological features are the presence of extracellular Aβ plaques and intracellular neurofibrillary tangles (NFT) of hyperphosphorylated tau in the brain (Chen and Mobley, 2019). These protein aggregates lead not only to neuronal dysfunction, but also impairment of other glial cells (microglia, astrocytes and oligodendrocytes) (Jantaratnotai et al., 2003; Desai et al., 2011). The increase in neuroinflammatory processes is relate to an increase in the oxidative stress and induction of further neuronal damage and apoptosis (Hardy and Allsop, 1991; Kametani and Hasegawa, 2018; Mayne et al., 2020) (**Figure I.12**).
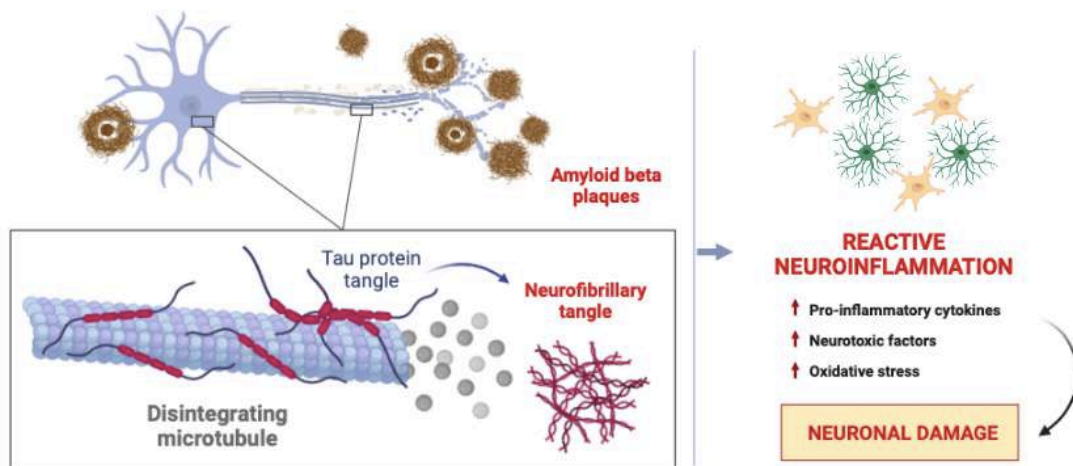
Figure I.12. **Schematic representation of Alzheimer's disease pathological events.** Created in BioRender.com.

The pathophysiological mechanism of AD remains unclear. The most accepted hypothesis is based on the impaired Aβ metabolism leading to its accumulation (amyloid-cascade hypothesis) (Soria Lopez et al., 2019). Overproduction and/or reduced clearance of Aβ promotes its self-assembly into oligomers and fibrils, inducing neurotoxicity, oxidative stress and neuroinflammation (Area-Gomez and Schon, 2017; Choi and Gandhi, 2018). Additionally, aberrations of tau protein (hyperphosphorylated) and its progressive spread through different brain areas as NFT have been well-characterized (Braak's stages) (Braak et al., 2006; Braak and Del Tredici, 2015). Although age is considered the main risk factor, some genes have been directly linked with its development, mainly Aβ

precursor protein (APP), the presenilin genes (PSEN1 and PSEN2) and the APOE4 (Chen and Mobley, 2019; Kloske and Wilcock, 2020).

Parkinson's disease. General aspects.

PD is a progressive, chronic, age-related and the second most common neurodegenerative disease (**Figure I.13**). The two principal histopathological hallmarks of this disorder are i) dopamine depletion (due to the death of dopaminergic neurons in the *Substantia Nigra pars compacta* (SNpc) and the loss of their terminals in the striatum) and ii) proteinaceous inclusions (enriched in misfolded α-synuclein) in neuronal cytoplasm, known as Lewy bodies (Cuenca et al., 2019; Poewe et al., 2017).
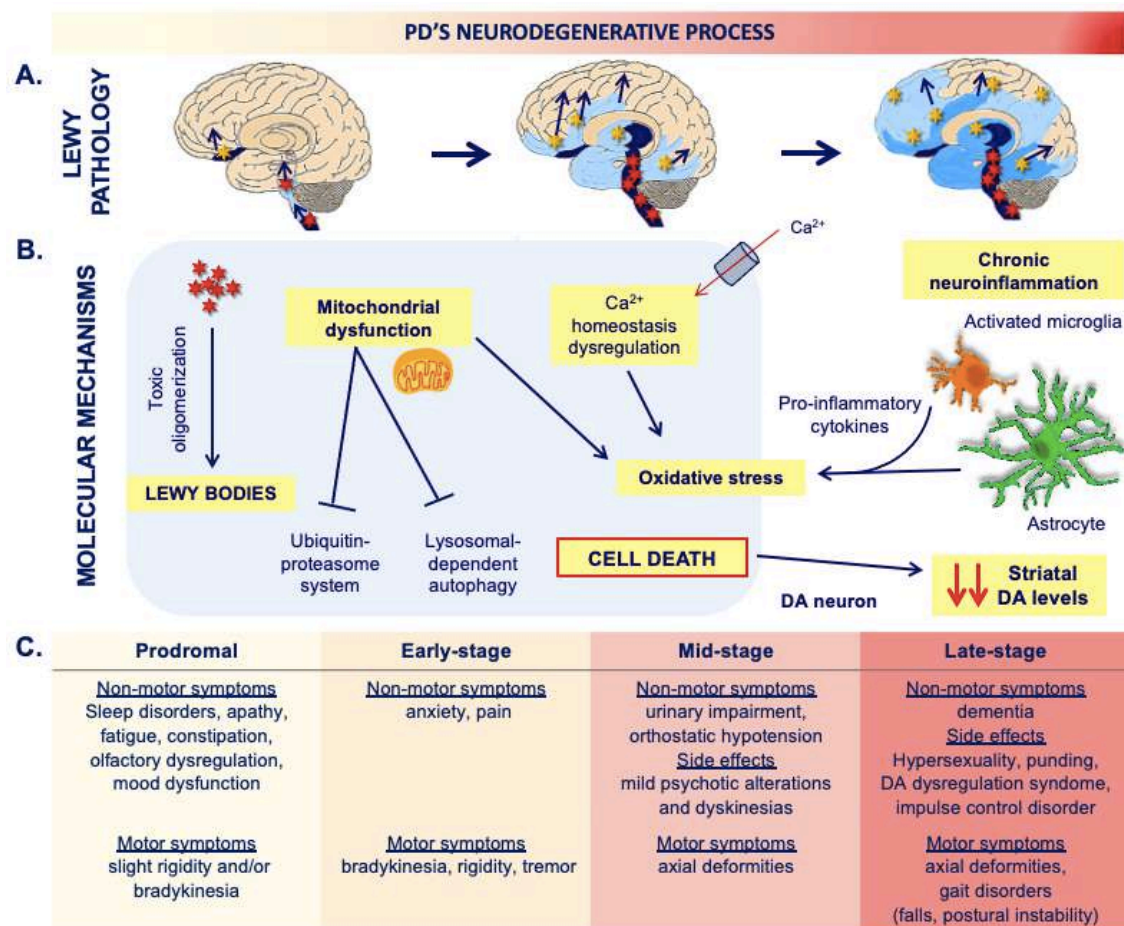
Figure I.13. Graphic summary of the components, factors and steps in PD's neurodegeneration. A. Sequential invasion of LB in the different brain areas as the disease progresses, as described by Braak et al., 2003. **B.** Scheme of the main contributing factors to DA neuronal death in the SNpc that leads to dopamine levels depletion in the striatum. **C.** PD stages and the associated non-motor and motor symptoms. (Illustration inspired by and adapted from (Halliday and McCann, 2010; Obeso et al., 2017; Poewe et al., 2017). Taken from Cuenca et al. 2019 under permission rights.

These features are accompanied by a number of contributing factors such as mitochondrial dysfunction (Surmeier, 2018; Zeng et al., 2018), oxidative stress (Jenner Peter, 2003; Kim et al., 2015), disruption of protein (Bandhyopadhyay and Cuervo, 2007; Chung et al., 2018) and neuroinflammation (Calabrese et al., 2018; Cuenca et al., 2019; Fuzzati-Armentero, Cerri, and Blandini, 2019) (**Figure I.13**).

Since Dr James Parkinson first named this disorder as "shaking palsy", PD has largely been considered to be a movement disorder affecting the CNS, but after years of research we know nowadays that several brain areas are affected in addition to SNpc and the striatum (i.e., the pedunculopontine nucleus, the locus coeruleus and the cerebellum) (Rolland et al., 2007; Heman et al., 2012; Gallea et al., 2017). For this reason, PD is considered a multisystemic syndrome, in which the nervous system is not only affected but also the autonomic system (Kalia and Lang, 2015; Braak and Del Tredici, 2017; Obeso et al., 2017; Cuenca et al., 2019).

A minor percentage of the cases are directly related to a genetic cause; however, 23 loci are currently linked to PD development, such as PARK1/4 (encoding for αsyn, SNCA), PARK8 (that encodes leucine-rich repeat kinase 2, LRRK2) and PARK21 (transmembrane protein 230 gene, TMEM230) (Cuenca et al., 2019; Deng, Wang, and Jankovic, 2018; Karimi-Moghadam, Charsouei, Bell, and Jabalameli, 2018).

I.4. The *Octodon degus* as a model for aging research

The elaboration of this part of the Introduction chapter is based on the published reference: Cuenca-Bermejo et al., 2020. Agreement documents for its use from all the co-authors and permission rights obtained from the journal can be found in the Annex II.

I.4.1. Generalities

The *Octodon degus (O. degus),* also known as degus, "brush tailed" or "trumpet-tailed" rat, belongs to the *Octodontidae* family and to the group of hystricomorphs (Ardiles et al., 2013) (**Figure I.14A**). In captivity, they live 5-8 years, and body weight varies between the values shown in **Figure I.14B** (data obtained along several years in the colony of our laboratory) (Cuenca-Bermejo et al., 2020).

O. degus are highly social and it has been described that they establish complex interindividual interactions, which are characterized by a rich vocal repertoire, tactile

communications, olfactory signals and chemical communication (Jechura and Lee, 2004; Edwards, 2009; Rivera et al., 2016; Cuenca-Bermejo et al., 2020).

Interestingly, from the cognitive ecological point of view, thanks to their manual dexterity to manipulate objects, the *O. degus* also use their tactile ability to integrate the environmental inputs into their neural circuits. This rodent develops a mental representation of tools, understand their functionality and spontaneously conceive flexible, compound and versatile ways to use them (Okanoya et al., 2008). In fact, their cognitive capacity to use tools requires the understanding of objects' physical properties and spatial relations (Kumazawa-Manita et al., 2013b; Tia et al., 2018; Cuenca-Bermejo et al., 2020).
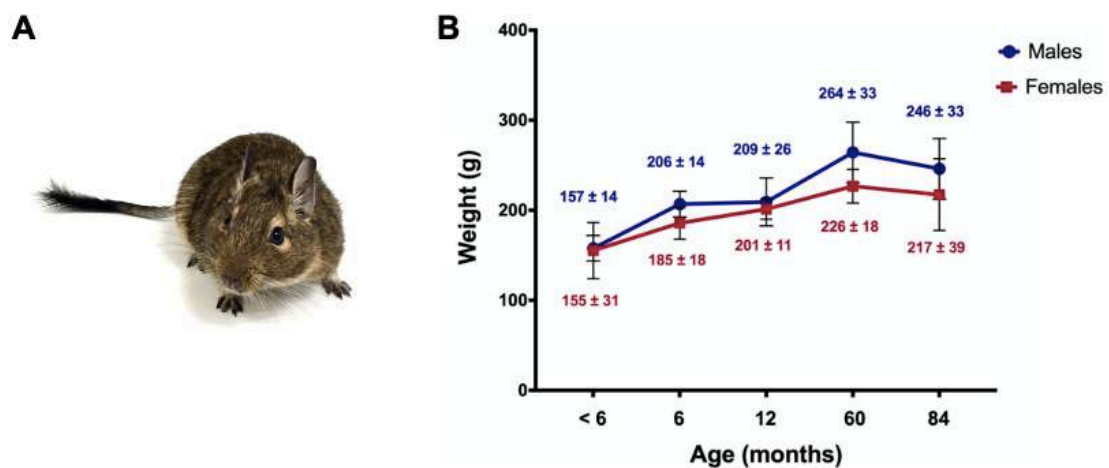
Figure I.14. Physical aspect and weights of *O. degus*. A) Picture of 1 year-old *O. degus.* **B)** Weights of *O. degus* considering age and sex (mean ± SD). Data were collected from animals belonging to the colony of our group; a minimum n of 10 animals per group was considered.

In the recent years, the *O. degus* has been claimed as a promising model for pre-clinical research in the field of biomedicine, since it has been reported to share some human-like traits, as complex social-affective behavior, diurnal circadian pattern and spontaneous development of age-related disorders (van Groen et al., 2011; Inestrosa et al., 2015; Hurley et al., 2018; Cuenca-Bermejo et al., 2020).

I.4.2. The *Octodon degus*' nervous system

An exhaustive analysis of the degus brain revealed that, compared to rats or mice, its forebrain is more compact, midbrain and fibers have a more rostral position, and superior and inferior colliculus are larger (Wright and Kern, 1992; Kumazawa-Manita et al., 2013b). Regarding the basic organization of the rhombencephalon, no differences have been found between *O. degus* and rats, although there are clear differences

regarding the length and the size of some rhombencephalic nuclei. Furthermore, there are no significant differences between males and females in brain asymmetry and size, and morphology of the dentate gyrus (Sobrero et al., 2016; Cuenca-Bermejo et al., 2020).

Evidence shows that after early life stress, the establishment and configuration of brain circuits at anatomical, neuronal, biochemical and behavioral levels are strongly affected in the *O. degus*. Briefly, stressful factors during their first weeks of life (e.g., maternal separation and social isolation from conspecifics) cause neuropsychological and neuroanatomical alterations at several levels, such as cortex, hippocampus and amygdala (Ardiles et al., 2013). Many isolation-induced alterations derive from components of the limbic systems and monoaminergic circuits, which are involved in human emotionality (Colonnello et al., 2011). Stressful events, like in humans, also influence the hormonal component, especially cortisol levels (Bauer et al., 2019), which strengths the use of *O. degus* as an experimental model for endocrinology research (Cuenca-Bermejo et al., 2020).

I.4.3. The *Octodon degus* as a model for neurodegeneration

O. degus has been classically known as a natural model of AD, since many works have validated the presence of AD-related signs in the brains of this species (Inestrosa et al., 2005). In contrast to other experimental models of the disease, *O. degus* spontaneously develops the main AD hallmarks and other age-associated changes similar to those observed in humans, which makes this diurnal rodent a key tool to investigate how sporadic AD develops. Inestrosa and collaborators were the first authors to find the existence of AD neuropathological markers in aged *O. degus* (over 3 years old): intracellular and extracellular accumulations of β-amyloid peptide (Aβ), and tau protein and ubiquitin de- posits in the frontal cortex and hippocampus (Inestrosa et al., 2005). They proposed that the high protein sequence homology of the O. degus and the human Aβ (97,5%) was the most contributing factor to the appearance of the AD-related (Inestrosa et al., 2005; Ríos et al, 2014). However, subsequent studies have shown that neuropathologic aggregation of Aβ depends on its quaternary structure and the influence of both biophysical and physiological factors, highlighting the importance of the ageing process (Lei et al., 2015). After the discovery of Inestrosa and colleagues, many authors have corroborated these results and enriched them with other findings (reported in the following paragraphs and collected in **Table I.2**), supporting *O. degus* as an adequate model for AD research (van Groen et al., 2011; Ardiles et al., 2012; Deacon et al., 2015; Inestrosa et al., 2015; Cisternas et al., 2018; Tan et al., 2022). In addition, genetic studies

performed on *O. degus*, complete the immunohistological detection of AD pathological hallmarks and promote its use in ageing research. In this sense, Altimiras and collaborators made an important contribution by elaborating the brain transcriptome of the *O. degus* (NCBI accession number: PRJNA326273) (Altimiras et al., 2017). In their work, they identified several genes with altered expression that have already been described in human AD and other age-related disorders (**Table I.2**) (Cuenca-Bermejo et al., 2020).

Table I.2. **Age-related and pathological changes observed in the *O. degus*' central nervous system**. [a] FRMD7, encodes a protein of unknown function; [b] ADAMTS9, Disintegrin and metalloproteinase with thrombospondin motifs 9; [c] CHRNA6, Neuronal acetylcholine receptor subunit α-6; [d] DEG AMD1, encodes an intermediate enzyme relevant to the polyamine biosynthesis; [e] WISP1, WNT1 inducible signaling pathway protein 1; [f] FGF9, fibroblast growth factor 9; [g] APOC-1, apolipoprotein C-I; [h] CPNE7, Copine VII; [i] COX8A, Cytochrome c oxidase subunit 8A. Taken from Cuenca-Bermejo et al., 2020.

Age-related changes	Reference
AD histopathological markers	
- Aβ oligomers and deposits	Inestrosa et al., 2005, 2015
	van Groen et al., 2011
	Tan et al., 2022
- Neurofibrillary tangles	Inestrosa et al., 2005
	van Groen et al., 2011
	Tan et al., 2022
- Altered cholinergic system	Inestrosa et al., 2005
- Degenerating axons	van Groen et al., 2011
- α-Synuclein and poly-ubiquitylated proteins	Bourdenx et al., 2017
Neuroinflammation	van Groen et al., 2011
	Inestrosa et al., 2005, 2015
Genetic dysregulations (in AD-like O. degus)	Altimiras et al., 2017
- Vision related genes (FRMD7[a], ADAMTS9[b])	
- AD related genes (CHRNA6[c], DEG AMD1[d], WISP1[e], FGF9[f], APOC-1[g], CPNE7[h])	
- Mitochondrial genes (COX8A[i]).	
- Diabetes-related genes (ADAMTS9[b])	
Biometals imbalance	Braidy et al., 2017
Cognitive decline	Ardiles et al., 2012
	Tarragon et al., 2013
	Estrada et al., 2015a, 2019
	Tan et al., 2022

Additionally, an increase in glial activation markers in different brain areas of aged *O. degus*, specifically for microglial cells (Iba1, CD11b) and astrocytes (vimentine, GFAP and S100β) (van Groen et al., 2011; Inestrosa et al., 2015). Moreover, it has also been demonstrated an increase in oxidative stress indicators (such as phosphorylated AMPK), interleukin-6 and neuronal apoptotic markers (by Hoechst and active caspase 3 immunofluorescence analysis) (Inestrosa et al., 2015). Together with this, other age-associated alterations found in the brain of aged *O. degus* is altered biometals imbalance, with an increase in Fe, Ca, Zn and Cu levels in cortex and hippocampus (Braidy et al., 2017). Moreover, impairment of metal homeostasis and altered lysosomal function

positively correlate with ageing, Aβ deposits and neuroinflammatory processes (Braidy et al., 2017; Cuenca-Bermejo et al., 2020).

Altogether, these brain alterations can give rise to cognitive decline. Different cognitive tests performed on *O. degus* have shown a significant cognitive impairment in old animals compared to young ones (Ardiles et al., 2012; Estrada et al., 2015b; Estrada et al., 2019; Tan et al., 2022). A positive correlation between cognitive decline and the progress of AD-like state has also been described (i.e., Aβ oligomers and hyperphosphorylated-tau protein) (Ardiles et al., 2013). In fact, some authors have already validated the *O. degus* as a proper model for transient cognitive decline induced by sleep deprivation (Tarragon et al., 2013) and tested some therapies with positive results, as memantine (Tarragon et al., 2014), transcranial magnetic stimulation (Estrada et al., 2015a, 2015b) or physical exercise (Estrada et al., 2019). Interestingly, creation of new neuronal circuits and synaptogenesis are observed in the dentate gyrus of adult *O. degus* after cognitive training (Kumazawa-Manita et al., 2013a; Cuenca-Bermejo et al., 2020).

A recent study using whole-genome sequencing techniques has identified single nucleotide polymorphisms for aging-related genes in the degu genome as potential candidates for the AD-like pathology in the *O. degus*: DNA repair, glucose metabolism, protein misfolding and lipid homeostasis (Hurley et al., 2022).

The *Octodon degus'* visual system

Degus' retina is similar to that in humans, regarding layers organization and cell types (Szabadfi et al., 2015) (**Figure I. 15A**). As in humans, in *O. degus'* retina there is a remarkably high cone density: 30% of its 9 million retinal photoreceptors are cones, which peaks near the optic nerve and decreases in the periphery (Verra et al., 2019). *O. degus* can make color discriminations between ultraviolet and visible lights, thanks to the presence of only two types of cones: M cones (507 nm) and UV-sensitive S cones (362 nm) in a 13:1 ratio. Interestingly, thanks to the presence of S cones *O. degus* lens selectively absorb short wavelength light and shows a progressive increase in optical density as a function of age (Jacobs et al., 2003; Cuenca-Bermejo et al., 2020).

Cataracts are one of the most frequent lesions seen in aged degus and are associated with the spontaneous occurrence of diabetes mellitus in this rodent (Jekl et al., 2011). In addition, the retina of this rodent is also subjected to age-related structural alterations. The retina of adult degus (average 48 months old) shows outer plexiform layer (OPL) thinning, nerve fiber layer (NFL) thinning and atrophy, apoptotic cells in the outer nuclear layer (ONL), retinal ganglion cells (RGCs) loss, altered vascular parameters and

sign of inflammation. While 6- and 12-months-old degus do not present alteration in arborization, pattern and number of cone and rod bipolar cells (**Figure I. 15B-I**), the retina of 36-months-old degus reveals empty cell spaces amidst bipolar cells (**Figure I.15J-M**) due to the loss of rods and their connecting neurons (Szabadfi et al., 2015). In addition, old degus retina reveals alterations of the retinal pigment epithelial layer, higher GFAP expression in the Müller glial cells, degeneration of the vertical pathway linked to rod receptors, with retracted dendrites of rod bipolar cells and fragmented ribbon synapses in the OPL, hence an overall compromised structure and functionality.
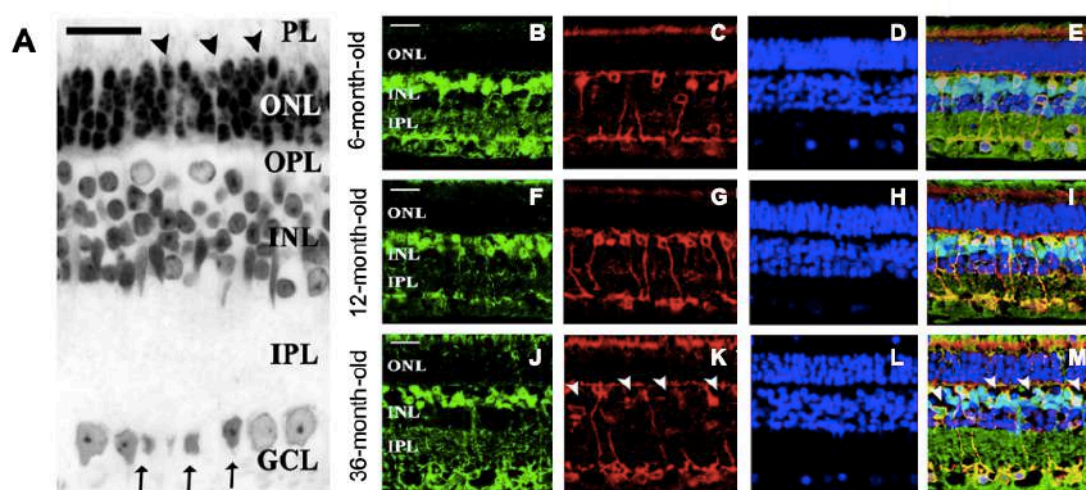
Figure I.15. Representative microphotographs of the O. degus' retina. **A)** Toluidine blue staining of the degus' retina, where the characteristic layers of the mammalian retina and cellular types appear very well visible (scale bar =20 μm). **B-M)** Retinal sections stained with bipolar cell markers. In green **(B,F,J)** and light blue **(E, I, M)** are labelled the somas and terminals of all bipolar cells, using Pan-bipolar cell marker (Chx10). In red **(C, G, K)** and yellow/white **(E, I, M)** are labelled the somas, dendrites and axon terminals of rod bipolar cells, using protein kinase Ca (PKCa). DAPI labels in dark blue the nuclei of all retinal cells **(D, H, L)**. The staining shape was similar in all groups, except for the presence of empty cell body shapes (arrowheads) among the bipolar cells in the 36-month-old degus retina **(J–M)** (scale bar =20 μm). Abbreviations: GCL = ganglion cell layer; INL = inner nuclear layer; IPL = inner plexiform layer; ONL = outer nuclear layer; OPL = outer plexiform layer; PL = photoreceptor layer (Images courtesy of Szabadfi et al., 2015 and Cuenca-Bermejo et al. 2020).

Interestingly, AD-related alterations, such as the deposition of β-amyloid oligomers and phosphorylated tau (pTau) has been described in the retina of this rodent as a function of age (Du et al., 2015; Hurley et al., 2018). Elevated levels of Aβ peptide species, particularly Aβ42, have been observed in the retinas of aged O. degus (>36 months old), as well as in its lens, vitreous humor, and choroid. Aβ deposits can appear in the NFL, ganglion cell layer (GCL), inner and outer segments of photoreceptors in young degus, but during ageing they expand throughout all retinal layers (Du et al., 2015; Hart et al., 2016). The NFL and GCL are also characterized by an aged-related increasing in pTau expression (Du et al., 2015; Hart et al., 2016). The recent study conducted by Chang and

collaborators demonstrated that the appearance of these AD-like markers triggers a chain of age-dependent events in the degus' retina that promotes synaptic remodeling, starting from young age (12 months old) (Chang et al., 2020). These changes include microglial activation and morphological changes, neurotransmitters alterations (e.g., decrease in cholinergic amacrinal cells and glutamate pattern), reduction of GCL density and imbalance of synaptic proteins (Chang et al., 2020).

I.4.3. Development of other age-related disorders

Together with the brain pathology, aged degus show other systemic changes, which have been reported in the elderly humans such as variations in the hematological parameters (Jekl et al., 2011), oral cavity alterations (van Groen et al., 2011), spontaneous tumors (Švara et al., 2020), type II diabetes (Opazo et al., 2004; Edwards, 2009), disruption of lipid metabolism, atherosclerosis (Homan et al., 2010), heart failure (Sanchez et al., 2019) and renal problems (Hagen et al., 2014) (**Figure I.16**).
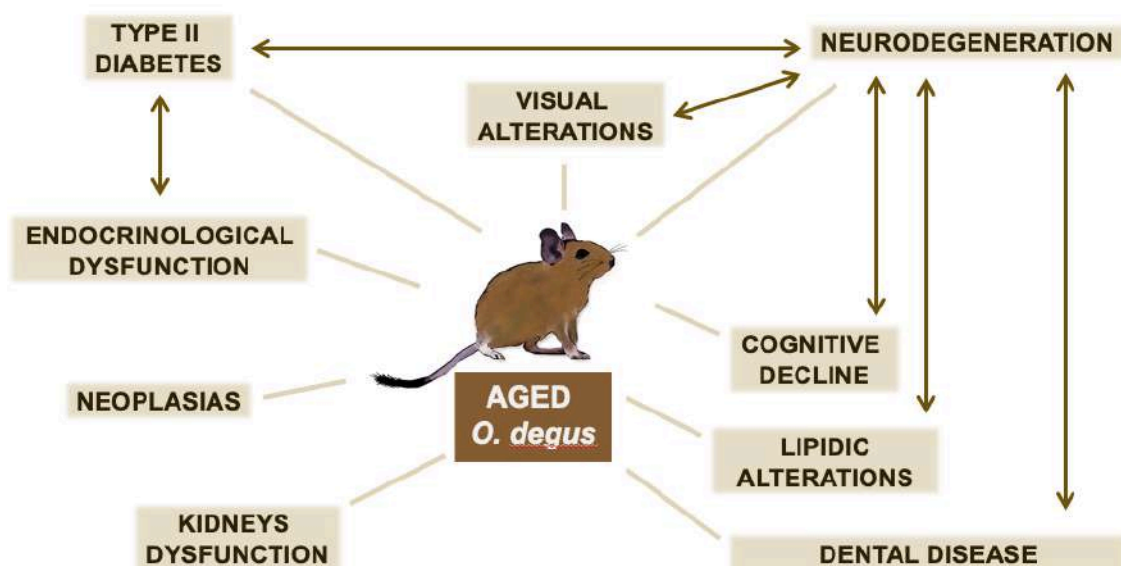
Figure I.16. **Age-related disorders in the *O. degus* and their relationship** (from Cuenca-Bermejo et al., 2020).

CHAPTER II

HYPOTHESIS AND OBJECTIVES

HYPOTHESIS

Different research groups have provided evidence to consider the *O. degus* as a unique tool to study age-related diseases, since the natural and simultaneous presence of different pathological hallmarks have been described in this model (Cuenca-Bermejo et al., 2020). However, even if the first studies in this diurnal rodent appeared more than 50 years ago, information regarding the aging process in the *O. degus* appreciating the sex-associated differences is scarce. Therefore, further research to complete its characterization would provide useful information for further research with potential translational perspective.

The conducting hypothesis of this thesis is that the *O. degus* is a natural experimental model of aging with sex-specific differences, thus representing a tool to explore the interactions among systemic alterations (multimorbidity) and cognitive decline.

OBJECTIVES
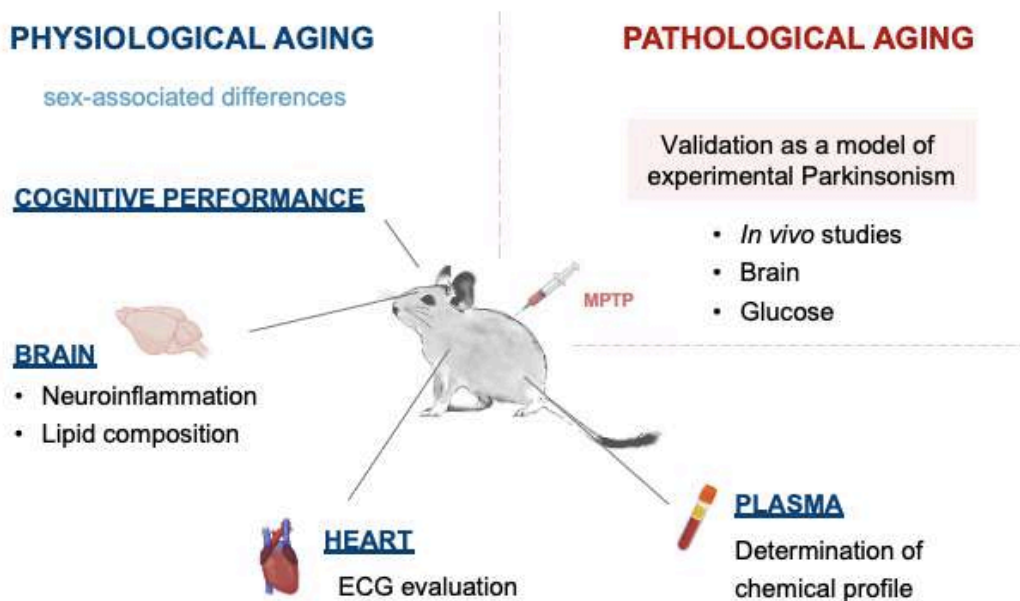
Figure II.1. Graphical summary of the objectives of this thesis. The aim of this research project was to characterize the *O. degus* as an experimental model for aging research (physiological and pathological), including the sex perspective. For this, both *in vivo* and *post mortem* analyses were carried out to determine systemic and brain change, as well as their interaction along aging.

II. 2. GENERAL OBJECTIVES

The general objectives proposed for this research project are (**Figure II.1**):

1. Evaluate the effect of age and sex in the plasmatic biochemical profile of the *O. degus*.
2. Establish the *in vivo* cardiac state of the *O. degus* in males and females along aging.
3. Analyze the age-associated cognitive decline and hippocampal changes with a sex perspective in the *O. degus*.
4. Determine the brain lipid composition in the *O. degus* and its changes along aging with a sex perspective.
5. Validate the *O. degus* as a model of experimental Parkinsonism.

II. 3. SPECIFIC OBJECTIVES

1. **Evaluate the effect of age and sex in the plasmatic biochemical profile of the *O. degus*.**
   1.1. Characterize the reference values of general metabolism parameters (e.g., total protein, glucose, cholesterol, among others) for males and females along aging.
   1.2. Study the effect of age and sex on the hepatic, kidney and pancreatic functions.
   1.3. Evaluate the plasmatic oxidation and inflammatory states along aging with a sex perspective.

2. **Establish the *in vivo* cardiac state of the *O. degus* in males and females along aging.**
   2.1. Establish the electrocardiogram's parameters for the species *O. degus* of different ages and sex.
   2.2. Study the influence of age and sex in the possible cardiac alterations.

3. **Analyze the age-associated cognitive decline and hippocampal changes with a sex perspective in the *O. degus*.**
   3.1. Cognitive evaluation of the animals along aging with a sex perspective.
   3.2. Study of neuroinflammatory processes in the hippocampus.
   3.3. Explore the relationship among neuroinflammation in different hippocampal subareas and cognitive performance.

4. **Evaluate the brain lipid composition in the *O. degus* and its changes along aging with a sex perspective.**

   4.1. Analyze of lipid composition in different brain areas (prefrontal cortex, striatum, cortex and cerebellum) and the age- and sex-associated changes.

   4.2. Study the lipid peroxidation in the prefrontal cortex along aging in males and females.

   4.3. Explore the relationship among lipid peroxidation in the prefrontal cortex and cognitive performance.

5. **Validate the *O. degus* as a model for experimental Parkinsonism.**

   5.1. Determine the O. degus sensitivity to the neurotoxin MPTP.

   5.2. Analyze the effect of MPTP subchronic administration on motor state and cognition.

   5.3. Study the effect of MPTP subchronic intoxication on the dopaminergic system: neuronal death, terminals loss and neuroinflammation.

   5.4. Analyze neuroinflammatory processes in the hippocampus after MPTP administration.

   5.5. Study the effect of MPTP subchronic intoxication on the *locus coeruleus*: neuronal death and neuroinflammation.

CHAPTER III

MATERIALS AND METHODS

III.1. MATERIALS

Commercial chemicals and reagents used were of the highest purity available, and they were purchased from Sigma-Aldrich. Water was doubly distilled in a glass device.

III.2. ANIMALS

The studies of this thesis were performed in a total of 110 *O. degus*, including males and females. Animals belonged to the colony of our research group, and they were bred and maintained under identical conditions in the animal house of the University of Alicante and the Institute for Biomedical Research of Murcia-University of Murcia (CEIB-IMIB-UMU). Maintenance conditions (detailed in the next paragraph) were optimal and under the supervision of expert personnel. Animals' ages ranged from 6 months old to 6-7 years old and they were divided into different experimental groups depending on the different studies of this thesis (**Table III.1**).

Degus were individually identified by microchips and housed in groups of 2 to 4 animals per cage in a room with controlled environmental conditions: 12:12h light:dark cycles, 22 ± 1 ºC and 60% humidity. The cages, which were cleaned once per week, were made of Plexiglas, the floor covered with wood shavings and with environmental enrichment placed on them. Animals had water and food *ad libitum* during all the experiment (Harlan Teklad Global Diet®, Harlan Laboratories, USA). The health status of animals was continuously examined by the expert veterinarian. Animals included in the studies showed normal physical examination.

Ethics statement

All experimental procedures involving animals were done strictly following the regulations standards indicated in experimental guidelines and procedures complied with the European Community Council Directive (2010/63/UE), the Spanish law (RD 53/2013) and the Ethics Committee of the University of Murcia (project number: A13170102 / CEEA-OH AMP/MOD 103/2014 + 2018). Additionally, the "3 R's principle" was applied throughout the study and important efforts were done to minimize the procedure's impact on animals. Additionally, All the animals used in these studies underwent handling by the experimenters (at least 5 minutes per day) to accustom them to manipulation and reduce the stressful condition.

Table III. 1. **Number of animals (n) included in each experimental group and their weights (g).** A total of 110 O. degus were used in this thesis. Animals were divided according to sex (males and females), age (juvenile, young, old and senile) or treatment (control, MPTP). In those studies, in which no significant differences were found between the juvenile and the young animals, they were grouped under the name of "young". Data are expressed as mean ± standard deviation.

Determination of plasmatic biochemical profile (n= 86)

	Young (6-12 months old)	Old (4-5 years old)	Senile (6-7 years old)
Males	n = 16	n = 16	n = 12
Weight (g)	211.0 ± 20.2	262.0 ± 31.6	247.0 ± 33.3
Females	n = 25	n = 8	n = 9
Weight (g)	187.0 ± 18.0	231.0 ± 16.9	225.0 ± 20.3

Determination of electrocardiographic parameters (n=98)

	Juvenile (6 months old)	Young (1 year old)	Old (4-5 years old)	Senile (6-7 years old)
Males	n = 13	n = 7	n = 20	n = 12
Weight (g)	194.6 ± 14.4	220.7 ± 18.5	264.3 ± 33.5	246.7 ± 33.3
Females	n = 4	n = 7	n = 16	n = 19
Weight (g)	202.5 ± 15.5	205.0 ± 11.4	226.8 ± 18.8	221.5 ± 33.9

Cognitive performance (n=98)

	Juvenile (6 months old)	Young (1 year old)	Old (4-5 years old)	Senile (6-7 years old)
Males	n = 13	n = 7	n = 20	n = 12
Weight (g)	194.6 ± 14.4	220.7 ± 18.5	264.3 ± 33.5	246.7 ± 33.3
Females	n = 4	n = 7	n = 16	n = 19
Weight (g)	202.5 ± 15.5	205.0 ± 11.4	226.8 ± 18.8	221.5 ± 33.9

Neuroinflammation in the hippocampus (n=45)

	Juvenile (6 months old)	Young (1 year old)	Old (4-5 years old)	Senile (6-7 years old)
Males	n = 6	n = 6	n = 6	n = 6
Weight (g)	209.0 ± 22.7	220.5 ± 16.8	259.0 ± 32.6	252.5 ± 31.7
Females	n = 6	n = 6	n = 6	n =3
Weight (g)	201.8 ± 34.5	181.9 ± 16.4	231.6 ± 16.9	215.6 ± 21.7

Lipids' analysis (n=41)

	Young (6-12 months old)	Old (4-5 years old)	Senile (6-7 years old)
Males	n = 10	n = 6	n = 3
Weight (g)	212.7 ± 22.7	269.4 ± 37.5	268.3 ± 2.9
Females	n = 11	n = 6	n = 5
Weight (g)	198.8 ± 16.6	220.8 ± 21.1	210.8 ± 62.1

The *O. degus* as an experimental model of Parkinsonism (n=10)

	CONTROL (1 year old)	MPTP (1 year old)
Males	n = 5	n = 5
Weight (g)	230. ± 32.2	240.0 ± 33.3

III.3. *IN VIVO* PROCEDURES

IN VIVO GLUCOSE MEASUREMENT

Glucose levels in the blood were determined *in vivo* with a glucometer (Accu-Chek Compact Plus, Roche, Switzerland) one week before the MPTP injections started and just before the animals were euthanized. For this procedure, *O. degus* were anesthetized with isoflurane and blood was taken from the femoral vein by puncture.

BLOOD SAMPLING AND PLASMATIC BIOCHEMICAL ANALYSIS

To minimize stress during the procedure, the animals were previously accustomed to handling and to the blood sampling procedure. *O. degus* were short-term anesthetized with isoflurane and they were placed in supine position on a thermal platform (34-36ºC). Hair from the posterior limbs was removed with a veterinary razor and blood was extracted from the femoral vein by puncture and collected in lithium heparin tubes (Microvette® CB 300 LH, Sarstedt, Germany). Variations associated to the time of the day were reduced by collecting blood samples at approximately the same time (10:00 am to 2:00 pm). Samples were placed in ice and subsequently centrifuged to obtain the plasma (10 minutes at 3500xg, 4ºC), which was transferred to a new plastic tube and stored at -80ºC until further processing.

The chemistry profile in the plasma was carried out by the Interdisciplinary Laboratory of Clinical Analysis of the University of Murcia (Interlab-UMU) on an automated chemistry analyzer (Olympus Diagnostica GmbH AU 600, Beckman Coulter, Ennis, Ireland). The analytes included in the chemistry profile were:

- Biomarkers of general metabolism and liver, muscle, and kidney: amylase, triglycerides, cholesterol, glucose, total proteins, albumin, phosphorus, total calcium, iron, ferritin and unsaturated iron-binding capacity (UIBC), total bilirubin, alkaline phosphatase (ALP), gamma-glutamyl transferase (gGT), aspartate aminotransferase (AST), alanine aminotransferase (ALT), creatine kinase (CK), creatinine and urea. All these analytes were measured using commercial kits (Beckman coulter) (Contreras-Aguilar et al., 2021).

- Biomarkers of redox-status: cupric reducing antioxidant capacity (CUPRAC), ferric reducing ability of the plasma (FRAP), trolox equivalent antioxidant capacity (TEAC), total thiol concentrations (THIOL), and total oxidant status (TOS), that were measured according previously described assays (Rubio et al., 2016, 2017).

- Inflammatory biomarkers: serum A-amyloid (SAA), butyrylcholinesterase (BChE) and paraoxonase-1 (PON1), measured using previously described assays (González-Barrio et al., 2021).

All the methods for the analyte measurements were previously validated in our lab in plasma of *O. degus* showing inter and intraassay imprecisions lower than 15% and linearity after serial sample dilutions.

ELECTROCARDIOGRAM EVALUATION

Electrocardiogram recordings

The ECG recordings were carried out in the facilities of the Veterinary Teaching Hospital of the University of Murcia using a commercially available 6-channel ECG machine (Siemens Megacart R, Electromedical Systems Division ECS, Sweden).

Animals were placed in an isolated room where the ECG recording would be performed at least 8 hours before the test started and they were kept undisturbed in order to reduce stress and promote acclimatization. All the ECGs were always performed at fixed times (between 4:00 pm - 8:00 pm) to reduce the influence of circadian variables during the analysis. Animals were anesthetized with an intramuscular combination of 20.0 mg/Kg of ketamine (Anesketin®l, Dechra Veterinary Products SLU, Barcelona) and 0.20 mg/Kg of medetomidine (Domtor®, Ecuphar®, Barcelona).
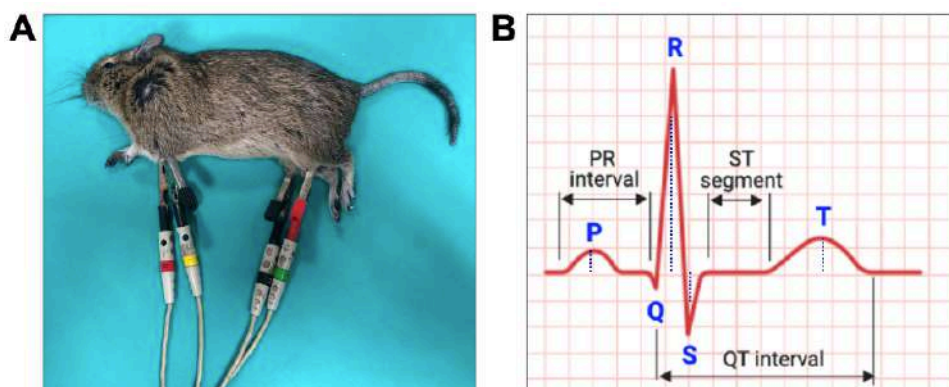
Figure III. 1. *In vivo* **electrocardiogram recording. A)** Photograph of an *O. degus* while the electrocardiography was performed; **B)** Schematic representation of the waves and intervals measured in the lead II of the electrocardiogram. Dotted blue lines indicate the voltages evaluated, while duration of the different intervals and waves measured are represented by horizontal delimitated arrows. Created in BioRender.com.

All *O. degus* were placed in right lateral recumbency, with the limbs held as nearly perpendicular to the body as possible. Surface electrodes made of flattened alligator clips were attached to the skin midway on the caudal area of the elbows and over the patellae on the rear limbs (**Figure III.1A**). Surgical alcohol was applied to maintain proper electrical contact. Standard bipolar and augmented unipolar 6-lead ECGs (leads I, II, III, aVR, aVL, and aVF) were recorded for all animals. According to heart rate (HR) and amplitude of the waves, the ECG recordings were calibrated at 50–100 mm/s and 10–20 mm/mV. For each animal, an effort was made to obtain an ECG tracing showing a proper isoelectric baseline with easily recognizable waveforms.

Electrocardiogram trace analysis

ECG were digitalized immediately after their acquisition The procedure of the ECG interpretation and nomenclature was done following standard methods (Talavera et al., 2008). A board-certified veterinary cardiologist performed a general analysis to ensure the quality of the ECG recording and evaluate cardiac rhythm. Then, two independent observers carried out the manual ECG analysis. Each observer evaluated three representative consecutive beats to measure various ECG variables for each animal, that is, 6 beats per animal were analyzed (588 cardiac beats in total). Then, data obtained for each variable was averaged to have a representative value for each animal. The variables analyzed included:

- Cardiac rhythm: was classified as normal sinus rhythm, sinus arrhythmia, and pathological arrhythmias.
- Heart rate (HR), in beats per minute (bpm), was calculated by determining the number of QRS complexes in a 3-s interval and multiplying this number by 20 (50 mm/s) or by 40 (100 mm/s).
- Using the bipolar lead II, the following variables were measured (**Figure III.1B**):
    - Amplitude and duration of the P wave
    - PR interval duration
    - Duration of the QRS complex
    - Amplitude of the R and S waves
    - QT interval duration
    - Amplitude of the T wave

Mean electrical axis (MEA) in the frontal plane was calculated by the vector method using the leads I and III and they were then classified as normal (from -30º to 100º), right axis deviation (RAD, from 100º to 180º), extreme right axis deviation (EAD, from -90º to -180º) and left axis deviation (LAD, from -30º to -90º) (Kashou et al., 2020).

BEHAVIORAL TESTS

Experimental rooms with the same noise and temperature conditions as those in which *O. degus* lived were used to perform all the behavioral tests, and animals were allowed to adapt to the experimental room for, at least, 2h before the experiments began. Since the *O. degus* is a diurnal rodent, all the behavioral tests were performed during the light period (from 8:00 am – 8:00 pm).

Barnes Maze test

The Barnes Maze (BM) is a circular platform of 160 cm diameter raised 75 cm from the ground and surrounded by a 55 cm high wall (Estrada et al., 2015b). The platform was made of white Plexiglas and contained eighteen circular holes (8 cm in diameter), equidistant (16 cm) from each other and 5.5 cm from the outer edge. The escape hole was the only one opened to a transparent plastic escape box, positioned under it, while the other holes were blocked with mesh. An open metallic box (20x9x15 cm) was used as start box. Different visual cues (a triangle, a square, a circle, a cross) were placed in the surrounding wall and remained unchanged during the experiments, so they served as visuospatial references (**Figure III.2A**). The room where the test was performed was illuminated by fluorescent lights located in the ceiling (normal room lighting) so that the maze was exposed to an illumination of 210 lux. The procedure was performed in the same way as previous published works, and it was divided into 3 phases: habituation, acquisition, and retrieval phases (Tarragon et al., 2014; Estrada et al., 2015b, 2019).

A   BARNES MAZE TEST   B   OPEN FIELD

Escape hole
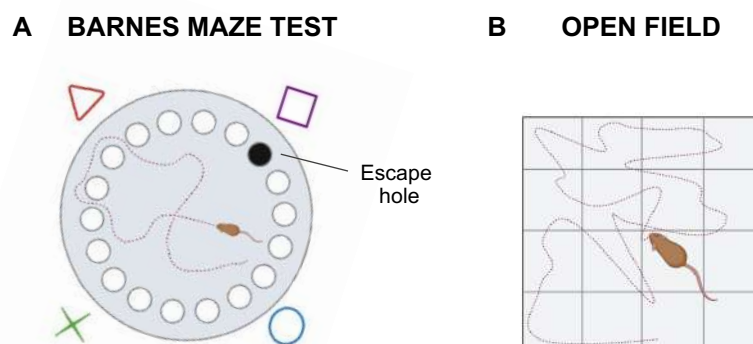
Figure III.2. **Schematic representation of the behavioral tests performed in this thesis. A)** The Barnes Maze test consists in a round platform from which the animal must scape through the escape hole, helped by the visual cues placed in the wall of the platform. **B)** The open field allows the monitorization of the animals' spontaneous locomotor activity. Created in BioRender.com.

Habituation Session. This phase lasts one day (day 1) and it consists in placing the animal in the escape cage (filled with bedding from its own home cage) for 2 minutes, after which it was placed on the platform near the escape hole and allowed 1 minute to explore the maze and escape. If the animal did not escape the maze, it was gently picked up and put through the target hole into the escape box. Again, the animal was left in the escape box for 2 minutes. Finally, the animal was put in the center of the platform, allowed 4 minutes to enter the escape box. If the *O. degus* did not enter in the escape box, it was put into the escape cage as explained above and left there for 2 minutes. All the activities described were separated by 5 minutes resting period time, in which the animals were returned to its home cage. During this period, the maze and the start point were cleaned with 70% ethanol to remove odors (Estrada et al., 2015b).

Table III. 2. **List of parameters evaluated in the Barnes Maze test.** Adapted from **(Gawel et al., 2019).**

NAME OF THE PARAMETER		DESCRIPTION
Escapes / correct answers		Number of times that the animal solves the maze during the trial (in total 4 per day)
Latencies (seconds)	Time to escape	Time needed to escape the maze with the whole body
	Time to find the first hole	Time needed to make a head deflection into the escape hole
	Time to find the escape hole	Time needed to make a head deflection into the escape hole
	Decision time	Time spent exploring the escape hole
Escape hole as first visited hole		The animal visits the escape hole before any other
Errors	Omission	Number of visits to the escape hole without escaping the maze
	Reference memory	The animal makes a head deflection and a nose into a non-escape hole
	Working memory	The animal makes a head deflection and a nose into a non-escape hole already visited during the same trial

Acquisition phase. One day after the habituation session, the *O. degus* were trained for seven consecutive days (training days, days 2-8), undergoing four trials of 4 minutes each per training session. Between trials, animals were left in their home cage for 5 minutes and the surfaces of the platform, start box, and escape box were thoroughly cleaned with 70% ethanol. At the beginning of each trial, each animal was kept in the start box for 30 seconds in the center of the platform before being allowed to explore the maze freely for the 4 minutes that the trial lasted. If the animal did not escape the maze, it was gently picked up and placed in the escape box, leaving it for 2 minutes before being

returned to its home cage for the 5 minutes rest. The escape hole was maintained in the same position throughout all trials and sessions. The different parameters evaluated in each session are shown in **Table III.2** (Estrada et al., 2015a).

Retention Session (retrieval phase). The day after the learning period (day 9), the *O. degus* were examined for task retention. The experimental procedure was identical to the one of the acquisition phase.

Open field test

The open field test, also known as actimetry, is one of the most common tests to asses motor conditions and the ability to move and explore the arena (Hutter-Saunders et al., 2012). The chamber consisted of a transparent open Plexiglas arena (44.5 cm wide x 44.5 cm long x 40 cm high) located inside a system of two sets of 16 infrared photocells (SAI Electronics & Engineering division, University of Murcia, Spain) (**Figure III.2B**). Horizontal locomotor activity and vertical movements were measured by the registration of the beam breaks, that were recorded and transmitted to a computerized system (Melo-Thomas et al., 2018). Every animal was placed in the center of the arena and its activity was recorded during 180 s. The chamber was cleaned with 70% ethanol after each trial (Cuenca-Bermejo et al., 2021b).

INDUCTION OF EXPERIMENTAL PARKINSONISM

O. degus from the MPTP group received two MPTP injections per week (10 mg/kg/injection, intraperitoneally, Sigma-Aldrich-Merck, US). This procedure was repeated for five weeks, until the animals reached a cumulative dose of 100 mg/kg. Injections were performed with 3-4 days interval, except for the last injection: we left 8 days from the 9th to the 10th injection in order to make compatible the performance of the Barnes Maze test with the day that the animals were euthanized (**Figure III.3**). This procedure was adopted because it has been previously described that, in other experimental models, the highest point of neuroinflammation appears 48 hours after the last MPTP injection (Huang et al., 2017).

Animals were anesthetized intramuscularly with a cocktail of ketamine (75 mg/Kg, Anesketin® 100 mg/ml, Dechra Veterinary Products SLU, Barcelona) and medetomidine (0.5 mg/Kg, Domtor®1 mg/ml, Ecuphar®, Barcelona). The responsible investigator followed the safety protocols described by Jackson-Lewis and Przendborski (Jackson-Lewis and Przedborski, 2007). In order to ensure that all animals received 10mg/kg in

every injection, doses were recalculated before each MPTP injection by weighting *O. degus*. The measurement of the weight before each injection allowed us to evaluate how the previous one had affected the weight of each animal. After MPTP intoxication, animals were placed inside cages with a negative pressure system (IVC transport rack, Techniplast, Italy) and 48 hours later (security period) they were returned to their original cages. Additional animal care was considered during the security period: heat lamps, hydration gel (gel diet water Safe®) and food placed in the floor of the cage to make it more accessible. Knowing that MPTP neurotoxicity is not exacerbated by the use of anesthetics, control animals were not anesthetized in order to avoid additional invasive procedures (Cuenca-Bermejo et al., 2021b).
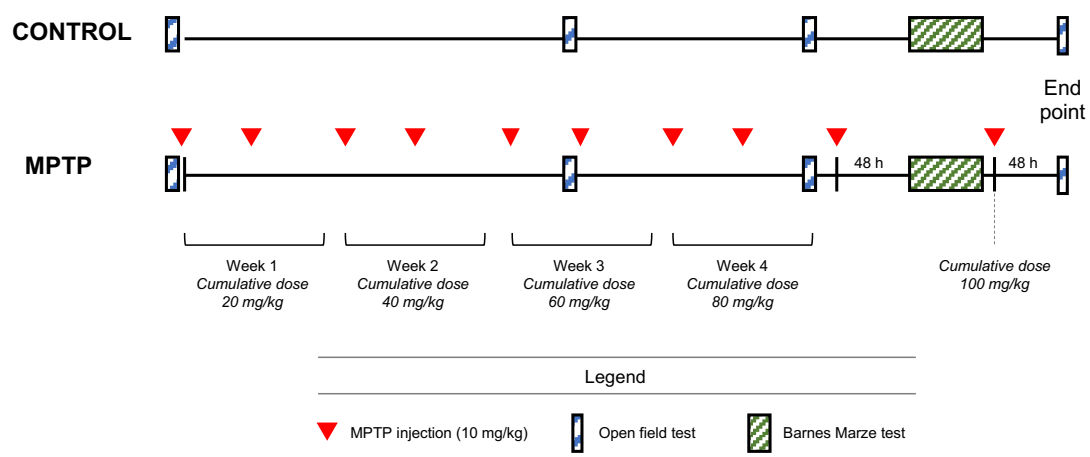
Figure III.3. MPTP administration regimen and behavioral tests. Animals received 5 MPTP injections (10 mg/kg). When cumulative dose was 90 mg/kg, the Barnes Maze test was performed. Animals were euthanized 48 hours after the 10th MPTP injection (cumulative dose of 100 mg/kg). The open field test was performed before the MPTP administrations started, at cumulative dose of 50 mg/kg, 80 mg/kg and 100 mg/kg. Control animals were subjected to the same behavioral tests as MPTP group.

III.4. END POINT AND *POST MORTEM* SAMPLES' COLLECTION

The end point method consisted in the introduction of the animals (individually) in a CO_2 flux chamber. For the aging studies, animals were euthanized at the time corresponding to their age group. For the MPTP studies, animals were euthanized 48h after the last MPTP injection. Then, organs were immediately collected and weighted. This thesis is part of a project which considers the analysis of different organs and tissues, and the samples' collection protocols were performed as follows:

- Tissues and organs dedicated to histological studies were fixed in 4% paraformaldehyde in 0.1M phosphate buffer saline (4% PFA in PBS, pH=7.4) for 48 hours, at room temperature. After, they were washed in distilled water (10 min,

3 times) and immersed in absolute ethanol until they were embedded in paraffin blocks (Cuenca-Bermejo et al., 2021b).

Paraffin embedding was performed by the Experimental Pathology Service of the Institute for Biomedical Research of Murcia (IMIB-Hospital Universitario Virgen de la Arrixaca). After the fixation period, the samples were processed using a conventional histological device (Excelsior, Thermo Scientific, Madrid, Spain), following the next steps: 50% ethanol (1 hour) > 70% ethanol (1 hour) > 96% ethanol (2 hours) > 100 ethanol (1 hour x 3 times) > xylene substitute (1 hour x 3 times) > paraffin inclusion (1 hour x 2 times, 2 hours x 1 time). Then, the samples were placed in the paraffin blocks using a modular inclusion system (Thermo Histostar, Thermo).

- Tissues and organs dedicated to molecular studies were immediately frozen and kept at -80ºC until further processing. In particular, frozen brains were used in this thesis. Once they were removed, they were quickly dissected into the following brain areas: prefrontal cortex (PFC), striatum, cortex (cerebral cortex excluding the PFC) and cerebellum. As the rest of the samples, the different brain areas were immediately frozen and kept at -80ºC until they were further used.

III.5. *POST MORTEM* STUDIES

HISTOLOGICAL ANALYSIS

Histological analyses were performed in the fixed brains in the Clinical and Experimental Neuroscience group at the University of Murcia. **Figure III.4** shows the general workflow performed regarding the *post mortem* studies carried out in the fixed brains.

Brain serial sections

Immunohistological analyses were performed in 5 μm coronal brain sections, obtained with a microtome (Thermo Scientific HM 325 Rotary Microtome, Thermo Fisher Scientific). The studies were performed in the prefrontal cortex (PFC), in the striatum, in the ventral mesencephalon (Substantia Nigra *pars compacta*, SNpc, and the ventral tegmental area, VTA) in the dorsal hippocampus, and in the *locus coeruleus* (LC) (**Figure III.4**). Brain areas in the *O. degus* brains were identified according to the mouse brain atlas (Franklin, Keith and Paxinos, 2004) and the Allen Reference Atlas, due to the anatomical similarities.
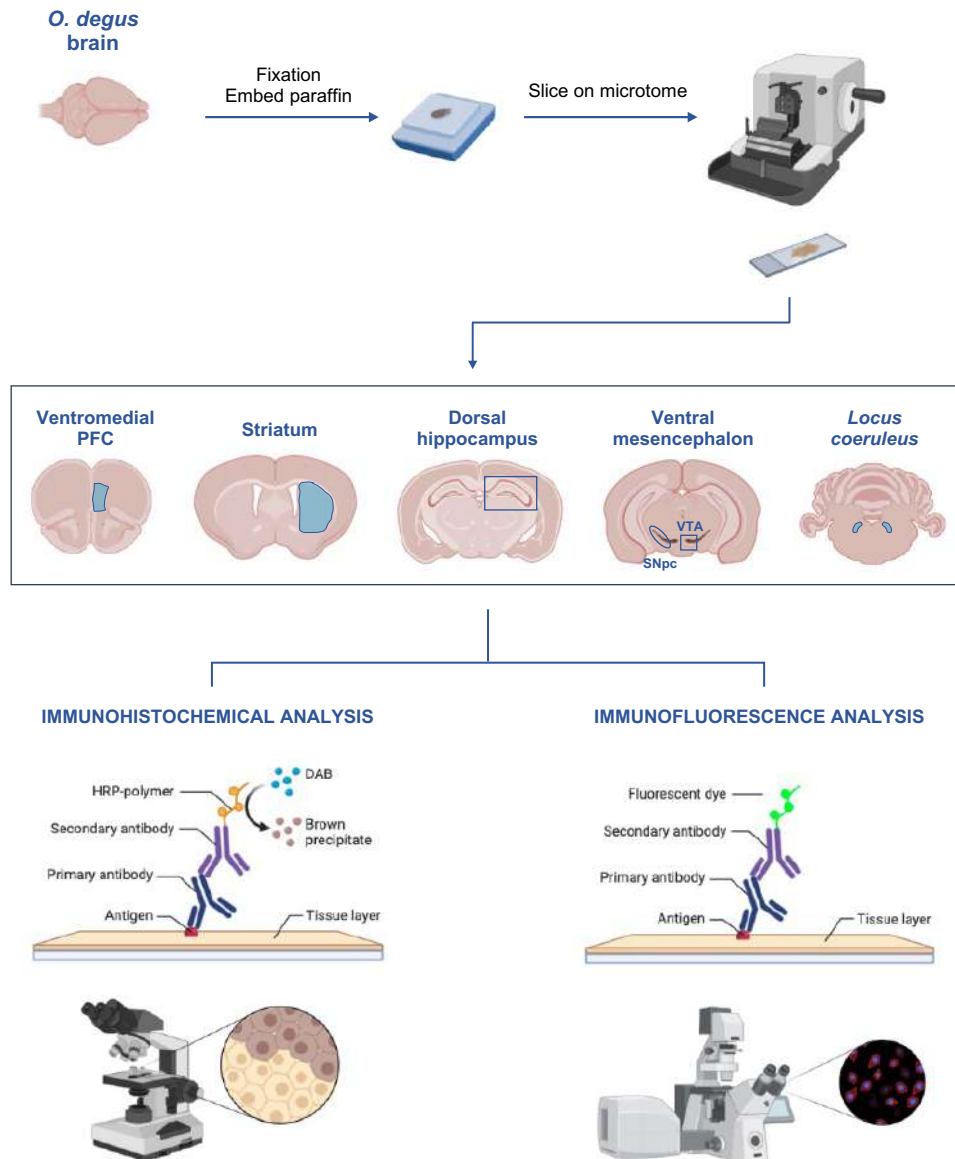
Figure III. 4. Schematic summary of the methods performed in the fixed brains. Degus' brains were fixed and embedded in paraffin blocks, to be subsequently sliced using a microtome. Histological analyses were performed in five different brain areas (ventromedial prefrontal cortex, striatum, hippocampus, ventral mesencephalon and cerebellum), which consisted in detection of different antigens of interest by immunohistochemical and immunofluorescence stainings. Abbreviations: PFC = prefrontal cortex.

Immunohistochemistry

The sections were dewaxed in the oven (at least 2 hours, 65ºC) and by subsequent immersion in xylene (10 minutes, RT). Then, they were hydrated by immersion in decreasing concentrations of ethanol (100, 95 and 70%) and finally in distilled water. The

antigen retrieval was performed using citrate buffer solution (pH=6.0, 20 min, 95ºC) and the sections were washed in PBS (2 x 3 minutes, RT).

Endogenous peroxidase was blocked with 0.3% hydrogen peroxide (20 minutes, RT) and unspecific bindings were blocked with 10% goat serum (in PBS + 0.5% Triton X-100, S-1000 Vector Laboratories) for 1 hour at 36ºC in a humid chamber. Primary antibody applied at appropriate dilution in PBS + 0.5% Triton X-100 + 1% goat serum, and kept overnight at 4ºC (**Table III. 3**). Sections were washed with PBS and incubated with the corresponding biotinylated secondary antibody diluted in PBS (1h, RT) (**Table III. 3**). Then, a signal amplifier was applied following the manufacturer's indications (ABC Elite Kit, Vectastain, Vector Labs). Sections were incubated with DAB substrate until reaction occurred (DAB Peroxidase HRP Substrate Kit, Vector Laboratories); finally, then they were dehydrated and mounted with cover-slip and DPX (Sigma-Aldrich-Merck, US). For TH immunohistochemistry in the ventral mesencephalon, sections were counterstained with Nissl (Cuenca-Bermejo et al., 2021b).

Immunofluorescence

The sections were dewaxed in the oven (at least 2 hours, 65ºC) and by subsequent immersion in xylene (10 minutes, RT). Then, they were hydrated by immersion in decreasing concentrations of ethanol (100, 95 and 70%) and finally in distilled water. The antigen retrieval was performed using citrate buffer solution (pH=6.0, 20 min, 95ºC) and the sections were washed in PBS (2 x 3 minutes, RT).

Then, samples were blocked with 10% animal-free blocker (in PBS + Triton 0.5%; SP-5035 Vector Laboratories) for 1 hour at 36ºC in a humid chamber. Primary antibodies were applied at appropriate dilution in PBS + 0.5% Triton X-100 + 1% animal-free serum, and kept overnight at 4ºC (**Table III. 3**). The primary antibodies were removed with PBS washes (3 x 5 minutes, RT) and secondary antibodies was added to the sections following the manufacturer's instructions (VectaFluor™ Duet Immunofluorescence Double Labeling Kit, Vector Labs). Then, the slices were washed in PBS (6 x 5 minutes, RT) and finally cover-slipped (VECTASHIELD Antifade Mounting Medium, Vector Laboratories) (Gil-Martínez et al., 2018a; Cuenca-Bermejo et al., 2021b).

Images' caption

The samples from immunohistochemistry were photographed with the Hall 100 ZEISS microscope. The images from immunofluorescence were taken with a confocal microscope using a 40X-oil objective (microscope Leica TCS-SP8, SACE, University of

Murcia). We selected the upper and lower limits in the z-position mode to acquire series of 10 images at 0,5 μm interval. Independently from the microscope used, all the images taken for the same analysis were acquired and quantified in the same conditions (including light and room temperature, and without editing them for analysis) in order to avoid bias.

Table III. 3. List of antibodies used in this thesis. The details of the antibodies used are collected, including commercial reference, application and dilution. Abbreviations: IF = immunofluorescence; IHC = immunohistochemistry.

PRIMARY ANTIBODIES

Name *(host species)*	Commercial reference	Application	Dilution
Anti-TH *(mouse)*	Millipore, MAB318	IHC / IF	1:500
Anti-Iba1 *(rabbit)*	Abcam, ab178846	IHC / IF	1:500
Anti-GFAP *(mouse)*	Millipore, MAB360	IHC / IF	1:500
NEUN *(mouse)*	Sigma-Aldrich, MAB377	IF	1:500
Anti-S100β *(rabbit)*	Abcam, ab52642	IF	1:500
Anti-4HNE *(mouse)*	Abcam, ab48506	IF	1:200

SECONDARY ANTIBODIES

Name	Commercial reference	Application	Dilution
Biotinylated Anti-IgG mouse	Vector Laboratories, BA-9200	IHC	1:250
Biotinylated Anti-IgG rabbit	Vector Laboratories, BA-1000	IHC	1:250
Anti-IgG rabbit 488- AlexaFluor	VectaFluor™ Duet Immunofluorescence Double Labeling Kit, Vector Labs	IF	Manufacturer's instructions
Anti-IgG mouse 594- AlexaFluor	VectaFluor™ Duet Immunofluorescence Double Labeling Kit, Vector Labs	IF	Manufacturer's instructions

Study of neuroinflammatory processes

The study of inflammatory markers was performed in the ventral mesencephalon (at the level of the exit of the third cranial nerve, IIIcn), striatum (anterior white commissure level) in dorsal hippocampus (dentate gyrus, CA1 and CA3; polymorph, granular regions) and in the LC.

At the ventral mesencephalon and at the striatum levels, both hemispheres were photographed (3 images per each, 2 slices per animal). At the hippocampal level, two

images per subarea were taken from both hemispheres of each animal (2 brain slices/animal). The LC was divided into three anatomical levels: rostral, medial and caudal. For each level, both hemispheres were photographed (3 images per each, 2 slices per animal). Quantification of Iba1 and GFAP immunolabeling was done by measuring the area occupied by each marker in the z-stack images and expressed relative to the total area (in percentage, %). The quantification of S100β+ astrocytes was done by counting the number of cells expressing three defined profiles: nuclear S100β, nuclear and cytoplasmic S100β and perinuclear S100β (Gil-Martínez et al., 2018a).

Study of the dopaminergic system

Series of 8 images (100 µm apart each) of the mesencephalon stained for TH were taken at 10X magnification, covering the entire SNpc and the VTA (from rostral to caudal axis). Both hemispheres were photographed and 4 replicates per area and sample were taken. Then, nuclei surrounded by TH+ immunostaining were counted by an automated plug-in of Fiji software in order to avoid bias in the cell count (based on the optical fractionator) (Schindelin et al., 2012). Nissl+ nuclei were also studied to ensure accurate neuronal count.

The striatal dopaminergic terminals were determined in the striatum using 6 brain slices per animal. The striatum was divided into two areas: ventral and dorsal. In each slice, four images per hemisphere and striatal area were taken at 20X magnification. Quantification of the TH immunoreactivity in striatal fibers was assessed by optical density using Fiji software, applying a plug in for color deconvolution for DAB staining (Schindelin et al., 2012; Gil-Martínez et al., 2018a).

Study of noradrenergic neuronal death

The sensitivity of the noradrenergic neurons of the LC to the MPTP neurotoxicity was evaluated by TH immunostaining, taking advantage of the presence of this enzyme in the noradrenaline biosynthesis. Series of images covering the LC in the rostro-caudal axis (5 µm apart each) were obtained at 10X magnification. Both hemispheres were photographed and 2 replicates per glass were acquired (in total 4 replicates per level). Then, nuclei surrounded by TH+ immunostaining were counted by an automated plug-in of Fiji software in order to avoid bias in the cell count (based on the optical fractionator) (Schindelin et al., 2012). Data were analyzed dividing the LC in three anatomical levels: rostral, medial and caudal.

Determination of lipid peroxidation in the prefrontal cortex

LPO was studied at the level of the ventromedial PFC (vmPFC) by 4HNE immunofluorescence. Two images per subarea were taken from both hemispheres of each animal (2 brain slices/animal). Quantification of 4HNE immunolabeling was done by measuring the area occupied by this marker in the z-stack images and expressed relative to the total area (in percentage, %).

LIPID ANALYSIS

Analysis regarding the lipid composition were performed in the frozen brains in the Department of Medical Biotechnology and Translational Medicine at the University of Milan. **Figure III. 5** shows the general workflow performed regarding lipids' analysis.

Brain homogenates

Brain areas were let to unfreeze in ice. Meninges were removed and the tissue were minced with a surgical blade and weighted. Then, the sample was homogenized in PBS containing protease inhibitors (1mM Na_3VO_4, PMSF and aprotinin) using a Dounce homogenizer (10 strokes). The whole procedure was performed at 4ºC and samples were stored at -20ºC until they were used.

Lipid extraction

Lipids from the lyophilized lysate of the four brain areas studied in this thesis were extracted by adding chloroform/methanol/water (2:1:0.1) by volume (Prinetti et al., 2000). Briefly, 50µL of water, 500µL of methanol and 1000 µL of chloroform, were added to the lyophilized lysates. Vortex and sonication steps were performed in the middle of the addition of each component. The solutions were mixed at 1100 rpm 20 minutes at 24ºC (Eppendorf Termomixer comfort Block, Hamburg, Germany) and subsequently centrifuged at 13200 rpm 20 minutes at 24ºC (Eppendorf 5415R, Hamburg, Germany). The supernatant obtained, herein the total lipid extract (TLE) was transferred to a new tube and the extraction was repeated 2 more times in the pellets, maintaining the same volume of the solvent system used in the first extraction.

TLE were dried under a N_2 flux and stored at 4ºC until they were further processed.
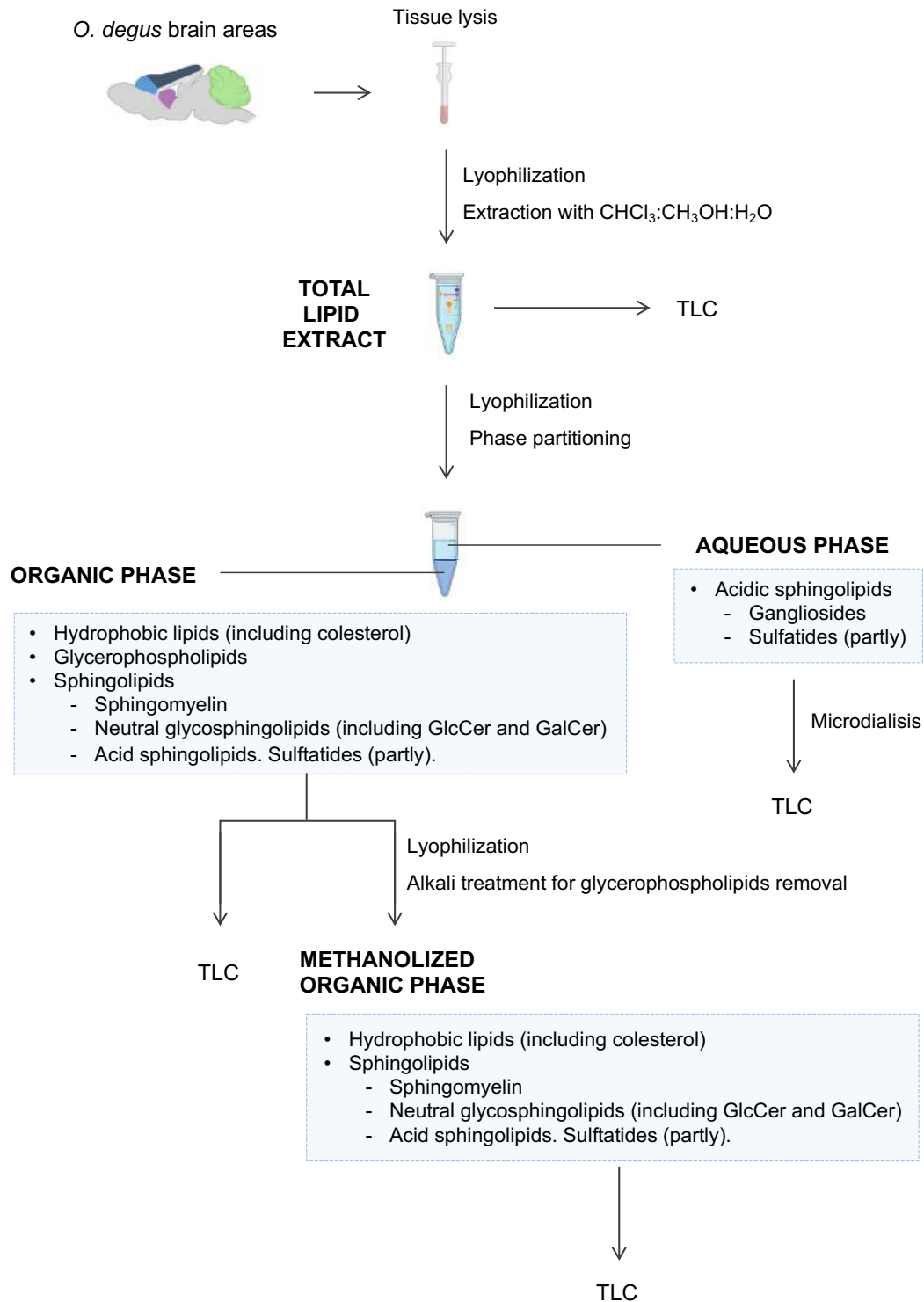
Figure III. **5. Schematic summary of the methods performed for the lipids' analysis.** Four different brain areas (prefrontal cortex, striatum, cortex and cerebellum) from the *O. degus'* brain were homogenized. Total lipid extracts were obtained from tissue lysates and were i) analyzed by TLC and ii) subjected to phase separation to obtain organic and aqueous phases. The lipid composition of both the organic and aqueous phases were analyzed by TLC. Organic phases were methanolized in order to remove glycerophospholipids and reduce the interferences to study the rest of the lipids contained in the phase. Abbreviations: TLC=thin layer chromatography.

Protein quantification

Pellets obtained from the TLE were used to determine protein content. When the pellets were completely dry, they were digested overnight with1N NaOH (at RT) and then diluted to 0.05N. The protein content was determined by the detergent compatible (DC) Protein Assay (Biorad Laboratories, Hercules, CA, USA). Sample's dilution was adjusted to meet in the range of reliability.

Phases' partitioning

TLEs were resuspended in chloroform/methanol 2:1 (by volume) and a volume containing a particular amount of protein was subjected to a two-phase partitioning, resulting in the separation of an aqueous phase containing gangliosides and an organic phase containing the rest of the lipids. The TLEs of the PFC and cerebellum were partitioned. The volume taken to partition was the equivalent to 3mg of protein for the PFC samples' and 4mg of protein for the cerebellum's samples. Briefly, an amount of water (20% of the volume of the sample) was added to the TLE and the sample was vortexed, sonicated, mixed (1000 rpm, 20 minutes, 24ºC) and centrifuged (13200 rpm, 20 minutes, 24ºC). The two phases were obtained and the aqueous phase (the upper one) was transferred to a new tube. An amount of methanol/water 1:1 by volume (40% of the starting volume of the sample) was added to the organic phase (the lower one).

The tubes were mixed and centrifuged with the previous conditions and the aqueous phase was transferred to the tube containing the previous aqueous phase (Scandroglio et al., 2008).

Both the aqueous and the organic phases were dried under a N_2 flux and stored at 4ºC until they were further processed.

Microdialysis of the aqueous phase

In order to remove the salts from the aqueous phases and reduce chromatographic interferences, they were subjected to a microdialysis step. Once dried, the aqueous phases were resuspended in 200µL of dH_2O and half of the volume was transferred to a new tube containing 200µL of dH_2O (final sample's dilution 1:3). Dialysis membranes (12-14 kD, Standard RC Tubing, Spectra/Por®, USA) were placed to cover the surface of the opened tubes, which were placed in glass container filled with decarbonated dH_2O. The system was covered and maintained at 4ºC with soft shaking to facilitate the salts

exchange. The water of the system was changed once per day and samples were recovered after 72 hours, which were then dried under a N_2 flux and stored at 4ºC until they were further used.

Methanolysis the organic phases

The organic phases were subjected to an alkaline treatment to remove glycerophospholipids from the organic phases and improve the TLC separation and analysis (Bjostad et al., 1987). The material used was equivalent to 700µg of protein for the PFC samples and 1200µg for the cerebellum ones. The dried aliquots of these organic phases were resuspended in 100µL of chloroform and then 100µL of 0.6M NaOH (in methanol) were added. The solutions were incubated for 3 hours at 37ºC and 600rpm shaking, and then left overnight at RT. The next day, the reaction was stopped by adding 120µL of 0.5M HCl (in methanol) (Scandroglio et al., 2009). These samples were subjected to phase separation by adding chloroform/methanol/water 70:18:17 (by volume), mixing at 1000rpm 20 minutes RT and the aqueous phase (upper phase) was discarded. The remaining organic phases (named herein methanolized organic phases) were used for TLC analysis.

Monodimensional thin layer chromatography

TLC is a useful and adequate method to obtain a first piece of information regarding the endogenous lipid content. Like other types of chromatographies, the basic principle of the TLC is the existence of a chromatographic system composed by a stationary and a mobile phase, which enable the separation of the components in a mixture due to their different affinities for the mobile and the stationary phases. In the TLC, the stationary phase is a thin solid layer, such as silica, attached to an inert base (e.g., glass or aluminum). The sample is applied at the bottom of this plate, which is then introduced in a closed chamber containing the solvent system (mobile phase). The mobile phase will advance vertically through the plate, allows the separation of the different lipidic components based on their mobility, i.e., their affinity for the solvent system. The plate can be further stained by colorimetric or immuno-based methods, among others (**Figure III. 6**).
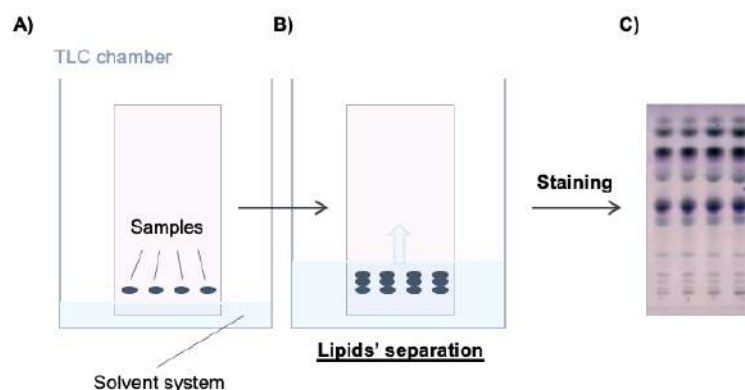
Figure III. 6. Thin layer chromatography procedure. **A)** Samples are placed at the bottom of the TLC plate, which is then immersed in the solvent system (inside the closed TLC chamber). **B)** Solvent systems move along the stationary phase, performing the lipids' separation according to their mobility. **C)** TLC is stained with colorimetric or immuno-based methods. Abbreviations: TLC = thin layer chromatography.

Thus, in this study, changes in the lipid composition along aging with a sex perspective were determined by the performance of TLCs in different solvent systems. TLCs were performed on silica high performance TLC (HPTLC) plates were purchased from Merck, aluminum back support for gangliosides' TLCs and glass support (size 20x10) for the rest of the TLCs. TLEs, dialyzed aqueous phases, organic phases and methanolized organic phases were used for the TLC separation and analysis. Lipid of these phases were dissolved in chloroform/methanol 2:1 and were spotted at 15mm from the bottom of the plate edge; different samples were applied maintaining a 3-5mm distance on an imaginary lane. 10mm were left as right and left edges. Different standards of lipids (3-5 nmol) were placed on the TLCs depending on the solvent system used. Once the samples and the standards were spotted, the plate was let dry before introducing it inside the closed tank containing the solvent system (∼10mm). The chromatography was carried out at RT in the range of 15-20ºC and it was left until the solvent reached the TLC top edge. Once finished, all TLCs were left overnight to ensure that the solvent was completely evaporated.

The solvent system used in this study are collected in **Table III. 4**.

Colorimetric staining

Depending on the lipids studied in each TLC, different colorimetric reagents were used (**Table III. 4**).

General profile of each phase was determined using the anisaldehyde reagent, because it recognizes all lipids. It was prepared dissolving 4-methoxybenzaldehyde (0.5 mL) in a mixture of glacial acetic acid (50 mL) and 97% sulfuric acid (1 mL). The TLC plate

was thoroughly sprayed and then maintained at 120°C in oven for 15 min (Lisboa, 1964). Lipid spots showed different colors: from green to brown (Scandroglio et al., 2009).

The TLC for glycerophospholipids' analysis was stained with the phosphorous reagent. It was prepared as follows: i) ammonium molybdate (16g) was dissolved in dH_2O (120mL) [solution 1]; ii) 80 mL of [solution 1] were added to concentrated HCl (80mL) and metallic mercury, which were shacked for 30 minutes and then filtered [solution 2]; iii) add 200 mL of sulfuric acid to the volume of solution 1 that was not used in step (ii) and add solution 2 [solution 3]; finally, once solution 3 returns to RT, take to a final volume of 1L with dH_2O (Vaskovsky and Kostetsky, 1968). The TLC must be slightly sprayed with this reagent and quickly taken into -20°C. Glycerophospholipids appear as blue bands (in white background).

Table III. 4. Solvent systems and staining method used in this study. Different solvent systems and staining methods were used depending on the purpose of the analysis. $CHCl_3$ =chloroform; CH_3OH=methanol; $CaCl_2$ 0.2%=calcium chloride (in water); C_6H_{14}=hexane; $C_4H_8O_2$=ethylacetate; CH_3COOH=acetic acid. [1] by volume; [2] colorimetric method; [3] immuno-based method.

PHASE (SAMPLE)	LIPIDS STUDIED	SOLVENT SYSTEM	STAINING
Total lipid extract	General lipidic profile	$CHCl_3$: CH_3OH : $CaCl_2$ 0.2% (60 : 35 : 8)[1]	Anisaldehyde[2]
Aqueous phase	General aqueous phase profile	$CHCl_3$: CH_3OH : $CaCl_2$ 0.2% (50 : 42 : 11)[1]	Anisaldehyde[2]
	Gangliosides	$CHCl_3$: CH_3OH : $CaCl_2$ 0.2% (50 : 42 : 11)[1]	Cholera toxin[3]
Organic phase	General organic phase profile	$CHCl_3$: CH_3OH : H_2O (110 : 40 : 6)[1]	Anisaldehyde[2]
	Cholesterol	C_6H_{14} : $C_4H_8O_2$ (3 : 2)[1]	Anisaldehyde[2]
	Glycerophospholipids	$CHCl_3$: CH_3OH : CH_3COOH : H_2O (30 : 20 : 2 : 1)[1]	Phosphorous reagent[2]
Methanolized organic phase	General methanolized organic phase profile	$CHCl_3$: CH_3OH : H_2O (110 : 40 : 6)[1]	Anisaldehyde[2]
	Glycosphingolipids	C : M : H_2O (110 : 40 : 6)[1]	Aniline[2]

All glycosphingolipids were recognized using the aniline/diphenylamine reagent prepared dissolving diphenylamine (4 g) and aniline (4 mL) in a mixture of 85% phosphoric acid (20 mL) and acetone (200 mL). After a moderate spraying the plate was maintained at 120°C for 5–10 min in oven (Schwimmer and Bevenue, 1956; Scandroglio et al., 2009).

Cholera toxin staining

The gangliosides belonging to the gangliotetraose series were detected directly on the TLC plate by the sialidase-cholera toxin procedure: sialidase converts gangliosides to GM1 and cholera toxin B specifically recognizes the oligosaccharide chain of GM1

ganglioside (Davidsson et al., 1991). Identification of the different lipids was accomplished by chromatographic and behavioral comparison with standard lipids in the TLC. Briefly, the procedure was as follows: after chromatographic running, the TLC plate was well dried and fixed with a polyisobutylmethacrylate solution prepared dissolving 1.3g of polyisobutylmethacrylate in 10mL of chloroform and diluting 8mL of this solution with 42mL of hexane. The TLC plate was immersed in this solution three times and then allowed to dry for 1–2 h. The dried TLC was soaked for 30 min in 0.1M Tris–HCl pH 8.0, 0.14M NaCl supplemented with 1% bovine serum albumin (BSA). The incubation with Clostridium perfringens sialidase was performed overnight at room temperature. The enzyme concentration was 2.40U/ml in 0.05 M acetate buffer pH 5.4, 4mM $CaCl_2$. Then the TLC was overlaid with HRP-conjugated cholera toxin subunit B diluted 1:1000 in PBS with 1% BSA for 1 hour (Sigma-Aldrich-Merck, US, C3741-1VL). After several washings with PBS, the TLC plate was developed with OPD-substrate (1 tablet in 50 ml citrate– phosphate buffer pH 5+20 µlH_2O_2) for 5 minutes (Sigma-Aldrich-Merck, US, P5412-50TAB) (Scandroglio et al., 2009).

TLC's analysis

Immediately after the TLC staining, images were acquired a Kyocera Taskalfa 4012i scanner. Changes in the lipid composition were determined by optical density of the different bands present in the samples, which was performed using the Fiji-ImageJ software. The protocol used consisted in the densitometric analysis using the same measuring window and identical parameters for all the bands, which allowed to reduce bias during the TLC analysis. The following information was derived from this data: i) relative abundance of each band in the sample (expressed in % respect to the total intensity); and ii) the intensity of each band, which was normalized with an internal control (optical density in relative units, RU). The lipid/protein relationship in the brain lysates was determined by the sum of all the lipids' bands in the TLC of the TLE, divided by the µg of protein loaded in the TLC ("total bands intensity of the TLE-TLC / µg of protein loaded in the TLC").

Identification of the different lipids was accomplished by chromatographic and behavioral comparison with standard lipids in each TLC. Pure GalCer and sulfatides were purchased from Avanti Polar Lipids; PC, PE, PI, PS, SM, and PA were purchased from Sigma-Aldrich-Merck. Ceramide, gangliosides (GM3, GM2, GM1, GD3, GD1a, GD1b, GT1b), GlcCer, glucosylsphingosine (GlcSph), lactosylceramide (LacCer) and trihexosylceramide were synthesized or purified in our laboratories.

Both general (e.g., organic phase stained with anisaldehyde) and specific TLC (e.g., for glycerophospholipids) were evaluated, but due to its higher accuracy, the quantification shown in this manuscript corresponds to that of the specific TLCs. That is:

- Gangliosides were quantified in the aqueous phase stained with the immuno-based method (cholera toxin staining).
- Glycerophospholipids and SM were quantified in the TLC sprayed with the phosphorous reagent.
- GlcCer, GalCer and GlcSph bands were analyzed in the methanolized organic phase stained with aniline.
- Cholesterol was quantified in the organic phase.
- Since no specific TLC nor reagent was used for sulfatides its quantification resulted from all the TLCs where it appeared.

III.6. STATISTICAL ANALYSIS

Normal distribution of the data obtained was checked by the Shapiro-Wilk test. The two-way analysis of variance (two-way ANOVA) and the post-hoc Tukey test were applied for multiple comparisons considering two variables (age and sex), when data presented a Gaussian distribution. When a single variable of study was considered among different experimental groups (> 2), ordinary one-way ANOVA (followed by Tukey multiple comparison test) or Kruskal-Wallis (followed by Dunn's multiple comparison test) were applied depending on the normal distribution of the data. On the other hand, comparisons performed between two experimental groups were performed using the t-test (unpaired or Mann-Whitney, depending on the normal distribution of the data). Spearman's test was applied for the correlations analyses. Statistical differences were always considered as significant when $p < 0.05$.

CHAPTER IV

RESULTS

IV.1. INFLUENCE OF AGE AND SEX ON BLOOD BIOCHEMICAL PROFILE

STATE OF THE ART

The comprehensive biochemical signature reflecting the physiological functions of the most important organ systems has undoubtedly offered the key information regarding the general health status of the organism. It may also provide a sufficient information to early diagnose several pathologies such as cancer, neurodegenerative disorders, cardiovascular alterations or diabetes, among others (Holdhoff et al., 2013; Arques, 2018; Jackson and Harris, 2018; Mayo et al., 2018). However, the progress of the development and application of novelties to advance health care depends on the availability of human samples or appropriate models in preclinical research, that could reflect the mode of the disease development and/or present pathogenetic pathways, behavior applicable and/comparable to humans.

Previous studies have provided data on different blood analytes on juvenile and adult degus (6 weeks to 3.5 years old) (Otalora et al., 2010; Jekl et al., 2011). However, the influence of sex and/or ages older than 4 years old have not been reported yet. In captivity, *O. degus* live 5-8 years and they spontaneously develop several age-related disorders with different degrees of individual susceptibility. Sex is a biological variable that represents a major contributor to the individual variability in the aging process (Hägg and Jylhävä, 2021). Indeed, several age-associated diseases show a sex-specific pattern (Austad and Fischer, 2016). Hence, completing the available data including older animals and appreciating the sexual differences in the lifespan, would provide useful information for further research with potential translation to interventions.

We hypothesize that age and sex can significantly influence the biochemical profile in the *O. degus*. Therefore, the main objective of the present study was to determine the biochemical parameters in the plasma of *O. degus* ranging from 6 months old (juvenile animals) to 7 years old (senile animals). In addition, we explored if the sex of the animals had an effect on the plasma biochemical profile (**Figure IV. 1**).

Determination of the effect of age and sex on plasma biochemical profile

EXPERIMENTAL GROUPS

IN VIVO STUDIES

Young

Males

• Blood collection
• Plasma separation and analysis

By age Old

By sex

Senile

Females
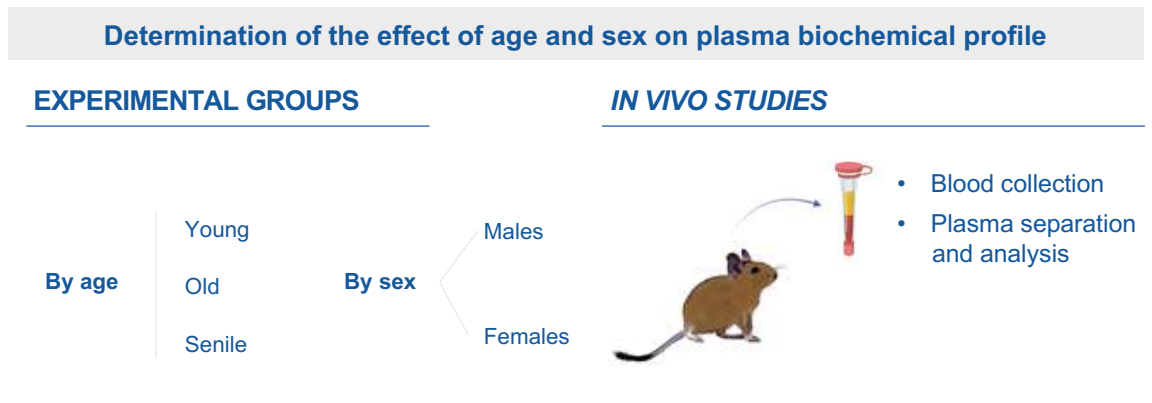
Figure IV. 1. Graphical summary of the experimental design to study the influence of age and sex on the blood biochemical profile.

RESULTS

Results of this section are organized in three main parts. The first one shows the effect of aging on the biochemical profile in the plasma of *O. degus*. The second part studies the sex-associated statistical differences. Finally, correlations studies were performed between the different plasma analytes measured in this study, that have been previously reported to show relationships.

1. Influence of age

Animals participating in this study ranged from 6 months old to 7 years old. Supplementary Table IV.1 shows the reference values for the different blood parameters analyzed regarding the general metabolism, whereas Supplementary Table IV.2 compiles the values for oxidative stress and inflammation biomarkers. The results obtained from the statistical analysis considering age as an experimental variable are presented in the following sections.

1.1. Study of the effect of age on biomarkers of general metabolism

Protein levels were significantly increased in the old group, compared to the young animals (**Figure IV. 2A**). Cholesterol levels were significantly increased in the old and senile animals when they were compared to the young group (**Figure IV. 2B**), although triglycerides were unaffected by the age of the animals (**Figure IV. 2C**).

No significant differences were found regarding glucose levels (**Figure IV. 2D**). Amylase and calcium were found significantly increased both in the old and senile animals compared to the young group (**Figure IV. 2E, F**).

The analytes detected to evaluate iron metabolism were iron levels, UIBC and ferritin (**Figure IV. 2G-I**). Animals from the old group showed significantly lower levels of iron in comparison to the young and the senile ones (**Figure IV. 2G**). UIBC was found significantly increased along aging, both in the old and senile animals (**Figure IV. 2H**). On the contrary, ferritin was found significantly decreased in the senile animals compared to the young ones (**Figure IV. 2I**).

Finally, a significant increase in CK was found along aging (**Figure IV. 2J**).
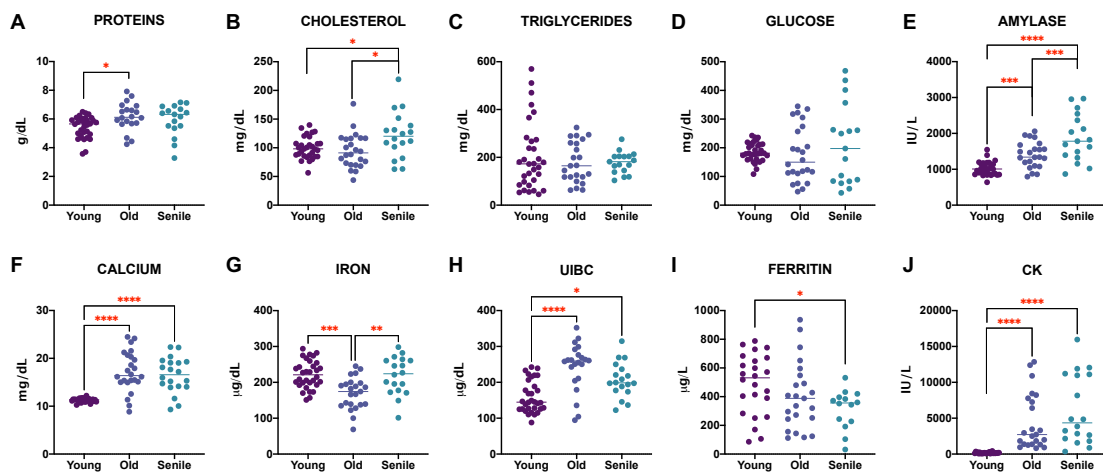
Figure IV. 2. Age effect on general plasmatic metabolites and iron metabolism. Animals were divided into young, old and senile groups, and the effect of age was studied on proteins levels **(A)**, cholesterol **(B)**, triglycerides **(C)**, glucose **(D)**, amylase **(E)**, calcium **(F)**, iron **(G)**, UIBC **(H),** ferritin **(I)** and CK **(J)**. Statistical differences among the different age groups were determined using the ordinary one-way ANOVA + Tukey multiple comparison test in cholesterol, calcium, amylase, iron and ferritin. Statistical differences among the different age groups were determined using Kruskal-Wallis + Dunn's multiple comparison test in proteins, glucose, triglycerides, UIBC and CK. Data are presented as individual values, being the horizontal line the mean or median of each group, depending on the normal distribution. Asterisks indicate the significance of statistical differences: *p<0.05, **p<0.01, ***p<0.001, **** p<0.0001. Abbreviations: CK = creatin kinase; IU = international units; UIBC = unsaturated iron-binding capacity.

1.2. Study of the effect of age on liver and kidneys analytes

Regarding the liver analytes, gGT and AST plasmatic concentrations were significantly increased in the old and senile animals, compared with the young ones (**Figure IV. 3A and B**, respectively). This was not the case of bilirubin, which was found significantly decreased in the older groups compared with the young animals (**Figure IV. 3C**). No significant differences were found for albumin, ALP and ALT levels when animals of different ages were compared (**Figure IV. 3D-F**).
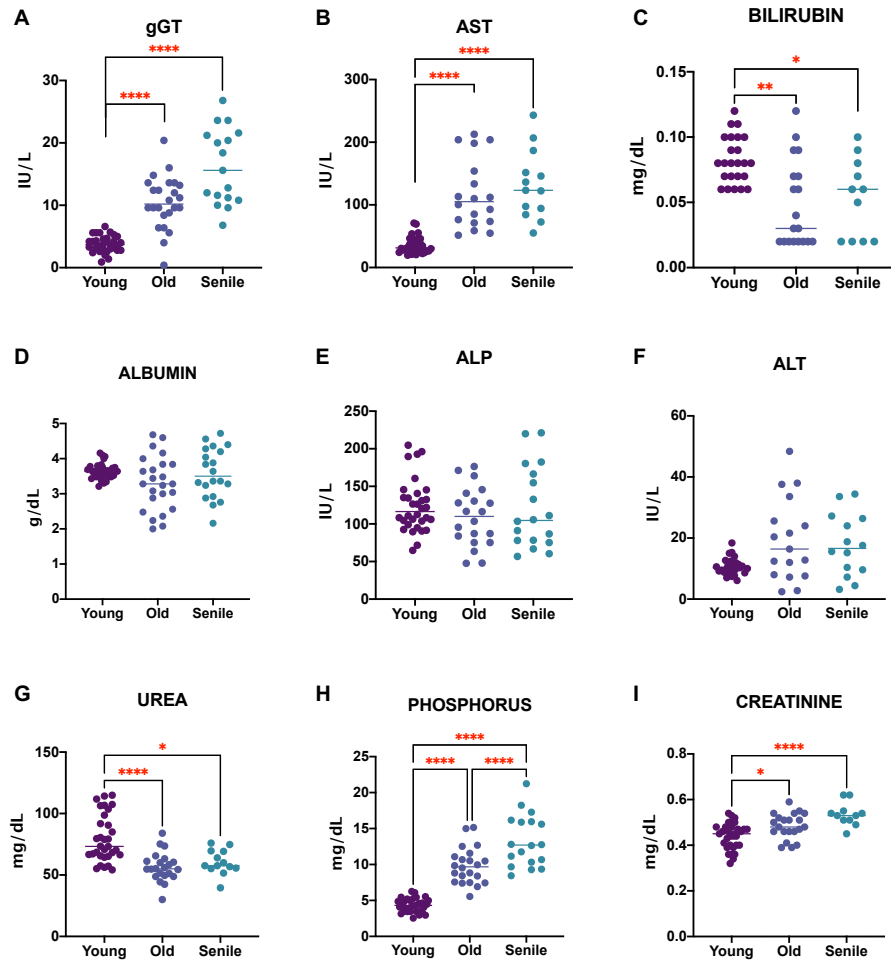
Figure IV. 3. Age effect on liver and kidneys analytes. Liver metabolism was evaluated by the following blood parameters: gGT **(A)**, AST **(B)**, bilirubin **(C)**, albumin **(D)**, ALP **(E)** and ALT **(F)**. The functional state of the kidneys was evaluated by urea **(G)**, phosphorus **(H)**, creatinine **(I)** levels. Statistical differences among the different age groups were determined using the ordinary one-way ANOVA + Tukey multiple comparison test in albumin and phosphorus. Statistical differences among the different age groups were determined using Kruskal-Wallis + Dunn's multiple comparison test in gGT, AST, bilirubin, ALP, ALT, urea and creatinine. Data are presented as individual values, being the horizontal line the mean or median of each group, depending on the normal distribution. Asterisks indicate the significance of statistical differences: *p<0.05, **p<0.01, ****p<0.0001. Abbreviations: ALP = alkaline phosphatase; ALT = alanine aminotransferase; AST = aspartate aminotransferase; gGT = gamma-glutamyl transferase; IU = international units.

The analytes related to the kidneys function analyzed in our study were significantly affected by the age of the animals. Urea levels were found significantly decreased in the old and in the senile groups, compared to the young animals (**Figure IV. 3G**). On the other hand, phosphorus was found to significantly increase as the animals aged (**Figure IV. 3H**). This significant increase was also detected when senile animals were compared with the old animals. Finally, creatinine was also found to increase (very significantly) along aging (**Figure IV. 3I**).

Figure IV. 4. **Effect of age on the different stress-related and inflammatory parameters.** The influence of the age of the animals was studied in the oxidative status was determined by the parameters CUPRAC **(A)**, FRAP **(B)**, TEAC **(C)**, TOS **(D)** a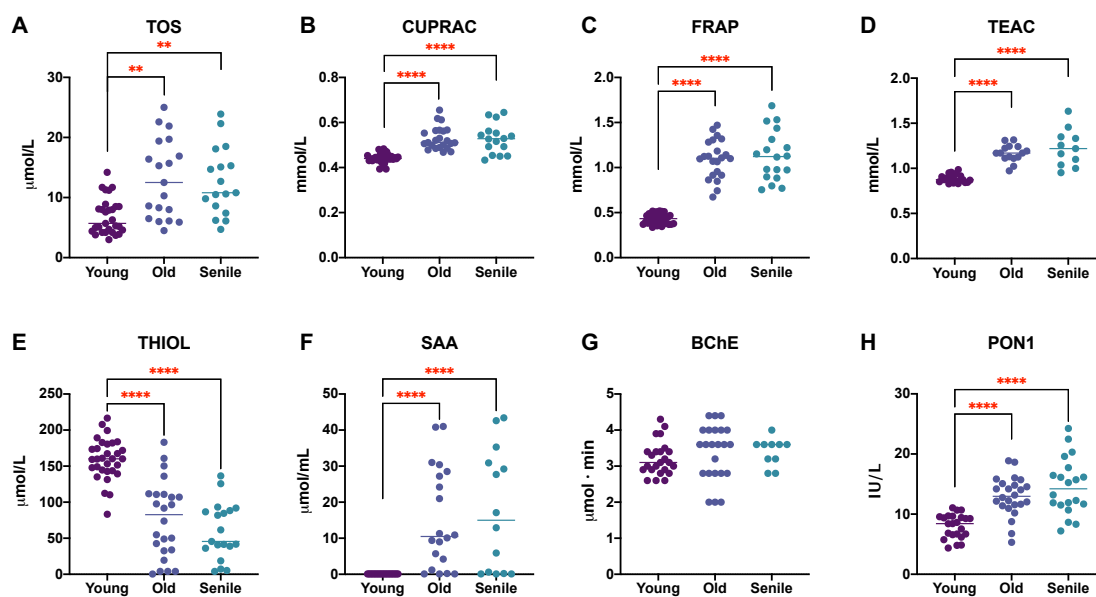nd THIOL **(E)**. The effect of age on acute inflammation was determined by SAA **(F)**. Additionally, other parameters indicating damage were measured in the plasma: BChE **(G)** and PON1 levels **(H).** Statistical differences among the different age groups were determined using the ordinary one-way ANOVA + Tukey multiple comparison test in TEAC and THIOL. Statistical differences among the different age groups were determined using Kruskal-Wallis + Dunn's multiple comparison test in CUPRAC, FRAP, TOS, SAA, BChE and PON1. Data are presented as individual values, being the horizontal line the mean or median of each group, depending on the normal distribution. Asterisks indicate the significance of statistical differences: **p<0.01, ***p<0.001. Abbreviations: BchE = butyrylcholinesterase; CUPRAC = cupric ion reducing antioxidant capacity; FRAP = ferric reducing ability of the plasma; IU = international units; PON1 = paraoxonase-1; SAA = serum A-amyloid; TEAC = trolox equivalent antioxidant capacity; THIOL = total thiol concentrations; TOS = total oxidant status.

1.3. Study of the effect of age on biomarkers of oxidative stress and inflammation

Oxidative stress-related biomarkers were significantly affected by the age of the animals (**Figure IV. 4A-E**). Total oxidative status was significantly increased both in the old and senile animals compared to the young ones (**Figure IV. 4A**). In this line, CUPRAC, FRAP and TEAC were significantly increased in the old and the senile animals, compared to the young ones (**Figure IV. 4B-D**). On the contrary, values for THIOL were significantly decreased in the old and the senile groups when they were compared to the young animals (**Figure IV. 4E**).

Regarding inflammation, we found that the SAA's values were significantly increased as the animals aged (old and senile *vs* young) (**Figure IV. 4F**). Other inflammation-related analytes that were studied are BChE and PON1(**Figure IV. 4G-I**). BChE values remained

constant along aging and no significant differences were found in this parameter (**Figure IV. 4G**). PON1 levels were determined by the age of the animals: old and senile groups showed very significant higher values when they were compared to the young one (**Figure IV. 4H**). A significant increase in CK was found along aging (**Figure IV. 4I**).

2. Influence of sex

The values obtained for the different parameters were compared between males and females of the same age, and those in which statistically significant differences were found are shown in **Figures IV. 5, 6 and 7**. **Figures IV. 5**.

Figure IV. 5. **Sex associated differences were found along aging for proteins (A), triglycerides (B) and UIBC (C).** Statistical differences between males and females were determined using the unpaired t-test or the Mann-Whitney test depending on the normal distribution of data. Asterisks indicate the significance of statistical differences: *$p<0.05$, **$p<0.01$. Data are presented as mean ± standard deviation. Abbreviations: UIBC= unsaturated iron-binding capacity.

Total proteins were higher in females than in males at all ages (**Figure IV. 5A**). In particular, this parameter was found significantly higher in old females compared with their males' counterpart. Triglycerides levels were significantly lower in young females compared with males from the same age (**Figure IV. 5B**). These differences were not present in the old and senile groups. Finally, UIBC levels in the old females were significantly superior to those of males of the same age; no significant differences were found in the young or senile animals (**Figure IV. 5C**).

The analytes related to liver and kidney that showed statistically significant differences when the variable sex was taken into account (**Figure IV. 6**). Bilirubin levels were higher in females than in males at all ages, but these differences became statistically significant in the senile age (**Figure IV. 6A**). ALP levels were found significantly higher in males than in females in the young age (**Figure IV. 6B**); at the old age males' levels

continued to be higher than those of females but at the senile age we found the opposite (**Figure IV. 6B**), although none of them reached the statistical significance. That is: ALP levels increased along aging for females, while for males they changed very slightly. In relation to ALT, both males and females reached the maximum levels at the old age (**Figure IV. 6C**). However, males' ALT plasmatic levels were higher at all ages, being especially very significant at the young age (**Figure IV. 6C**). Phosphorus levels significantly increased along aging; however, this increment was higher in males than in females, since phosphorus levels were significantly higher in senile males than in senile females (**Figure IV. 6D**).
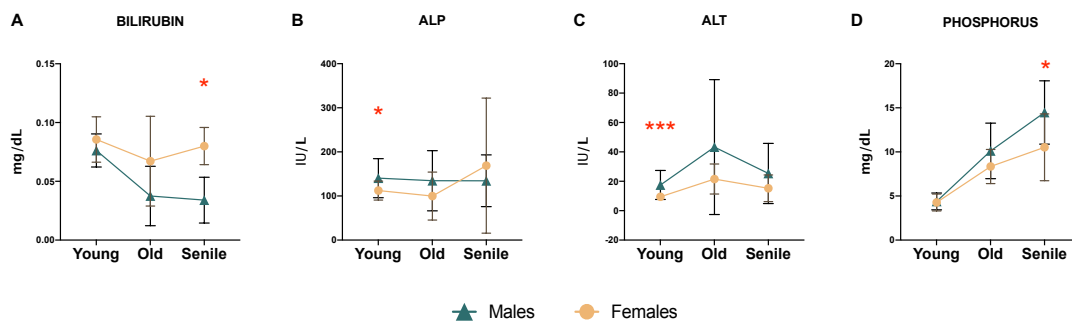
Figure IV. 6. **Sex associated differences were found along aging for liver and kidneys parameters:** bilirubin **(A)**, ALP **(B)**, ALT **(C)** and phosphorus **(D)**. Statistical differences between males and females were determined using the unpaired t-test or the Mann-Whitney test depending on the normal distribution of data. Asterisks indicate the significance of statistical differences: *$p < 0.05$, ***$p < 0.001$. Data are presented as mean ± standard deviation. Abbreviations: ALP = alkaline phosphatase; ALT = alanine aminotransferase; IU = international units.

Finally, **Figure IV. 7** shows the analytes related to oxidative stress and damage that showed statistically significant differences between males and females. When animals got older (i.e., old and senile ages), the TOS was found higher in males than in females, being statistically significant in the old age (**Figure IV. 7A**). In relation to FRAP levels, differences were found in males and females along aging: they progressively increased in the senile males, but in females they increased from the young to the old stage and then decreased in the senile group (**Figure IV. 7B**). For this reason, FRAP levels in the senile males were found significantly increased when they were compared to senile females (**Figure IV. 7B**).

The situation described for FRAP levels was found identical for SAA: its levels in the senile males were found significantly increased when they were compared to senile females (**Figure IV. 7C**).
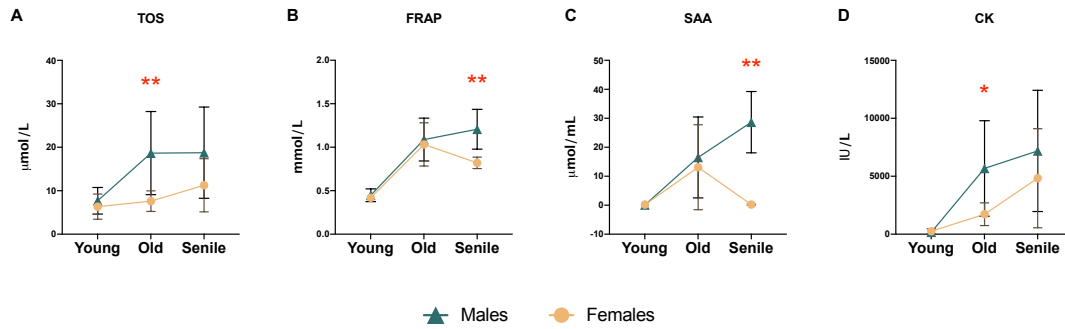
Figure IV. 7. **Sex associated differences were found along aging in the stress-related parameters:** TOS **(A)**, FRAP **(B)**, SAA **(C)** and CK **(D)**. Statistical differences between males and females were determined using the unpaired t-test or the Mann-Whitney test depending on the normal distribution of data. Asterisks indicate the significance of statistical differences: *p<0.05, **p<0.01. Data are presented as mean ± standard deviation. Abbreviations: CK = creatin kinase; FRAP = ferric reducing ability of the plasma; SAA = serum A-amyloid; TOS = total oxidant status.

Finally, although CK levels increased along aging in both sexes, this increment was more pronounced in males than in females, being CK activity in the old males significantly higher in males than in females (**Figure IV. 7D**).

3. Correlations

Next, in order to deepen in the relationship among the variations of the different analytes evaluated, we performed correlation analyses between those that have been previously related in literature.
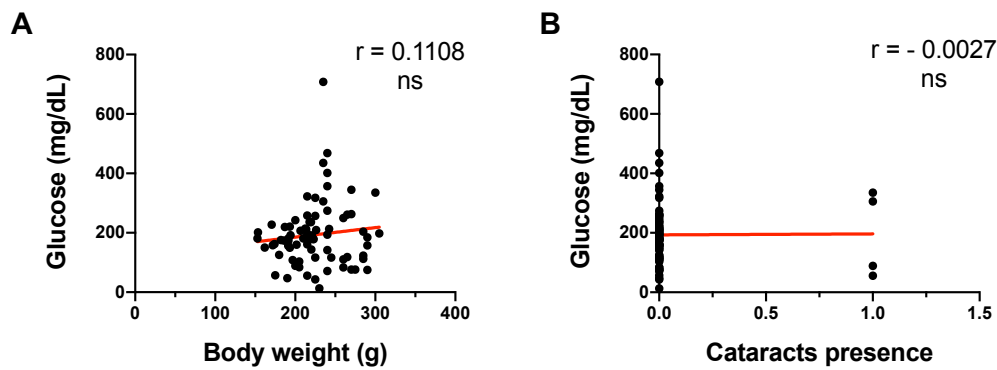
Figure IV.8. **Spearman correlations for glucose levels with body weight and cataracts presence**. Plasmatic glucose levels were correlated with body weight **(A)** and cataracts presence **(B)** (number of XY pairs = 75). Data are presented as individual pairs of values and the linear regression calculated is traced as the red line. No significant differences were found. Abbreviations: ns = non-significant; r = Spearman's coefficient.

Firstly, the possible correlation between plasmatic glucose concentration and body weight or cataracts presence was evaluated (**Figure IV. 8**). Regarding body weight, a

positive correlation with glucose levels was found, although it did not reach statistical significance (**Figure IV. 8A**). Similarly, no significant correlation was found for glucose levels and the cataracts presence (**Figure IV. 8B**).

Iron concentration was negatively correlated with UIBC levels (**Figure IV. 9A**), while positively correlated with ferritin levels (**Figure IV. 9B**). Both correlations were found statistically significant, being the one with UIBC most significant (**Figure IV. 9A and B**).

The relationship between the kidneys weight and the different renal analytes measured appears in **Figure IV. 9C-F**. Higher plasmatic phosphorus levels were very significantly correlated with higher kidneys weight (**Figure IV. 9C**). No correlation was found between creatinine and the kidneys weight (**Figure IV. 9D**). Urea showed a negative relationship with the kidneys size, which was statistically very significant (**Figure IV. 9E**). When we studied the correlation between albumin and kidneys weight, a very significant negative correlation was found (**Figure IV. 9F**).
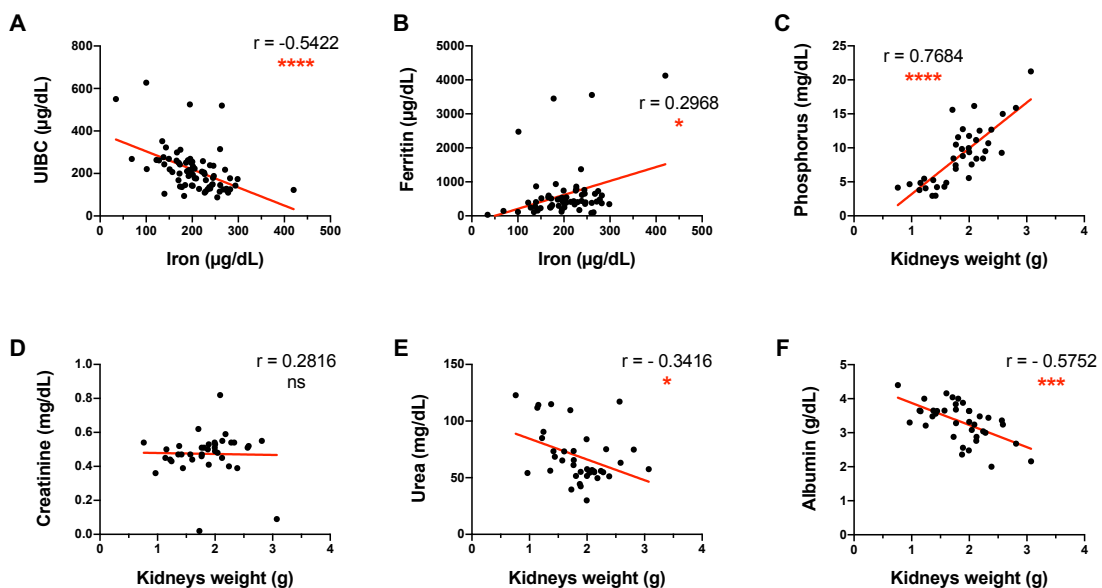
Figure IV. 9. **Spearman correlations for iron metabolism and kidneys analytes**. Plasmatic iron was correlated with UIBC **(A)** and ferritin **(B)** levels (number of XY pairs = 68). Correlation analysis was performed between kidneys weight and: phosphorus **(C)**, creatinine **(D)**, urea **(E)** and albumin **(F)** (number of XY pairs = 38). Data are presented as individual pairs of values and the linear regression calculated is traced as the red line. Asterisks indicate the significance of the statistical differences: *$p < 0.05$; ***$p<0.001$; **** $p<0.0001$. Abbreviations: UIBC = unsaturated iron-binding capacity; ns = non-significant, IU=international units; r = Spearman's coefficient.

Correlations to explore the relationship between liver hypertrophy (estimated by the liver weight) and the different plasmatic levels of liver analytes were performed (**Figure IV. 10**).

Regarding bilirubin and ALP levels, although a slight negative relationship was found the correlation did not reach statistical significance (**Figure IV. 10A and B**). A very significant negative correlation was found for albumin levels and the liver weight (**Figure IV. 10C**). On the contrary, very significant positive correlations were found between liver weight and gGT (**Figure IV. 10D**), AST (**Figure IV. 10E**) and ALT (**Figure IV. 10F**). Finally, no significant correlation was found between levels of gGT and hepatic tumors (**Figure IV. 10G**).
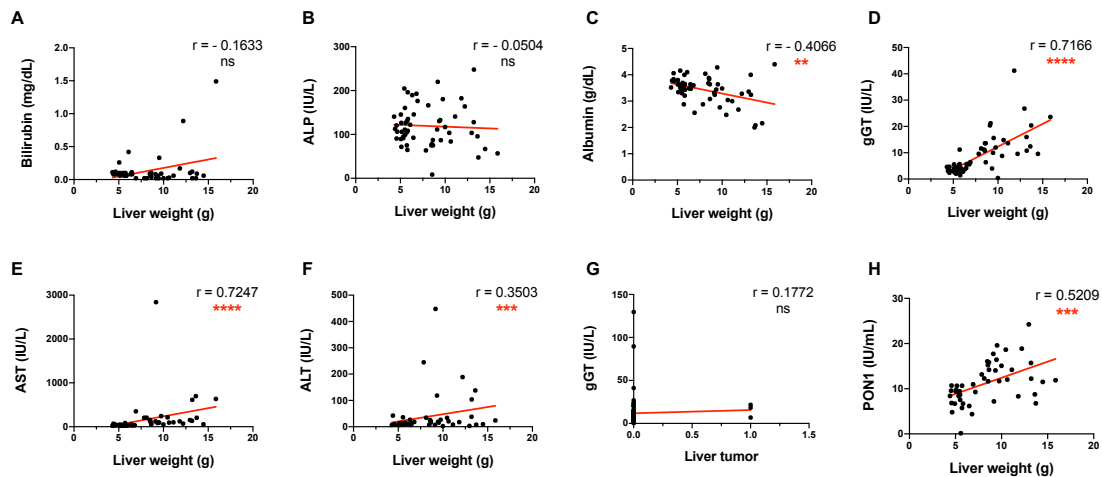
Figure IV. 10. **Spearman correlations to determine the relationship between hepatomegaly and the different plasmatic liver analytes.** The liver weight was correlated with different analytes detected in plasma: bilirubin **(A)**, ALP **(B)**, albumin **(C)**, gGT ©, AST **(E)**, ALT **(F)** and the presence of liver tumors **(G)**. Also, the possible relationship between the liver hyprtrophy and PON1 levels was studied **(H)**. Data are presented as individual pairs of values and the linear regression calculated is traced as the red line. Number of XY pairs = 56. Asterisks indicate the significance of the statistical differences: **p < 0.01; ***p<0.001; **** p<0.0001. Abbreviations: ALP = alkaline phosphatase; gGT = gamma-glutamyl transferase; ALT = alanine aminotransferase; AST = aspartate aminotransferase; PON1 = paraoxonase-1; IU=international units; ns = non-significant; r = Spearman's coefficient.

PON1 is a multifunctional enzyme and it has been related to liver damage, diabetes, oxidative stress, inflammation and cardiovascular diseases (James, 2006; Ceron et al., 2014). Thus, we performed several correlation studies between this enzyme plasmatic levels and liver weight, body weight, tumor presence, glucose and amylase levels (**Figure IV. 10H and 11**). PON1 levels were positively correlated with the liver weight, and this relationship was statistically very significant (**Figure IV. 10H**). In addition, a very significant positive correlation was found for PON1 levels and body weight (**Figure IV. 11A**), glucose (**Figure IV. 11B**) and amylase levels (**Figure IV. 11C**). No significant correlation was found between the presence of tumors and PON1 plasmatic levels (**Figure IV. 11D**)
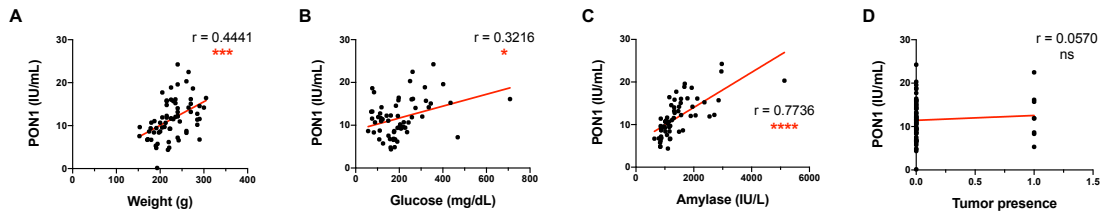
Figure IV. 11. Spearman correlations between PON1 and related variables. The role of PON1 in different clinical outcomes was evaluated by its correlation with weight **(A)**, glucose levels **(B)**, amylase values **(C)** and the tumor presence **(D)**. Data are presented as individual pairs of values and the linear regression calculated is traced as the red line. Number of XY pairs = 72. Asterisks indicate the significance of the statistical differences: *$p < 0.05$; ***$p < 0.001$. Abbreviations: IU=international units; PON1 = paraoxonase-1; ns = non-significant; r = Spearman's coefficient

DISCUSSION

Discussion of the method. Study limmitations

The number of animals used on this study was sufficient to find significant changes and tendencies along aging in the *O. degus*. However, this should be considered as a pilot study and future research should use a bigger population size, and might include different maintenance conditions (diet or stress, among others) in order to elucidate their possible influence on different blood biomarkers. Although the methods adopted were chosen to be the most adequate, some sources of variation can be named. One of them is the use of anesthesia. Several evidence point out that the use of isoflurane is highly recommended for blood collection in small rodents (Marquardt et al., 2018), although it can affect glucose levels by decreasing them (Ochiai et al., 2016). Another source of variation in the results obtained could be the collection site (Fernández et al., 2010). Therefore, future studies should evaluate the effect of different types of anesthesia, as well as different points of blood collection, such as the retroorbital plexus.

Discussion of results

The present work provides, for the first time, reference values for basic plasmatic biochemical analytes in the degus from a wide range of ages including senile individuals (6-7 years old), with a sex perspective. The analytes that are included in this study are biomarkers of general metabolism as well as liver, muscle and renal function, oxidative status and inflammatory markers. We found that age and sex had a substantial effect on most of the analytes studied: 21 out of 27 analytes were significantly affected by the age of the animals and differences between males and females were detected in 11 of them.

Regarding the biochemical parameters related to general metabolism, aged degus are characterized by significant increased concentrations of total protein, cholesterol and calcium. In addition, sex-associated differences were found in these parameters. For example, proteins levels were significantly higher in females than in males and triglycerides were found significantly higher in the juvenile males compared with juvenile females, while in older ages the females' levels are slightly superior than those of males. These findings are in agreement with what has been previously described for different strains of mice and rats (Zhou and Hansson, 2004; Wiedmeyer et al., 2014; He et al., 2017; Silva-Santana et al., 2020); therefore, these results highlight the sex-specific metabolic rates along aging, which can be related to the different incidence of different age-related disorders in men and women. Altered CK levels can indicate several degrees of tissular damage, including muscle (Mansour et al., 2017), heart (Mikolka et al., 2020), and kidneys (Mansour et al., 2017), among others. In agreement with the previously described alterations in the O. degus along aging, CK levels were significantly increased in the old and senile animals, being the levels in males' higher than those in females. Future studies should focus on the deeper characterization of these altered CK levels in order to understand its biological meaning.

Iron metabolism analytes values were significantly influenced by the age and sex of the animals. Significantly reduced levels of iron were detected in the old group compared to both the juvenile and the senile ones. In parallel, a significant increase of UIBC and a significant decrease of ferritin were found along aging. Correlation studies confirmed that the reduction in iron levels was significantly linked to an increase in UIBC and the significant reduction of ferritin. Therefore, there is an age-related iron deficit (including its storage as ferritin). From the sex perspective, females were the ones showing the most significant changes: UIBC levels in the old females group were significantly higher than those of males. A critical source of iron is diet (Siah et al., 2006). Since animals were fed in identical conditions, our findings highlight that age and sex are crucial co-factors determining iron metabolism. The pathophysiological consequences (e.g., associated neurodegeneration) of this iron deficit need to be further characterized.

Liver function was significantly compromised by the age of the animals, since a significant decrease in bilirubin and an increase in AST and gGT were detected along aging. The study conducted by Jekl and collaborators (2011) found that liver enzymes were decreased in animals from 2 years old when compared to animals of 7 weeks old (Jekl et al., 2011). Based on these evidence, liver enzymes decrease during the adulthood. Bilirubin levels were significantly determined by the sex of the animals, since males and females show different trends in bilirubin along aging: males showed a continuous

decrease of the levels of this analyte as the animals aged, whereas females showed a significant increase. On the other hand, hepatic enzymes ALP and ALT were significantly higher in males than in females. Further research needs to explore whether these parameters might increase the predisposition to suffer non-alcoholic liver disease in males. In the present study we analyzed if hepatomegaly (liver hypertrophy) could be related to the altered plasmatic liver analytes. Hepatomegaly was found significantly correlated with reduced albumin levels that could indicate an alteration in liver function and increased levels of gGT, AST, ALT and PON1 that could indicate liver damage (James, 2006; Ceron et al., 2014). Increased levels of gGT have been related to hepatic tumors (Xia et al., 2016); however, we could not find this correlation with our data, which might be explained by the population size.

The kidneys function was also found to be altered as the O. degus aged, since a significant increase in the phosphorus and creatinine levels was detected. The highest levels of phosphorus were found in the senile males, which were significantly increased compared to females. In humans, plasma phosphorus concentration is not significantly different between elderly men and women (Honour, 2018), whereas a study conducted in dogs revealed that in the growth phase males had higher plasma phosphorus levels than females. Since increased phosphorus and creatinine levels can indicate renal dysfunction, we analyzed if the concentrations of these analytes were related to kidneys hypertrophy (increased size). A significant positive correlation was found for phosphorus. Another kidneys-related analyte is urea, which increased levels are associated to kidneys dysfunction. Surprisingly, significantly decreased levels of urea were found along aging in the O. degus, and a significant negative correlation was found between urea levels and the kidneys weight. This finding suggest that decreased urea levels cannot be explained by renal failure but for other causes such as liver damage, as suggested by other authors (Lum and Leal-Khouri, 1989).

Significant alterations were found along aging with the sex perspective in the redox status related parameters. Firstly, the TOS significantly increased along aging. This finding can be explained by the decrease of thiol levels in the older animals, leading to a reduction in the reductive capacity. CUPRAC, FRAP and TEAC significantly decreased along aging, indicating that anti-oxidant mechanisms along aging are activated. Importantly, TOS levels were found higher at all ages in males than in females. One of the most popular and accepted theories to explain biological aging is the reactive oxygen species theory of aging: the accumulation of free radicals and oxidative damage across the life-span induces damage that cannot be repaired (Liochev, 2013), and this is influenced by the sex (Hägg

and Jylhävä, 2021). Therefore, these results are of special relevance when considering the O. degus as a tool to study aging.

In relation to the inflammatory state, the acute phase protein SAA that is usually increased acute in response to inflammatory stimuli was also significantly increased in the old and senile animals, thus suggesting a potential pro-inflammatory environment associated with aging. When the variable sex was taken into account, we found that significantly higher levels of SAA were found in senile males compared to females. Elevation of acute phase proteins has been related to neurodegenerative conditions, including Parkinson's and Alzheimer's diseases (de Pablos et al., 2011). Knowing that the O. degus spontaneously develop several hallmarks associated to neurodegeneration, such as the β-amyloid deposits, this could be considered as a strong point to deepen on the relationship between systemic sustained inflammation and neurodegenerative processes.

The O. degus have been described to show hyperglycemia and have been proposed to be an interesting model for type II diabetes (Nishi and Steiner, 1990; Opazo et al., 2004). In this study, in agreement with published data, no significant differences were found regarding blood glucose levels along aging (Jekl et al., 2011). However, when looking at our individual data, dispersion of the data is evident in the aged animals (both old and senile) but not in the young ones, which might explain why significant differences were not found. This observation leads to the thought that age is related to dysregulation of glucose metabolism in the O. degus, producing an individual-specific phenotype. In this line, both hyperglycemic and hypoglycemic values were found along aging in this species, which has been previously associated with systemic comorbidities (Al-Awar et al., 2016). Since no correlation was found between glucose levels and body weight, we discarded that in our experimental conditions the dysregulated glucose levels are linked to obesity. Also, some animals presented cataracts, but no relationship was found among higher glucose levels and this visual alteration.

When we analyzed pancreatic function, we found that amylase levels were significantly increased in an age-dependent manner and it was positively correlated, as well as glucose levels, with PON1. Altogether, these findings may suggest that dysregulated glucose metabolism is linked to impaired pancreatic function in the O. degus as a result of aging. The relationship between type II diabetes and cognitive decline has gained attention in the last decades (Hölscher, 2020; Riching et al., 2020). Thus, since this experimental model is a natural tool for both conditions (i.e., cognitive decline and impaired glucose metabolism), it would offer the possibility to better characterize this relationship along aging in the future.

Data dispersion was observed especially at older ages and for glucose, amylase, CK, oxidative stress and inflammatory analytes (TOS, THIOL, FRAP, SAA) and several indicators of liver metabolism (gGT, AST, bilirubin, ALP, ALT). Therefore, these findings highlighting the individual susceptibility of this species to the development of several pathological situations at subclinical level.

This study concurs with previous reports performed in *O. degus* (Otalora et al., 2010; Jekl et al., 2011) further strengthening the importance of considering both age and sex as experimental variables. However, some differences existed that could be explained by the fact that different ages were considered, since age has been demonstrated to exert a significant effect on these values. On the other hand, if we compare the data obtained for young animals in this study with the one conducted by Jekl and collaborators (2011) for adult (2 years old), the most divergent values were for cholesterol, amylase, ALP, ALT, bilirubin, creatin and urea. Since their study was conducted in degus pets, the way in which they are fed and maintained might be different from the laboratory food (Jekl et al., 2011). On the other hand, some analytes measured here, such as oxidative stress markers, have not been previously published for the *O. degus*.

Collectively, the results reported here provide data to better characterize this experimental model and support that *O. degus* are a natural tool for aging research in the context of multimorbidity. In addition, the data presented here is important for future studies about pathophysiology, early diagnosis and monitorization of disorders. Since environmental conditions can be modulated in experimental conditions, the inter-individual variability represents a potential tool to explore how genetic background can influence different clinical outcomes, and the identification of plasma diagnostic biomarkers.

SUMMARY OF RESULTS

In conclusion, values for blood biochemical profile, oxidative status and inflammatory biomarkers for the *O. degus* along aging with a sex perspective are provided. Most of blood chemical parameters significantly change along aging (with sex-associated differences), in some cases towards values that could potentially indicate subclinical pathological situations, such as systemic inflammation, liver dysfunction or increase in the oxidative stress. Therefore, not considering age and sex as experimental variables in further studies, might lead to results bias. It is expected that this data could be of use for consider the effect of age and sex when interpreting analytes in *O. degus*.

IV.2. AGE AND SEX DETERMINE ELECTROCARDIOGRAM PARAMETERS

STATE OF THE ART

Since Willem Einthoven introduced the surface electrocardiogram (ECG) in 1903, this technique has become one of the most commonly used methods to evaluate the heart physiology, both in humans and animals (Yang et al., 2015). Actually, ECG is the most important clinical test for the interpretation of the cardiac rhythm, detection of myocardial ischemia and infarction, preexcitation, long QT syndromes and difficulties in the electrical transmission between the different parts of the heart (Singh and Peter, 2016; Nikus et al., 2018). In animal models, several studies have reported the ECG-derived parameters in healthy and diseased animals under different experimental conditions, including aging, myocardial infarction or systemic arterial hypertension (Liu et al., 2012; Speerschneider and Thomsen, 2013; Konopelski and Ufnal, 2016; Locati et al., 2018).
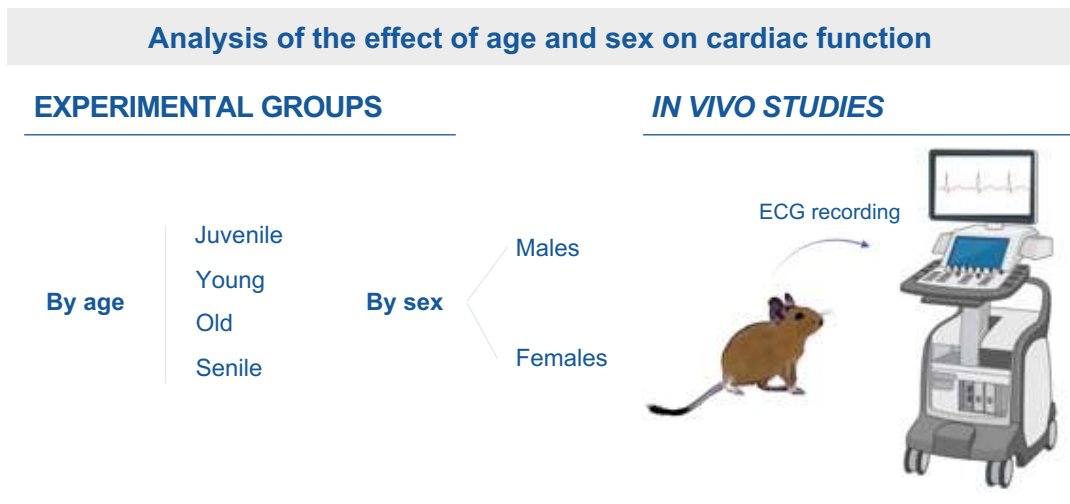
Figure IV. 12. Graphical summary of the experimental design to study the influence of age and sex on the electrocardiogram's parameters.

Even though current data reinforce the association between aging and cardiovascular disease, it is still not fully understood how this interaction works and how sex influences different clinical outcomes (Evans et al., 2020). The diurnal rodent *Octodon degus (O. degus)* has been proposed as a relevant tool in biomedical research because some of its similar age-related features with humans (Cuenca-Bermejo et al., 2020). However, to the authors' knowledge, no data have been reported on the electrocardiographic parameters in the *O. degus*.

We hypothesize that the ECG parameters in *O. degus* are influenced by the age of the animals and thus, could be used as a natural model for age-associated cardiac alterations. Hence, the aims of this study were to determine the normal surface ECG parameters in the *O. degus* and to evaluate the effect of age and sex on them (**Figure IV. 12**).

RESULTS

The protocol adopted for the ECG recordings in anesthetized *O. degus* allowed us to obtain tracings of sufficient quality to analyze the HR, cardiac rhythm, as well as the evaluation of the different waves and intervals, considering a minimum of three consecutive cardiac cycles. However, the movement of the baseline of the ECG tracing was commonly found. The values obtained for each parameter of the ECG, are presented in Supplementary Table IV.3 and Supplementary Table IV.4. Results obtained from the statistical analysis considering age and sex as experimental variables (isolated and simultaneous effect) are presented in the following sections.

1. Heart rate

The values for HR of all the animals used in this study ranged from 110 (old male) to 340 (senile female) bpm (Supplementary Table IV.3). No significant differences were found when all females and all males were compared (**Figure IV. 13A**, Supplementary Table IV.3B). On the contrary, when animals were grouped by age, HR significantly decreased in the old and senile animals compared with the young ones (**Figure IV. 13B**, Supplementary Table IV.3C). Along aging, HR values of the males appeared more affected than the ones from females: even if we detected a decrease in HR within the aging process in both sexes, this became statistically significant only when young and old females were compared (**Figure IV. 13C**, Supplementary Table IV.4).

The possible correlation between HR and other parameters was evaluated in all the animals (**Figure IV. 13D-H**). HR showed a very significant negative correlation with body weight (**Figure IV. 13D**). Regarding the duration of the different waves and intervals, HR showed a significant negative correlation with PR duration (**Figure IV. 13E**) and the duration of QT segment (**Figure IV. 13F**). A negative correlation between QRS complex and heart rate was found, although it did not reach the statistical significance (**Figure IV. 13G**). No significant relationship was found between HR and P wave duration (**Figure IV. 13H**).
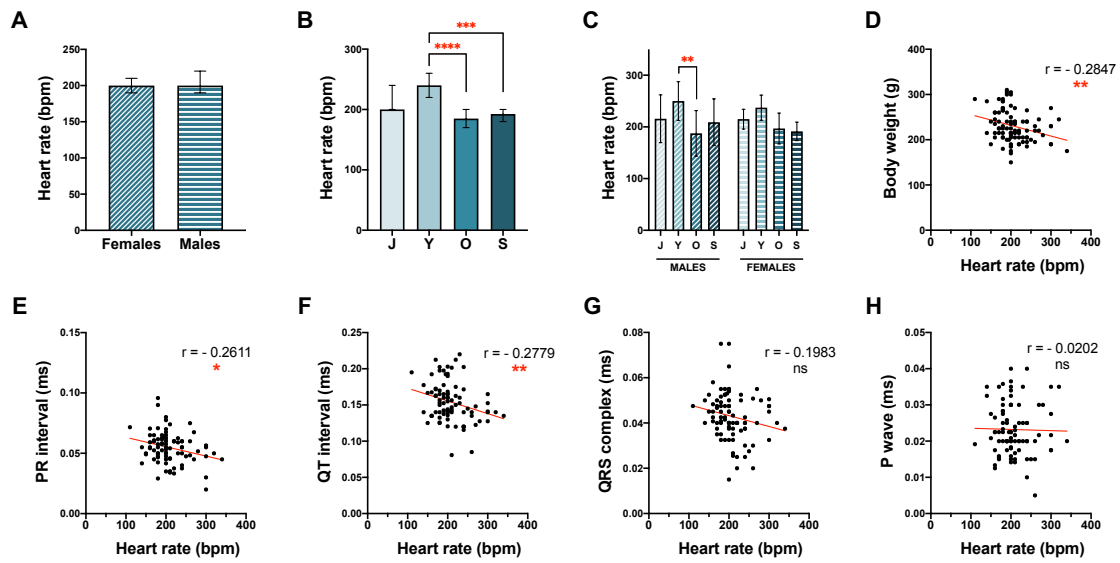
Figure IV. 13. **Heart rate values in the *O. degus***. Graphical representation of the heart rate regarding sex **(A)**, age **(B)** or both variables simultaneously **(C)**. **(D-H)** Correlations between heart rate values and: body weight **(D)**, PR interval duration **(E)**, QT interval **(F)**, QRS complex duration **(G)** and duration P wave duration **(H)**. Statistical analysis to study the differences between males and females in the heart rate was performed by the Mann-Whitney test. Statistical analysis to study the effect of age on heart rate was performed by Kruskal-Wallis + Dunn's multiple comparison test. Data are expressed as mean ± standard deviation in the column graphs. Data are presented as individual points in the correlation graphs, with the red line indicating linear regression. Number of XY pairs = 87. In both types of graphs, asterisks indicate statistical differences: * $p<0.05$, ** $p<0.01$, *** $p<0.001$, **** $p<0.0001$. Abbreviations: bpm = beats per minute; HR = heart rate; ms = milliseconds; r = Spearman's coefficient; ns = not significant; J = juvenile; Y = young; O = old; S = senile.

2. Rhythm

The evaluation of the cardiac rhythm showed that both sex and age influence the appearance of altered cardiac rhythm (**Table IV. 1**). In the females, more than 95% of the ECG tracings evaluated were classified as regular sinusal rhythm, and only 2/45 animals presented arrhythmia: one from the old group (frequent VPCs) and the other from the senile group (isolated VPCs, couplets or triplets) (**Table IV. 1**). On the opposite, alterations in the rhythm were more predominant in males, and unexpectedly in the juvenile ones. Bigeminal rhythm was detected in the 50.00% of the juvenile males and in the 33.33% of the young ones. Also, 33.33% of the senile males showed VPCs: 3/12 had frequent VPCs and 1/12 showed isolated VPCs, couplets and triplets (**Table IV. 1**). The 100% of animals from the group of old males showed a normal sinusal rhythm (**Table IV. 1**). **Figure IV. 14** shows a representative ECG recording of a physiological rhythm, while **Figure IV. 15** represents the different pathological rhythms found during aging in the *O. degus*.

Table IV. 1. **Cardiac rhythm in *O. degus* and incidence of the cardiac rhythm alterations**. The proportion of animals, expressed as percentage (%) from the total of individuals of the corresponding group, was quantified according to sinusal rhythm and different types of arrhythmias (bigeminal rhythm, ventricular premature complexes and ventricular tachycardia). Ventricular premature complexes were subdivided into frequent or isolated, couplets or triplets.

	Sinusal rhythm (%)	Arrhythmia			Ventricular tachycardia
		Bigeminal rhythm (%)	Ventricular premature complexes (VPC)		
			Frequent VPC (%)	Isolated VPC, couplets or triplets (%)	
Males					
Juvenile	37.50	50.00	-	-	12.50
Young	66.67	33.33	-	-	-
Old	100.00	-	-	-	-
Senile	66.67	-	25.00	8.33	-
Females					
Juvenile	100.00	-	-	-	-
Young	85.71	-	-	14.29	-
Old	93.75	-	6.25	-	-
Senile	100.00	-	-	-	-

Alterations in several plasmatic analytes, such as PON1, CK or BChE have been associated with cardiovascular alterations (Horjus et al., 2011; Stojanov et al., 2011; Ponce-Ruiz et al., 2020). For this reason, correlation studies were performed to understand if the presence of arrhythmias was related with those analytes in the *O. degus* (**Figure IV. 16**). We did not find a significant correlation for these analytes and cardiac impairment.

3. P wave

The duration of P wave (ms) of all the animals oscillated between 0.005 (young females) – 0.040 (senile females and juvenile males) (Supplementary Table IV.3 continuation-A and Supplementary Table IV. 4 continuation). Females and males exert an opposite behavior regarding the duration of P wave during aging: the duration of P wave decreases as males got older, while it increments along aging in females (**Figure IV. 17A**).

All the values for the voltage (mV) of P wave were found between the range 0.006 (young females) – 0.083 (senile males) (Supplementary Table IV.3A and Supplementary Table IV.4). No significant differences were found in the multiple comparison test, neither regarding sex nor age (**Figure IV. 17B**).
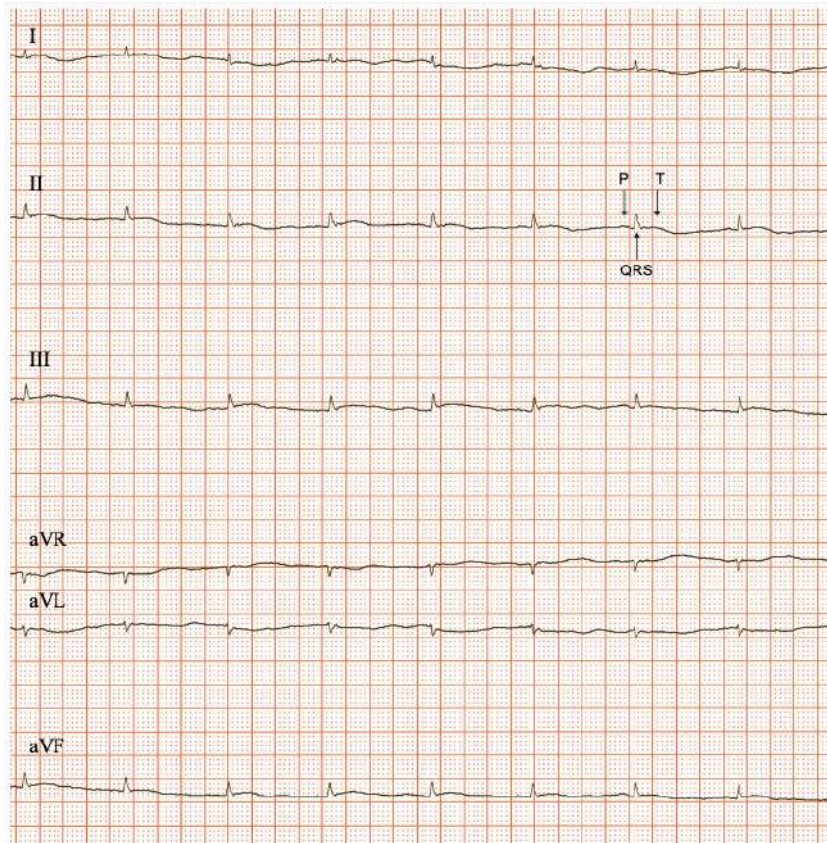
Figure IV. 14. Representative six-leads electrocardiograms of sinusal rhythm. 50 mm/s and 20 mm/mV.

4. PR interval

The values of PR interval (ms) ranged from 0.020 (senile males) to 0.096 (senile females) (Supplementary Table IV. 3 continuation-A and Supplementary Table IV. 4 continuation). Significant differences in the PR interval duration were found when males and females were compared: males showed significantly smaller values than females (Supplementary Table IV. 3 continuation-B). This parameter did not change significantly along aging in the *O. degus* (Supplementary Table IV. 3 continuation-C, **Figure IV. 17C**).

5. QRS complex

The QRS complex duration (ms) ranged from 0.020 (young females) to 0.075 (senile females) (Supplementary Table IV. 3 continuation-A and Supplementary Table IV. 4 continuation). The statistical analysis determined that the effect of "age" was extremely significant. In particular, the duration of the QRS is enlarged during aging in the species *O. degus*: senile animals presented significant larger QRS complexes compared with the young animals (Supplementary Table IV. 3 continuation-C). The effect of age on this parameter was more pronounced in the females than in the males: there were no significant differences along aging in males, whereas in the group of females, the duration of the QRS complex in the senile females was significantly higher (increase of 51.51%)

and very significantly higher (increase of 61.29%) when it was compared to juvenile and young females, respectively (**Figure IV. 17D**).

Finally, the effect of "sex" (females *vs* males) on the QRS duration was not found statistically significant (Supplementary Table IV. 3 continuation-B).
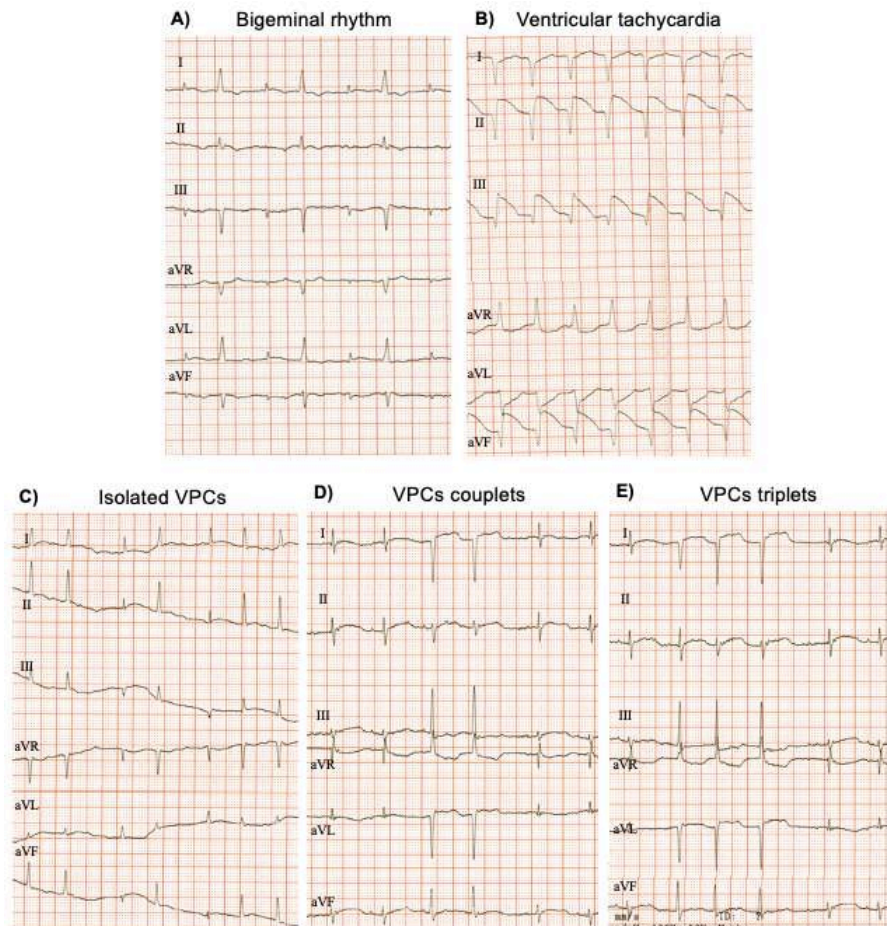
Figure IV. 15. **Representative electrocardiograms of the main different pathological ECG recordings found in the study: A)** Bigeminal rhythm; **B)** Ventricular tachycardia; **C)** Isolated ventricular premature complexes (VPCs) **D)** VPCs couplets and **E)** triplets. 50 mm/s and 20 mm/mV.

6. R wave (mV)

The amplitude of R wave (mV) was inside the values 0.013 (old females) and 0.525 (juvenile males) (Supplementary Table IV. 3A and Supplementary Table IV. 4). The statistical analysis showed no significant differences when the multiple comparison test was done (**Figure IV. 17E**). The effect of "age" and "sex" were not significant to explain the variations observed in the values among the different experimental groups (Supplementary Table IV. 3C).
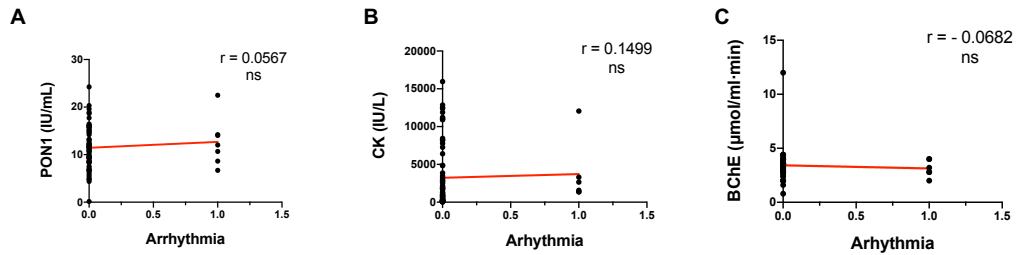
Figure IV. 16. Spearman correlations between different plasmatic parameters and cardiac functional alterations. Cardiac function was evaluated by electrocardiography (Result's section IV. 2) and the presence of arrhythmia was correlated with PON1 **(A)**, CK **(B)** and BChE **(C)**. Data are presented as individual pairs of values and the linear regression calculated is traced as the red line. Number of XY pairs = 62. Significant differences were considered when p<0.05. Abbreviations: BChE = butyrylcholinesterase; CK = creatine kinase; IU=international units; ns = non-significant; PON1 = paraoxonase-1; r = Spearman's coefficient.

7. S wave (mV)

The values of S wave voltage (mV) in lead II relied between 0.002 (old females) and 0.363 (juvenile males) (Supplementary Table IV. 3A and Supplementary Table IV. 4). The variable "sex" exerts a very significant effect on the total variance of this parameter. Independently of the age, the S wave voltage values were higher in males than in females (Supplementary Table IV. 3B, **Figure IV. 17F**). The aging process did not influence this parameter significantly (Supplementary Table IV. 3C).

8. T wave (mV)

Voltage values of the T wave in lead II ranged from 0.006 (young males) to 0.200 mV (juvenile males) (Supplementary Table IV. 3A and Supplementary Table IV. 4). The values of T wave voltage were higher in the juvenile animals (both females and males) than in the rest of the groups, although no significant differences were found (Supplementary Table IV. 3C). No sex-associated significant differences were found (Supplementary Table IV. 3B, **Figure IV. 17G**).

9. QT interval (ms)

The values of the duration (ms) of QT interval oscillated between 0.081 (senile females) and 0.235 (senile females) (Supplementary Table IV. 3 continuation-A and Supplementary Table IV. 3 continuation). Total variance of this parameter is mainly caused by the variable "age" (Supplementary Table IV. 3 continuation-C), while "sex" did not significantly affect it (Supplementary Table IV. 3 continuation-B). Interestingly, statistical differences associated to the age of the animals were found just in males (young vs juvenile) (**Figure IV. 17H**). When animals were grouped by sex and age simultaneously,

significant differences were found when males and females of the groups juvenile and senile were compared (**Figure IV. 17H**).
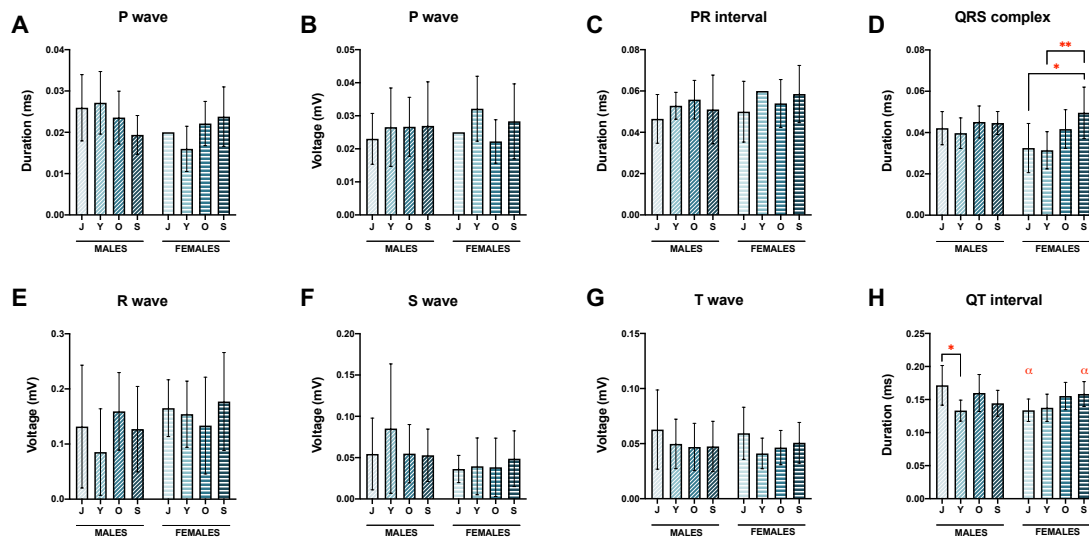
Figure IV. 17. **Effect of sex and age on the electrocardiographic parameters in the *O. degus*. A)** P wave duration (ms); **B)** P wave voltage (mV); **C)** PR interval duration (ms); **D)** QRS complex duration (ms); **E)** R wave voltage (mV); **F)** S wave voltage (mV); **G)** T wave voltage (mv); **H)** QT interval duration (ms). Statistical analysis to study the effect of age on the ECG parameters was performed by Kruskal-Wallis + Dunn's multiple comparison test. Statistical analysis to study the sex-associated differences in the different ECG parameters was performed by the unpaired t-test. Data are expressed as mean ± standard deviation. Asterisks indicate statistical differences comparing animals of the same sex and different age: * p<0.05, ** p< 0.01. Alpha character (α) indicates statistical differences when males and females of the same age are compared (α p<0.05). Abbreviations: ms = milliseconds; r = Spearman coefficient; J = juvenile; Y = young; O = old; S = senile.

10. Electrical axis

The MEA in the frontal plane of all the animals ranged from -138º (juvenile males) and +180º (senile females) (Supplementary Table IV. 3 and Supplementary Table IV. 4). The widest range of MEA was found in juvenile males (-138.0º to +169.0º), while the narrowest one corresponded to young males (-67.0 º to +20.5º). When the variable sex was studied, it was found that males had significant lower mean values of MEA (**Figure IV. 18A**). Regarding the variable age, MEA values did not show significant statistical differences (**Figure IV. 18B**).

Three representative ECG with normal electrical axis and left and right deviations are shown in **Figure IV. 19**.
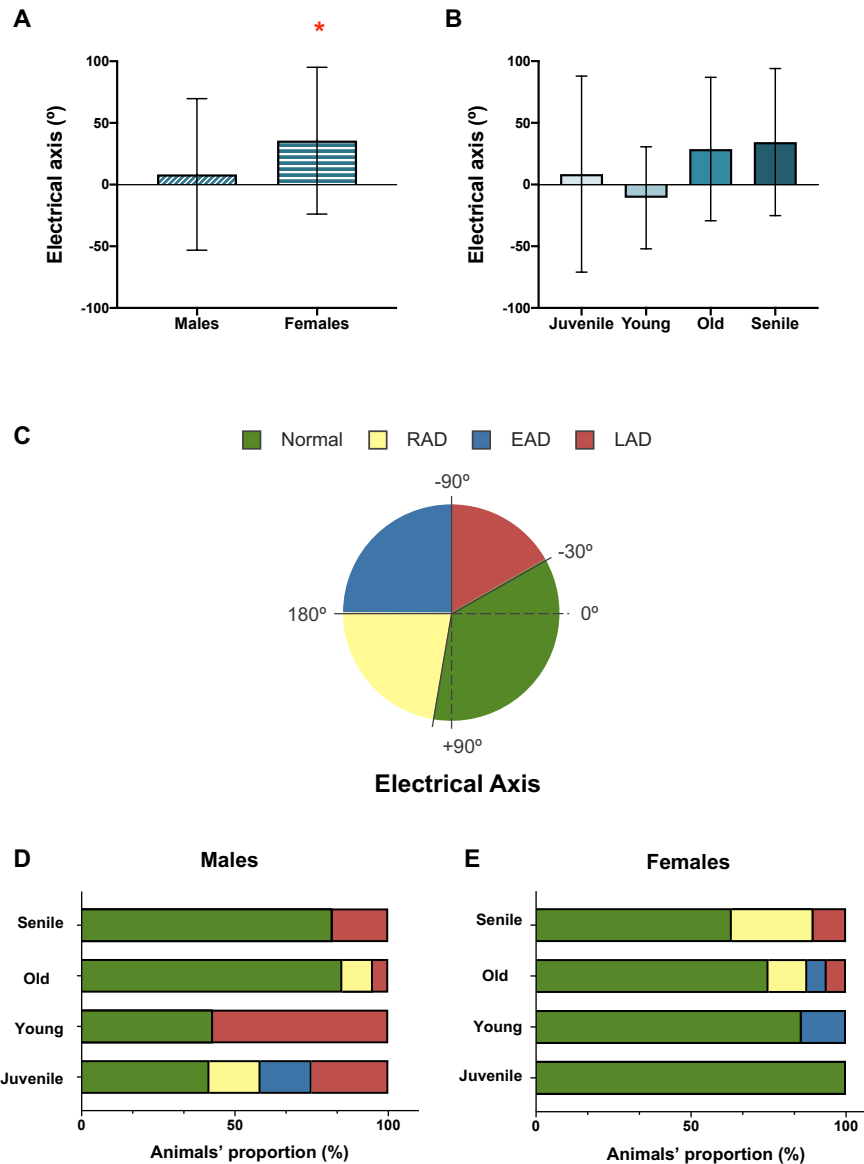
Figure IV. 18. Electrical axis in the *O. degus'* females and males during aging. A) Graphical representation of the electrical axis values in the *O. degus* regarding sex and **(B)** age. **C)** Classification of the electrical axis: normal, right axis deviation (RAD), extreme axis deviation (EAD) and left axis deviation (LAD). According to this classification, the electrical axis of the animals was calculated to express the proportion of animals with each axis deviation in males **(D)** and females **(E).** Statistical analysis to study the sex-associated differences in the different ECG parameters was performed by the unpaired t-test. Statistical analysis to study the effect of age on the ECG parameters was performed by ordinary one-way ANOVA + Tukey multiple comparison test. Asterisks indicate statistical difference between males and females: * $p < 0.05$. Data are expressed as mean ± SD in the column graphs.

Animals were classified according to their electrical axis values and the proportion (as percentage, %) of animals per group was calculated (**Figure IV. 18C**). The distribution of males and females showed clear differences. Males showed a different behavior (**Figure IV. 18D**). In contrast, in the females, a normal electrical axis predominates, although deviations of the axis appeared as age increases (**Figure IV. 18D**). In the young

male group, more than 50% of the animals presented deviations from the axis: 3/12 showed LAD, 2/12 EAD and 2/12 RAD. In adult males, only LAD was found, but it was present in more than 50% of the animals of the group. Surprisingly, in the old and senile group of males the 85 and 81.82% of the animals, respectively, showed a normal electrical axis and none of them showed an extreme deviation from the axis.
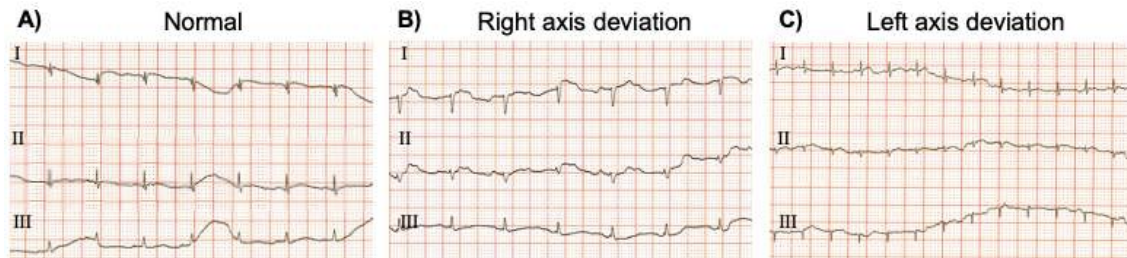
Figure IV. 19. **Representative electrocardiograms of the main different electrical axis deviations identified in the study:** A) normal axis deviation; B) right axis deviation: and C) left axis deviation. 50 mm/s and 20 mm/mV.

11. Heart/body weight ratio is increased in the aged *O. degus*

We studied whether heart weight was influenced by sex and age in the *O. degus* by calculating the ratio heart weight:body weight (expressed as %). There were not significant differences between females and males regarding this parameter (**Figure IV. 20A**). However, along aging, the heart size increases significantly, mainly in the old and in the senile animals compared to both juvenile and young animals (**Figure IV. 20B**).

Additionally, a possible correlation between heart weight and the ECG parameters measured was evaluated (**Figure IV. 20C-K**). Among them, a very significant negative correlation between R wave amplitude and the heart weight was found (**Figure IV.20H**).

DISCUSSION

Discussion of the method. Limitations of the study

The main limitation of this study was that the ECGs were recorded with the animals under anesthesia, and individual variations in heart rate and rhythm are known to occur with the anesthetic agents used in this study (Heaton-Jones et al., 2002; Barrasa et al., 2008; Chen et al., 2013). In this study we cannot know if medetomidine has contributed to the appearance of arrhythmias or not since the electrocardiograms have not been done without anesthesia in the same animals. However, anesthesia is necessary and recommended to most clinical procedures in small animals and the combination of dexmedetomidine and ketamine is commonly used and has shown to be sure.
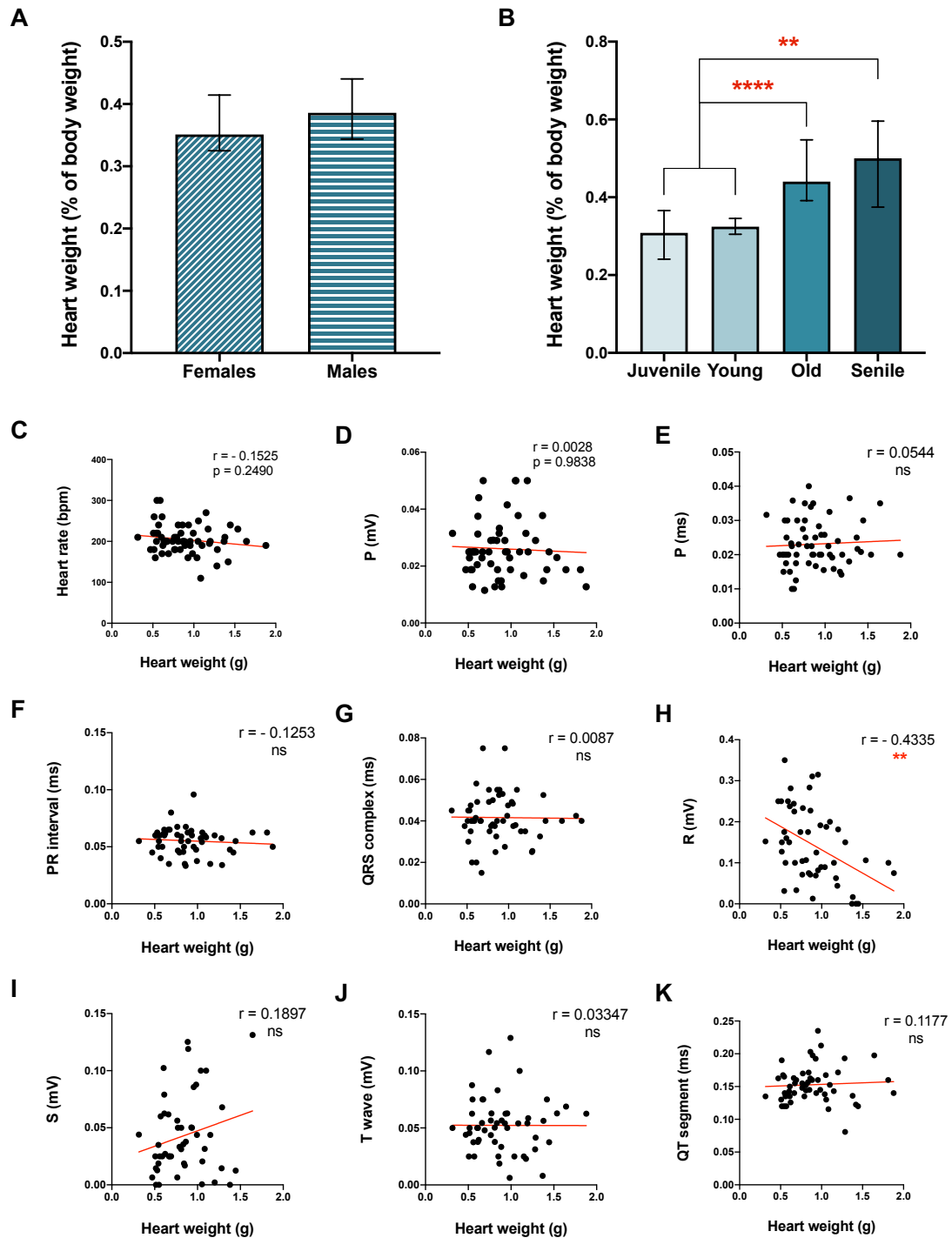
Figure IV. 20. Heart weight changes along aging and its relationship with ECG parameters. Heart weight (% respect to the total body weight) regarding sex **(A)** and age **(B)**. Statistical analysis to study the differences between males and females in the heart rate was performed by the Mann-Whitney test. Statistical analysis to study the effect of age on heart rate was performed by ordinary one-way ANOVA + Tukey multiple comparison test. Data are expressed as mean ± standard deviation. **(C-K)** Correlations between all heart weight (g) and the different ECG parameters. Data are expressed as individual values in the correlations, with red line indicating linear regression. Number of XY pairs = 55. Asterisks indicate the significance of the statistical differences: ** p<0.01, **** p<0.0001. Abbreviations: bpm = beats per minute; HR = heart rate; ms = milliseconds; ns = not significant; r = Spearman's coefficient.

Discussion of results

This is the first study that comprehensively reports the EGC measurements in the *O. degus*. Animals were divided into 8 groups depending on age and sex. The results showed that age is the most determinant variable that influences the amplitude and the duration of the waves and segments in the ECG recording, although particular sex-related differences were also found. In particular, the QRS complex and the QT segment were the most age-dependent measurements. On the opposite, electrical axis values and the outcome of different type of arrhythmias are more affected by the sex of the animals. To the author's knowledge, this is the first study that has shown that sex and age can influence the ECG parameters in the species *O. degus*.

Cardiovascular diseases (CVD) are the ones with the biggest impact and the first cause of death worldwide (Bray et al., 2021). The electric activity of the heart changes throughout life and it has been found to be particularly altered during aging (Paneni et al., 2017). Several studies have found impairment in the myocites' cell-cell communication, molecular and membrane properties changes or remodeling of the extracellular matrix, among others (Wagner and Dimmeler, 2020). This cellular and molecular variations have structural and functional consequences, such as the altered electric activity of the heart evidenced by ECG recordings. It is known that aging is important risk factor to develop CVD in both sexes in humans, but increasing evidence suggest that there are sex differences regarding the cardiac changes that happen during the aging process, as well as in the onset and progression of the cardiac diseases (Merz and Cheng, 2017; Azizi et al., 2021). For example, atrial hypertrophy and fibrosis are more prevalent in men but have a worse outcome in women. On the other side, left ventricular fibrosis, alterations in calcium metabolism or vascular stiffness are more prevalent in women but shows worse outcomes in men (Kane and Howlett, 2018). However, the current strategies in the clinical procedures applied to CVD have been established from information inferred from studies performed mostly in men because, historically, clinical trials have been made considering the male sex (Merz and Cheng, 2017; Kane and Howlett, 2018; Leonard and Marshall, 2018; Macfarlane, 2018).

Despite the fact that both age and sex strongly influence cardiac parameters, few studies have incorporated simultaneously these variables. In this line, the diurnal rodent *O. degus* represents an interesting alternative as an experimental model for age-related pathologies, since it spontaneously develops some age-associated traits, including atherosclerosis (Cuenca-Bermejo et al., 2020). However, the cardiac parameters of this species have not been determined yet. Thus, in the present work we have studied the

ECG of the *O. degus* along aging and with a sex perspective, under anesthesia conditions. We have found that that some ECG values are sex- and age-dependent in this species.

In these animals, HR values reach their maximum value in young animals (1 year old) and decrease with age. We found that this decrease was particularly significant in old males compared to young. These results are in line with what has been established for humans, mice and rats (Jones et al., 1990; Farraj et al., 2011; Rossi et al., 2014; Vicent and Martínez-Sellés, 2017). Sex does not influence the mean HR value in the *O. degus*.

Heart rhythm analysis revealed that abnormal rhythms are more frequent in males than in females, and that they occur mainly in younger groups (juvenile and young males). It is known that sedation or anesthesia with α-2 agonists in small animals induce arrythmias associated with increased parasympathetic tone, including a sinus arrhythmia further characterized as a sinus bigeminy (Singletary et al., 2010). Therefore, it might be speculated that sexual dimorphism could have implications regarding the response to anesthesia.

The P waves reflects the atrial depolarization, and it has been established in humans that its shape and duration have clinical importance (Konopelski and Ufnal, 2016). In general, an increase in P-wave duration may be associated with an increased susceptibility to arrhythmias. In the *O. degus*, we observed an opposite behavior when we compared males and females: in females, the duration increases with age, while in males it decreases. As for the amplitude of the P wave, the males showed homogeneous values with age. In contrast, females showed an increase in the value of old and senile ages. Increased P wave duration is indicative of decreased atrial and atrio-ventricular node conduction, possibly due to altered conductive function of myocytes by modifying expression of key proteins in the myocyte-to-myocyte connection-communication (Kane and Howlett, 2018).

Regarding the duration of PR interval, we observed an increase of this parameter as the animals age, in agreement with what is described for humans (Xing et al., 2009). Noteworthy, the highest values of PR interval duration in females were found in the young and the senile groups, while in males its prolongation was linear within the age. Atrio-ventricular blocks of first grade have been related with the increase of PR interval in humans during aging (Rodriguez and Schocken, 1990; Farraj et al., 2011).

The QRS complex, which corresponds to the depolarization of the ventricles, gives important information about the electrical function of the heart and is one of the most affected parameters during aging in humans and rodents (Xing et al., 2009; Konopelski and Ufnal, 2016).

We found that its duration increased significantly with the age in females, while in males this increase was smaller. No differences were found when comparing males and females of the same age, although the values for males had tendency to be higher at all ages except for the senile ones. These results are consistent with human studies, since it has been shown that the duration and voltage of this complex increases with age and that values for men are higher than those for women (Macfarlane, 2018). An increase in the duration of this complex is associated with alteration of ventricular rhythms and ventricular conduction which, in turn, is related to heart failure and myocardial ischemia (Konopelski and Ufnal, 2016).

Within the QRS complex, analysis of R and S wave amplitude also showed a gender-dependent behavior. In females, the R-wave showed a decrease from young-old ages, but increased in senile females. On the contrary, the trend with age in males was found to be very variable, and adult males showed a large decrease in the voltage of this wave. In the S-wave amplitude, the values for females remain similar at juvenile, young and old ages, although they increase slightly in the senile animals. In males, the values were higher at all ages and significantly higher in young males. Alterations in S and R wave amplitudes suggest alterations in the depolarization of the ventricles in young males. Of special relevance for the translational point of view, is that we found in the Octodon's ECG the presence of the Q wave, similar to humans and not found in rats and mice ECG (Farraj et al., 2011).

In relation to T wave amplitude, the maximum values were found in the juvenile group of both sexes. Then, these values decreased in the young groups and then tend to increase in the old and senile females, while to decrease in the old and senile males. Knowing that T wave corresponds to ventricular repolarization, abnormal values for this wave may suggest cardiac pathology, such as arrhythmias (Farraj et al., 2011; Konopelski and Ufnal, 2016). Higher values of T wave voltage may indicate hyperkalaemia, while lower values are indicative of hypokalaemia (Akita et al., 1998; Konopelski and Ufnal, 2016; Macfarlane, 2018).

Ventricular repolarization is measured as the duration of QT interval in the ECG. In the *O. degus*, the duration of this segment was prolonged in the aged females, which values where higher to those observed in the males of the same age (old and senile). On the contrary, young males showed a significant decrease in QT duration compared with the young ones. The prolongation of the QT interval has been closely related to toxicity of exogenous compounds and can predispose to myocardial infarction, channelopathies, ischemia or arrhythmias in both humans and laboratory animals (Konopelski and Ufnal, 2016; Mladěnka et al., 2018).

The study of the electrical axis can provide important information for finding underlying pathologic states and better characterization of the disease (Kashou and Kashou, 2018). Axis deviation is more frequent with aging. This behavior was observed in the females of this study. Surprisingly, the juvenile and young males were the ones that presented the greatest axis deviation, which decreased with age (similar to arrhythmias). The most frequent axis deviation in males was LAD, which has also been described as the most frequent in humans, and which has been related to changes in the position of the heart and anterior fascicle fibrosis (Vicent and Martínez-Sellés, 2017).

Aged animals (independently from the sex) showed heart weight/body weight ratio: old and senile animals had a 1.64-fold and a 1.75-fold, respectively, to the juvenile ones. This cardiac hypertrophy was negatively correlated (very significantly) with the R wave voltage. Several lines of evidence have pointed out that increase in the heart weight can be both a physiological response or a pathological situation (McMullen and Jennings, 2007; Nakamura and Sadoshima, 2018). Thus, future studies might focus on a deeper cellular and molecular characterization of the heart hypertrophy in the *O. degus*.

In summary, we observed that young males presented more variations on the ECG than the older ones, specifically in relation to R and S waves, QT segment, incidence and severity of arrhythmias, and electrical axis deviation. Arrhythmias and mean electrical axis deviations in young males can be explained by the confluence of increased R-wave duration and T-wave amplitude, and decreased S-wave and QT-segment duration.

Altogether, these findings provide the reference values for the ECG recording in the *O. degus*, providing evidence that this model may represent a valuable tool to study cardiac function in the context of aging. The variability observed in the data provides the opportunity of understanding the individual susceptibility to different pathological conditions. In addition, this study reinforces the need of including both sexes in preclinical research, since significant differences were found between males and females in the different ages considered. In this sense, further research might focus on exploring the role of sex hormones in the influence of sex in the ECG recording. Therefore, these results might serve as the starting point for future studies aiming at deciphering the aging heart mechanisms from the perspective of sex differences and individual susceptibility.

SUMMARY OF RESULTS

In this study we have characterized for the first time the electrocardiographic parameters in the *Octodon degus* during the aging process, considering both females and males. The data obtained showed spontaneous cardiac alterations within the age that differs in females and males. Therefore, we suggest that degus may act as an attractive a natural model for cardiovascular research since its shares features relevant to human aging and presents signs of sex specific alterations.

IV.3. AGE AND SEX EFFECT ON COGNITIVE DECLINE AND NEUROINFLAMMATION IN THE HIPPOCAMPUS

STATE OF THE ART

Cognitive decline is the most important age-related change in cognitive function, characterized by a progressive deterioration of physiological function and behavior, including memory loss (Amarya et al., 2018). Spatial memory is a subtype of long-term memory that depends on the capacity of remembering information within a spatio-temporal context, and it is especially vulnerable to normal aging (Tulving, 1972; Wahl et al., 2017). Spatial memory is learned over the time and it allows to integrate spatial references to maintain a particular trajectory from one place to another (Klencklen et al., 2012). Strong evidence show that the hippocampus in the most critical area for learning and memory consolidation, as well as for age-associated cognitive deficits (Corkin et al., 1997; Smith et al., 1999; Martin and Clark, 2007). In particular, cognitive deficits have been associated to changes in the dorsal part of the hippocampus (Maguire et al., 1996; González-Ramírez et al., 2014).

Since cognitive impairment is a shared feature for physiological aging and several types of dementia (e.g., AD), understanding how natural aging affects cognition and behavior is one of the main areas of interest in the field of neuroscience. In this line, evaluation of behavior and cognition in experimental models is a gold standard tool to uncover mechanistic and interventional studies of brain aging and neurodegeneration. Different behavioral tests are used in rodent models to reflect different aspects of the human memory (Vorhees and Williams, 2014). Among them, the BM represents an important task to evaluate the hippocampal-dependent spatial learning and memory (Barnes, 1979; Kennard and Woodruff-Pak, 2011; Negrón-Oyarzo et al., 2015; Pitts, 2018). The BM is based on the assumption that, given an aversive environment (platform), the animal should learn and remember the path to an escape box located below the platform (Gawel et al., 2019). This test has provided useful information, not only to assess brain damage (e.g., neurodegenerative disorders), but also to evaluate the effect of toxic substances or therapeutical strategies (Inman-Wood et al., 2000; Tarragon et al., 2014; Estrada et al., 2015a).

Previous studies have performed the BM in the *O. degus* to evaluate sex differences in young animals (Popović et al., 2010), the effect of sleep deprivation (Estrada et al., 2015b) and transcranial stimulation (Estrada et al., 2015a). However, no studies have been conducted along aging with a sex perspective. Our working hypothesis was that

cognitive impairment associated to aging, has an important sex component in the *O. degus*, which is manifested in the BM performance and in the hippocampal inflammatory processes (**Figure IV. 21**).
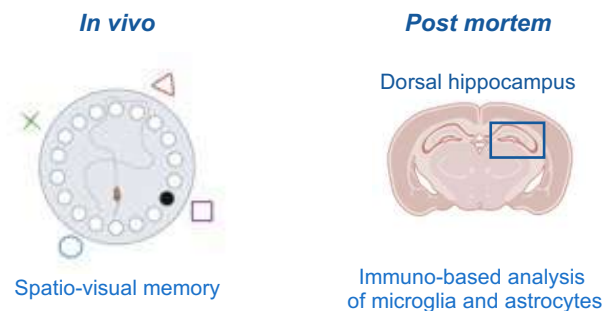
Figure IV. 21. Graphical summary of the experimental design to study the influence of age and sex on cognitive performance and neuroinflammatory processes in the dorsal hippocampus.

RESULTS

1. Barnes Maze performance in the acquisition phase

1.1. Effect of age

In general terms, evident differences considering the age of the animals were observed in the evolution of the performance of the test during de training sessions (acquisition phase): the juvenile and the young animals showed a better cognitive performance than the old and the senile groups (**Figure IV. 22**). Since juvenile and young groups behave similarly and the old and senile animals' behaviors also showed a similar tendency, animals will be referred as "younger" (including juvenile and young groups) and "older" (including old and senile groups) in this section.

During the training period, all the groups were able to improve their performance in the test, as seen by the increase in the number of escapes (**Figure IV. 22A**), the reduction

in the time to find the escape hole (**Figure IV. 22C**) or the reduction in the number of working memory errors (**Figure IV. 22I**). Noteworthy, we observed that the animals from the old and the senile groups were the ones showing a higher improvement, but their cognitive performance was always worse than the younger ones (juvenile and young) (**Figure IV. 22**).

Number of escapes

The older animals showed a lower number of escapes than the younger ones (**Figure IV. 22A**, Supplementary Table IV.5A). Although they improved along the training days, animals from the old group were the ones with fewer number of escapes, compared with the other three groups.
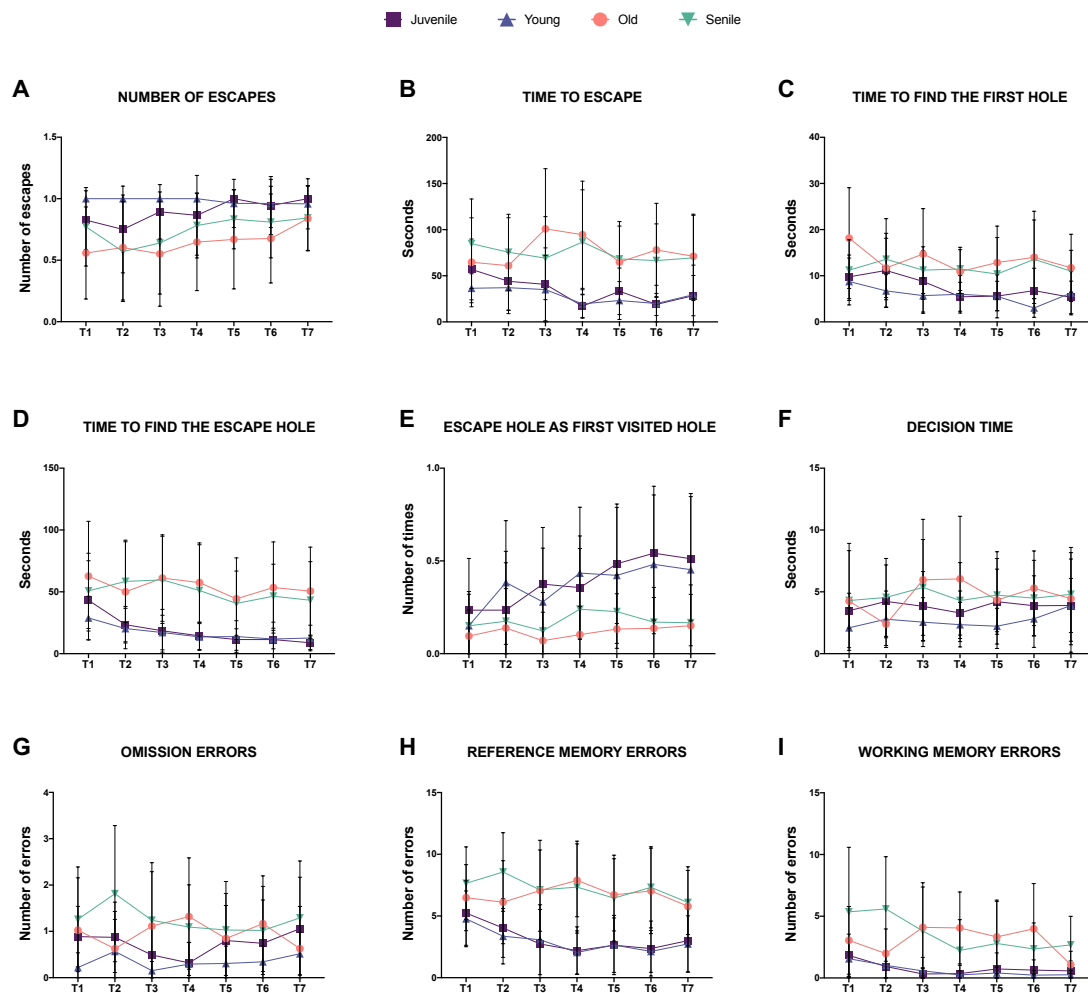
Figure IV. 22. **Barnes maze performance along the acquisition phase.** The different parameters evaluated during the training sessions are presented, grouping the animals by age (juvenile, young, old and senile): **A)** number of escapes; **B)** time to escape the maze; **C)** time to find the first hole; **D)** time to find the escape hole; **E)** number of times that the animals visited the escape hole as first visited hole; **F)** time spent exploring the escape hole before going through it; **G)** number of times that the animals visited the escape hole without escaping; **H)** number of reference memory errors; and **I)** number of working memory errors. Data are presented as mean ± standard deviation.

139

Time to escape

The older animals took more time to solve the maze and escape than the younger ones (**Figure IV. 22B**). Although all animals reduced the time to solve the maze, the older animals took significantly more time to escape compared to the young ones during the whole training sessions (Supplementary Table IV.5B).

Time to find the first hole

Juvenile and young animals were the ones that spent significantly less time to find any hole compared with the older animals (**Figure IV. 22C**, Supplementary Table IV.5C). These differences between younger and older animals were ameliorated along training, although the time needed for the old animals was still found significantly higher when it was compared with the juvenile and the young ones in the last day of training (Supplementary Table IV.5C).

Time to find the escape hole

Regarding the time to find the escape hole, the younger animals clearly spent less time than the older ones during the whole process (**Figure IV. 22D**), even if all the animals were able to reduce with the training sessions (Supplementary Table IV.5D).

Escape hole as first visited hole

In the younger animals, the number of times in which the escape hole was the first visited hole was higher than the older ones (**Figure IV. 22E**). Both the juvenile and the young animals showed a higher improvement in this parameter, since very significant differences were found in the last training sessions when they were compared with the old and the senile groups (Supplementary Table IV.5E). On the contrary, the older animals did not show an improvement in this parameter (**Figure IV. 22E**).

Decision time

The time that all the animals spent exploring the escape hole before deciding to escape appeared considerably stable during the whole training and retrieval day (**Figure IV. 22F**). The biggest statistical differences were found in the middle of the training period (Supplementary Table IV.5F), coinciding with the moment in which the younger animals reduced this parameter (**Figure IV. 22F**).

Omission errors

Notably, senile animals were the ones with the highest omission errors at the retrieval day (**Figure IV. 22G**). Statistical differences tend to decrease when the different

age-groups were compared along the training (Supplementary Table IV.5G). This parameter changed in a particular way along the training. In the young animals, which were the ones performing fewer omission errors during the whole training, this parameter stayed stable during all the procedure. On the other hand, the juvenile group increased the number of omission errors during the training, but their values were always lower than the older animals. The animals from the old group committed increasing omission errors in the first training days, but then this parameter was reduced until the end of the test. The senile animals, were the group showing the highest number of omission errors, which initially decreased in the training days, but then turned to increase.

Reference memory errors

The younger animals committed significantly less RME than the older ones during the whole training period (**Figure IV. 22H**, Supplementary Table IV.5H). The four groups were able to improve the performance of this parameter along training, particularly the young group.

Working memory errors

The younger animals performed significantly less WME than the older ones (**Figure IV. 22I**, Supplementary Table IV.5I). However, these differences were attenuated along the training due to the fact that the older animals could reduce the WME. In particular, this improvement was more evident in the senile group (**Figure IV. 22I**, Supplementary Table IV.5I).

1.2. Effect of sex

Number of escapes

Both males and females of the different ages increased the number of escapes to the maze along the training sessions (**Figure IV. 23A**). Although no statistical differences were found, males and females showed different behaviors along aging. Juvenile males had a worst performance compared to females in the beginning of the sessions, but at the end of the training, values for both sexes were very similar. Regarding the young age, males decreased the number of correct answers from the training day 4, while females were always able to escape the maze. The behavior observed in the old age was very similar in males and in females. During the senile period, females had more correct answers than males during the whole training, except from the last day.

Time to escape

In general, females were faster to escape the maze than males, in all ages (**Figure IV. 23B**). These differences were particularly significant in the third day of training in the young period.
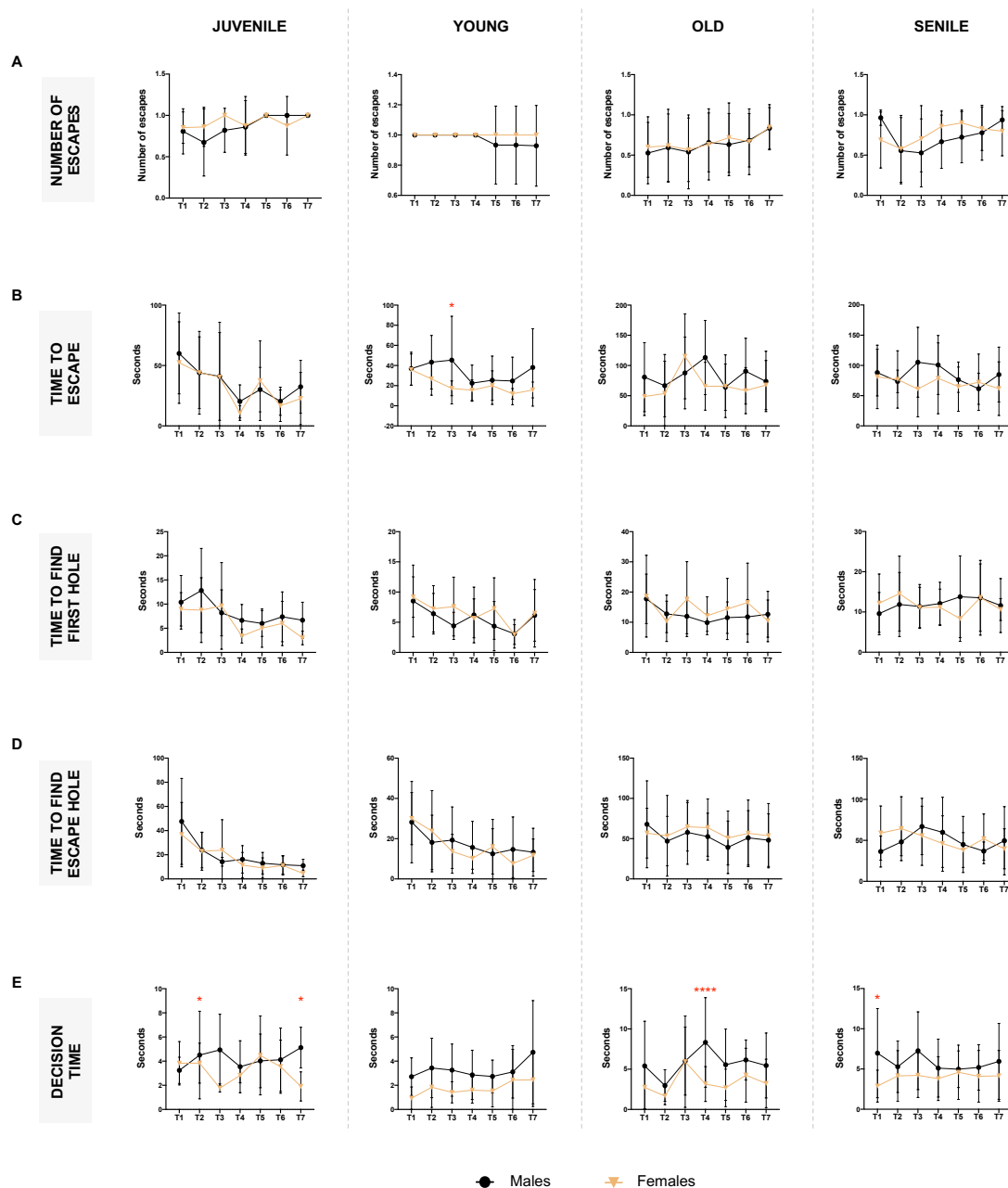
Figure IV. 23. Sex-associated differences in parameters evaluating time in the Barnes maze performance along the acquisition phase. The different parameters evaluated during the training sessions are presented, grouping the animals by sex (males and females): **A)** number of escapes; **B)** time to escape the maze; **C)** time to find the first hole; **D)** time to find the escape hole; **E)** time spent exploring the escape hole before going through it. The effect of sex on the training sessions was determined by using the t-test to compare males and females of the same age, same day of the test. Asterisks indicate statistical differences: * $p < 0.05$, **** $p < 0.0001$. Data are presented as mean ± standard deviation. T1 – T7 = training sessions 1 to 7.

Time to find the first hole

The training sessions allowed the animals to reduce the time to explore the first hole, with no sex-associated differences (**Figure IV. 23C**).

Time to find the escape hole

The time spent to find the escape hole was reduced along the training sessions and no significant differences were found when males and females of the different ages were compared (**Figure IV. 23D**).

Decision time

Decision time was significantly affected by the sex of the animals in the acquisition phase (**Figure IV. 23E**). At all ages, males spent more time exploring the escape hole than females. In particular, significant differences were found in the juvenile age, the young and in the senile. In addition, the behavior observed in males for this parameter tended to the increment of the decision time in the last days of trainings; whereas females tended to maintain or to decrease along the acquisition phase.

Escape hole as first visited hole

The ability to find the escape hole as first visited hole also exerted a sex- and age-dependent outcome, although it did not reach statistical significance (**Figure IV. 24A**). Younger (juvenile and young) females were better at going directly to the escape hole. However, when animals age (old and senile periods), females were less able to find the escape hole as first visited hole.

Omission errors

Females committed less omission errors than males at all ages (**Figure IV. 24B**). These differences were found especially significant at the juvenile and young ages. At these ages, females tended to commit less (or maintain) omission errors, while males improved this parameter in the first sessions but then increased the number of errors. For old and senile animals, both males and females, the number of errors was reduced along the training sessions.

Reference memory errors

Along the acquisition phase, females performed less reference memory errors than males, although significant differences were just found in the young age (**Figure IV. 24C**).

Working memory errors

No significant differences were found regarding the working memory errors committed during the training sessions when males and females were compared (**Figure IV. 24D**). Importantly, at the senile age, females were better at reducing the number of working memory errors during the training.

2. Barnes Maze performance in the retrieval day

2.1. Effect of age

Number of escapes

All the animals belonging to the juvenile and the young groups were able to escape the maze (**Figure IV. 25A**). After the training sessions, a high percentage of animals from the old and senile groups were able to solve the maze; however, some of them did not. Thus, compared to both the juvenile and the young animals, the old and senile groups showed significantly reduced number of escapes (**Figure IV. 25A**).

Time to escape

The time spent to solve the maze in the old and senile animals was very significantly increased, compared to the young group (**Figure IV. 25B**). The young animals showed a slight decrease in the time spent to escape the maze compared to the juvenile animals, although it did not reach statistical significance (**Figure IV. 25B**).

Time to find the first hole

The animals from the young group were the ones that spent less time to visit a first hole in the maze, followed by the juvenile animals (**Figure IV. 25C**). The old animals needed more time to explore any hole compared to the young group (statistically very significant). Similarly, the time spent to find the first hole by the senile animals was very significantly superior compared to the young group and also to the juvenile one (**Figure IV. 25C**).

Time to find the escape hole

In line with the previous results, we did not find significant differences when young and juvenile animals were compared. The young animals were the quickest ones to find the escape hole (**Figure IV. 25D**). Both the old and the senile animals showed a very significant increase in the time to find the escape hole compared with the young group (**Figure IV. 25D**). Statistical differences were also found when old and juvenile animals were compared.
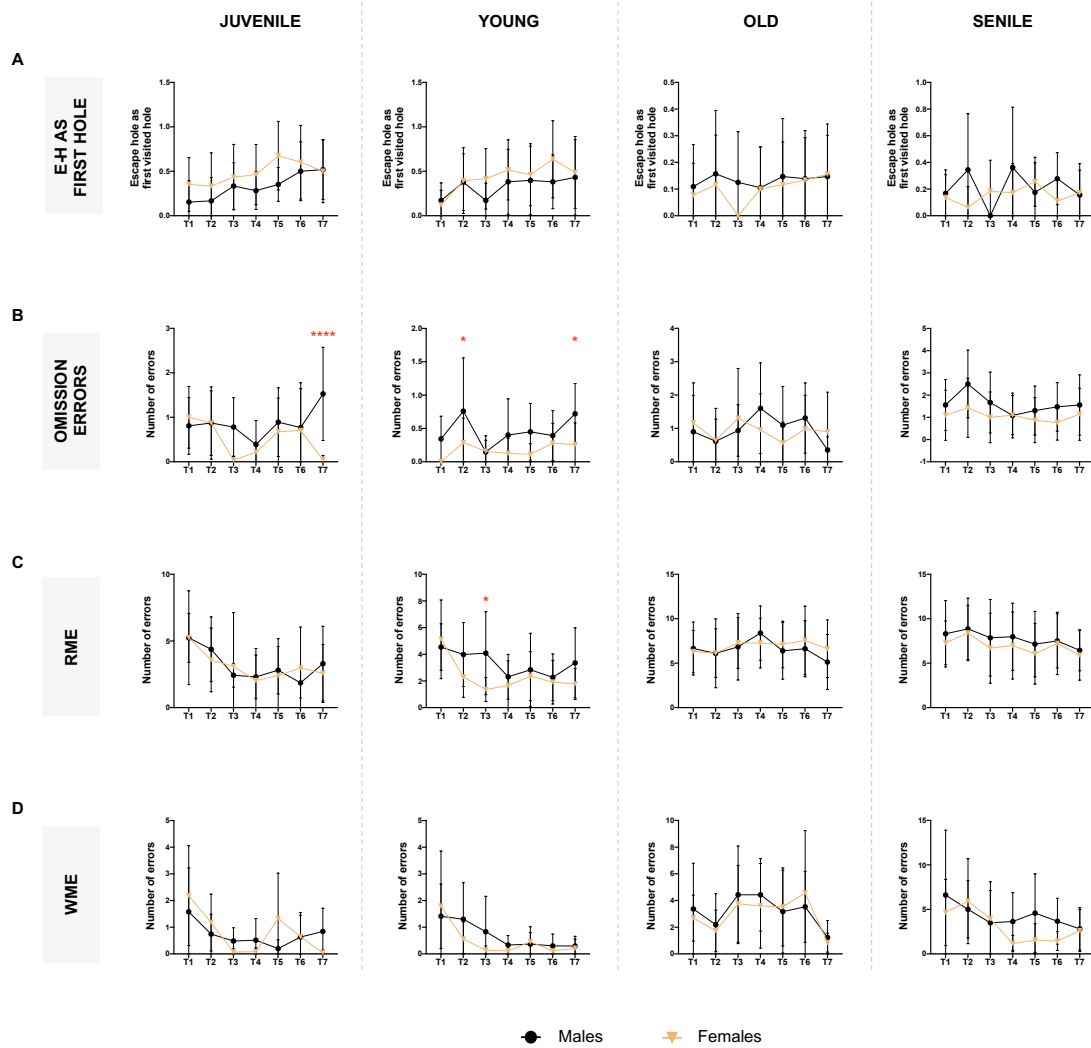
Figure IV. 24. Sex-associated differences in the errors committed in Barnes maze performance along the acquisition phase. The different parameters evaluated during the training sessions are presented, grouping the animals by sex (males and females): **A)** number of times that the animals visited the escape hole as first visited hole; **B)** number of times that the animals visited the escape hole without escaping (omission errors); **C)** number of reference memory errors; and **D)** number of working memory errors. The effect of sex on the training sessions was determined by using the t-test to compare males and females of the same age, same day of the test. Asterisks indicate statistical differences: Asterisks indicate statistical differences: * $p<0.05$, **** $p<0.0001$. Data are presented as mean ± standard deviation. Abbreviations: E-H = escape hole; RME =reference memory errors; WME = working memory errors; T1 – T7 = training sessions 1 to 7.

Escape hole as first visited hole

The young animals were the ones with the highest number of times going to the escape hole as first visited hole (**Figure IV. 25E**). This parameter appeared slightly decreased in the juvenile animals, but it did not reach statistical significance. Old and senile animals went to the escape hole as first visited hole fewer times than the young group, which was found to be very significant in the case of the old animals (**Figure IV. 25E**).

Figure IV. 25. Effect of age in the different parameters evaluated in the retrieval day of the Barnes Maze test. The influence of the age of the animals was studied in the different parameters of the BM test: **A)** number of escapes; **B)** time to escape the maze; **C)** time to find the first hole; **D)** time to find the escape hole; **E)** number of times that the animals visited the escape hole as first visited hole; **F)** time spent exploring the escape hole before going through it; **G)** number of times that the animals visited the escape hole without escaping; **H)** number of reference memory errors; and **I)** number of working memory errors. Age-associated differences were determined by ordinary one-way ANOVA + Tukey multiple comparison test. Asterisks indicate statistical differences vs the juvenile animals: * $p<0.05$, ** $p<0.01$; alpha character indicates statistical differences vs the young group: α $p<0.05$; $\alpha\alpha\alpha$ $p<0.001$. $\alpha\alpha\alpha\alpha$ $p<0.0001$; # symbol indicates statistical differences vs the old group: # $p<0.05$. Data are presented as individual values, being the horizontal line the mean of each group.

Omission errors

The number of times that the senile animals visited the escape hole without escaping though it, was significantly increased compared to all the other ages (**Figure IV. 25G**).

Reference memory errors

The young group was the one with the lowest number of RME (**Figure IV. 25H**). Compared to it, the juvenile showed a little increase in the RME, but it was not found statistically significant. On the other hand, the number of RME was very significantly increased in the old and senile animals compared to both the juvenile and the young groups (**Figure IV. 25H**).

Working memory errors

The number of WME was found to increase in parallel with the age of the animals: the juvenile group showed the lowest mean of WME committed, while this parameter significantly increased in the senile group (**Figure IV. 25I**).

2.2.   Effect of sex

The effect of sex on the performance of the Barnes Maze test was studied (Supplementary Table IV.6) and some parameters were found significantly different between males and females (**Figure IV. 26**). Regarding the retrieval day, the number of escapes (**Figure IV. 26A**), the time to escape (**Figure IV. 26B**), the omission errors (**Figure IV. 26G**), the RME (**Figure IV. 26H**) and the WME (**Figure IV. 26I**), were not affected by the sex of the animals. On the contrary, significant differences between males and females were found in the time spent to find the first hole (**Figure IV. 26C**) and the escape hole (**Figure IV. 26D**), the number of times in which the escape hole was the first visited hole (**Figure IV. 26E**) as well as the decision time (**Figure IV. 26F**).

Time to find the first hole. Significant differences were found at the juvenile age: males spent more time to find the first hole in the maze than females (**Figure IV. 26C**).

Time to find the escape hole. Coinciding with the previous parameter, at the juvenile age, males spent significantly more time to find the escape hole than females. This situation was inverted as the animals aged: old females spent significantly more time to find the escape hole than males (**Figure IV. 26D**).

Escape hole as first visited hole. At the young age, the number of times in which females went to the escape hole as the first visited hole was higher than males, although it did not reach statistical significance (**Figure IV. 26E**). This situation was inverted at the old age: the number of times in which females chose the escape hole as first visited hole was significantly reduced compared to males.

Decision time. Differences along aging according to the sex of the animals were found when old males and females were compared: females spent significantly less time exploring the escape hole before solving the maze than males (**Figure IV. 26F**).
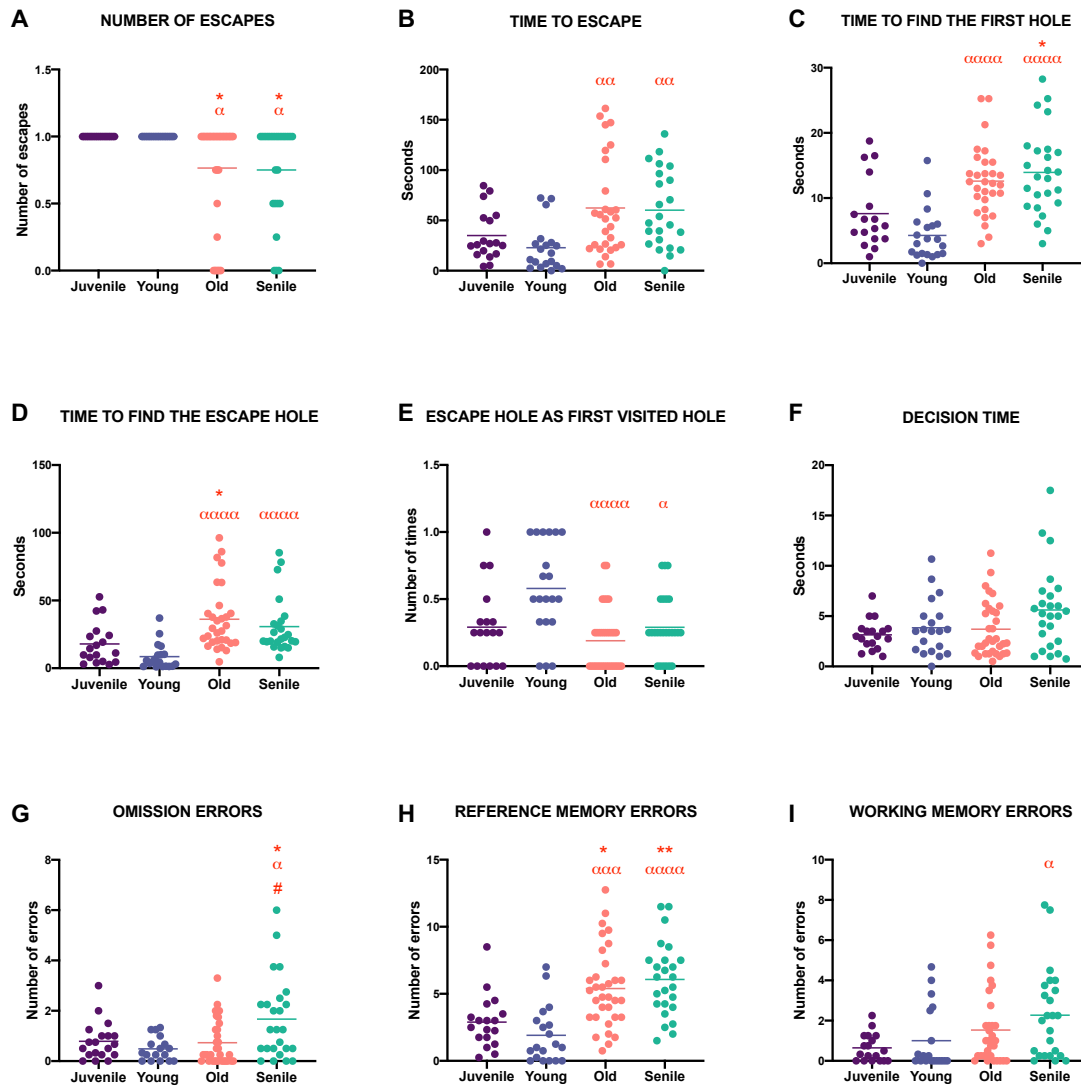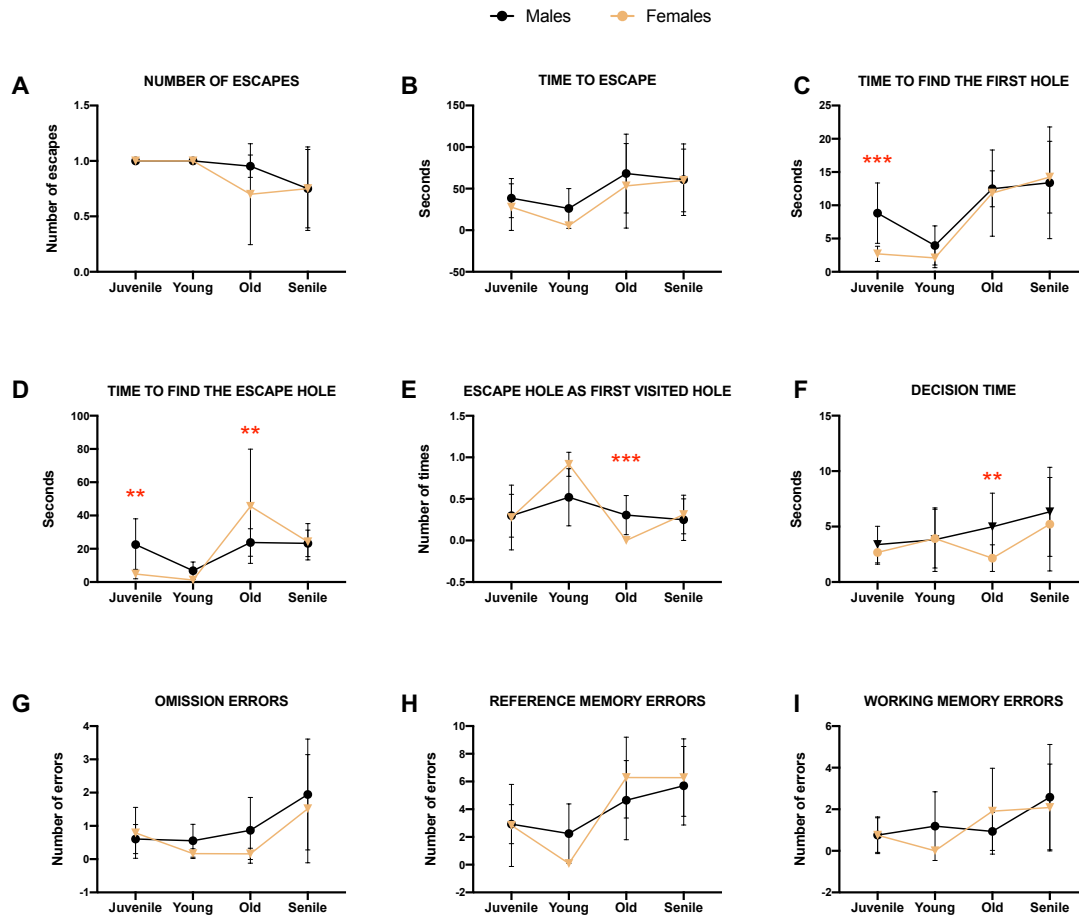

Figure IV. 26. **Effect of sex in the different parameters evaluated in the retrieval day of the Barnes Maze test.** The influence of the sex of the animals was studied in the different parameters of the BM test: **A)** number of escapes; **B)** time to escape the maze; **C)** time to find the first hole; **D)** time to find the escape hole; **E)** number of times that the animals visited the escape hole as first visited hole; **F)** time spent exploring the escape hole before going through it; **G)** number of times that the animals visited the escape hole without escaping; **H)** number of reference memory errors; and **I)** number of working memory errors. The effect of sex on the training sessions was determined by using the t-test to compare males and females of the same age. Asterisks indicate statistical differences when males and females of the same age were compared: ** $p < 0.01$; *** $p < 0.001$. Data are presented as mean ± standard deviation.

3. Microglia in the hippocampus along aging and sex differences

Neuroinflammatory processes associated to microglial cells was studied by Iba1 immunolabeling in the hippocampus. Results are presented according to the hippocampal subareas analyzed: DG (**Figure IV. 27**), CA1 (**Figure IV. 28**) and CA3 (**Figure IV. 29**).

3.1. Dentate gyrus

The Iba1+ area showed a sex-dependent behavior along aging in the DG. Males did not show changes when the different ages were compared (**Figure IV. 27A**), whereas a very significant increase in this microglial marker in females along aging (**Figure IV. 27B**). Although no significant differences were found when both sexes were compared along aging, **Figure IV. 27C** shows that males and females are most divergent at the young stage.

DENTATE GYRUS

Figure IV. 27. Study of the microglial state in the dentate gyrus of the dorsal hippocampus. Quantification of the surface immunostained for Iba1 (area expressed as % of the total area) in the molecular **(A-C)** and in the polymorphic layers **(D-F)**. In both areas, the study was performed along aging in males **(A, D)** and females **(B, E)**. Statistical differences along aging were tested using the one-way ANOVA + Tukey multiple comparison test. Males and females were compared **(C, F)**. Sex-related differences were evaluated by using the t-test to compare males and females of the same age. In the graphs, asterisks are used to indicate the significance of statistical differences: * p<0.05, ** p<0.01, **** p<0.0001. Data are expressed as mean ± standard deviation.

The opposite situation was found in the polymorph layer: the surface immunoreactive for Iba1 was significantly increased as males aged (**Figure IV. 27D**), but not changes were observed in females (**Figure IV. 27E**). When males and females were compared, microglia immunostaining was significantly elevated in the juvenile and young males compared with females of the same age (**Figure IV. 27F**). These differences disappeared in the older ages (**Figure IV. 27F**).

A Males
CA1 SLM

B Females
CA1 SLM

C Males *vs* Females

D Males
CA1 *stratum radiatum*

E Females
CA1 *stratum radiatum*

F Males *vs* Females
CA1 *stratum radiatum*

G Males
CA1 *stratum oriens*

H Females
CA1 *stratum oriens*
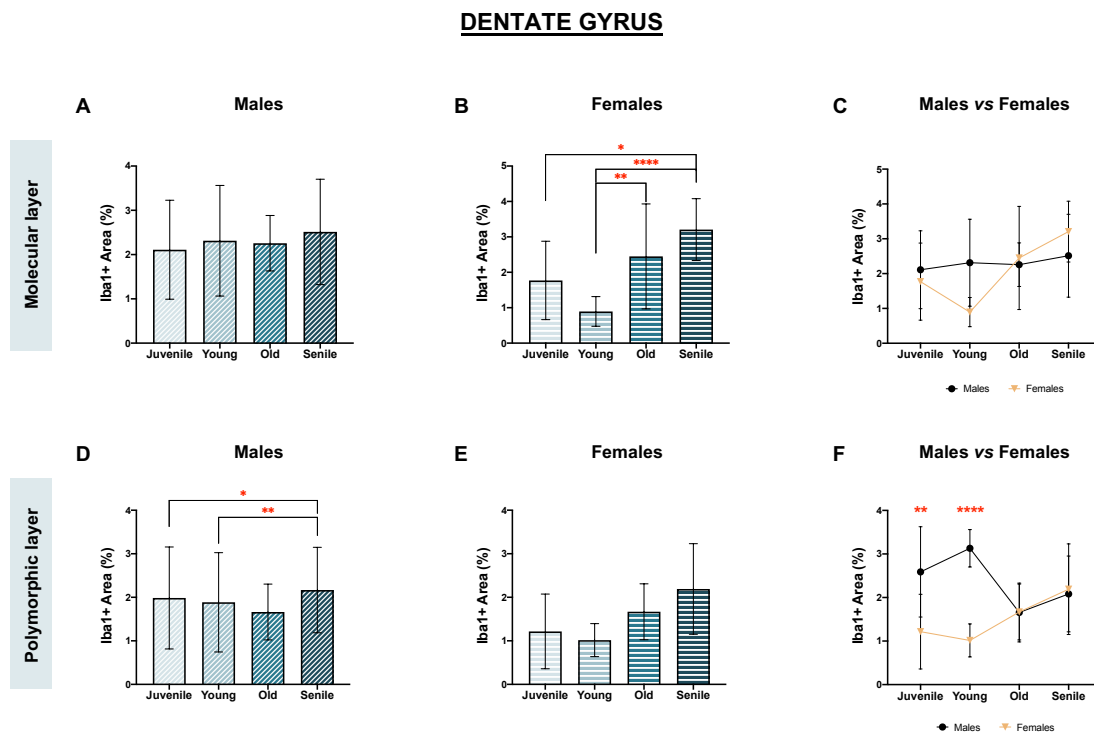
I Males *vs* Females
CA1 *stratum oriens*

Figure IV. 28. Study of the microglial state in the CA1 region of the dorsal hippocampus. Quantification of the surface immunostained for Iba1 (area expressed as % of the total area) in the *stratum lacunosum moleculare* **(A-C)** in the *stratum radiatum* **(D-F)** and in the *stratum oriens* **(G-I)**. In the three areas, the study was performed along aging in males **(A, D, G)** and females **(B, E, H)**. Statistical differences along aging were tested using the one-way ANOVA + Tukey multiple comparison test. Then, males and females were compared **(C, F)**. Sex-related differences were evaluated by using the t-test to compare males and females of the same age. In all graphs, asterisks are used to indicate the significance of statistical differences: * p<0.05, ** p<0.01, *** p<0.001, **** p<0.0001. Abbreviations: CA1 = C*ornu Ammonis* region 1; SLM = *stratum lacunosum moleculare.* Data are expressed as mean ± standard deviation.

3.2. CA1

Results obtained for both the SLM and SR regions showed a sex-dependent behavior. In SLM and SR, males' levels Iba1 immunoreactive surface remained stable along aging (**Figure IV. 28A**). On the contrary, females showed a very significant increment of this parameter (**Figure IV. 28B**). No significant differences were found when both sexes were compared along aging (**Figure IV. 28C**). The analysis of males' SR region showed

CA1 *stratum radiatum* CA1 *stratum radiatum* CA1 *stratum radiatum*

a tendency to increase the fraction occupied by Iba1 immunostaining along aging, with no significant differences when the different ages were compared (**Figure IV. 28D**). This parameter was significantly affected by the age of the animals for females (**Figure IV. 28E**): the area immunostained for Iba1 significantly increased from the younger ages to the old one, and then decreased when senile animals were compared with the old ones. When males and females were compared along aging, we detected that young males had a significant higher Iba1 area in this CA1 region (**Figure IV. 28F**).

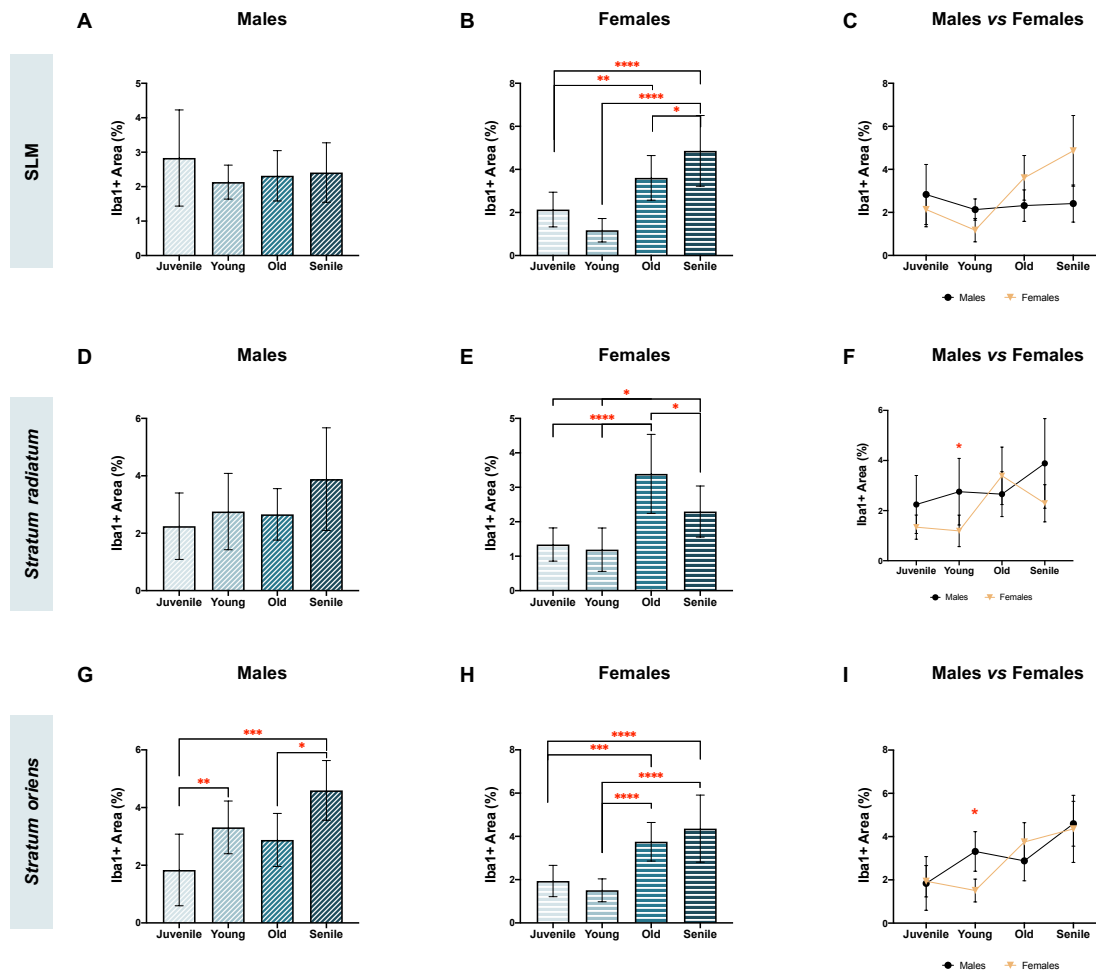CA1 *stratum oriens* CA1 *stratum oriens* CA1 *stratum oriens*
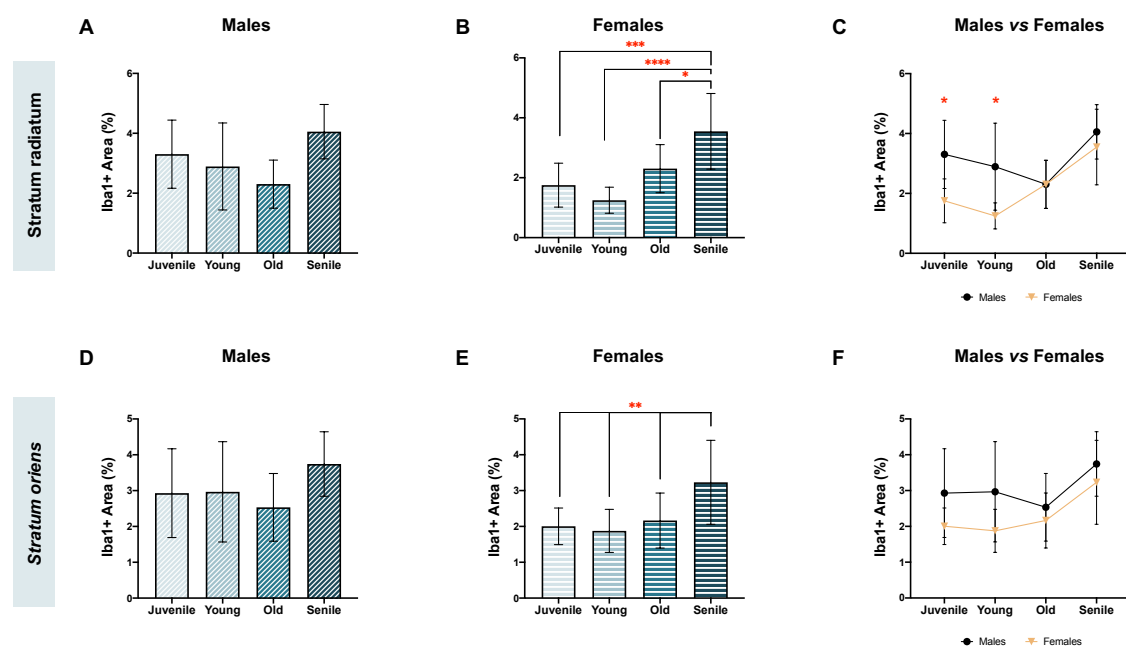
Figure IV. 29. **Study of the microglial state in the CA3 region of the dorsal hippocampus.** Quantification of the surface immunostained for Iba1 (area expressed as % of the total area) in the *stratum radiatum* **(A-C)** and in the *stratum oriens* **(D-F)**. In both areas, the study was performed along aging in males **(A, D)** and females **(B, E)**. Statistical differences along aging were tested using the one-way ANOVA + Tukey multiple comparison test. Then, males and females were compared **(C, F)**. Sex-related differences were evaluated by using the t-test to compare males and females of the same age. In all graphs, asterisks are used to indicate the significance of statistical differences* $p<0.05$, ** $p<0.01$, *** $p<0.001$, **** $p<0.0001$. Data are expressed as mean ± SD. Abbreviations: CA3 = *Cornu A*mmonis region 3. Data are expressed as mean ± standard deviation.

In the SO, both males and females showed a very significant increase in the Iba1+ area (**Figure IV. 28G, H**). Differences between both sexes were statistically significant at the young age, males having the highest values (**Figure IV. 28I**).

3.3. CA3

The two CA3 subareas analyzed, the SR and the SO, showed a similar pattern along aging. In males, expression of the microglial marker Iba1 tends to decrease from the

juvenile age to the old, and then increased in the senile age, although no statistical significance was found in these changes (**Figure IV. 29A, D**). On the contrary, the surface immunolabeled for Iba1 significantly increased along aging in females, both in the SR and in the SO (**Figure IV. 29B, E**).

Interestingly, when the results for males and females were confronted, we found that the Iba1+ area was higher in males than in females (in all ages, except from old in the SR) (**Figure IV. 29C, F**). These differences were especially significant in the juvenile and young period in the SR (**Figure IV. 29C**).

4. Astroglia in the hippocampus along aging and sex differences

Changes in the astrocytes were analyzed by GFAP immunolabeling in the hippocampus. Results are presented according to the hippocampal subareas analyzed: DG (**Figure IV. 30**), CA1 (**Figure IV. 31**) and CA3 (**Figure IV. 32**).

4.1. Dentate gyrus

The expression of GFAP in the molecular layer of the DG was extremely affected by the age of the animals: both males and females showed a very significant increase of this astroglial marker along aging (**Figure IV. 30A, B**). When both sexes were contrasted, the area occupied by GFAP was significantly increased in males compared to females at all ages (**Figure IV. 30C**).

In the polymorph layer, GFAP+ area was significantly increased along aging, both in males and females (**Figure IV. 30D, E**). In this layer, no significant differences were found when males and females were compared (**Figure IV. 30F**).

When the two GD subareas are compared, changes in the astrocytes were more exacerbated in the molecular region than in the polymorph one (**Figure IV. 30**).

The fraction immunostained for GFAP in the SO area of the CA1 was significantly influenced by the age and the sex of the animals. When males from the younger ages (juvenile and young) were compared with the older ones (old and senile), a very significant increase in the expression of GFAP was detected (**Figure IV. 31D**). In females, proportion of GFAP immunolabeled area significantly increased from the younger animals to the old age, but it was reduced in the senile animals (**Figure IV. 31E**). Sex-associated differences were found in all ages, having males significantly higher levels of GFAP (**Figure IV. 31F**).

In the SO, GFAP expression also incremented along aging, especially in females (**Figure IV. 31G, H**). Sex-related differences were observed in all ages: males presented significant higher level of GFAP+ area than females (**Figure IV. 31C**).

DENTATE GYRUS

Figure IV. 30. Study of the astrocytic state in the dentate gyrus of the dorsal hippocampus. Quantification of the surface immunostained for GFAP (area expressed as % of the total area) in the molecular **(A-C)** and in the polymorphic layers **(D-F)**. In both areas, the study was performed along aging in males **(A, D)** and females **(B, E)**. Statistical differences along aging were tested using the one-way ANOVA - Tukey multiple comparison test. Males and females were compared **(C, F)**. Sex-related differences were evaluated by using the t-test to compare males and females of the same age. In all graphs, asterisks are used to indicate the significance of statistical differences: * p<0.05, ** p<0.01, **** p<0.0001. Data are expressed as mean ± standard deviation.

4.2. CA1

In the CA1 SLM region, the GFAP+ area significantly increased from the juvenile to the old age, then decreased in the senile stage both in males (**Figure IV. 31A**) and females (**Figure IV. 31B**). Sex-related differences were found at the young stage (**Figure IV. 31C**).

The fraction immunostained for GFAP in the SO area of the CA1 was significantly influenced by the age and the sex of the animals. When males from the younger ages (juvenile and young) were compared with the older ones (old and senile), a very significant increase in the expression of GFAP was detected (**Figure IV. 31D**). In females, proportion of GFAP immunolabeled area significantly increased from the younger animals to the old age, but it was reduced in the senile animals (**Figure IV. 31E**). Sex-associated differences were found in all ages, having males significantly higher levels of GFAP (**Figure IV. 31F**).

In the SO, GFAP expression also incremented along aging, especially in females (**Figure IV. 31G, H**). Sex-related differences were observed in all ages: males presented significant higher level of GFAP+ area than females (**Figure IV. 31C**).
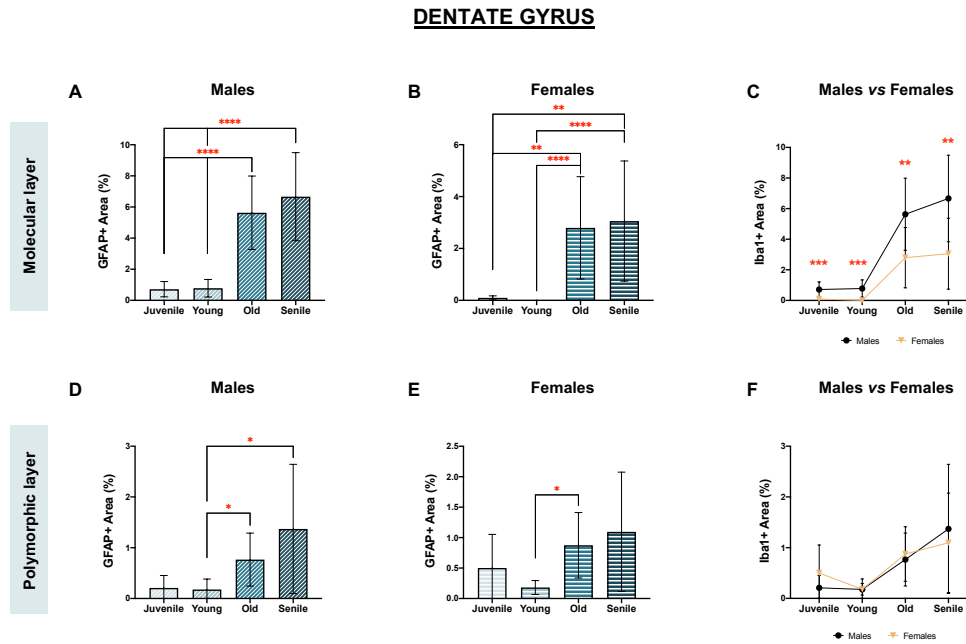
153

Figure IV. 31. Study of the astrocytic state in the CA1 region of the dorsal hippocampus. Quantification of the surface immunostained for GFAP (area expressed as % of the total area) in the *stratum lacunosum moleculare* **(A-C)** in the *stratum radiatum* **(D-F)** and in the *stratum oriens* **(G-I)**. In the three areas, the study was performed along aging in males **(A, D, G)** and females **(B, E, H)**. Statistical differences along aging were tested using the one-way ANOVA + Tukey multiple comparison test. Then, males and females were compared **(C, F)**. Sex-related differences were evaluated by using the t-test to compare males and females at the same age. In all graphs, asterisks are used to indicate the significance of statistical differences: p<0.05, ** p<0.01, *** p<0.001, **** p<0.0001. Abbreviations: CA1 = *Cornu Ammonis* region 1; SLM = *stratum lacunosum moleculare*. Data are expressed as mean ± standard deviation.

4.3. CA3

Age and sex significantly affected GFAP levels in the CA3 hippocampal subregion (**Figure IV. 32**).

At the level of the SR, males showed a significant increase the surface immunostained for GFAP from the juvenile animals to the old ones, but then significantly decreased in the senile period (**Figure IV. 32A**). A very significant increase in this astroglial

marker was found for females along aging (**Figure IV. 32B**). When both sexes were compared, old males showed significantly high levels of GFAP compared to females (**Figure IV. 32C**).

Finally, the area fraction immunoreactive for GFAP significantly increased along aging in both males (**Figure IV. 32D**) and females (**Figure IV. 32E**). Sex-associated differences were found: males showed significantly higher levels of GFAP compared to females (**Figure IV. 32F**).
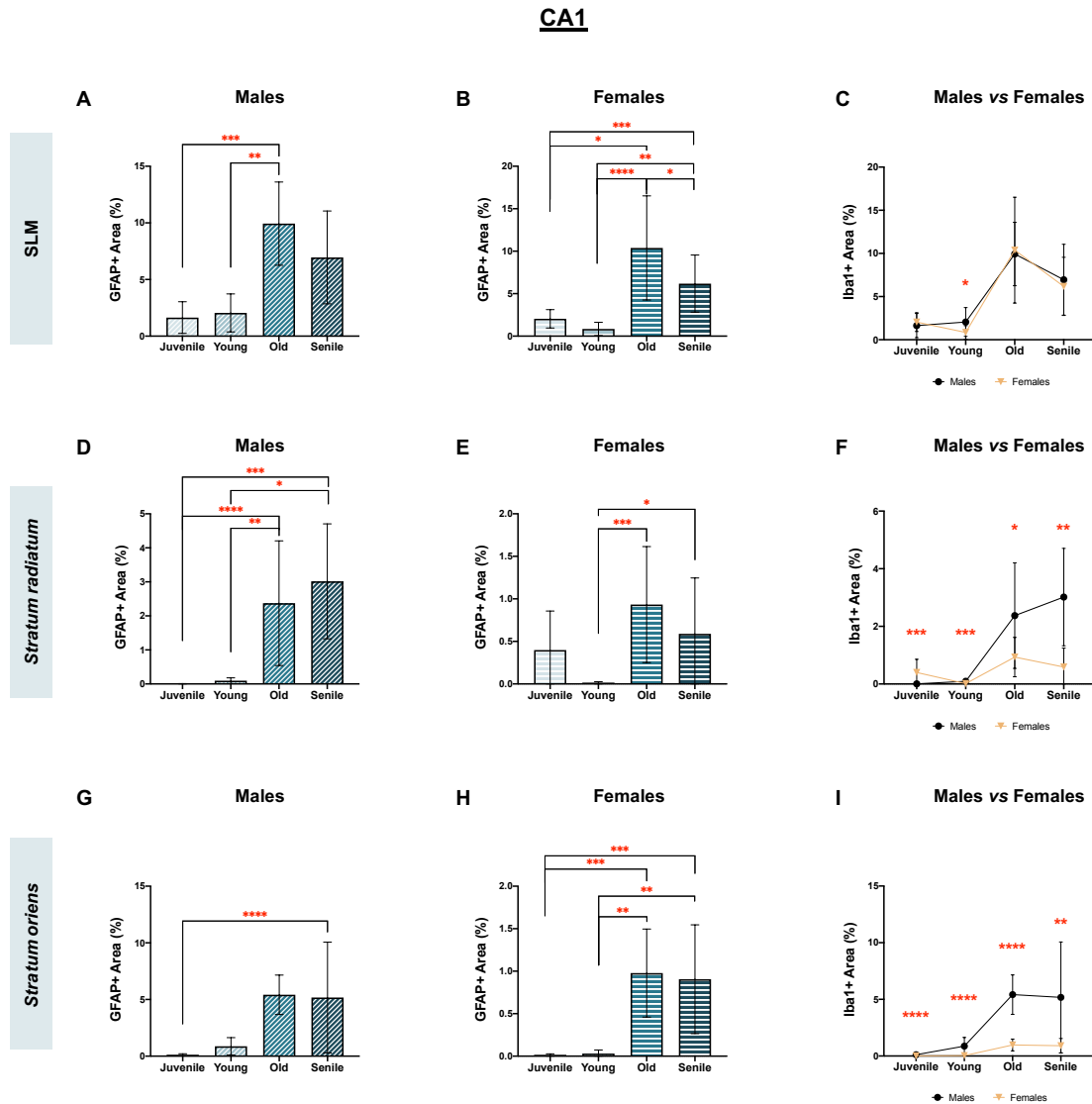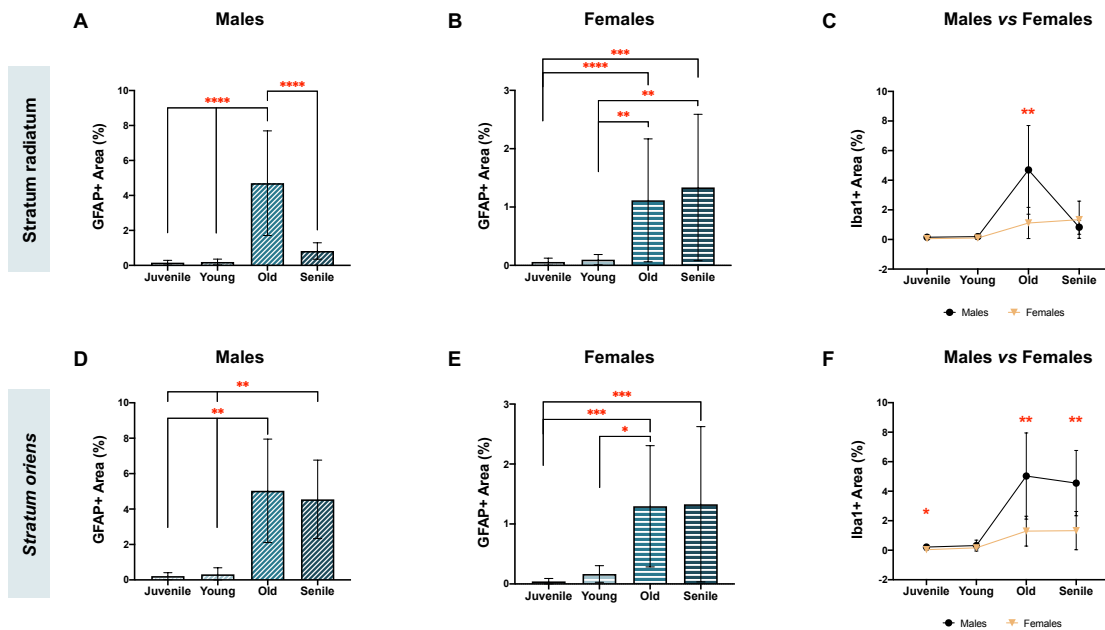

Figure IV. 32. **Study of the astrocytic state in the CA3 region of the dorsal hippocampus.** Quantification of the surface immunostained for GFAP (area expressed as % of the total area) in the *stratum radiatum* **(A-C)** and in the *stratum oriens* **(D-F).** In both areas, the study was performed along aging in males **(A, D)** and females **(B, E)**. Statistical differences along aging were tested using the one-way ANOVA + Tukey multiple comparison test. Then, males and females were compared **(C, F)**. Sex-related differences were evaluated by using the t-test to compare males and females of the same age. In all graphs, asterisks are used to indicate the significance of statistical differences* p<0.05, ** p<0.01, *** p<0.001, **** p<0.0001. Data are expressed as mean ± SD. Abbreviations: CA3 = *Cornu A*mmonis region 3. Data are expressed as mean ± standard deviation.

Table IV. 2. **Relationship between microglia immunostaining and BM performance.** Spearman correlations were performed among the different parameters evaluated in the BM test and the Iba1+ area in the different hippocampal subregions. Asterisks indicate that the correlation was found statistically significant at the level of: * p<0.05; ** p<0.01. Abbreviations: CA1 = *Cornu Ammonis* region 1; CA3 = *Cornu Ammonis* region 3; DG = dentate gyrus; SLM = *stratum lacunosum moleculare*; SO = *stratum oriens*; SR = *stratum radiatum*; r = Spearman's coefficient.

	DG		CA1			CA3	
	Molecular layer	Polymorphic layer	SLM	SR	SO	SR	SR
A. Number of escapes							
r	-0.086	0.072	0.014	-0-257	-0227	-0,039	0,069
p value	ns	ns	ns	ns	ns	ns	ns
B. Time to escape							
r	0.229	0.114	0.279	0.262	0.236	0,089	0,160
p value	ns	ns	ns	ns	ns	ns	ns
C. Time to find the first hole							
r	0.399	0.174	0.334	0.440	0.329	0,287	0,133
p value	*	ns	*	**	*	ns	Ns
D. Time to find the escape hole							
r	0.355	0.027	0.402	0.504	0.419	0,218	-0,007
p value	*	ns	*	**	*	ns	ns
E. Escape hole as first visited hole							
r	0.078	0.111	-0.094	-0.304	-0,217	-0,019	0,170
p value	ns	ns	ns	ns	ns	ns	ns
F. Decision time							
r	- 0.076	-0.070	-0.123	-0.094	-0,152	-0,192	0,010
p value	ns	ns	ns	ns	ns	ns	ns
G. Omission errors							
r	-0.010	0.024	0.124	0.080	0,071	0,140	0,107
p value	ns	ns	ns	ns	ns	ns	ns
H. Reference memory errors							
r	0.169	-0.050	0.373	0.412	0,353	0,217	0,008
p value	ns	ns	*	**	*	ns	ns
I. Working memory errors							
r	0.152	0.060	0.263	0.379	0,316	0,182	0,041
p value	ns	ns	ns	*	*	ns	ns

5. Neuroinflammatory processes correlate with BM performance

In order to explore the relationship among the neuroinflammatory changes in the different hippocampal subareas and the BM performance, correlation studies were performed. The results obtained for microglia are reported in **Table IV. 2**, whereas the ones regarding astrocytes are collected in **Table IV. 3**.

5.1. Microglial changes and BM performance

Among all the parameters studied, the following significant correlations were found:

- A significant positive relationship was found for microglia in the DG molecular layer and the CA1 (all three subregions) and the time to find any hole and the escape hole (**Table IV. 2C, D**).

- Microglia in the CA1 region (SLM, SR and SO) was positively correlated with RME (**Table IV. 2H**).

- The increase in the number of WME was significantly correlated with higher levels of Iba1 in the CA1 SO and SR subareas (**Table IV. 2HI**).

Table IV. 3. **Relationship between astroglia immunostaining and BM performance.** Spearman correlations were performed among the different parameters evaluated in the BM test and the GFAP+ area in the different hippocampal subregions. Asterisks indicate that the correlation was found statistically significant at the level of: * $p<0.05$; ** $p<0.01$, *** $p<0.001$, **** $p<0.0001$. r = Spearman's coefficient; DG = dentate gyrus; CA1 = *Cornu Ammonis* region 1, CA3 = *Cornu Ammonis* region 3, SLM = *stratum lacunosum moleculare*, SR = *stratum radiatum*, SO = *stratum oriens*.

	DG		CA1			CA3	
	Molecular layer	Polymorphic layer	SLM	SR	SO	SR	SO
A. Number of escapes							
r	-0406	-0,387	-0,374	-0,422	-0,295	-0,454	-0,388
p value	**	*	*	**	ns	**	*
B. Time to escape							
r	0,130	0,306	0,216	0,234	0,052	0,156	0,124
p value	ns	ns	ns	ns	ns	ns	ns
C. Time to find the first hole							
r	0,439	0,458	0,476	0,343	0,356	0,433	0,422
p value	**	**	**	*	*	**	**
D. Time to find the escape hole							
r	0,442	0,595	0,563	0,448	0,220	0,540	0,385
p value	**	***	***	**	ns	**	*
E. Escape hole as first visited hole							
r	-0,099	-0,458	-0,314	-0,306	-0,004	-0,295	-0,030
p value	ns	**	ns	ns	ns	ns	ns
F. Decision time							
r	0,054	-0,257	-0,007	0,019	0,140	0,109	-0,041
p value	ns	ns	ns	ns	ns	ns	ns
G. Omission errors							
r	0,017	0,026	-0,030	-0,047	0,045	0,071	-0,063
p value	ns	ns	ns	ns	ns	ns	ns
H. Reference memory errors							
r	0,451	0,632	0,554	0,523	0,282	0,505	0,399
p value	**	****	***	***	ns	**	*
I. Working memory errors							
r	0,280	0,417	0,291	0,283	0,118	0,327	0,207
p value	ns	*	ns	ns	ns	*	ns

5.2. Astrocytic changes and BM performance

The GFAP expression showed a significant influence in the BM performance, since the following significant correlations were found:

- The number of escapes was negatively correlated with GFAP expression in all the hippocampal subregions, except from the CA1 SO (**Table IV. 3A**).

- The time spent to find the first hole was positively correlated with GFAP immunostaining in all the hippocampal subareas (**Table IV. 3C**).

- The time spent to find the escape hole was positively correlated with the area fraction immunolabeled for GFAP in all the hippocampal subareas, except from the CA1 SO (**Table IV. 3D**).

- The ability of visiting the escape hole as first hole showed a significant negative correlation with GFAP levels in the polymorphic layer of the DG (**Table IV. 3E**).

- Very significant positive correlations were found between reference memory errors and GFAP immunostaining in all areas, except from CA1 SO (**Table IV. 3H**).

- Working memory errors appeared positively correlated with GFAP expression in the polymorphic layer of the DG and the SR of the CA3 (**Table IV. 3I**).

DISCUSSION

Discussion of the method. Limitations of the study

The main limitation that we encountered was regarding the glial markers used. Although Iba1 and GFAP are well-accepted markers for the neuroinflammatory studies, detection of these proteins does not enable the complete visualization of microglia and astrocytes and, therefore, cannot be used as a single tool to explore morphological changes. In this line, pro- or anti-inflammatory profiles cannot be determined by the use of these markers and future studies must complement the results obtained here to completely understand the role of glia in cognitive changes associated to aging.

Discussion of results

In the present study the effect of age and sex in the cognitive performance in the *O. degus* has been determined, as well as the possible link with the neuroinflammatory state (microglia and astroglia) in the dorsal hippocampus.

The BM is one of the most preferred behavioral approaches to assess the hippocampal-based spatial reference memory in rodent models (Sharma et al., 2010; Pitts, 2018). Since it was first described by Carol Barnes (Barnes, 1979), different BM's protocols have been described, adapting and optimizing the original guidelines to the experimental conditions and strain used (Gawel et al., 2019). The protocol used in this

thesis was previously demonstrated to be suitable to explore differences in the cognitive performance in the *O. degus* (Estrada et al., 2015a; b, 2019; Rivera et al., 2020).

In the recent years, studies evaluating the effect of age in cognitive performance in the *O. degus* have been performed (Ardiles et al., 2012; Rivera et al., 2021), while others have analyzed sex differences in the BM performance in young animals (Popović et al., 2010). However, no studies have characterized the simultaneous effect of age and sex on cognition in this species. Our study was conducted in *O. degus* aged from 6 months old (juvenile) to 6-7 years old (senile), both males and females. Significant differences in the BM performance were found along aging and when males and females were compared, both along the training sessions and in the retrieval day.

Age-related differences in the BM performance

As expected, younger animals (juvenile and young groups) showed better results in the BM than the older ones (old and senile). However, even if cognitive performance was better in the younger animals in all the experimental phases, statistical differences among the different age groups tended to be reduced as the training sessions advanced. That is, even in the advanced ages, cognitive decline can be rescued (in part) by memory training in the *O. degus*. These results are in agreement with those previously reported that showed that aging is associated with cognitive decline (De Lima et al., 2005; Burke et al., 2010; Ardiles et al., 2012; Rivera et al., 2021).

The younger animals were faster in solving the maze than the older ones, i.e., they spent less time to escape or to find the escape hole. Some authors have suggested that older animals might spend more time to solve the maze due to their reduced locomotor activity (Gawel et al., 2019). However, a recent study conducted by Rivera and collaborators demonstrated that for the *O. degus*, no significant differences were found in the motor activity (evaluated by the Open field test) along aging. The evaluation of decision time did not show significant age-associated differences, which means that even if older animals spent more time to find the escape hole (motor-dependent task), once they found it, they recognized it as the exit of the maze. All in all, as suggested by other authors, when aged animals are evaluated, other parameters analyzed in the test are more sensitive than those based on the time (Barrett et al., 2009; O'Leary and Brown, 2013; Gawel et al., 2019). Instead, the number of visits to the escape hole as first visited hole and the number of errors (omission, reference and working memory) are the most accurate to measure the animal's performance (O'Leary and Brown, 2013).

In the juvenile and young animals, the number of times choosing the escape hole as the first explored hole was significantly increased along the training sessions. This cognitive performance was accompanied by a reduction in the number of reference and working memory errors, thus indicating that younger animals follow a learning strategy based on the spatial references. It is worthy to mention that, in parallel with this behavior, the number of omission errors recorded in the last days for the juvenile animals increased when it was compared with the initial measurements (instead of decreasing). This behavior is in agreement with the data provided by other authors showing that, along training, the animals can worsen some parameters of the BM, not because they are cognitively impaired but because they lose the motivation to escape (Harrison et al., 2006). This lack of motivation has been explained by the familiarization with the environment and the aversive stimuli of the test (Inman-Wood et al., 2000; Gawel et al., 2019). The protocol used in this study solely included bright light as an aversive stimulus since supporting evidence points out that the open platform where the test is performed acts as an aversive stimulus itself, since rodents tend to avoid open spaces (Locklear and Kritzer, 2014). In addition, other works demonstrate that placing aversive stimulus such as fans or sound, can actually impair animals from focusing on the spatial task (Gawel et al., 2019). Indeed, previous pilot tests of our group confirmed that adding aversive sounds while the test was performed had a negative effect for the *O. degus*, making them completely freeze and preventing them from escaping the maze.

Another alternative to explain these findings is that once identified the escape path, younger animals are motivated to explore other alternatives, resulting in the higher number of errors at the end of the test (Grootendorst et al., 2001; Rivera et al., 2016).

The older animals increased their ability to solve the maze as shown by the increment in the number of escapes along the training sessions and in the retrieval day. However, differently to the younger animals, they did not use a learning strategy based on spatial references as they did not reduce the number of reference and working memory errors performed, nor went to the escape hole as first visited hole. These data are in contrast with previous studies showing that no significant differences were found in the number of reference and memory errors in the aged degus (Ardiles et al., 2012), which might be explained by the different ages evaluated. Therefore, in our experimental conditions, the aged degus (>4-5 years old) are able to remember that there is an escape hole, but they move randomly along the platform to find it.

Importantly, although no significant differences were found in the BM performance between juvenile and young animals, we observed that the juvenile group showed a slight worse performance than the young one; e.g., they spent more time to escape the maze,

more omission and reference errors. These observations have been described by other authors (Campbell and Campbell, 1962; Hayne, 2004; Li et al., 2014), and are supported by the incomplete development of the neural connections for long-term memory (Rudy and Morledge, 1994).

Sex-related differences in BM performance

Few studies have considered the simultaneous effect of age and sex in the BM performance. Along the training sessions, the *O. degus* females had a better cognitive performance than males in all ages. These findings are in contrast with the general available literature, since the main part of studies indicate that males to have better cognitive performance than females (Vorhees and Williams, 2014; Gawel et al., 2019).

Surprisingly, this behavior was maintained in the retrieval day for juvenile and young females, but in the old and senile ages, females showed a worse cognitive performance than males of the same age. The data obtained might indicate that along aging, males integrate the spatial information acquired during the training sessions more effectively than do females, although females were better at the beginning of the test. These *in vivo* results agree with the electrophysiology study conducted by Olivia and collaborators, in which aged male degus showed a more efficient synaptic plasticity than aged females (Olivia et al., 2022). Further research might focus on the role of sex hormones in these age-related physiological changes that occur differently in males and females.

Neuroinflammation in the hippocampus

Few studies have analyzed how age-related glial changes in the different hippocampal subareas can influence cognition with a sex perspective. Here, we analyzed neuroinflammation in the dorsal hippocampus by Iba1 immunostaining for microglia and by GFAP immunolabeling for astrocytes, considering both age and sex of the animals.

In line with previous studies, both glial markers were significantly increased along aging (Valero et al., 2017). In general, we found that microglia was incremented in the hippocampus of aged degus. However, this response was not homogeneous between males and females. Females showed increased Iba1 levels along aging in both the molecular and in the polymorphic layers of the DG. On the other hand, males showed no changes in Iba1 immunolabeling in the molecular layer, but a significant reduction of this microglial marker in the polymorphic one. Indeed, when males and females were compared along aging, we found that in the younger period (i.e., juvenile and young animals), females presented less surface occupied by microglia, but due to the increment in Iba1 along aging, in the older females its levels were higher than the ones reported in

males. Results obtained for the CA1 and CA3 regions, were in line with the ones in the DG: the most significant changes (increments) regarding Iba1 immunolabelling were detected in females along aging. However, differently to what it was observed in the DG, even if Iba1 levels were more affected by age in females than in males, these levels were higher in all ages in the latter than in the former. This observation was repeated in all the CA1 and CA3 subareas, except from the CA1 SLM, in which old and senile females had higher Iba1 levels than males of the same age.

The astrocytic response exerted more age- and sex-related changes than the ones observed for microglia. Actually, all hippocampal subareas showed significant age-related changes in both males and females. A very significant increase in the GFAP+ area was found in all areas when younger animals were compared with the older ones. However, GFAP levels decreased when animals reached the senile age in the CA1 SLM (in both sexes), in the CA1 SR of females and in the CA3 SR of males; even though these levels were always superior to the ones found in the younger ages.

Interestingly, although significant increases of GFAP immunolabeling were detected in the polymorphic layer of the DG, this layer was found to be the less sensitive to the age-related changes and no significant differences were found when males and females were compared.

Important differences were found when we compared males and females along aging. In the molecular layer of the DG, males' GFAP levels were significantly higher in all the groups of ages than the ones of females. No sex-associated differences were found in the DG polymorphic layer. In the CA1 SLM, although males and females had similar behaviors along aging, significant higher levels of GFAP were found at the young stage. In the CA1 SR and SO, as well as in the CA3 SO, GFAP levels were similar in the younger ages, but as animals aged, males showed significantly higher levels of this astrocytic marker than females. At the CA3 SR level, the highest differences between males and females were found in the old age.

The next step in this study was to explore if Iba1 and GFAP levels were correlated with cognitive performance. Interestingly, higher levels of Iba1 and GFAP were correlated with a worse cognitive performance in the BM, such as increased number of errors or higher latency to escape the maze. Among all the hippocampal subareas studied, changes in the neuroinflammatory state in the CA1 and the DG were the ones having a higher influence on cognitive performance; that is, the increase in the glial markers analyzed was significantly correlated with a worse cognitive performance.

Increasing amount of evidence has indicated that neuroinflammatory processes have an effect on cognition and can even accelerate the progression of protein deposits in AD (Lana et al., 2021). The results provided here suggest that the microglia and astrocytes present in the older animals, would be balance to the detrimental phenotype, as indicated by the correlations with cognitive decline. However, further studies are required to completely understand the interplay among glia-neuronal circuits' integrity-cognitive performance, since neuroinflammatory processes are also for neurogenesis and synapse maintenance (Sierra et al., 2014; Araki et al., 2021). For example, the study conducted by Sampedro-Piquero showed higher GFAP levels in the hippocampus (from the DG, the CA1 and the CA3) of aged rats, which were positively correlated with cognitive improvement after environmental enrichment (Sampedro-Piquero et al., 2014).

In addition, further research is necessary to understand the particular susceptibility of the hippocampal subfields to the age-related neuroinflammation.

SUMMARY OF RESULTS

Taken together, the data presented here provides a first piece of information regarding cognitive decline along aging and the hippocampal-related neuroinflammatory processes with a sex perspective in the *O. degus*. Several lines of evidence might emerge from these results with the aim of deepening in the characterization of the role of glial processes in the age-related cognitive decline. In addition, the use of the *O. degus* as an experimental model offers some key points. Like in humans, we found that although animals followed a tendency along aging comparable to the studies performed in other rodent models, some old and senile individuals presented a young-like cognitive performance. These findings support the idea that changes in memory associated to the aging process presents an individual variability and, therefore, places the degus as a potential tool to explore the individual susceptibility. In line with this idea, and supported by previous studies reporting AD-like histopathological markers, the cognitive decline observed in the *O. degus* could serve to explore whether it corresponds with normal aging or with more severe pathological conditions, and how sporadic AD might be initiated. Thus, the information derived from these findings could give important clues to uncover the age-related mechanisms associated to cognitive impairment and help us to deepen in the pathological course of aging, with the advantage of including the sex perspective.

IV.4. DIFFERENTIAL BRAIN LIPID COMPOSITION, A MATTER OF AGE AND SEX

STATE OF THE ART

Although massive neuronal loss was thought to be the main responsible for brain functional decline in the past, further research demonstrated that cognitive impairment is caused by progressive and relative subtle changes (Mesa-Herrera et al., 2019). Lipids are the major constituents of the CNS and they are crucial for cell architecture and brain function. Accumulating evidence indicates that both lipid metabolism and homeostasis are altered during brain aging, as well as in several pathological conditions such as AD or PD (Kracun et al., 1992; Soreghan et al., 2003; Martinez et al., 2007; Pirman et al., 2011). Indeed, several works have reported specific brain lipid changes related to aging and neurodegeneration (Mesa-Herrera et al., 2019). Some examples of the age-associated lipid changes include modifications of the phospholipids' and gangliosides' proportions and imbalance in the polyunsaturated fatty acids profile (Rouser and Yamamoto, 1968; Farooqui et al., 1988; Svennerholm et al., 1994; Díaz et al., 2018; McFarlane and Kędziora-Kornatowska, 2019). Furthermore, studies analyzing the brain lipid composition have reported that the occurrence of lipid alterations with age does not occur homogeneously but in a region-dependent manner (Söderberg et al., 1990; Svennerholm et al., 1991; Fitzner et al., 2020).

Therefore, a better characterization of the brain composition and the age-related changes in different brain areas, is of particular relevance to understand early neurodegenerative events and the development of early diagnostic tools and pharmacological interventions. In this sense, the availability of adequate experimental models is of vital importance. The *O. degus* has been proposed as an interesting experimental model for aging research, since spontaneous development of several age-associated treats similar to the human ones have been found in this species (Cuenca-Bermejo et al., 2020). However, the lipid composition of its brain has not been explored yet.

Thus, the working hypothesis of this section is that the lipid composition of the *O. degus* changes along aging, with sex-associated differences, and that these alterations are related to the *in vivo* cognitive performance (**Figure IV. 33**).

Determine the brain lipid composition along aging with a sex perspective

EXPERIMENTAL GROUPS

	By age	Young	By sex	Males
		Old		
		Senile		Females

POST MORTEM STUDIES

O. degus **brain areas**   Studies of lipid composition

Prefrontal cortex   Cortex

Cerebellum

Striatum
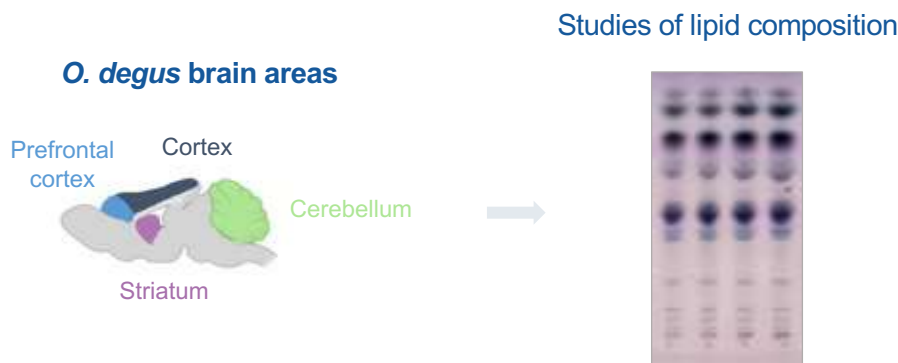
Figure IV. 33. Graphical summary of the experimental design to study the influence of age and sex on brain lipid composition.

RESULTS

1. Protocol optimization for the study of brain lipid content in the *O. degus*.

The lipids' distribution obtained after the TLE partitioning was confronted to the general scheme proposed when the protocol described in the Materials and Methods section was performed (**Figure III. 5**). As shown in **Figure IV. 34A**, the aqueous phase contained exclusively gangliosides and, in minor extend, the glycosphingolipids sulfatides and trihexosylcermides. The rest of the lipids contained in the TLE moved to the organic phase: the most hydrophobic lipids (including cholesterol), glycerophospholipids, neutral sphingolipids (GlcCer and GalCer) and sulfatides (**Figure IV. 34B**). As expected, methanolized organic phase contained most of the lipids found in the organic phase, except from the glycerophospholipids (**Figure IV. 34C**).

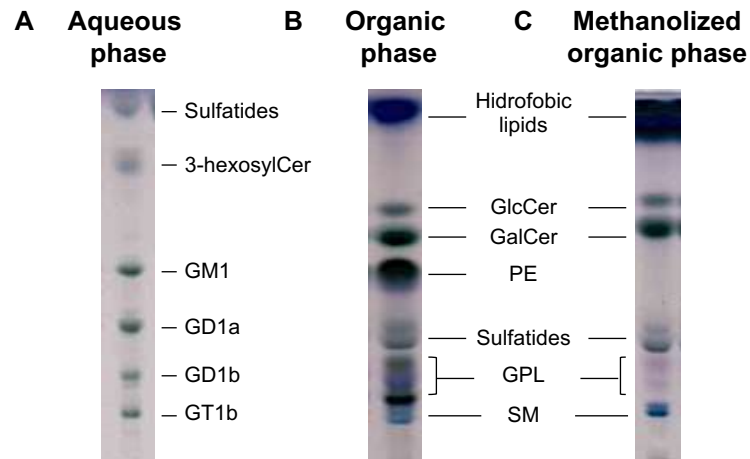**Figure IV. 34. General distribution of the lipid content in the partitioned phases in the brain of *O. degus*. A)** The most hydrophilic lipids (i.e., sulfatides, 3 hexosylCer and gangliosides) were resolved by the TLC of the aqueous phase using the solvent system $CHCl_3:CH_3OH:CaCl_2$ 0.2% (50:42:11, by volume) and stained with anisaldehyde. **B)** Organic phase composition was analyzed by TLC in $CHCl_3:CH_3OH:H_2O$ (110:40:6, by volume), in which the lipids that were not distributed into the aqueous phase were visualized. **C)** Methanolized organic phase corresponds to the organic phase in which the main proportion of glycerophospholipids was removed. Lipid content in the methanolized organic phase was resolved by TLC in $CHCl_3:CH_3OH:H_2O$ (110:40:6, by volume). Abbreviations: 3-hexosylCer = trihexosylceramide; GalCer = galactosylceramide; GlcCer = glucosyceramide; GPL = glycerophospholipids; PE = phosphatidylethanolamine; SM = sphingomyelin; TLC = thin layer chromatography.

2. Protein content and lipid/protein relationship are region-dependent

Total protein content was determined in the brain lysates of the four brain areas used in this study (the PFC, the striatum, the cortex and the cerebellum). The protein content in the PFC (78.4 ± 15.1), in the striatum (85.4 ± 22.0) and in the cortex (83.0 ± 15.1) was very similar, while the cerebellum's one was found to be very significantly lowered compared to them (67.1 ± 15.4) (**Figure IV. 35A**).

The lipid/protein relationship is shown in **Figure IV. 35B**. The PFC was the brain region with an intermediate lipid/protein ratio. Compared to it, the striatum had a very significant increase in this ratio (1.35-fold the PFC ratio), whereas the cortex's and the cerebellum's ones were very significantly reduced (0.84- and 0.86-fold, respectively).
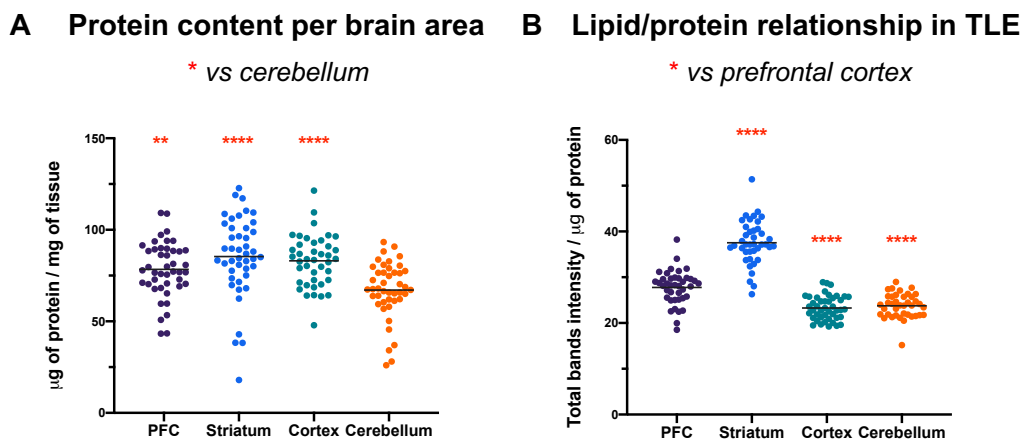
A   Protein content per brain area

* vs cerebellum

B   Lipid/protein relationship in TLE

* vs prefrontal cortex

Figure IV. 35. **Protein content and lipid-protein relationship are region-dependent. A)** Protein content per brain area. Statistical differences among the different brain areas were analyzed by Kruskal-Wallis + Dunn's multiple comparison test. Asterisks indicate statistical differences when the brain areas were compared to the cerebellum: ** $p<0.01$ in cerebellum *vs* prefrontal cortex comparison, **** $p<0.0001$ when cerebellum *vs* striatum and cerebellum *vs* cortex comparisons. **B)** Lipid/protein relationship in the TLE was calculated as the ratio of total lipids bands intensity in the TLE divided by the protein content. Statistical differences among the different brain areas were analyzed by ordinary one-way ANOVA + Tukey multiple comparison test. Asterisks indicate statistical differences when the brain areas were compared to the PFC: **** $p<0.0001$ *vs* striatum, *vs* cortex and *vs* cerebellum. In both graphs, data are presented as individual values and horizontal black lines represent the mean of each data set. Abbreviations: PFC = prefrontal cortex; TLE = total lipid extracts.

3.   General lipid composition of PFC, striatum, cortex and cerebellum

Firstly, data obtained from the analysis of TLE-TLC were used to determine the general lipid composition of the PFC, the striatum, the cerebral cortex and the cerebellum (**Figure IV. 36**).

The general lipid composition followed a common pattern in the four brain areas: glycerophospholipids are the most abundant lipid species, while gangliosides represent a small portion of the TLE (**Figure IV. 36A-D**). The neutral glycosphingolipids (i.e., the bands that co-migrate with the standards GlcCer+GalCer) in the cerebellum appear to be less abundant compared to the rest of the areas analyzed (**Figure IV. 36A-D**).

Regarding the ganglioside's composition, the PFC, the striatum and the cortex showed a similar profile, where GD1b and GT1b were the most abundant ones (**Figure IV. 36E-G**). In the cerebellum, the GT1b ganglioside continued to be the most abundant one, but GD1b relative abundance was slightly reduced compared to the rest of the brain areas (**Figure IV. 36H**).
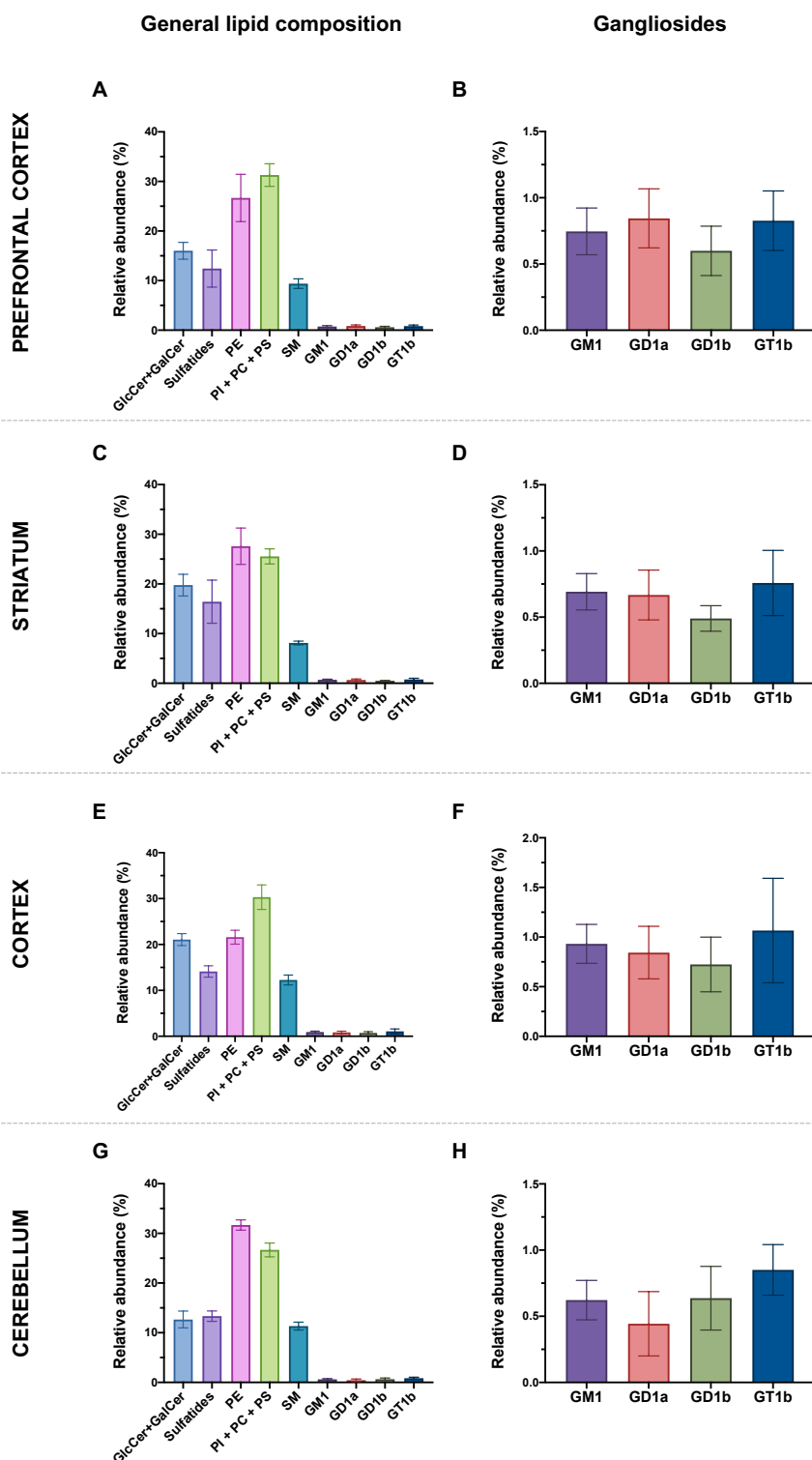
Figure IV. 36. Lipid composition of the total lipid extracts of the different brain areas analyzed. The lipids species of the total lipid extracts were resolved by TLC in the solvent system $CHCl_3$: CH_3OH : CaCl2 0.2% (60 : 35 : 8, by volume). Their lipid composition is expressed as the relative abundance (%) of the main groups of lipids. The left graphs show all the lipidic species identified in the four brain areas, while the right ones are the magnification of the gangliosides fraction of each of them. **A-B)** Lipid composition of the TLE of the prefrontal cortex, **C-D)** striatum, **E-F)** cortex and **G-H)** cerebellum. Data are presented as mean ± standard deviation.

4. Differential effect of age and sex in the lipid composition of the brain areas

Secondly, the quantification of the different bands in the TLE-TLC from the four brain areas was used as a first approach to study the age-associated changes considering sex as an experimental variable.
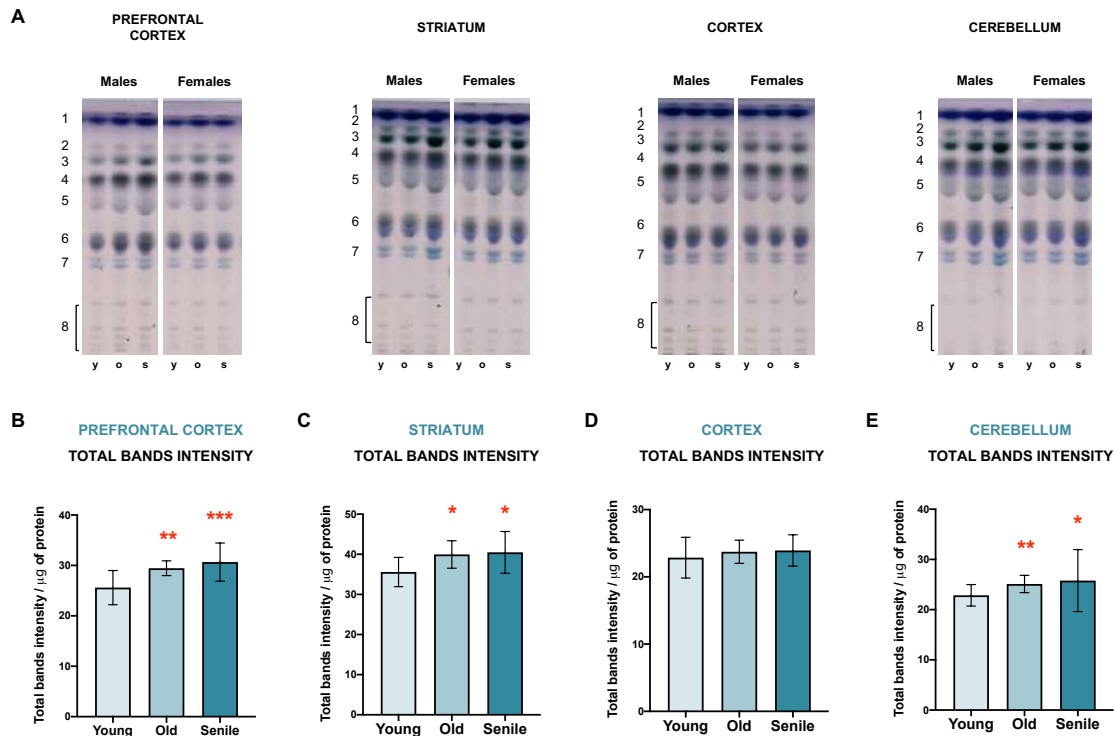

Figure IV. 36. Changes in the total lipid content of the total lipid extracts along aging. A) The lipids species of the total lipid extracts were resolved by TLC in the solvent system CHCl$_3$: CH$_3$OH : CaCl2 0.2% (60 : 35 : 8, by volume). **(B-E)** Total bands intensity was calculated as the sum of the optical densities of all the bands present in the total lipid extracts, and adjusted to the amount of protein loaded in the TLC (Total bands intensity/µg of protein). Quantification was performed in the **B)** prefrontal cortex, **C)** striatum, **D)** cortex and **E)** cerebellum. Age-associated statistical differences in the prefrontal cortex and in the striatum were analyzed by ordinary one-way ANOVA + Tukey multiple comparison test, whereas Kruskal-Wallis + Dunn's multiple comparison test was used for cortex and cerebellum. Asterisks indicate statistical differences *vs* the young group: * $p<0.05$, ** $p<0.01$; ***$p<0.001$. Data are presented as mean ± standard deviation. Legend: 1=hydrophobic lipids; 2=glucosylceramide; 3=galactosylceramide; 4=phosphatidylethanolamine; 5=sulfatides; 6=rest of glycerophospholipids; 7=sphingomyelin; 8=gangliosides, from top to bottom: GM1, GD1a, GD1b and GT1b; y=young; o=old; s=senile.

In the PFC, total lipid content was significantly increased along aging, without sex-associated differences (**Figure IV. 36A**). The neutral glycosphingolipids were the most sensitive ones to the effect of age: i) the GlcCer family was significantly increased in the senile animals compared with the old and the young ones (**Figure IV. 37A**); and ii) the GalCer family band was very significantly increased in the senile animals compared with

the young ones (**Figure IV. 37B**). No sex-related differences were found for any of the lipid species analyzed (**Figure IV. 37C-J**).
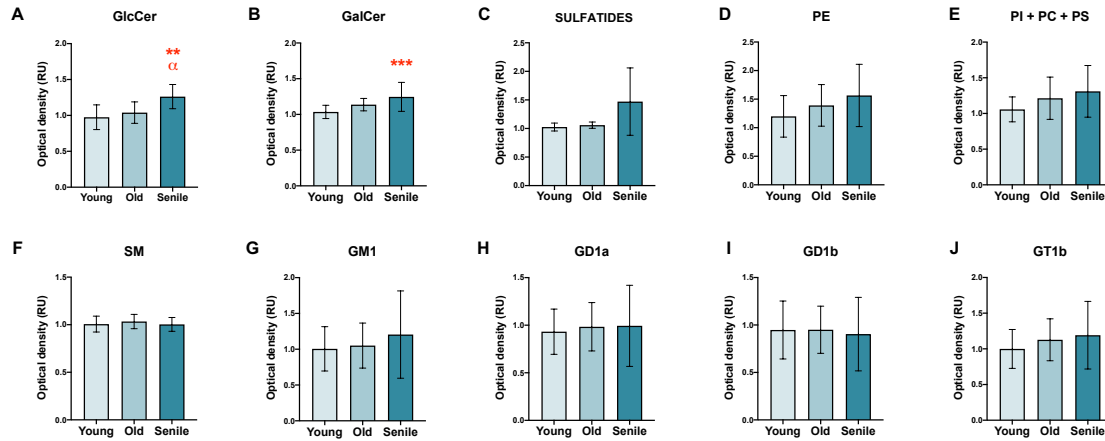

Figure IV. 37. **Changes in the abundance of the lipid-associated bands in the total lipid extracts of the prefrontal cortex.** The lipids species of the total lipid extracts were resolved by TLC in the solvent system $CHCl_3 : CH_3OH : CaCl2$ 0.2% (60 : 35 : 8, by volume). **A-J)** The effect of age in the abundance of the different lipid species was studied by optical density quantification of their corresponding bands in the TLC. Statistical differences along aging were analyzed by ordinary one-way ANOVA + Tukey multiple comparison test for GlcCer, GalCer, PE and the gangliosides' family; Kruskal-Wallis + Dunn's multiple comparison test was used for sulfatides, PI+PC+PS and SM. Asterisks indicate statistical differences *vs* the young animals; alpha character indicates statistical differences vs the old group: ** $p<0.01$, *** $p<0.001$, α $p<0.05$. Data are presented as mean ± standard deviation. Abbreviations: GalCer = galactosylceramide; GlcCer = glucosylceramide; PC = phosphatidylcholine; PE = phosphatidylethanolamine; PI = phosphatidylinositol; PS = phosphatidylserine; SM = sphingomyelin; RU = relative units.

In the striatum, the total lipid content was significantly increased in the old and senile groups, independently from the sex of the animals (**Figure IV. 36B**). From all the lipids analyzed (**Figure IV. 38**), SM was the one showing the highest changes in relation to aging: it significantly increased in the senile age compared with the young one (**Figure IV. 38F**). Sex-related differences were found in the gangliosides: independently from the age of the animals, relative intensity of GD1a and GD1b bands were significantly lower in females than in males (**Figure IV. 38K, L**).

In the cortex, changes in the total bands' intensity were not found significant, neither along aging nor between males and females (**Figure IV. 36C**). However, when specific lipid bands were analyzed (**Figure IV. 39**), a significant increase along aging was found in GlcCer, GalCer, sulfatides and PE (**Figure IV. 39A-C, F**). In particular, changes in the sulfatides were more pronounced along aging in males than in females (**Figure IV. 39D,**

E). Age and/or sex did not show a significant effect in phospholipids, SM nor the different gangliosides' species (**Figure IV. 39G-L**).

Figure IV. 38. Changes in the abundance of the lipid-associated bands in the total lipid extracts of the striatum. The lipids species of the total lipid extracts were resolved by TLC in the solvent system $CHCl_3 : CH_3OH : CaCl2$ 0.2% (60 : 35 : 8, by volume). **A-J)** The effect of age in the abundance of the different lipid species was studied by optical density quantification of their corresponding bands in the TLC. **K-L)** Significant sex-related differences were found for GD1a and GD1b; lipids in which significant differences were not found are not shown. Statistical differences along aging were analyzed by ordinary one-way ANOVA + Tukey multiple comparison test for GalCer, PI+PC+PS, SM and the gangliosides' family; Kruskal-Wallis + Dunn's multiple comparison test was used for GlcCer, PE and sulfatides. Asterisks indicate statistical differences *vs* the young animals: ** $p<0.01$, *** $p<0.001$. Statistical differences between males and females were analyzed by unpaired t-test. # symbol indicates statistical differences when males and females are compared: ## $p<0.01$, ### $p<0.001$. Data are presented as mean ± standard deviation. Abbreviations: GalCer = galactosylceramide; GlcCer = glucosylceramide; PC = phosphatidylcholine; PE = phosphatidylethanolamine; PI = phosphatidylinositol; PS = phosphatidylserine; SM = sphingomyelin; RU = relative units.
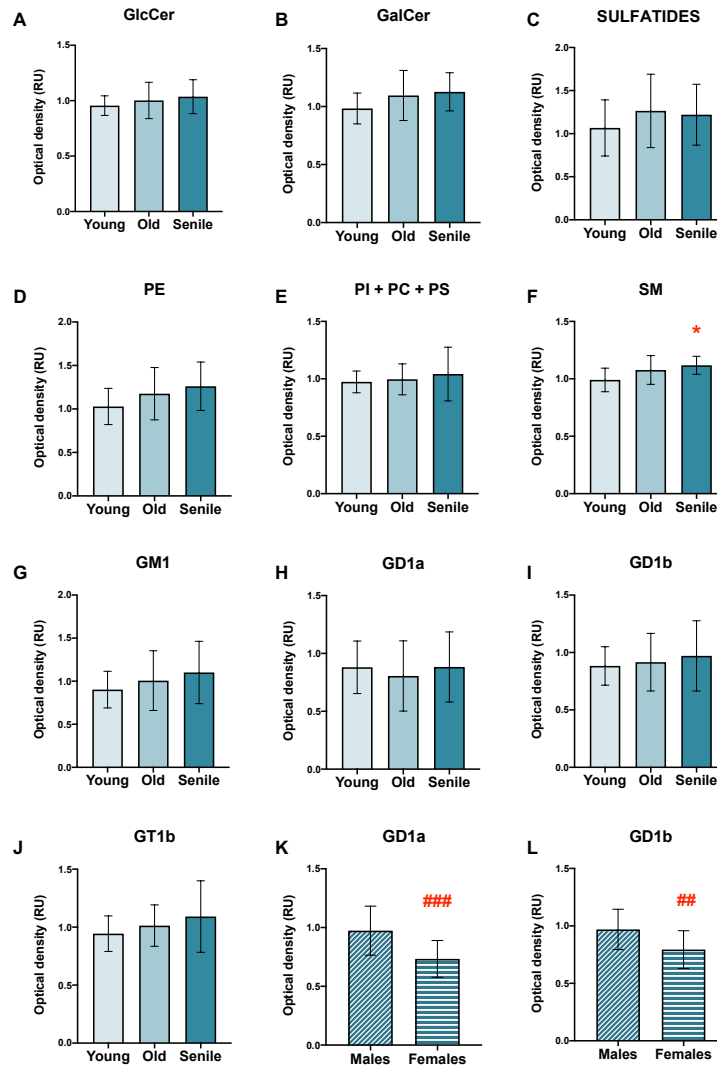
Figure IV. 39. Changes in the abundance of the lipid-associated bands in the lipid extracts of the cortex. The lipids species of the total lipid extracts were resolved by TLC in the solvent system $CHCl_3 : CH_3OH : CaCl2$ 0.2% (60 : 35 : 8, by volume). **A-L)** The effect of age in the abundance of the different lipid species was studied by optical density quantification of their corresponding bands. **D, E)** Significant sex-related differences were found along aging for sulfatides; lipids in which significant differences were not found are not shown. Statistical differences along aging were analyzed by ordinary one-way ANOVA + Tukey multiple comparison test for GlcCer, GalCer, sulfatides, PI+PC+PS and the gangliosides' family; Kruskal-Wallis + Dunn's multiple comparison test was used for SM. Asterisks indicate statistical differences vs the young group: * $p < 0.05$, ** $p < 0.01$, *** $p < 0.001$. Data are presented as mean ± standard deviation. Abbreviations: GalCer = galactosylceramide; GlcCer = glucosylceramide; PC = phosphatidylcholine; PE = phosphatidylethanolamine; PI = phosphatidylinositol; PS = phosphatidylserine; SM = sphingomyelin; RU = relative units.

In the cerebellum, both sex ang age significantly influenced the lipid profile (**Figure IV. 36C**). The optical density of the total bands was significantly increased in the old and senile animals compared to the young ones (**Figure IV. 40D**). Particularly, this increase

was found very significant in the bands of GalCer, sulfatides, glycerophospholipids (PE+PI+PC+PS), sphingomyelin and ganglioside GM1 (**Figure IV. 40B-G**). When the variable sex was explored, it was found that males and females were not affected the same by the aging process (**Figure IV. 40K-O**). Additionally, the relative intensity of GlcCer, GalCer, glycerophospholipids, sphingomyelin and ganglioside GM1 bands was significantly higher in the senile
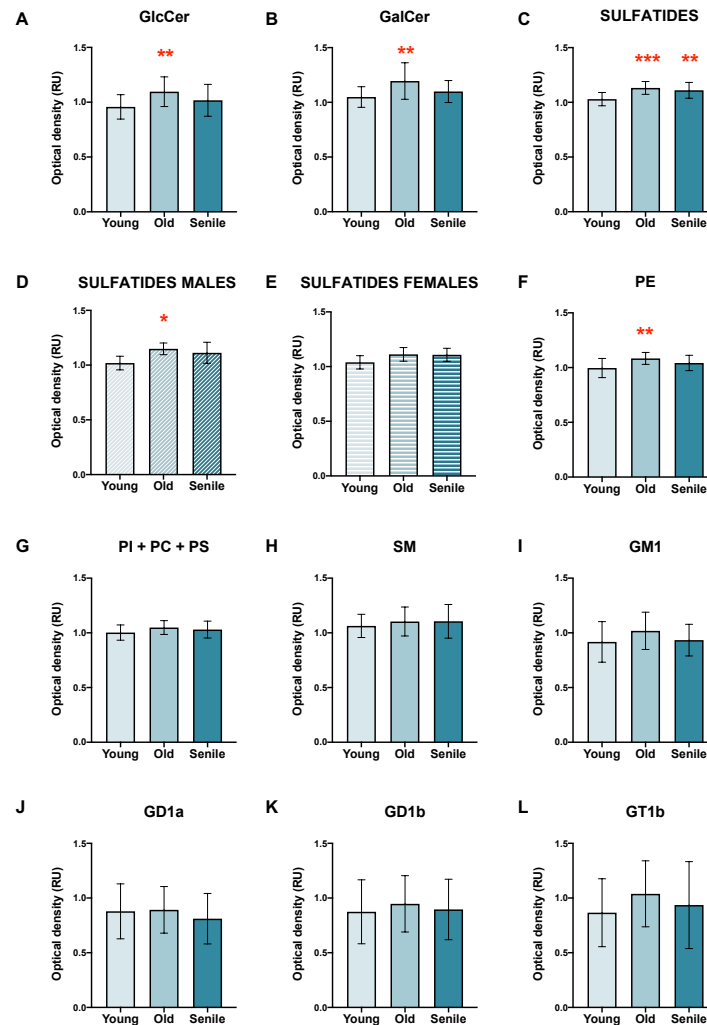
Figure IV. 40. Changes in the abundance of the lipid-associated bands in the lipid extracts of the cerebellum. The lipids species of the total lipid extracts were resolved by TLC in the solvent system $CHCl_3 : CH_3OH : CaCl2$ 0.2% (60 : 35 : 8, by volume). **A-J)** The effect of age in the abundance of the different lipid species was studied by optical density quantification of their corresponding bands. Statistical differences along aging were analyzed by ordinary one-way ANOVA + Tukey multiple comparison test for all the lipid species except from GD1a. Kruskal-Wallis + Dunn's multiple comparison test was used for GD1a. Asterisks indicate statistical differences vs the young group: * $p < 0.05$, ** $p < 0.01$, *** $p < 0.001$. **K-O)** Significant sex-related differences were found along aging for **K)** GlcCer, **L)** GalCer, **M)** PI+PC+PS, **N)** SM and **O)** GM1; lipids in which significant differences were not found are not shown. Statistical differences along aging and sex were analyzed by two-way ANOVA + Tukey post-hoc test. Asterisks indicate statistical differences among animals of the same sex (e.g., old females vs senile females); # symbol indicate statistical differences between males and females of the same age group (e.g., young males vs young females): * $p < 0.05$, ** $p < 0.01$, *** $p < 0.001$, **** $p < 0.0001$, # $p < 0.05$, ## $p < 0.01$, ### $p < 0.001$. Data are presented as mean ± standard deviation. Abbreviations: GalCer = galactosylceramide; GlcCer = glucosylceramide; PC = phosphatidylcholine; PE = phosphatidylethanolamine; PI = phosphatidylinositol; PS = phosphatidylserine; SM = sphingomyelin; RU = relative units.
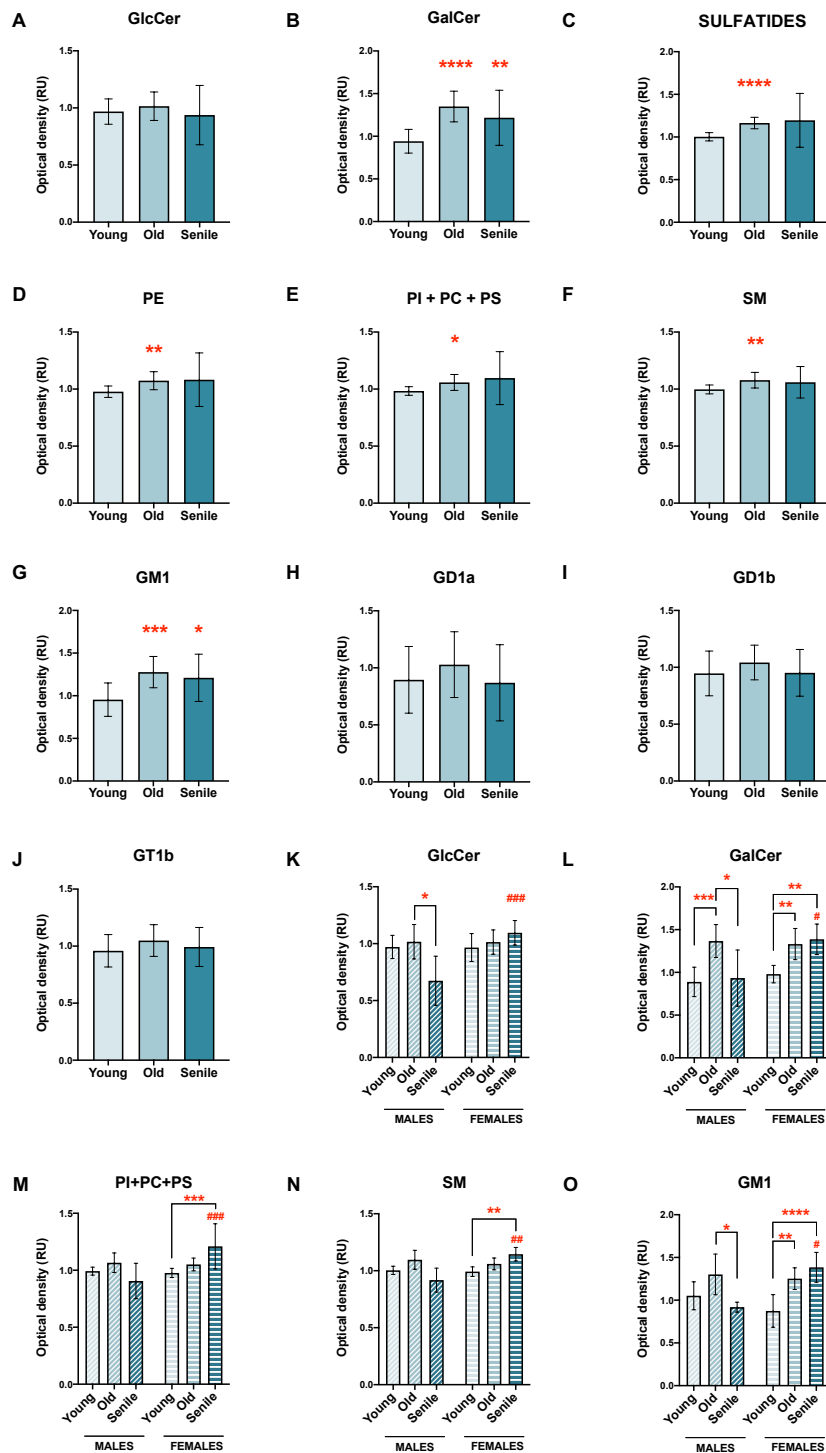
Based on the results of this section, the PFC and the cerebellum were used for a deeper characterization of the lipid changes along aging in males and females.

5. Study of the effect of age and sex on the lipid composition in the PFC

Figure IV. 41. Changes in the glycerophospholipids presence in the prefrontal cortex along aging. The glycerophospholipids' species (organic phases) were resolved by the TLC with the solvent system $CHCl_3 : CH_3OH : CH_3COOH : H_2O$ (30 : 20 : 2 : 1, by volume). **A-D)** Age-associated changes in the abundance of the lipids was studied by optical density quantification. Statistical differences along aging were analyzed by ordinary one-way ANOVA + Tukey multiple comparison test. No significant differences were found. **E-I)** Sex-associated changes in the abundance of the lipids was studied by optical density quantification. Statistical differences between males and females were analyzed by unpaired t-test. Asterisks indicate statistical differences vs the young group: * $p < 0.05$, ** $p < 0.01$, *** $p < 0.001$. Data are presented as mean ± standard deviation. Abbreviations: PC = phosphatidylcholine; PE = phosphatidylethanolamine; PI = phosphatidylinositol; PS = phosphatidylserine; RU = relative units.

5.1. Glycerophospholipids

The analysis of the PFC's glycerophospholipids revealed no significant changes along aging in none of the subspecies identified (**Figure IV. 41A-D**).

However, when animals were grouped by sex, significant differences were found in the presence of all the glycerophospholipids identified: males showed significantly higher levels of the different glycerophospholipid species compared to females (**Figure IV. 41F-I**).

5.2. Neutral glycosphingolipids

The analysis of neutral glycosphingolipids (mainly the family of GlcCer and GalCer) showed a significant increase of this kind of lipids along aging (**Figure IV. 42A-C**), which was mainly explained by a significant increase in the lipids of GalCer family (**Figure IV. 42C**). Interestingly, GlcSph levels were found to be very significantly higher in males than in females (**Figure IV. 42E**)
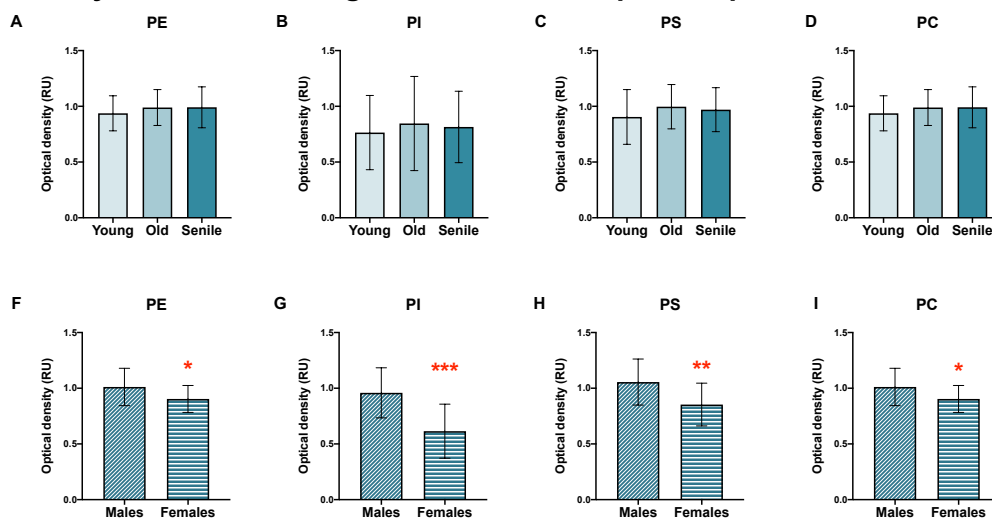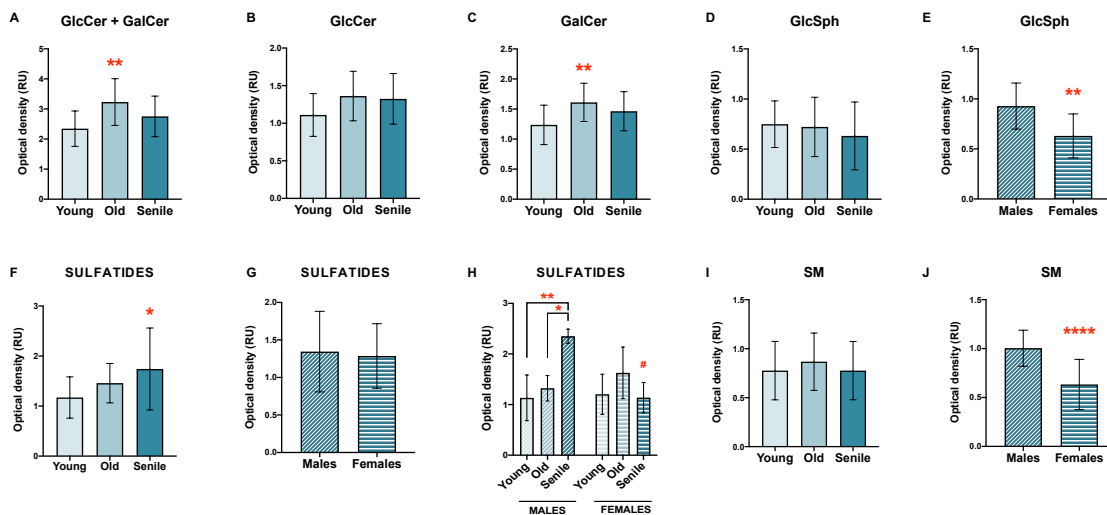

Figure IV. 42. Changes in the sphingolipid presence in the prefrontal cortex along aging. The sphingolipids' species (methanolized organic phases) were resolved by TLC with the solvent system C : M : H_2O (110 : 40 : 6, by volume). Age-associated changes in the abundance of the lipids was studied by optical density quantification: **A)** GalCer+GlcCer, **B)** GlcCer, **C)** GalCer, **D)** GlcSph, **F)** sulfatides and **I)** SM. Statistical differences along aging were analyzed by ordinary one-way ANOVA + Tukey multiple comparison test. Asterisks indicate statistical differences vs the young group: * $p < 0.05$, ** $p < 0.01$. Sex-associated changes in the abundance of the lipids was studied by optical density quantification, and those in which significant differences were detected are shown: **E)** GlcSph, **G-H)** sulfatides, **J)** SM.
Statistical differences between males and females were analyzed by unpaired t-test. Statistical differences along aging and sex were analyzed by two-way ANOVA + Tukey post-hoc test. Asterisks indicate statistical differences among animals of the same sex (e.g., old females vs senile females); # symbol indicate statistical differences between males and females of the same age group (e.g., young males vs young females): * $p < 0.05$, ** $p < 0.01$, **** $p < 0.0001$, # $p < 0.05$. Data are presented as mean ± standard deviation. Abbreviations: GalCer=galactosylceramide; GlcCer = glucosylceramide; GlcSph = glucosylsphingosine; SM = sphingomyelin; RU = relative units.

5.3. Sulfatides

Quantification of sulfatides revealed that both age and sex have a significant effect on its presence. A significant accumulation of this lipid species was found as the animals aged, which was more pronounced in males than in females (**Figure IV. 42F, H**). The analysis of the simultaneous effect of age and sex showed that sulfatides levels were significantly higher in senile males than in senile females (**Figure IV. 42H**). However, these differences disappeared when the variable age was eliminated and animals were grouped by sex (males vs. females) (**Figure IV. 42G**).

Figure IV. 43. **Changes in the gangliosides' presence in the prefrontal cortex along aging.**
A) The gangliosides' species (aqueous phases) were resolved by TLC in the solvent system $CHCl_3$: CH_3OH : $CaCl_2$ 0.2% (50 : 42 : 11, by volume). Age-associated changes in the abundance of the lipids was studied by optical density quantification: **B)** GM1, **C)** Band 2, **D)** GD1a, **E)** GD1b, **F)** GT1b and **G)** GQ1b. Statistical differences along aging were analyzed by ordinary one-way ANOVA + Tukey multiple comparison test. No significant differences were found. Sex-associated changes in the abundance of the lipids was studied by optical density quantification, and those in which significant differences were found are shown: **H)** GQ1b. Sex-related statistical differences were analyzed by unpaired t-test. Asterisks indicate statistical differences when males and females were compared: *** $p < 0.001$. Data are presented as mean ± standard deviation. Abbreviations: y = young; o = old; s = senile; RU = relative units.

5.4. Sphingomyelin

Behavior of SM in the *O. degus* was identical to that of glycerophospholipids: no significant age-associated differences were found (**Figure IV. 42I**), while comparisons between males and females showed significant lower levels in females compared to males (**Figure IV. 42J**).

5.5. Gangliosides

Gangliosides' composition in the PFC was not significantly affected by the age of the animals (**Figure IV. 43A-G**). The effect of sex alone (males vs. females) was found statistically significant just for the ganglioside GQ1b: females had significantly reduced levels of this lipid compared to males (**Figure IV. 43H**). When the effect of age and sex was explored together, a different behavior was observed for males and females along aging for the different gangliosides (**Figure IV. 44**). Some gangliosides (GM1, band 2, GD1a, GD1b, GT1b) were similar for males and females in the young and old ages; however, in the senile age, these gangliosides became accumulated by males while constant/reduced in females (**Figure IV. 43A-D**). On the contrary, GT1b and GQ1b were found higher at all ages for males compared with females (**Figure IV. 44E,F**).

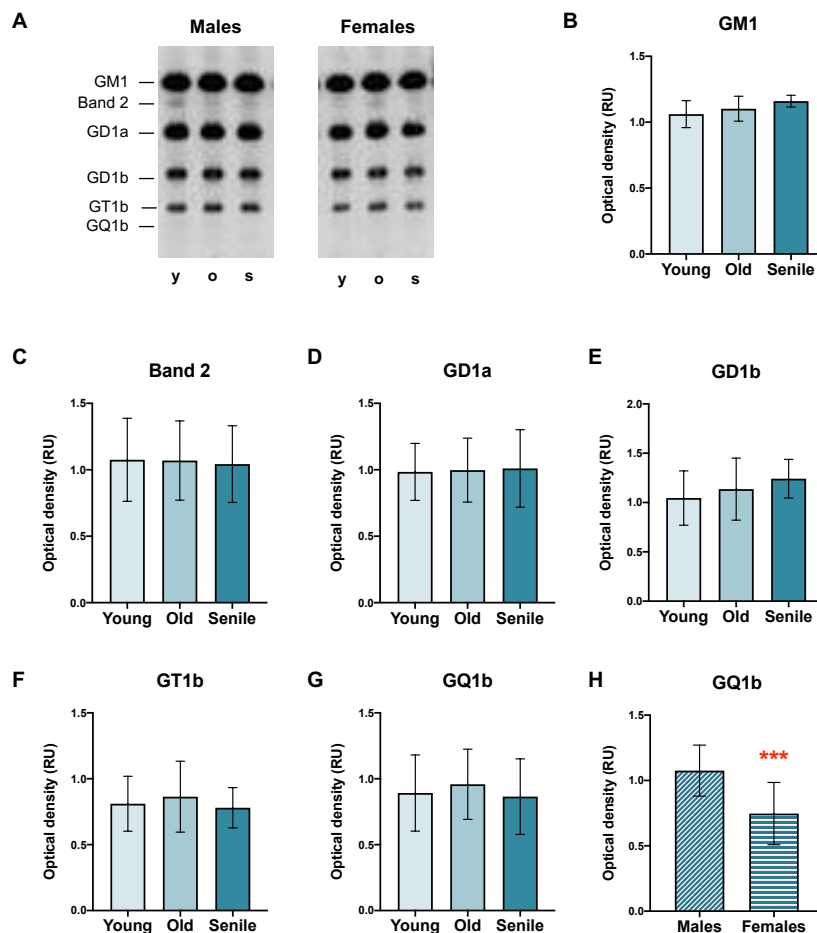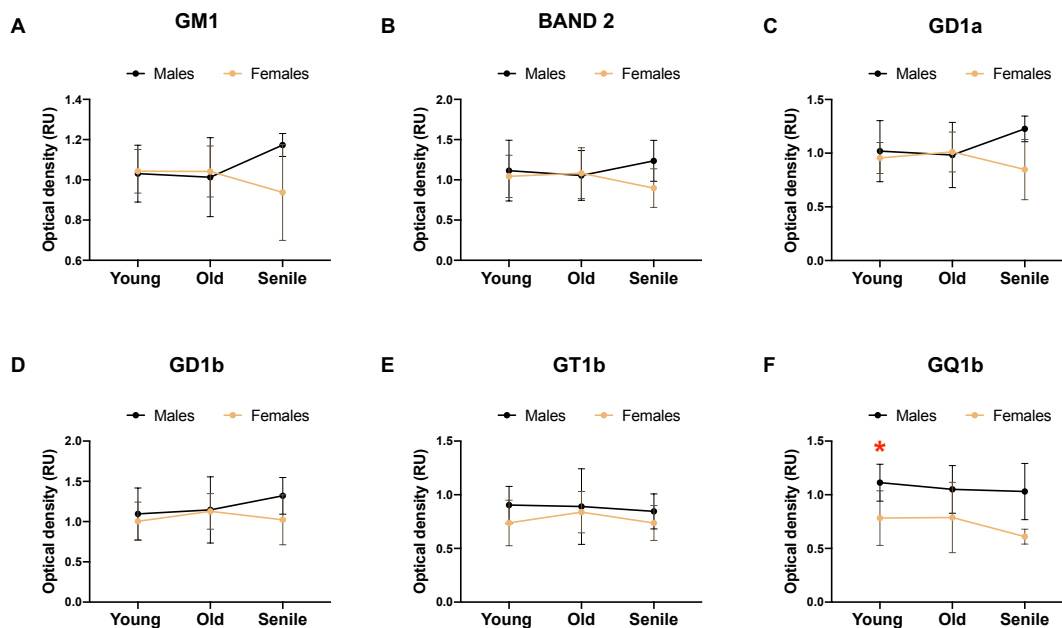**Figure IV. 44. Sex-related changes along aging in the gangliosides' presence in the prefrontal cortex.** The gangliosides' species (aqueous phases) were resolved by TLC in the solvent system $CHCl_3 : CH_3OH : CaCl_2$ 0.2% (50 : 42 : 11, by volume). Differences in the gangliosides' abundance along aging was analyzed with a sex perspective by optical density quantification: **A)** GM1, **B)** Band 2, **C)** GD1a, **D)** GD1b, **E)** GT1b and **F)** GQ1b. Statistical differences were determined by comparing males and females of the same age using the unpaired t-test, asterisks indicating the statistical differences found: * $p<0.05$. Data are presented as mean ± standard deviation. Abbreviations: RU = relative units.

5.6. Cholesterol

Cholesterol levels in the PFC were found to significantly accumulate significantly along aging (**Figure IV. 45A, B**), without sex-associated differences (**Figure IV. 45C**).
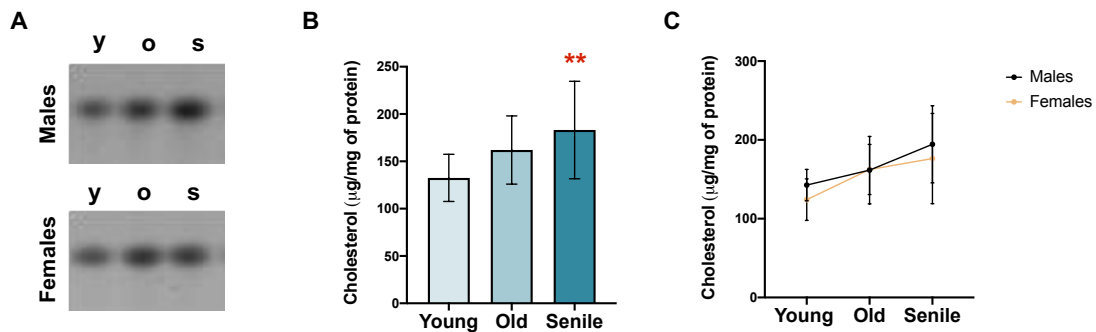
Figure IV. 45. **Study of cholesterol levels in the prefrontal cortex.** The organic phases were resolved by TLC in the solvent $C_6H_{14} : C_4H_8O_2$ (3 : 2, by volume) to study cholesterol levels. **A)** Representative image of the cholesterol TLC. **B)** Changes in cholesterol along aging were evaluated by optical density quantification of its bands. Data were analyzed by the ordinary one-way ANOVA + Tukey multiple comparisons test. Asterisks indicate statistical differences when animals were compared *vs* the young group: ** $p<0.01$. **C)** Changes in cholesterol along aging with a sex perspective were determined by comparing males and females of the same age using the unpaired t-test. No differences were found. Data are presented as mean ± standard deviation. Abbreviations: y = young; o = old; s = senile.

6. Study of the effect of age and sex on the lipid composition in the cerebellum

6.1. Glycerophospholipids

Glycerophospholipids were the lipid species less affected either by age and sex in the cerebellum, since no significant age-associated differences were detected along aging (**Figure IV. 46A-D**), and the effect of sex was found significant just for PI (**Figure IV. 46E**).
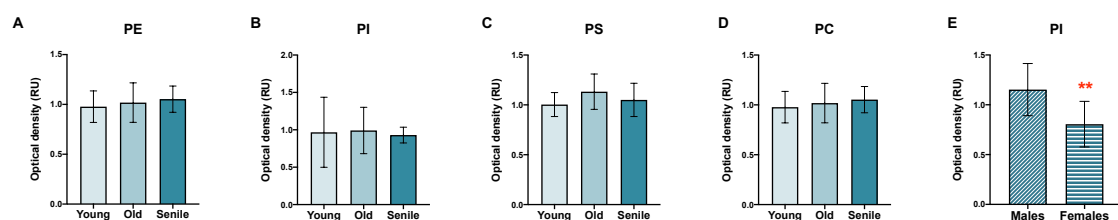
Figure IV. 46. **Changes in the glycerophospholipids presence in the cerebellum along aging.** The glycerophospholipids' species (organic phases) were resolved by the TLC with the solvent system $CHCl_3 : CH_3OH : CH_3COOH : H_2O$ (30 : 20 : 2 : 1, by volume). **A-D)** Age-associated changes in the abundance of the lipids was studied by optical density quantification. Statistical differences along aging were analyzed by ordinary one-way ANOVA + Tukey multiple comparison test. No significant differences were found. **E)** Sex-associated changes in the abundance of the lipids was studied by optical density quantification; lipids in which significant differences were not found are not shown. Statistical differences between males and females were analyzed by unpaired t-test: ** $p<0.01$. Data are presented as mean ± standard deviation. PE=phosphatidylethanolamine; PI=phosphatidylinositol; PS=phosphatidylserine; PC=phosphatidylcholine; RU=relative units.

6.2. Neutral glycosphingolipids

Neutral glycosphingolipids were significantly elevated in old and senile animals, compared to the young ones (**Figure IV. 47A**), although no sex-associated differences were found. This increment was explained by the significant increase in GalCer rather than in GlcCer (**Figure IV. 47B, C**). GlcSph showed a slight increase along aging (**Figure IV. 47D**), and significant lower levels were detected for females than males (**Figure IV. 47E**).
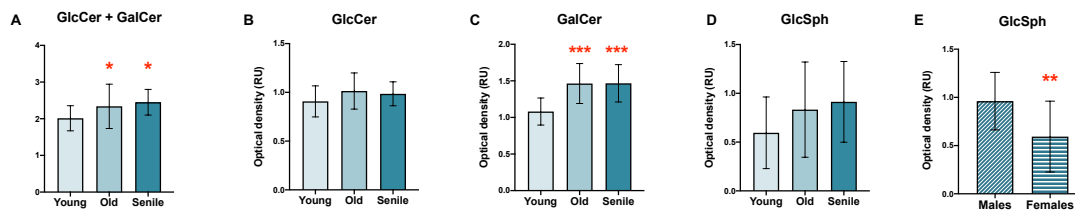
Figure IV. 47. Changes in the sphingolipid presence in the prefrontal cortex along aging. The sphingolipids' species (methanolized organic phases) were resolved by TLC with the solvent system C : M : H_2O (110 : 40 : 6, by volume). Age-associated changes in the abundance of the lipids was studied by optical density quantification: **A)** GalCer+GlcCer, **B)** GlcCer, **C)** GalCer and **D)** GlcSph. Statistical differences along aging were analyzed by ordinary one-way ANOVA + Tukey multiple comparison test. Asterisks indicate statistical differences vs the young group: *** $p<0.001$. Sex-associated changes in the abundance of the lipids was studied by optical density quantification, and those in which significant differences were detected are shown: **E)** GlcSph. Statistical differences between males and females were analyzed by unpaired t-test, asterisks indicating statistical differences: ** $p<0.01$. Data are presented as mean ± standard deviation. Abbreviations: GalCer = galactosylceramide; GlcCer = glucosylceramide; GlcSph = glucosylsphingosine; RU = relative units.

6.3. Sulfatides

In the cerebellum, sulfatides significantly accumulate as the animals aged, both in the old and in the senile groups compared to the young one (**Figure IV. 48A**). Although no significant differences were found when animals were grouped by sex (**Figure IV. 48B**), the accumulation along aging was found to be more exacerbated in females than in males (**Figure IV. 48C**).

6.4. Sphingomyelin

SM in the cerebellum showed a tendency to increase along aging, although it did not reach statistical significance (**Figure IV. 49A**). When males and females were compared, we found that, independently of the variable age, females had very significantly lower levels than males (**Figure IV. 49B**). In addition, these changes between males and females were observed along the aging process: at the senile age, males had a slight decrease in this lipid species, whereas females showed a significant accumulation (**Figure IV. 49C**).

Figure IV. 48. Changes in the sulfatides' presence in the cerebellum along aging and with a sex perspective. Sulfatides' species (methanolized organic phases) were resolved by TLC with the solvent system C : M : H_2O (110 : 40 : 6, by volume). **A)** Age-associated changes in the abundance was studied by optical density quantification. Data were analyzed by ordinary one-way ANOVA + Tukey multiple comparison test. Asterisks indicate statistical differences *vs* the young group: ** $p < 0.01$, *** $p < 0.001$. **B)** Sex-associated changes in the abundance of sulfatides was studied by optical density quantification. Statistical differences between males and females were calculated by unpaired t-test; no significant differences were found. **C)** Study of sulfatides' changes in males and females along aging. Data were analyzed by two-way ANOVA + Tuckey multiple comparison test. Asterisks indicate statistical differences *vs* the young group: * $p < 0.05$. Data are presented as mean ± standard deviation. Abbreviations: RU = relative units.
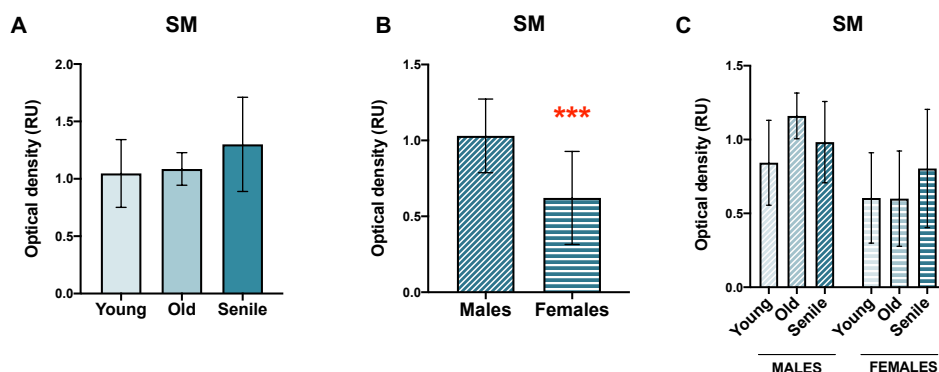
Figure IV. 49. Changes in the sphingomyelin's presence in the cerebellum along aging and with a sex perspective. Sphingomyelin (methanolized organic phases) was resolved by TLC with the solvent system C : M : H_2O (110 : 40 : 6, by volume). **A)** Age-associated changes in the abundance was studied by optical density quantification. Data were analyzed by ordinary one-way ANOVA + Tukey multiple comparison test. No significant differences were found. **B)** Sex-associated changes in the abundance of sphingomyelin was studied by optical density quantification. Statistical differences between males and females were calculated by unpaired t-test, asterisks indicating statistical significance: *** $p < 0.001$. **C)** Study of sphingomyelin's changes in males and females along aging. Data were analyzed by two-way ANOVA + Tuckey multiple comparison test. No significant differences were found. Data are presented as mean ± standard deviation. Abbreviations: RU = relative units; SM = sphingomyelin.
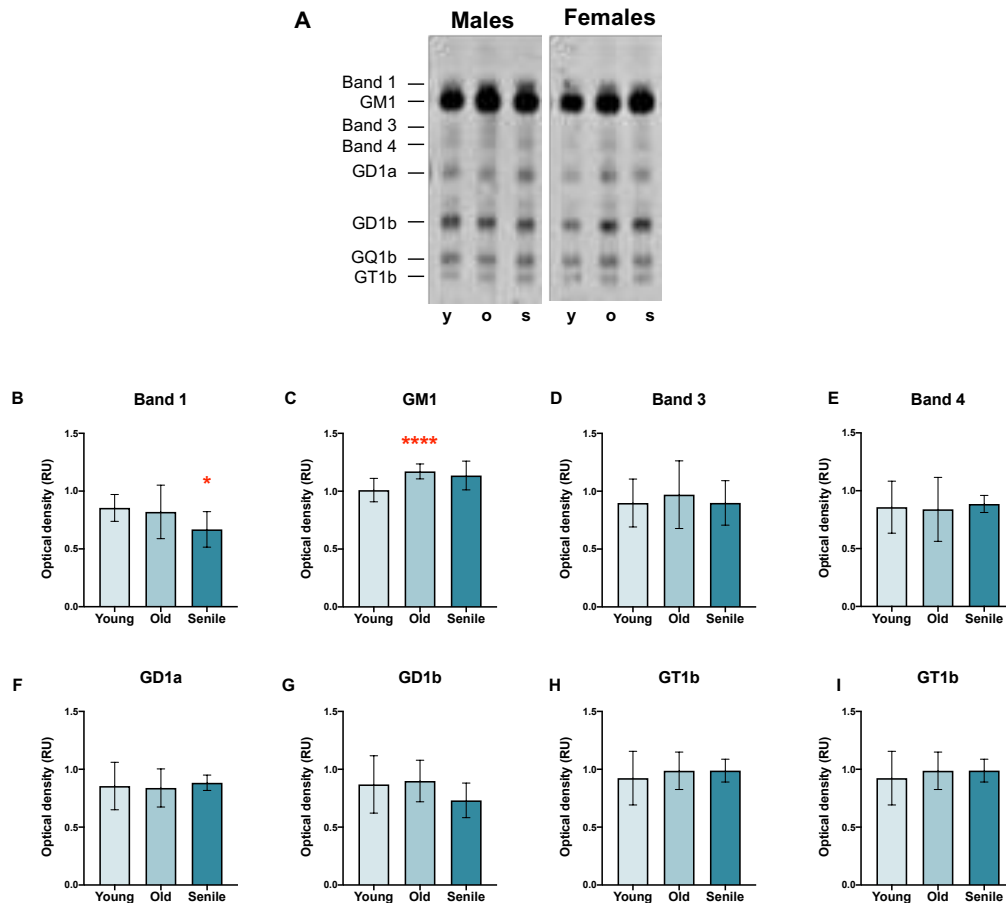
Figure IV. 50. **Changes in the gangliosides' presence in the cerebellum along aging. A)** The gangliosides' species (aqueous phases) were resolved by TLC in the solvent system $CHCl_3$: CH_3OH : $CaCl_2$ 0.2% (50 : 42 : 11, by volume). Age-associated changes in the abundance of the lipids was studied by optical density quantification: **B)** Band 1, **C)** GM1, **D)** Band 3, **E)** Band 4, **F)** GD1a, **G)** GD1b, **H)** GT1b, **I)** GT1b. Statistical differences along aging were analyzed by ordinary one-way ANOVA + Tukey multiple comparison test. Asterisks indicate statistical differences when animals were compared *vs* the young group: * $p<0.05$, *** $p<0.001$. Data are presented as mean ± standard deviation. Abbreviations: y = young; o = old; s = senile; RU = relative units.

6.5. Gangliosides

Gangliosides' composition was affected both by age and sex in the cerebellum (**Figure IV. 50A**). Gangliosides' subspecies particularly affected by age were band 1 (significant decrease in the senile group, **Figure IV. 50B**), GM1 (very significant accumulation along aging, especially in the old animals, **Figure IV. 50C**) and GD1b (decrease in the senile group although it did not reach statistical significance, **Figure IV. 50G**).

When animals were grouped by sex, females showed significant lower levels compared to males of the following gangliosides: bands 3 and 4 (**Figure IV. 51A** and **B**, respectively), GD1a (**Figure IV. 51C**), GD1b (**Figure IV. 51D**), GT1b (**Figure IV. 51E**), GQ1b (**Figure IV. 51F**).
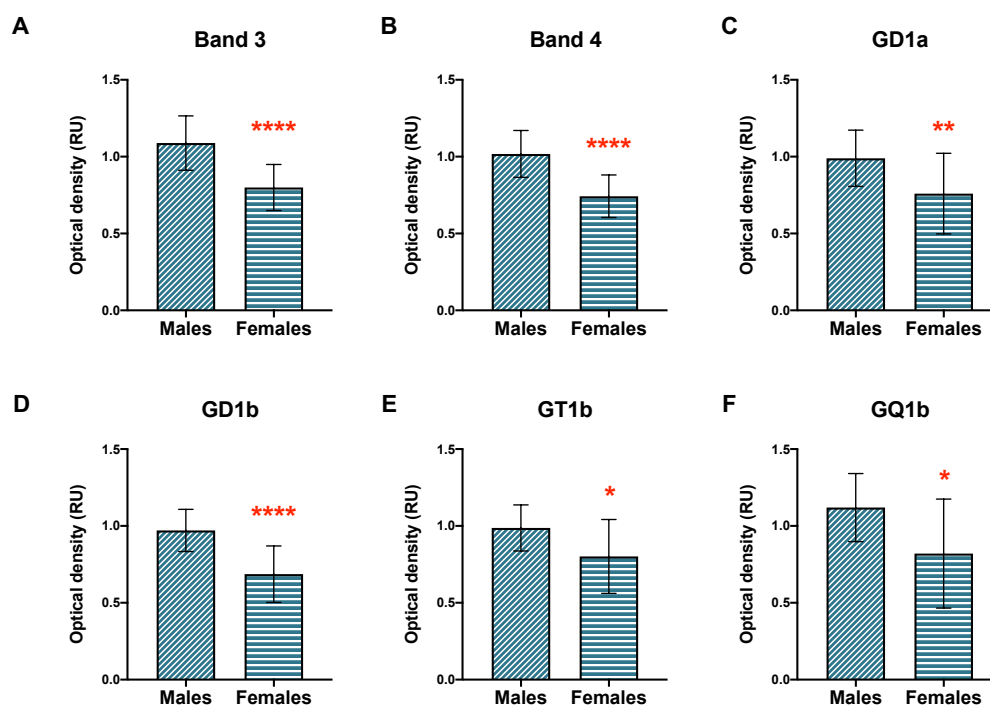
Figure IV. 51. Sex differences in the gangliosides' presence in the cerebellum. The gangliosides' species (aqueous phases) were resolved by TLC in the solvent system $CHCl_3$: CH_3OH : $CaCl_2$ 0.2% (50 : 42 : 11, by volume). Sex-related changes in the abundance of the lipids was studied by optical density quantification. Gangliosides' species in which statistical differences were found are shown: **A)** Band 3, **B)** Band 4, **C)** GD1a, **D)** GD1b, **E)** GT1b, **F)** GQ1b. Data were statistically analyzed by unpaired t-test, asterisks indicating statistical differences when males and females were compared: * $p<0.05$, ** $p<0.01$, **** $p<0.0001$. Data are presented as mean ± standard deviation. Abbreviations: RU = relative units.

6.6. Cholesterol

Cholesterol levels were significantly influenced by both age and sex of the animals (**Figure IV. 52**). When all the animals were grouped according to their age, a significant increase of cholesterol was found (**Figure IV. 52A**). However, when the variable sex was taken into account, it was observed that males and females behaved differently: cholesterol significantly increased along aging in females, whereas it was found to significantly decrease when senile males were compared with the young ones (**Figure IV. 52B**).

7. Correlations among changes in the lipids' species and systemic parameters

7.1. Plasmatic cholesterol and brain cholesterol correlation

Correlation analyses to explore a possible relationship between plasmatic cholesterol and PFC cholesterol revealed a positive correlation, although it did not reach statistical significance (**Figure IV. 53A**). On the contrary, a negative relationship between plasmatic cholesterol and cerebellum cholesterol was found (without statistical significance) (**Figure IV. 53B**).
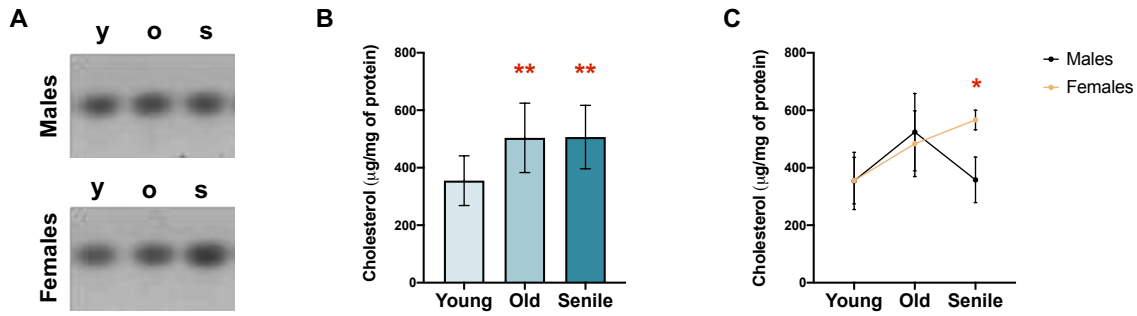
Figure IV. 52. Study of cholesterol levels in the cerebellum. The organic phases were resolved by TLC in the solvent $C_6H_{14} : C_4H_8O_2$ (3 : 2, by volume) to study cholesterol levels. **A)** Representative images of the cerebellum cholesterol TLC. **B)** Changes in cholesterol along aging were evaluated by optical density quantification of its bands. Data were analyzed by the ordinary one-way ANOVA + Tukey multiple comparisons test. Asterisks indicate statistical differences when animals were compared *vs* the young group: ** $p<0.01$. **C)** Changes in cholesterol along aging with a sex perspective were determined by comparing males and females of the same age using the unpaired t-test. Asterisks indicate statistical differences when males and females of the same age were compared: * $p<0.05$ Data are presented as mean ± standard deviation. Abbreviations: y = young; o = old; s = senile.

7.2. Brain lipid changes and cognitive performance

Correlation analyses were done to explore the relationship between the WME done in the BM test and the significant lipid changes found in the PFC.
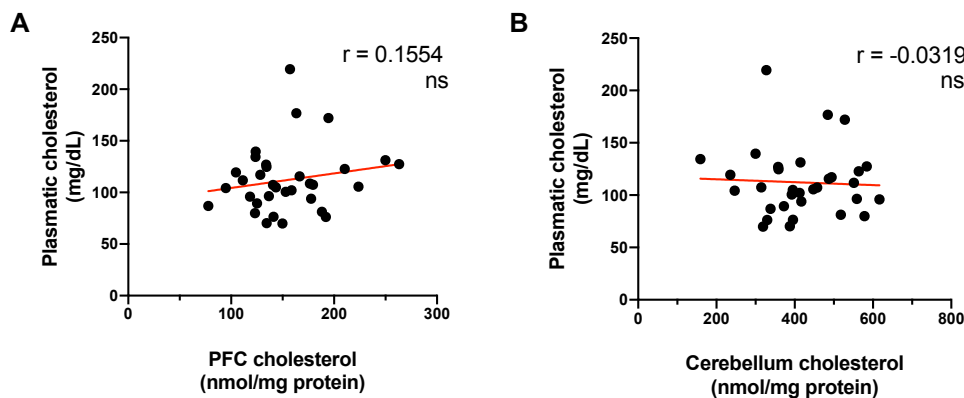
Figure IV. 53. Spearman correlations between plasmatic cholesterol and both PFC (A) and cerebellum (B) cholesterol. Data are presented as individual pairs of values and the linear regression calculated is traced as the red line. XY pairs = 33. Significant differences were considered when $p<0.05$. Abbreviations: PFC = prefrontal cortex; ns = not significant; r = Spearman's coefficient.
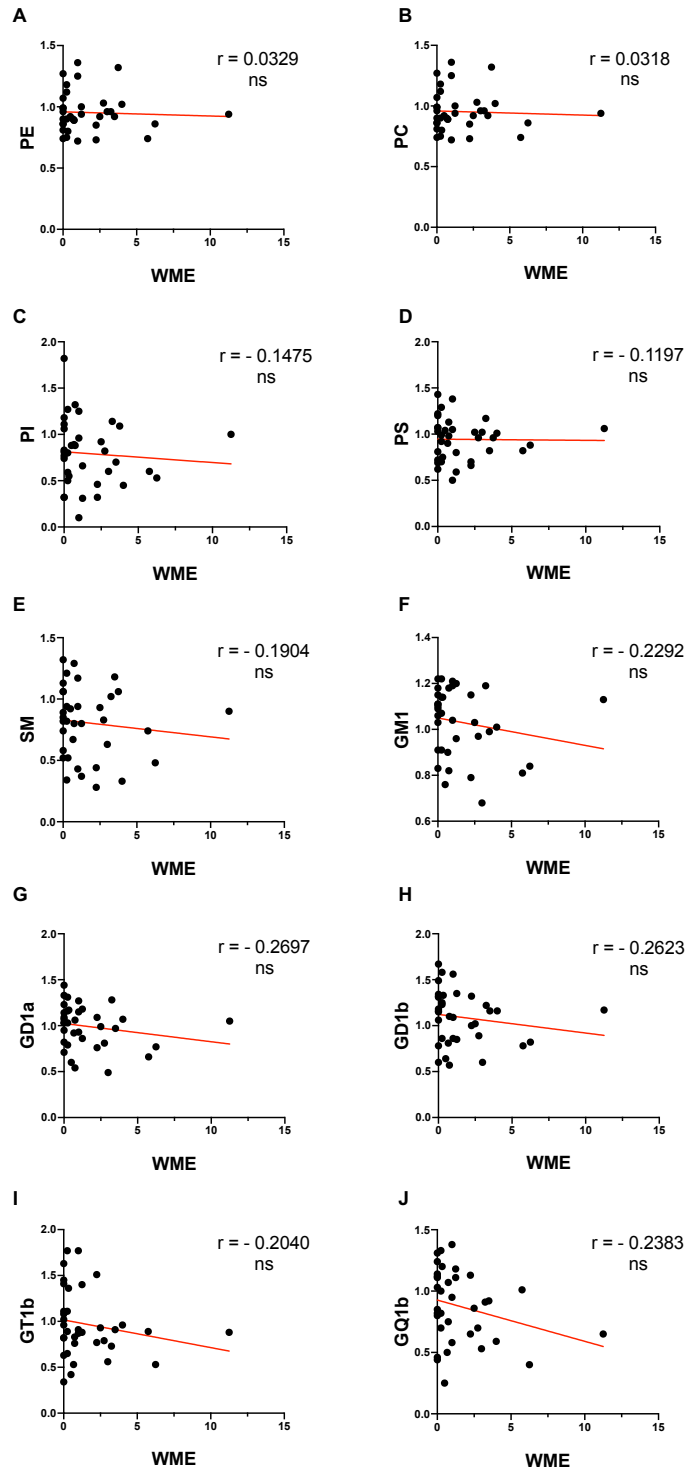
Figure IV. 54. Spearman correlations between the working memory errors done in the Barnes Maze test and glycerophospholipids (A-E) and gangliosides (F-J) of the PFC. Data are presented as individual pairs of values and the linear regression calculated is traced as the red line. XY pairs = 36. Significant differences were considered when p<0.05. Abbreviations: ns = not significant; PC = phosphatidylcholine; PE = phosphatidylethanolamine; PS = phosphatidylserine; PI = phosphatidylinositol; SM = sphingomyelin; r = Spearman's coefficient; WME = working memory errors (performed in the retrieval day).

None of correlations studied between the lipid changes and the WME showed statistical significance; however, some tendencies were observed, as detailed in the following lines. Regarding glycerophospholipids, a positive correlation was found between the WME and PE and PC (**Figure IV. 54A, B**). On the other hand, a negative correlation was found between the WME and PI, PS and SM (**Figure IV. 54C-E**). The levels of all the gangliosides (GM1, GD1a, GD1b, GT1b and GQ1b) were negatively correlated with the WME (**Figure IV. 54 continuation F-J**). The accumulation of GlcCer, GalCer and sulfatides showed a positive correlation with WME (**Figure IV. 54 continuation A-C**), whereas Sph1P was negatively correlated with the cognitive parameter (**Figure IV. 54–D**).
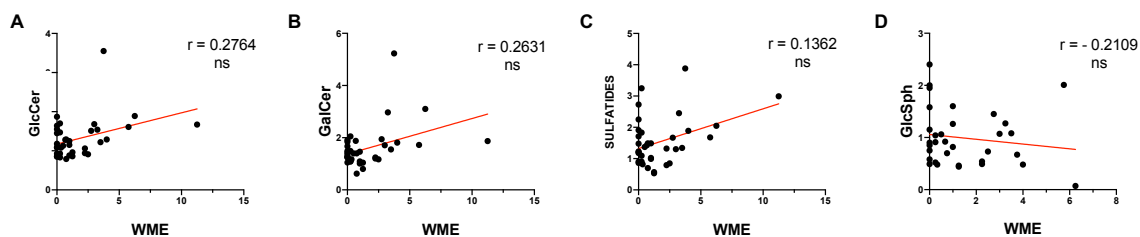
Figure IV. 54 - continuation. Spearman correlations between the working memory errors done in the Barnes Maze test and glycosphingolipids (A-B), sulfatides (C) and GlcSph (D). Data are presented as individual pairs of values and the linear regression calculated is traced as the red line. XY pairs = 36. Significant differences were considered when $p<0.05$. GalCer = galactosylceramide; GlcCer = glucosylceramide; GlcSph = glucosylsphingosine; ns = not significant; r = Spearman's coefficient; WME = working memory errors (performed in the retrieval day).

7.3. Lipid peroxidation in the prefrontal cortex

We found that the immunostaining for 4-HNE was very significantly increased along aging in the PFC of both males (**Figure IV. 55A, B**) and females (**Figure IV. 55A, C**). Interestingly, this increment did not affect equally to males and females: lipid peroxidation was found very significantly higher in old and senile males when they were compared with females of the same age groups (**Figure IV. 55D**).

4-HNE immunostaining had a very significant positive correlation with cognitive decline: higher area immunostained by 4-HNE was associated with higher WME (**Figure IV. 55E**).
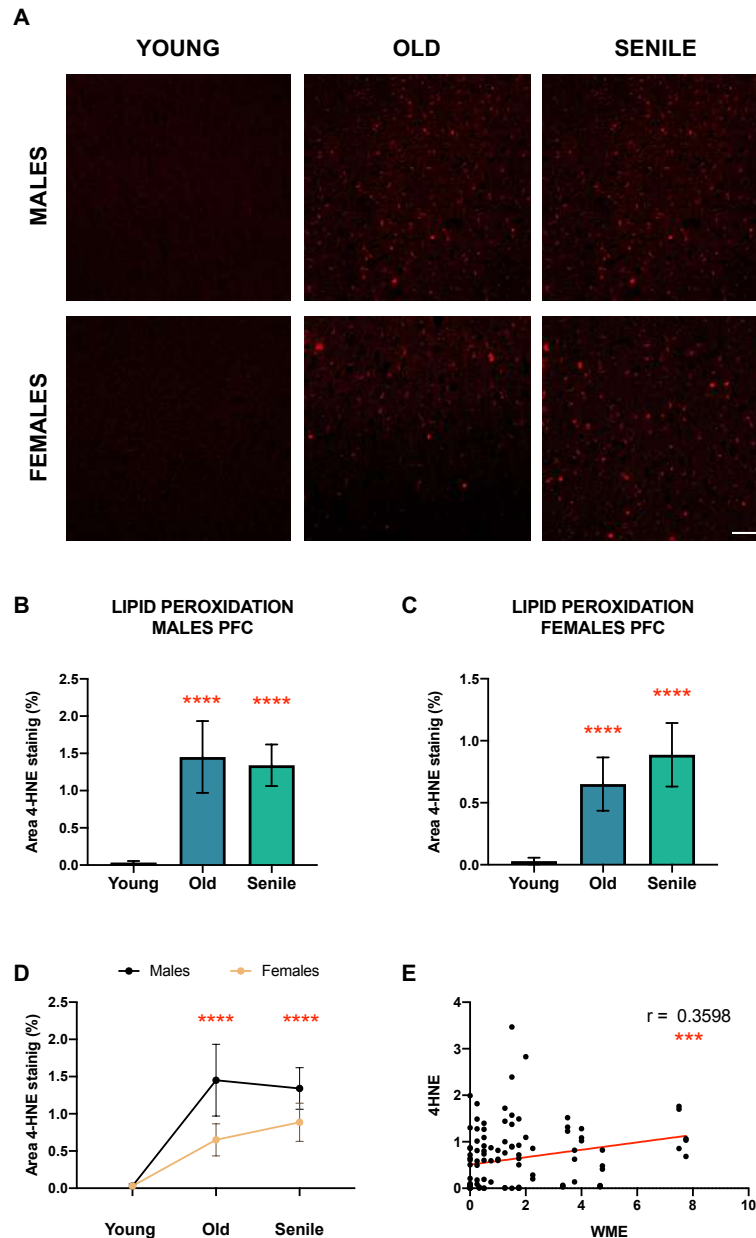
Figure IV. 55. Lipid peroxidation in the PFC and its correlation with cognitive performance. A) Representative microphotographs of 4-HNE immunofluorescence staining in the prefrontal cortex of the different experimental groups. Scale bar=50µm. Quantification of the 4-HNE staining along aging in the prefrontal cortex of males **(B)** and females **(C)** *O. degus*. Age-related differences were determined by one-way ANOVA + Tukey multiple comparison test. Asterisks indicate statistical differences when animals were compared *vs* the young group: **** $p < 0.0001$. Data are presented as mean ± standard deviation. **D)** Sex-related differences regarding lipid peroxidation in the PFC along aging were analyzed by the unpaired t-test. Statistical differences between males and females of the same age are indicated with asterisks: **** $p < 0.0001$. Data are presented as mean ± standard deviation. **E)** Spearman correlations between the working memory errors done in the Barnes Maze test and the 4-HNE staining. Data are presented as individual pairs of values and the linear regression calculated is traced as the red line. Number of XY pairs=111. Abbreviations: 4-HNE = 4-hydroxynoneal; WME = working memory errors (performed in the retrieval day).

DISCUSSION

Discussion of the method. Limitations of the study

The main limitation of this study was the number of animals that were used, especially for the senile ones, which resulted in bigger data dispersion for some lipids. Whether this situation is due to the fact that these animals are not genetically identical or to the sample size, needs to be determined in further studies with enlarged sample size. In addition, the use of the TLC allowed us to obtain information regarding the lipid content of the samples. However, the specificity of the lipid changes found will need further characterization by complementing our results with other high-resolution techniques (e.g., mass spectrometry analyses).

Discussion of results

Impaired lipid metabolism and changes in lipid composition in the brain have been increasingly recognized as key contributing factors to both brain aging and neuropathologies (Hallett et al., 2019; Grassi et al., 2020; Moll et al., 2020, 2021; Yoon et al., 2022; Cuenca-Bermejo et al., Under review). Based on the evidence that the *O. degus* is a natural model for age-associated neurodegeneration, the determination of its brain lipid profile would provide useful information for its characterization and further research. In the present work, the lipid content of the *O. degus* brain has been characterized for the first time. The results revealed region-specific changes in the lipid composition along aging, with sex-associated differences.

First place, the protocol optimization for brain samples of *O. degus* was carried out. Among all the available protocols in literature, we chose the one that had been previously used by our group and others to analyze lipid content in the rodent brain (Scandroglio et al., 2009). We found that this protocol was appropriate to answer our scientific questions, since it allowed the study of the lipidic composition with a good resolution and reduced interferences during the analysis.

In the second step, the general lipid composition of TLEs of the four brain areas (PFC, striatum, cortex, cerebellum) was determined. In agreement with previous studies performed in mouse and human brain samples, the predominant class of lipids were glycerophospholipids (Wood et al., 2015; Otoki et al., 2021) and, among them, PE was the most abundant one (Naudí et al., 2015). On the contrary, gangliosides were the less abundant ones, being GM1, GD1a, GD1b and GT1b the most common species (Tettamanti et al., 1973).

The analysis of the particular lipid species that are present in the TLE of the four brain areas revealed that there is a significant increase in the total lipid content along aging. This result is in contrast with previous studies in humans in which an increase in the total lipid content is associated with maturity, but it decreases with advancing age (Burger and Seidel, 1958). The age- and sex-associated lipid changes were specific for each region analyzed. The lipid profile in the PFC, the striatum and the cortex were mainly determined by the age of the animals; while both age and sex significantly influence the lipid composition of the cerebellum. These data support the idea that aging does not affect heterogeneously the different brain areas (Mattson and Magnus, 2006; Wang et al., 2010; Jové et al., 2014).

To better characterize the differences found in the TLE, a deeper analysis on glycerophospholipids, sphingolipids, sulfatides, gangliosides and cholesterol was performed in the PFC and the cerebellum. Both age and sex had an effect in the lipid content of the two areas, although the cerebellum was more susceptible to them.

Regarding glycerophospholipids, no significant differences were found along aging (neither in the PFC nor in the cerebellum), which is in line with previous findings (Naudí et al., 2015). In both brain areas, glycerophospholipids were significantly affected by the sex of the animals: females showed lower levels of this lipid species than males. Previous works found no significant differences when males and females were compared (Svennerholm et al., 1994) or found that some PC species were higher in females (Chabrun et al., 2020). These differences could be explained by i) the subjects participating in Svennerholm and collaborators' work were human, and numerous variables are known to influence the brain lipid composition in humans (e.g., diet); ii) the mice used in the study of Chabrun and colleagues were not old ones and, therefore sex-associated differences had not manifested yet.

Neutral (GlcCer and GalCer) and acidic sphingolipids (sulfatides) significantly accumulated along aging, in agreement with what has been previously described (Tu et al., 2018). Gangliosides were not significantly affected by age in the PFC. However, when males and females were compared, the greatest differences were observed: senile females had lower gangliosides levels than senile males. These sex-associated differences became very significant in the cerebellum. Regarding age, we found that GM1 in the cerebellum accumulated along aging, while GD1b significantly decreased as the animals aged. These findings are consistent with those described in aged mice and in the senescence-accelerated mouse strain (SAMP-8) (Ohsawa and Shumiya, 1991; Yamamoto et al., 2008; Sipione et al., 2020).

Since the PFC is directly implicated in the circuits of working memory (Chao et al., 2020), correlation analyses were done to explore the relationship between WME done in the BM test and the significant lipid changes found in this brain area. Interestingly, correlations among the glycerophospholipids and cognitive performance showed a very specific pattern: PE and PC higher levels resulted to be positively correlated with the number of WME (worse cognitive performance), while the increased levels of PI, PS and SM were correlated with a better cognitive performance in this species. Correlations between cognitive performance and sphingolipids also showed a particular tendency: whereas neutral sphingolipids and sulfatides were positively correlated with the WME, negative correlations were found for gangliosides. The meaning of these changes must be studied in detailed (e.g., by the analysis of particular sphingolipidic species), however, they reinforce the implications of impaired lipid metabolism in cognitive decline.

Cholesterol is a key structural and functional component in the brain. We found that cholesterol significantly accumulated along aging both in the PFC and in the cerebellum. A growing number of evidence highlights the relationship between high cholesterol levels and AD (Segatto et al., 2013; Skowronska-Krawczyk and Budin, 2020).

Importantly, we found that some lipids show the highest significant differences between males and females in the senile age (e.g., SM and sulfatides), thus suggesting a sex-specific change in the aging process. Importantly, even if some lipids remained unaltered along aging or when animals were grouped just by sex, when both variables were taken into account, the significant changes were evidences. That is, not appreciating that males and females age differently may induce bias in the results.

Lipid peroxidation has been found significantly increased in AD patients (Li et al., 2022). Our results are in agreement with the ones previously published, showing that lipid-associated oxidative stress increases with advancing age and are lower in females than in males (Sobočanec et al., 2003).

Altogether, these findings have several implications. On the one side, these results are a first piece of information on the characterization of the lipid profile of this species. One of the strongest points of this experimental model is the inter-individual variability (under controlled environmental conditions). This scenario is closer to the human situation compared with other traditional rodents (mice and rats), in which genetic background importantly influences the development of physiological or pathological aging. Since some studies have found AD-like histopathological hallmarks in the brain of this rodent but others not, one might think that (as in humans), some individuals are more predisposed than others. Therefore, taking the available information and the present study as a starting

point, further research may investigate how particular lipid changes might correlate with or predispose to the appearance of, for example, detrimental protein deposits. On the other side, these results support that underestimating the effect of sex might lead to bias in research studies, since we found that males and females show differences during their whole lifespan.

SUMMARY OF RESULTS

Taken together, the data presented in this section provide the first brain lipid profile in the *O. degus*, which is vulnerable to both the age and sex effect, in a region-specific manner.

IV.5.	A NEW TOOL TO STUDY PARKINSONISM IN THE CONTEXT OF AGING: MPTP INTOXICATION IN A NATURAL MODEL OF MULTIMORBIDITY

The elaboration of this section is based on the published reference: (Cuenca-Bermejo et al., 2021b). Agreement documents for its use from all the co-authors and permission rights obtained from the journal can be found in the Annex III.

STATE OF THE ART

In the last decades, Parkinson's disease (PD) has become one of the neurodegenerative pathologies with the highest impact in our society (Hayes, 2019). Throughout the years, diverse approaches have been used to analyze different aspects of the disease, ranging from toxin-based models to transgenic animals. Currently, a model that fully recapitulate the human disease is not available yet, although all experimental approaches have advantages and limitations that must be considered when it comes to the study design (Grandi et al., 2018). Among the most commonly used models to mimic human PD, of great relevance is the experimental model based on the neurotoxin 1-methyl-4-phenyl-1,2,3,6-tetrahydro-pyridine (MPTP). Several lines of evidence have shown that MPTP reproduces motor and non-motor symptoms of PD, and it can simulate early and late disease stages of the disease depending on the administration regimen (Grandi et al., 2018; Hamadjida et al., 2019).

When MPTP is administered systemically, it acts as a pro-toxin that is able to cross the blood brain barrier. Then, it is taken up by astrocytes, it is metabolized to MPP+, released and finally captured by the dopaminergic neurons of the ventral mesencephalon and their terminals in the striatum via dopamine transporters. Once inside the cell, MPP+ induces the disruption of the mitochondrial electron chain, which triggers oxidative stress and neurotoxic effects, with neuronal death as a result (Kopin and Markey, 1988). Additionally, several studies have shown that MPTP also induces an exacerbated inflammatory response, which has been shown to be a key element in neurodegeneration (Annese et al., 2013; Huang et al., 2017; Gil-Martínez et al., 2018a).

Administration regimens, as well as their characterization, have been well-established in monkeys and mice. Non-human primates are the most valuable experimental model due to their greater similarity to humans, but their use is limited by certain disadvantageous aspects, such as associated costs, ethics and time consumption (Grandi et al., 2018). For this reason, the use of rodents is a common choice in these trials

even though many of their physiological and pathological processes greatly differ from the ones in humans.

Therefore, taking into account that aging is the main risk factor to develop sporadic PD (which represents the majority of cases) and that this disease co-occurs with other age-related alterations that influence its progression, if we were able to induce Parkinsonism in the *O. degus*, it could represent a promising scenario to investigate the physiopathology of the disease and how comorbidity influences its progression.

Taking this background as a starting point, we hypothesize that the *O. degus* is sensitive to subchronic MPTP-induced neurotoxicity and thus, could be a suitable model for experimental Parkinsonism (**Figure IV. 56**).
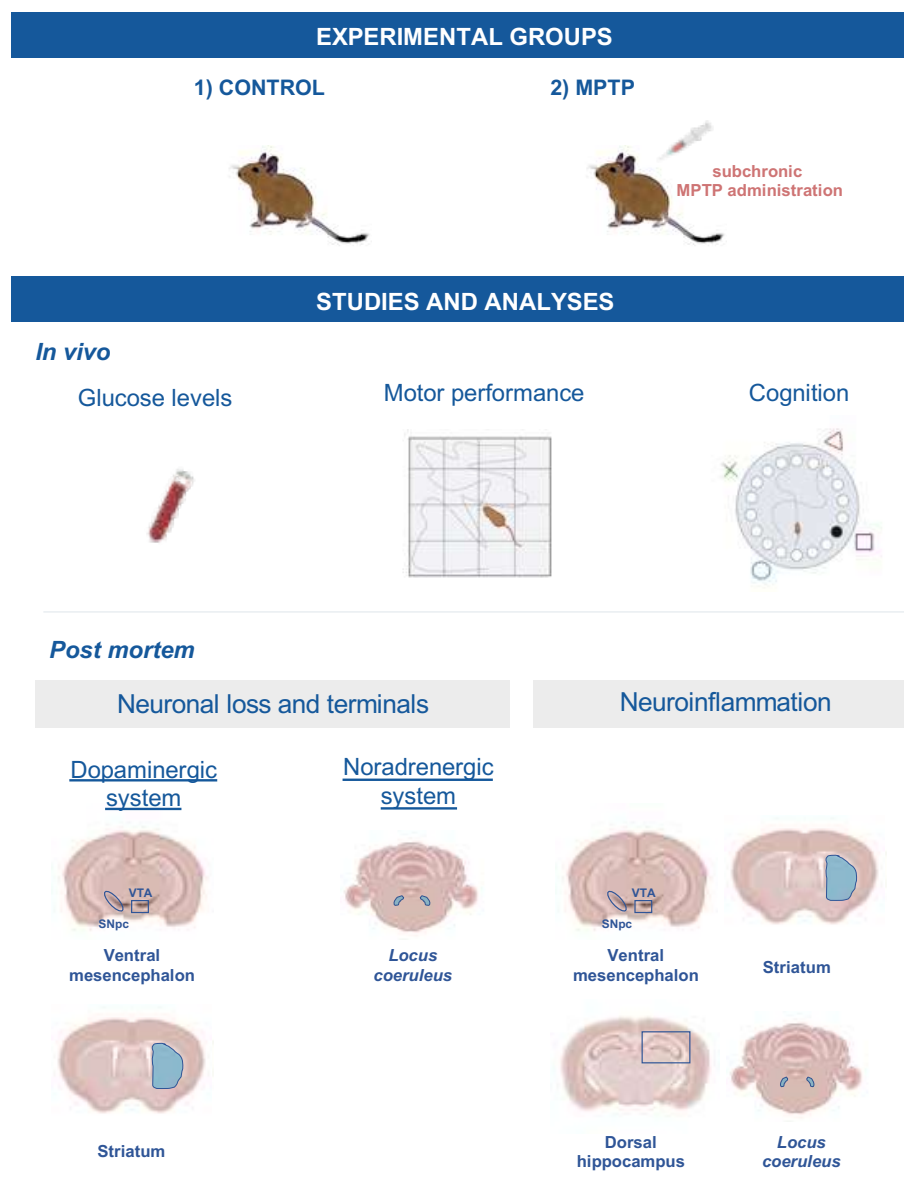
Figure IV. 56. Graphical summary of the experimental design to validate the *O. degus* as an experimental model for Parkinsonism.

RESULTS

1. MPTP intoxication affects body weight

During the entire experiment, the weight of the animals was monitored (**Figure IV. 57A**). In general, weight loss was observed as the dose of MPTP increased, and this decrease was very significant from the first (10 mg/kg) to the fourth dose (40 mg/kg). At this point, a little non-significant weight regain was observed, but a significant decrease was detected again at the time-point corresponding to doses of 80 and 90 mg/kg. No significant changes were observed in the weight of control animals (**Figure IV. 57A**).
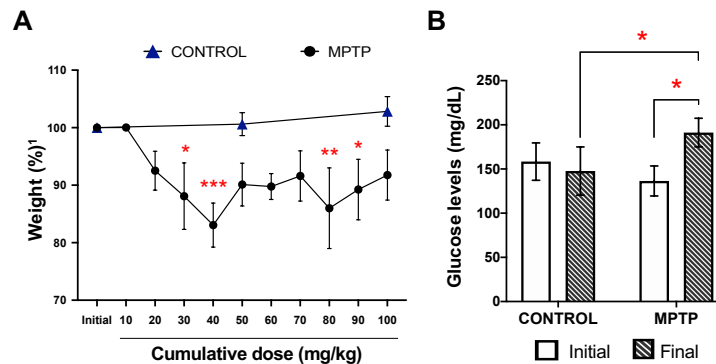
Figure IV. 57. **Weight and glucose levels are affected by MPTP intoxication. A)** Animals were weighted along the experiment, and results are expressed as percentage relative to their own initial weight[1]. **B)** Glucose levels were measured *in vivo* with a glucometer at two time points: before the MPTP injections started (initial) and the day in which the animals were euthanized (final). The same time points were taken as a reference for the control animals. Statistical differences were analyzed by two-way ANOVA + the post-hoc Tukey for weight comparisons and unpaired t-test for glucose levels. Asterisks indicate statistical differences: * $p<0.05$, ** $p<0.01$ *** $p<0.001$. Data are expressed as mean ± standard deviation.

2. Increase of glucose levels induced by MPTP administration

Glucose levels of the two experimental groups were measured at the beginning of the experiment (one day before the injections started) and at the end of the experiment (**Figure IV. 57B**). At baseline, there were no significant differences between the glucose levels of the control and MPTP groups. However, after MPTP intoxication, animals showed significantly higher glucose levels compared with both their baseline levels and with the control animals (**Figure IV. 57B**).

3. MPTP affects motor condition in the *O. degus*

The motor condition of the animals was evaluated at different time-points taking the accumulated doses of MPTP as time reference: baseline (prior to MPTP injections), and the doses of 50, 80 and 100 mg/kg. The traveled distance (cm) and the number of occasions they tried to escape from the platform were measured, and both parameters are

expressed in % with respect to the baseline measurements of each group (**Figure IV. 58**). Animals intoxicated with MPTP showed a decrease in the distance traveled as cumulative dose of MPTP increased, while control animals did not (**Figure IV. 58A**). These differences between MPTP-intoxicated animals and control ones were significant and very significant at the doses 50 and 80 mg/kg respectively, while at the dose 100 mg/kg a decrease in the distance travelled was still observed but it did not reach statistical significance.
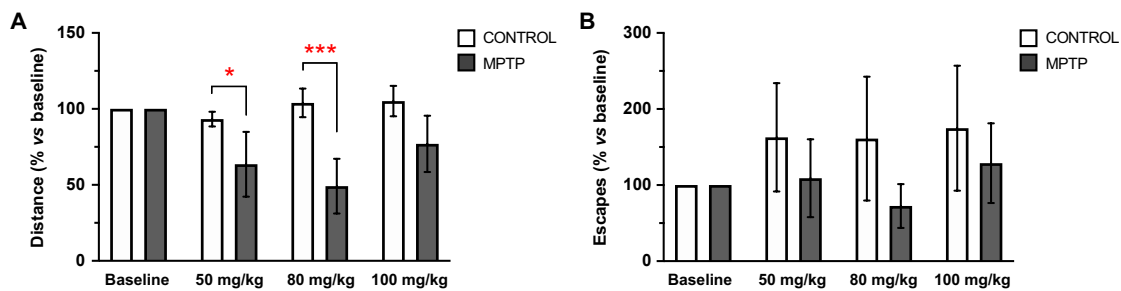
Figure IV. 58. **Travelled distance and escapes in the open field test decrease in the *O. degus* intoxicated with MPTP**. Motor condition was evaluated by the open field test at four time points, taking the cumulative dose of MPTP as reference: before the MPTP injections started (baseline), 50 mg/kg, 80 mg/kg and 100 mg/kg**. A)** Distance travelled by the animals expressed as a percentage in relation to its own baseline data. **B)** Number of escapes from the arena of the open-field expressed as a percentage in relation to its own baseline data. Statistical differences between control and MPTP animals were analyzed by unpaired t-test. Asterisks indicate statistical differences: * $p<0.05$; *** $p<0.001$. Data are expressed as mean ± standard deviation.

Regarding the number of escapes, we observed that the control animals made more escapes within time, while the MPTP animals reduced the number of escapes as the MPTP dose increased, although no significant differences were found (**Figure IV. 58B**). Surprisingly, in line with the data obtained in relation to spontaneous locomotor activity, at the 100 mg/kg dose, a recovery of motor capacity was observed.

4. *O. degus* intoxicated with MPTP show cognitive alterations

In order to understand if MPTP intoxication had an effect on the cognition of these animals, the Barnes Maze test was performed when the animals had received a cumulative dose of 90 mg/kg. No significant differences were observed in relation to the number of times the animals escaped from the maze (**Figure IV. 59A**), although the rest of the evaluated parameters showed differences when the two groups were compared (**Figure IV. 59B-H**).

Regarding the latency to find any hole, the MPTP animals reduced the time in finding it after training, although no significant differences were found (**Figure IV. 59B**). However, even if these animals improved this parameter with training, the time spent to find the

escape hole was always higher when it was compared with the control group, reaching statistical significance in the first day of training (**Figure IV. 59C**).
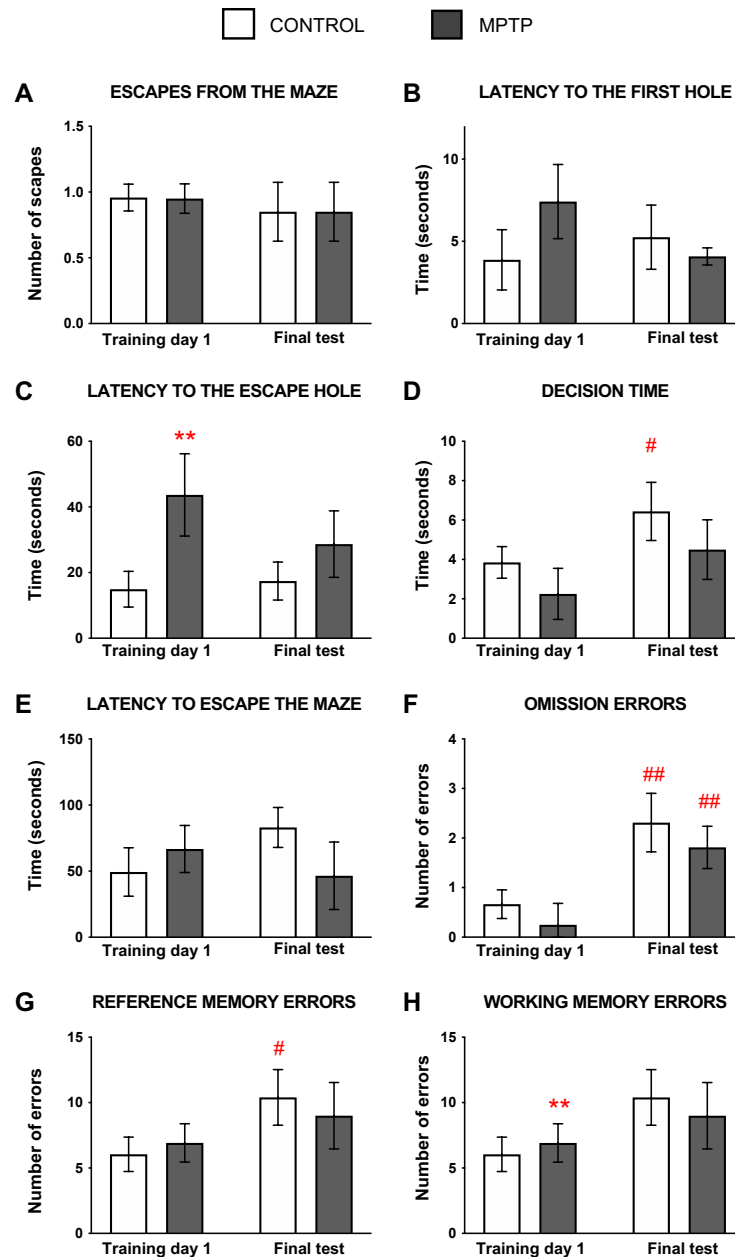
Figure IV. 59. **MPTP alters visuospatial memory in the *O. degus*.** Changes in cognitive performance (visuospatial memory) were studied by evaluating the following parameters in the Barnes Maze test: **A)** Number of escapes from the maze; **B)** Time spent (seconds) to find the first hole of the maze; **C)** Time spent (seconds) to find the escape hole; **D)** Time spent exploring the escape hole before leaving the maze; **E)** Total time taken to escape the maze; **F)** Number of visits to the escape hole without escaping through it; **G)** Number of non-escape holes visited; **H)** Number of repeated visits to non-escape holes. Data are expressed as mean ± standard deviation; $p<0.0001$. Statistical differences between control and MPTP animals were analyzed by two-way ANOVA and the post-hoc Tukey. Asterisks (*) indicate comparison between control and MPTP group in the same time point: ** $p<0.01$; pound sign (#) indicate comparison between the training day 1 and the final test of the same group: # $p<0.05$, ## $p<0.01$.

The time spent exploring the escape hole was always shorter in the MPTP animals compared with the control group. We observed that, after training, animals from both groups reduced their decision time, being these differences significant between control animals (**Figure IV. 59D**).

The time animals spent escaping from the maze was higher in the control animals as the number of trainings increased, while the opposite occurred in the MPTP group (**Figure IV. 59E**).

Omission errors were significantly higher in the two groups of animals as they were trained, although these errors were lower in the MPTP group compared to the control (**Figure IV. 59F**). In order to evaluate the reference memory and the working memory, we evaluated the reference memory errors and the working memory errors, respectively. The same pattern was seen in reference memory errors (**Figure IV. 59G**) and working memory errors (**Figure IV. 59H**) than in the omission ones: errors increased with training but the animals intoxicated with MPTP made fewer errors than the controls at the end of training.

5. Dopaminergic alterations in the MPTP-intoxicated animals

The dopaminergic system was studied by immunostaining of tyrosine hydroxylase (TH) in the ventral mesencephalon (SNpc and VTA), and in the striatum (**Figure IV. 60A, C**).

We found a very significant decrease in the number of TH+ neurons in both the SNpc and in the VTA (**Figure IV. 60D**), being this loss slightly more accused in the VTA. Counterstaining with Nissl confirmed the dopaminergic cell death in the ventral mesencephalon (**Figure IV. 60B**). In the striatum, we found a slight decrease in the optical density of the dopaminergic terminals in the MPTP group compared to the control, without significant statistical differences (**Figure IV. 60E**).

6. Increase of neuroinflammatory cells in the MPTP-intoxicated *O. degus*

Possible MPTP-induced neuroinflammatory processes were studied by detecting microglia (**Figure IV. 61A-C**) and astroglia (**Figure IV. 61D-F**). In both the ventral mesencephalon and the striatum, a very significant increase in the area occupied by these cells was observed (**Figure IV. 61B, C** and **Figure IV. 61E, F**). Both microglial and astroglial responses were more exacerbated in the ventral mesencephalon than in the striatum.

In addition, we observed clear morphological differences in the microglia and astrocytes when the two groups were compared. Regarding microglia, in the MPTP we found shorter processes and an ameboid-like shape (**Figure IV. 61A**). Astrocytes found in

in the control animals had thin GFAP+ branches, while in the MPTP one we detected hypertrophy and increase in the body size (**Figure IV. 61D**).
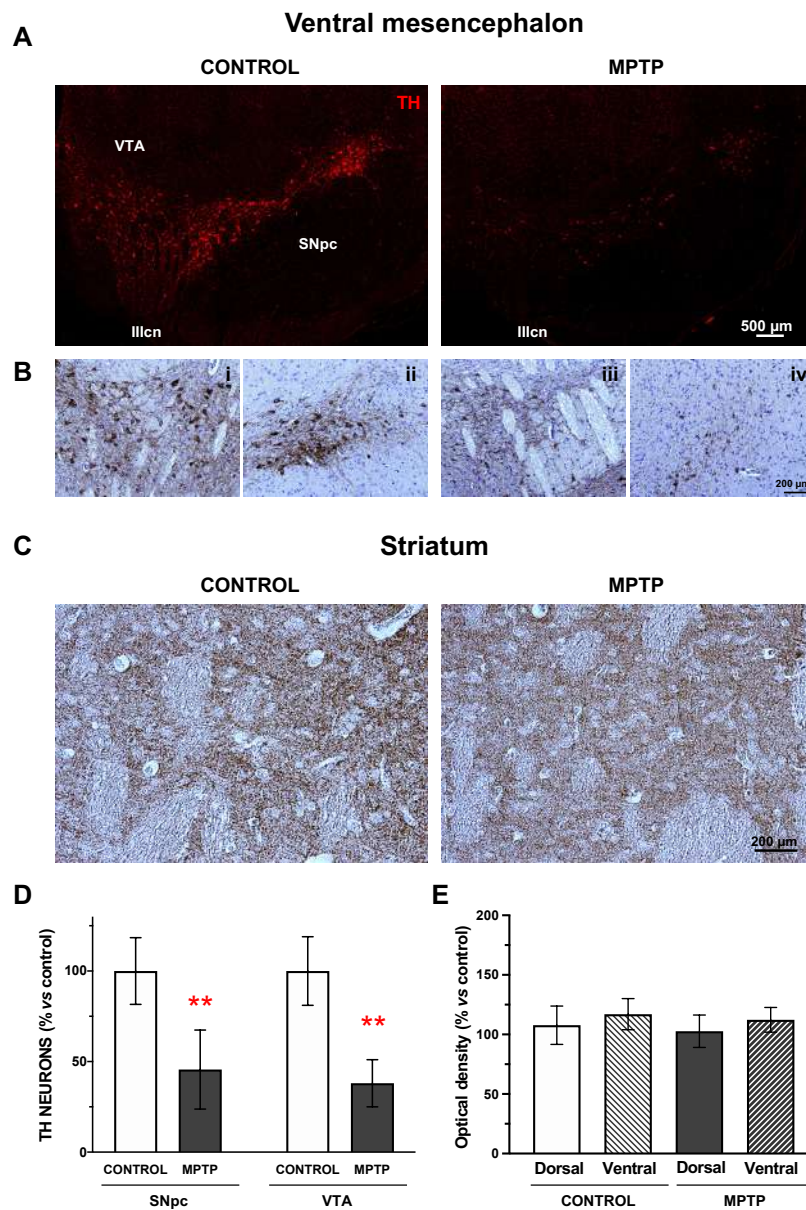
Figure IV. 60. **The dopaminergic pathway is compromised in the *O. degus* after chronic intoxication with MPTP. (A)** Representative microphotographs of TH immunostaining performed in the ventral mesencephalon (SNpc and VTA) of control and MPTP animals; **(B)** TH immunohistochemistry counterstained with Nissl at the level of the exit of the third cranial nerve in VTA and lateral SNpc of control (i, ii) and MPTP animals (iii, iv); **(C)** Representative microphotographs TH immunostaining in the striatum of control and MPTP animals; **D)** Quantification of TH+ neurons in the SNpc and in the VTA; **E)** Optical density quantification of TH+ terminals by in the striatum. Statistical differences between control and MPTP animals, as well as differences among the striatal levels, were analyzed by unpaired t-test. Asterisks indicate statistical differences: ** $p < 0.01$. Data are expressed as mean ± standard deviation. Abbreviations: SNpc = Substantia Nigra pars compacta; VTA = ventral tegmental area; IIIcn = exit of the third cranial nerve.
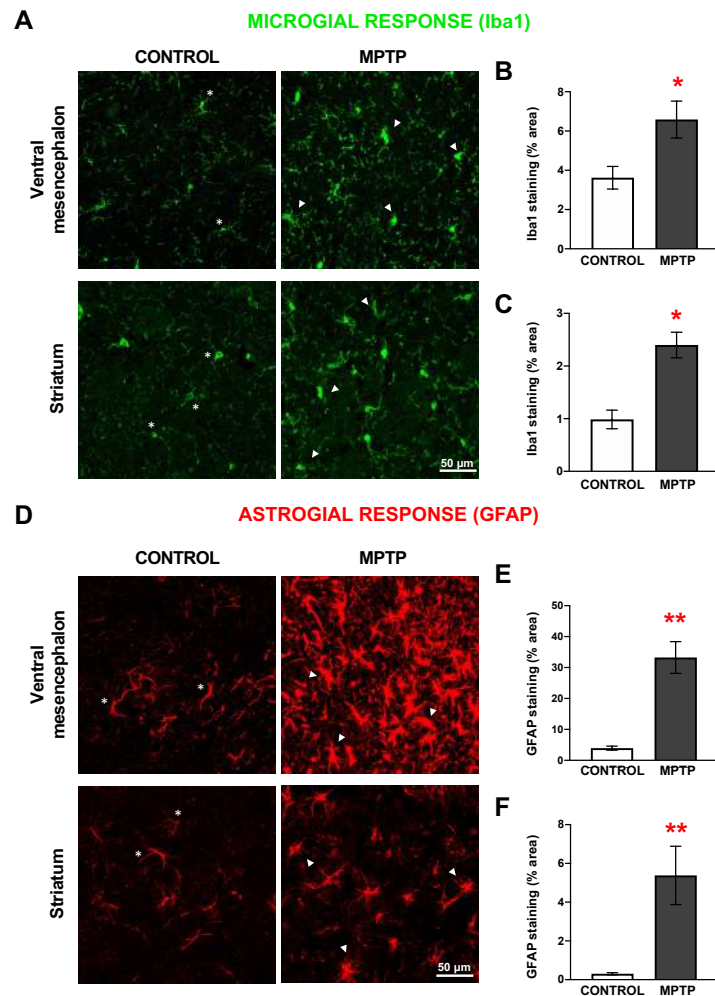
Figure IV. 61. Neuroinflammation is exacerbated both in the ventral mesencephalon and in the striatum of MPTP-*Octodon degus*. A) Representative microphotographs of microglial response, evaluated by Iba1 immunostaining. **B)** Quantification of the Iba1+ surface (area expressed as % of the total area) in the ventral mesencephalon and **(C)** in the striatum. **D)** Representative microphotographs of astroglial response, evaluated by GFAP immunostaining. **E)** Quantification of the GFAP+ surface (area expressed as % of the total area) Quantification of in the ventral mesencephalon and **(F)** in the striatum. White asterisks (*) indicate physiological-like morphology, while white triangles (△) point active or hypertrophic morphology. Statistical differences between control and MPTP animals were analyzed by unpaired t-test. Asterisks indicate statistical differences: * p<0.05; ** p<0.01. Data are expressed as mean ± standard deviation.
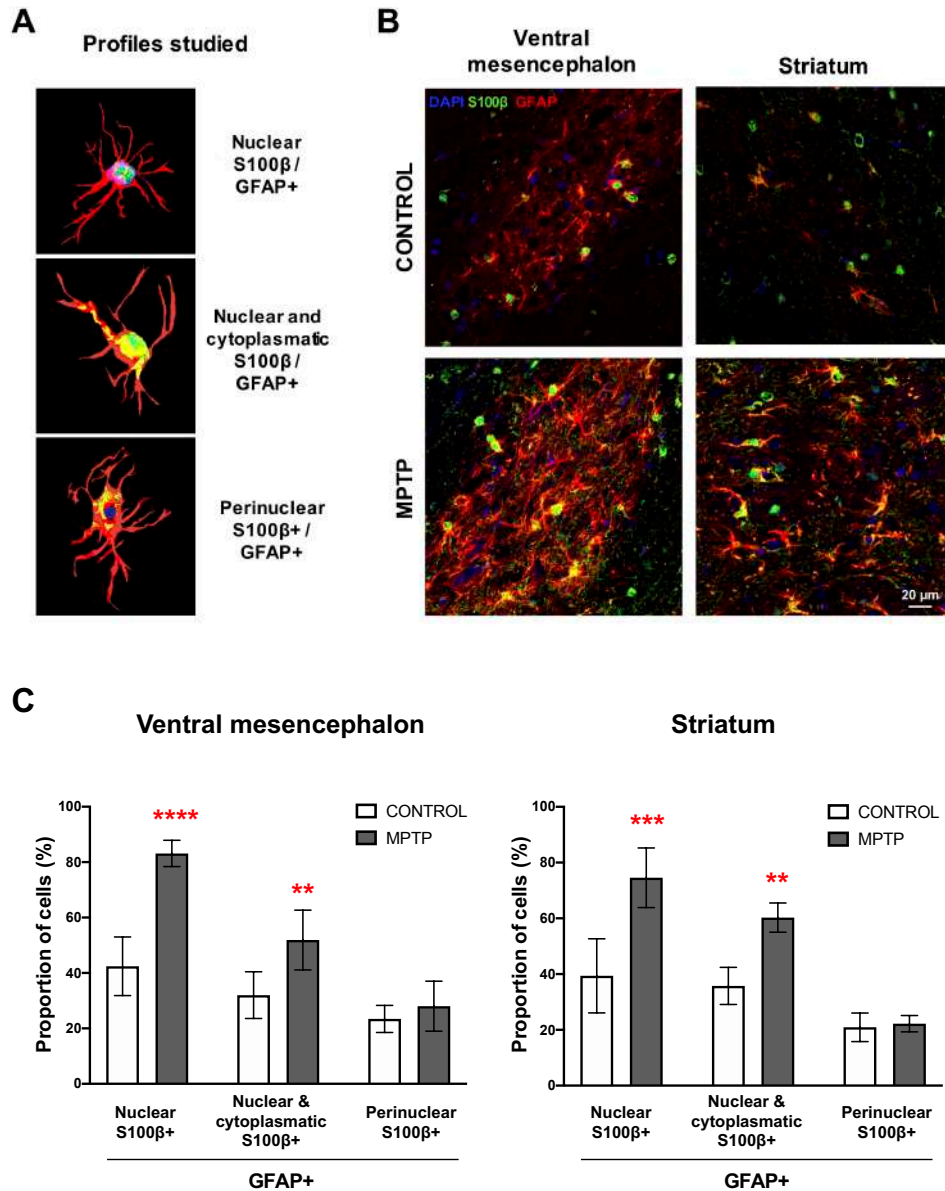
Figure IV. 62. Changes in subcellular localization of S100β in astrocytes cells. A) Schemes of the three profiles of GFAP+/S100β+ astrocytes studied. **B)** Representative microphotographs of the GFAP/S100β immunostaining in the ventral mesencephalon and in the striatum. GFAP+/S100β+ astrocytes cell count in the **(C)** ventral mesencephalon and **(D)** in the striatum. Statistical differences between control and MPTP animals were analyzed by unpaired t-test. Asterisks indicate statistical differences: ** $p < 0.01$, *** $p < 0.001$, **** $p < 0.0001$. Data are expressed as mean ± standard deviation.

7. MPTP promotes reactive astrogliosis in the *O. degus*

The calcium-binding protein S100β is mainly expressed by astrocytes and the increase in its expression levels has been related to neuronal damage. For this reason, we studied different subpopulations of astrocytes according to the subcellular localization of S100β (Gil-Martínez et al., 2018b). We identified three main types of GFAP+/ S100β+

cells (**Figure IV. 62A**): i) S100β exclusively co-localizing with DAPI (nucleus); ii) S100β present in the nucleus and in the astrocyte's cytoplasm; and iii) S100β outside the nucleus (perinuclear). We found that the together with the increase of GFAP expression, the pattern of distribution of S100β in the MPTP animals was different than the one in the control group (**Figure IV. 62B**). In particular, we observed a very significant increase in the number of astrocytes with profiles ii and iii in both the ventral mesencephalon and in the striatum of the *O. degus* intoxicated with MPTP compared with the control group (**Figure IV. 62C**). Interestingly, the increase of astrocytes with nuclear S100β was more significant than the rest of astrocytic profiles. We did not find significant differences in the number of GFAP+ cells with perinuclear S100β.

8. Increase of microglial cells in the hippocampus

Since cognitive alterations were found in the Barnes Maze test, inflammatory state in the dorsal hippocampus was analyzed. For this, we studied the surface immunolabeled for Iba1 in the whole dorsal hippocampus and in its subareas: dentate gyrus, CA1 and CA3 (**Figure IV. 63A**). When the analysis was performed on the entire hippocampus, a significant increase in the area occupied by Iba1+ cells was observed (**Figure IV. 63B**). This increase was also detected in the individual area analysis, although the differences were not statistically significant (**Figure IV. 63C-G**). Notably, the polymorphous areas had a greater increase than the molecular ones (**Figure IV. 63D-G**).

9. MPTP effect on the noradrenergic system: neuronal death in the *locus coeruleus*

TH immunostaining in the LC revealed a very significant reduction in the number of TH+ neurons when MPTP animals were compared with the control ones (**Figure IV. 64A, B**). This decrease was found along the whole rostro-caudal axis of the LC, i.e., the rostral (**Figure IV. 64C**), medial (**Figure IV. 64D**) and caudal (**Figure IV. 64E**) portions of this nucleus were equally affected by the neurotoxin.

10. MPTP effect on the noradrenergic system: neuroinflammation in the *locus coeruleus*

Results regarding the neuroinflammatory response in the LC showed differences along the rostro-caudal axis.
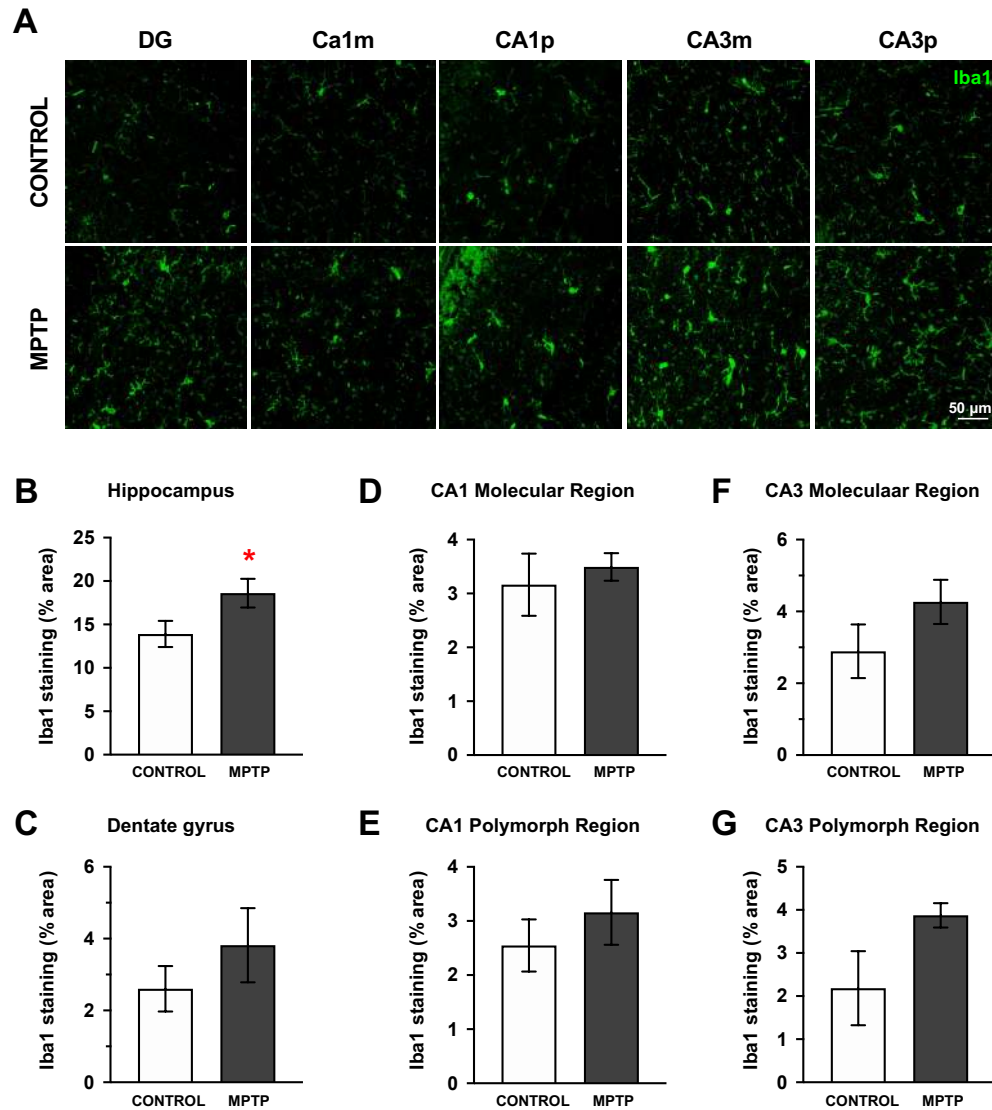
Figure IV. 63. Microglial response is also increased in the dorsal hippocampus. A) Representative images of the Iba1 immunostained sections. Quantification of the surface immunostained for Iba1 (area expressed as % of the total area) in the complete hippocampus **(C)**, the dentate gyrus **(D)**, CA1 molecular **(E)** and polymorph regions **(F)**, CA3 molecular **(G)** and polymorph regions **(H)**. Statistical differences between control and MPTP animals were analyzed by unpaired t-test. Asterisks indicate statistical differences: * $p<0.05$. Data are expressed as mean ± standard deviation. Abbreviations: CA1m = CA1 molecular layer; CA1p = CA1 polymorph layer; CA3m = CA3 molecular layer; CA3p = CA3 polymorph layer; DG = dentate gyrus.

Astrocytes in the control animals showed a ramified morphology, these cells presented a hypertrophic morphology in the MPTP group (**Figure IV. 65A**). The GFAP+ area (%) slightly increased in the whole LC in the MPTP animals, although it was not found statistically significant (**Figure IV. 65B**). A deeper analysis considering the three anatomical levels revealed that this increment reached statistical significance in in the rostral and medial portions of this area when the Parkinsonian animals were compared

with the control ones (**Figure IV. 65C, D**). No significant differences were found in the caudal part of the LC (**Figure IV. 65E**).
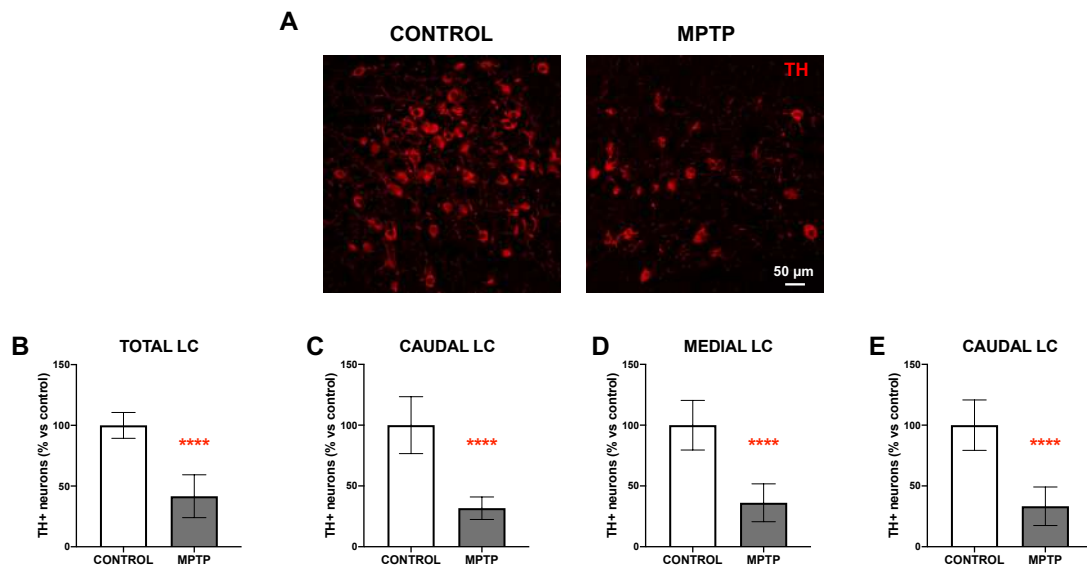
Figure IV. 64. **Neuronal death in the *locus coeruleus* after MPTP intoxication in the *O. degus***. **(A)** Representative microphotographs of TH immunostaining performed in the LC (medial level). Quantification of TH+ neurons in the LC along the rostro-caudal axis: **B)** total LC (sum of all the areas), **C)** rostral portion, **D)** medial portion and **E)** caudal portion. Statistical differences between control and MPTP animals were analyzed by unpaired t-test. Asterisks indicate statistical differences: **** $p < 0.0001$. Data are expressed as mean ± standard deviation. Abbreviations: LC = *locus coeruleus*; TH = tyrosine hydroxylase.

Microglial morphology changed from the ramified and little soma in the control animals, to the ameboid phenotype in the MPTP group (**Figure IV. 66A**). Regarding the area immunostained by the microglial marker Iba1 (**Figure IV. 66**), we did not find any changes at none of the LC anatomical levels considered (**Figure IV. 66B-E**).

DISCUSSION

Discussion of the method. Limitations of the study

Our experimental design allowed us to confirm that the O. degus in sensitive to MPTP intoxication, but we encountered some limitations. In the first place, although some results are consistent enough, others suggest that increasing the number of animals would have helped us to reduce heterogeneity among individuals. For example, the increase in the inflammatory response in the hippocampus was not found statistically significant in the hippocampal subareas, although analyzing the complete hippocampus showed a significant increase in neuroinflammation. Another point we would like to emphasize is that it would be interesting to perform experiments of molecular biology, such as the de-

termination of MPP+ levels in the striatum or the study of the suggested striatal nerve recovery. We hope that the present results will inspire future lines of research and these questions would be addressed.
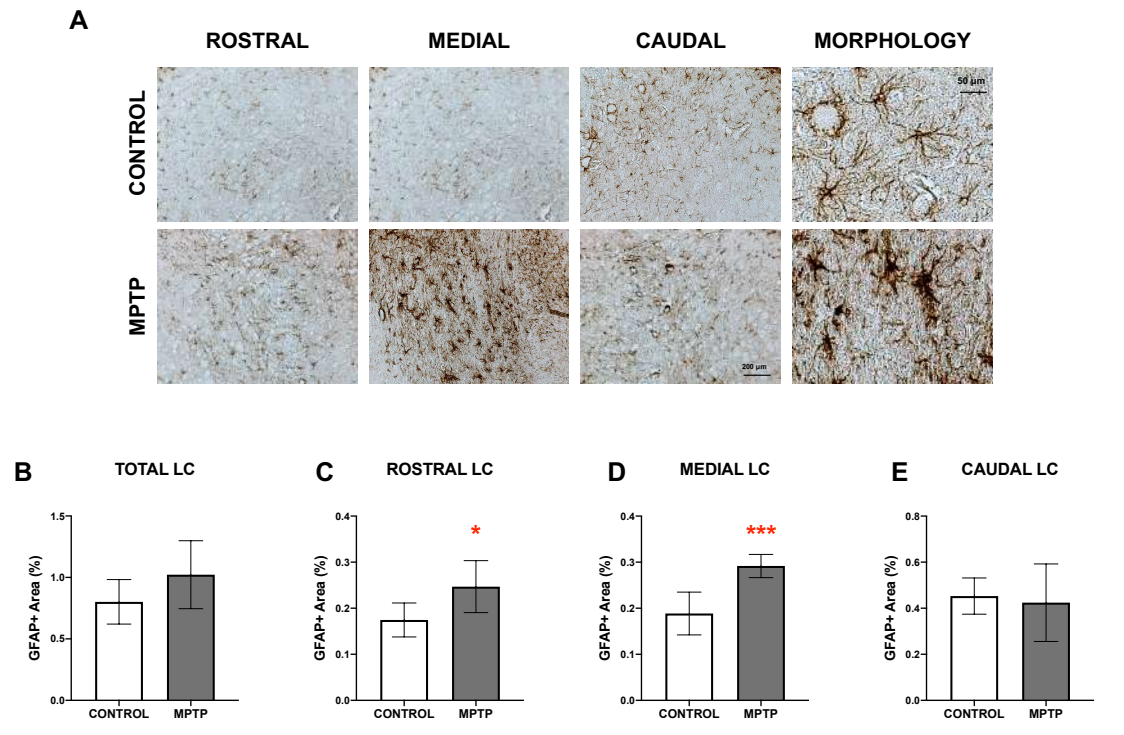
Figure IV. 65. **Astrocytes response is increased in the *locus coeruleus* in the MPTP animals. (A)** Representative microphotographs of GFAP immunostaining performed along the rostro-caudal axis. Quantification of GFAP+ area in the LC along the rostro-caudal axis: **B)** total LC (sum of all the areas), **C)** rostral portion, **D)** medial portion and **E)** caudal portion. Statistical differences between control and MPTP animals were analyzed by unpaired t-test. Asterisks indicate statistical differences: * $p<0.05$, *** $p<0.0001$. Data are expressed as mean ± standard deviation. Abbreviations: LC = *locus coeruleus*.

Discussion of results

In this study, we have validated for the first time that the diurnal rodent *Octodon degus* is sensitive to the subchronic intoxication with MPTP, by the examination of both behavioral performance and postmortem analysis in the dopaminergic system and other PD-related areas (hippocampus and LC).

It has been more than 200 years since PD was first described, but given the complexity of the neurodegenerative process many questions remain unsolved and although there are many available therapies that improve the patients' quality of life, they are not completely effective. In this sense, basic research and the use of experimental models are keys to understand the mechanisms that participate both in the onset and in

the progression of the disease and, therefore, to develop diagnostic tools and accurate treatments.

It is widely accepted that a perfect experimental model has not been found yet and, therefore, it is important to be aware of the advantages and limitations of the chosen experimental model. In this line, animal models for PD research are classically divided in genetic and toxin-based models (Chia et al., 2020). Genetically engineered animals have provided valuable information on the role of specific proteins and metabolic pathways, especially for genetic forms of Parkinson's disease. Their main disadvantage is that they are not able to induce dopaminergic nigral loss. On the other hand, models based on toxins often produce neuronal loss and decrease in dopamine levels, but they usually do not show the formation of Lewy bodies. Hence, a more ideal experimental scenario might be obtained by the combination of the two types of models, always keeping in mind that there is not a perfect experimental model of PD, but we can be able to use the most appropriate model that can answer a specific scientific question.
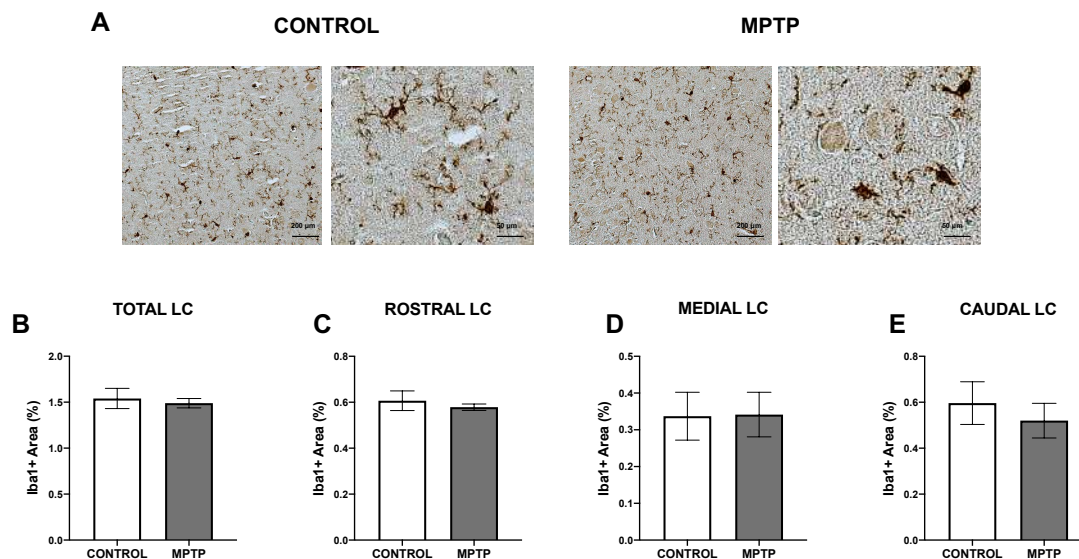
Figure IV. 66. Microglial response is not altered in the *locus coeruleus* in the MPTP animals. (A) Representative microphotographs of Iba1 immunostaining performed in the LC (medial level). Quantification of Iba1+ area in the LC along the rostro-caudal axis: **B)** total LC (sum of all the areas), **C)** rostral portion, **D)** medial portion and **E)** caudal portion. Statistical differences between control and MPTP animals were analyzed by unpaired t-test. No significant differences were found when control and MPTP animals were compared. Data are expressed as mean ± standard deviation. Abbreviations: LC = *locus coeruleus*.

The experimental approach for PD based on the intoxication with MPTP is one of the most preferred because its use has provided important contributions to the understanding of idiopathic PD (Meredith and Rademacher, 2016). Since its discovery, the effects of MPTP have been widely described and this prodrug is known to cause motor

impairment, selective death of the dopaminergic neurons in the SNpc and loss of their striatal terminals, neuroinflammation and oxidative stress, both in humans and in experimental models (mainly non-human primates and mice) (**Figure IV. 59**) (Chia et al., 2020). Moreover, the effect of this neurotoxin can be modulated by different intoxication schedules and doses, offering the possibility to induce a variety of PD-like stages (Grandi et al., 2018). Among them, the chronic regimen (MPTP administration during several weeks) is the one that best reproduces the PD scenario regarding neuronal loss (Hamadjida et al., 2019).

In relation to the in vivo tests, we observed a significative reduction in the spontaneous exploratory movement of the animals within the cumulative dose of MPTP, although a slight increase in the locomotor activity was detected at the end of the experiment. This motor alteration directly correlates with the postmortem analysis of the dopaminergic system performed in the nigrostriatal pathway. The number of TH+ neurons in the ventral mesencephalon of MPTP-intoxicated *O. degus* was dramatically reduced: ~45% of survival in the SNpc and ~38% of survival in the VTA. Surprisingly, optical density of the dopaminergic striatal terminals remained unaffected. These results might explain the slight recovery observed in the motor performance of the MPTP animals in the last injection compared to the lower doses. In this line, previous studies have shown a spontaneous partial motor recovery after MPTP intoxication, which at the striatal levels corresponds with compensatory mechanisms in order to maintain the dopaminergic circuits (Schneider et al., 1998; Mounayar et al., 2007; Gagnon et al., 2018). This neuroadaptive changes can be dopamine-mediated, such as the promotion of dopamine re-uptake and promotion of striatal sprouting of the survival nigral neurons (Rothblat and Schneider, 1994; Blesa et al., 2017; Monje et al., 2020), but they can also be independent, like the participation of external structures, serotonergic compensation or changes in the neuronal arborization in order to increase the postsynaptic contacts with the surviving neurons (Bezard et al., 2003; Obeso et al., 2004; Mounayar et al., 2007). These evidence are compatible with our findings, since despite we performed several weekly injections, the last dose was time-spaced 8 days with the previous one. Therefore, during that time phenomena of recovery could had taken place and the last dose might have not been as strong as to provoke a significant decrease in the dopaminergic terminals. In this sense, future studies might focus on the characterization of the changes induced by MPTP intoxication, conducting different intoxication regimens and different time points for collecting the samples. Moreover, this model could be used to explore the compensatory mechanisms underlying the dopaminergic cell loss in PD.
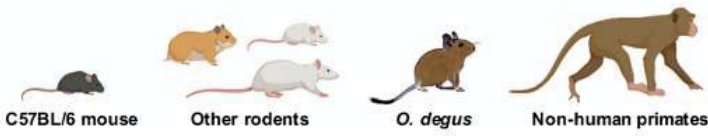
On the other hand, the results concerning dopaminergic cell death in the mesencephalon were impressive to us since several lines of evidence have demonstrated that the TH+ VTA neurons are more resistant to the toxic effect of MPTP and they generally appear unaffected (Langston, 2017). However, in the MPTP-intoxicated *O. degus*, the dopaminergic neurons of the VTA were dramatically reduced, as they were the SNpc ones. It is clear that more studies are needed to understand what are the differential elements in the response against MPTP intoxication in this species compared to other experimental models. An interesting line to explore could be the neuromelanin, calbindin or UCP2 content of these neurons (Herrero et al., 1993a; Paradis et al., 2003; Blesa and Vila, 2019; Peng et al., 2019). Other emerging questions are the ones related to the catecholaminergic system: are other dopamine-innervated regions altered? Is the noradrenergic system affected in the cerebellar pathways? (Heman et al., 2012).

The increase of neuroinflammatory processes is a key hallmark of both PD and experimental models of the disease (Annese et al., 2013; Fuzzati-Armentero et al., 2019; Guzman-Martinez et al., 2019). We also confirmed this feature in the MPTP-intoxicated *O. degus*, since a very significative increase was detected in the surface occupied by microglia (immunodetected with Iba1) and astroglia (immunodetected with GFAP), both in the ventral mesencephalon and in the striatum. This increment was more exacerbated at the ventral mesencephalon level. This behavior was also described by our group in MPTP-intoxicated monkeys 1 year after the injections finished: the glial response was significantly detected in the ventral mesencephalon but not in the striatum (Barcia et al., 2004). Moreover, this increase in the number of glial cells was accompanied by morphological changes in the degus administered with MPTP (reactive microglia and astroglia), according to what has been described in PD patients and experimental models (Kam et al., 2020). To deepen in the inflammatory response, we studied the astroglial population regarding the subcellular distribution of S100β protein, which has been demonstrated to have an important role in PD (Muramatsu et al., 2003; Angelopoulou et al., 2020). We found that the number of astrocytes (GFAP+ cells) expressing S100β in the nucleus and in the cytoplasm was very significantly increased in the ventral mesencephalon and in the striatum of MPTP animals, as previously described in mice (Gil-Martínez et al., 2018b). The increase in the number of GFAP+ cells with S100β+ cytoplasm supports its role as a regulator of proliferation and migration (Donato et al., 2009). Our study was limited to explore the intracellular functions of S100β; however, it would be relevant to analyze extracellular concentrations of this protein, since they have been described to be determinant to exert neuroprotection or detrimental effects (Angelopoulou et al., 2020).

Non-motor symptoms are also present in PD patients. In order to evaluate memory loss and cognitive performance, animals were subjected to Barnes Maze test. The results obtained suggest visuospatial alterations in the performance of the intoxicated animals. MPTP animals had reduced number of escapes from the maze compared with the control group, as well as they spent more time to find the escape hole. These findings might reflect the altered dopaminergic innervation in the VTA. However, it is interesting to see that, after training, MPTP animals reduced the latency to find the first hole and also the escape hole, although their performance was still worse than the control animals. This fact is important to explore new disease modifying strategies in order to improve non-motor signs.

Control animals presented more errors (omission and reference and working memory errors) and spent more time to find the escape from the maze. These differences that were observed by comparison of the parameters of control and MPTP animals might reflect alterations in the dopaminergic system: after training, control animals spent more time exploring the maze and deciding whether to exit or not; on the contrary, MPTP animals seemed more impulsive (impaired dopaminergic circuits) and made less errors because they did not explore the maze. These behaviors could also be due to a different motivation to escape, to motor alterations or to the development of different strategies to solve the maze. This result can be explained by the fact that animals were not as afraid as in the beginning, as previously explained by our group (Tarragon et al., 2014). But, at the end, control animals were able to find the escape hole before the MPTP ones because they were able to remember it and made more correct answers. These findings represent a novelty, since the previous published works have only detected cognitive alterations at low MPTP doses.

Once that we had detected these alterations in visuo-spatial memory and the loss of dopaminergic neurons in the VTA, we decided to study neuroinflammation in the hippocampus, as it is a key brain area for the memory processes (Knierim, 2015). Other studies have demonstrated that, after MPTP intoxication, the hippocampal neuronal population was not altered, but microgliosis is detected (Zhu et al., 2012; Cataldi et al., 2017; Singh et al., 2019). Accordingly, we observed an increase in the area occupied by Iba1+cells (trend). Therefore, this scenario could be interesting to study the role of hippocampus on PD and how it influences the progression of the neurodegenerative process, although a deeper characterization of the nature of the inflammatory response should be carried out.

	C57BL/6 mouse	Other rodents	*O. degus*	Non-human primates
Age-associated traits related to neurodegeneration				
Natural proteinaceous deposits (β-amyloid, tau)	X	X	✔ (1)	X
Spontaneous diabetes	X	X	✔ (2)	X
Chronic MPTP intoxication	↓	↓	↓	↓
Motor alterations	✔ (3)	X (5)	✔ (a)	✔ (6)
Non-motor symptoms (e.g. cognitive decline)	✔ (4)	X (5)	✔ (a)	✔ (7)
Dopaminergic death	✔ (3)	X (5)	✔ (a)	✔ (6)
Neuroinflammation	✔ (3)	X (5)	✔ (a)	✔ (8)
***Locus coeruleus* damage**	✔ (9)	X (5)	✔ (a)	✔ (10)
Dysregulation of blood glucose levels	X	X	✔ (a)	X

Figure IV. 67. Summary of the effects of the chronic MPTP intoxication in different experimental models. "X" symbol indicates that the feature has not been found in the experimental model, while the check symbol means the presence of the feature. (1) Inestrosa et al. 2005; (2) Spear and Caple, 1984; (3) Luchtman et al. 2009; (4) Deguil et al. 2010; (5) Riachi et al. 1989; (a) Demonstrated in the present study; (6) Pérez-Otaño et al. 1994; (7) Vezoli et al. 2004.; (8) Barcia et al. 2004; (9) Seniuk et al., 1990; (10) Forno et al., 1986.

The alteration of other non-dopaminergic areas has been confirmed during the progression of PD, even years before the motor symptoms appear (Cuenca et al., 2019). Several studies, both in human brains and in experimental models of the disease, evidence that alterations in the LC in the early phases of PD are related to the neuropsychiatric symptoms, such as anxiety or sleep alterations (Bari et al., 2020). After MPTP administration, we found that TH+ neurons in the LC were significantly reduced. These results are in agreement with the results obtained in other experimental models of the disease (Chan-Palay and Asan, 1989; Herrero et al., 1993b; Gesi et al., 2000). Regarding neuroinflammation, an increase in the astrocytic response was found in the LC, which was particularly significant at the rostral and media levels. Ascending projections emerge from the rostral segments of the LC to the superior nuclei and cortex (especially the hippocampus), while the more caudal areas of the LC project to the cerebellum and spinal cord (Berridge and Waterhouse, 2003; Dahl et al., 2019). In addition, the rostral

portion of the LC also receives afferents from structures such as the infralimbic cortex and the lateral preoptic area (Luppi et al., 1995). Therefore, most rostral and medial portions of the LC are connected to other areas involved in the severe non-motor symptoms of PD such as depression, anxiety, and disorders of behavior, attention, learning and memory (Berridge and Waterhouse, 2003; Sara, 2009; Dahl et al., 2019).

On the other hand, no significant changes were observed regarding the area occupied by microglial cells (although they exerted evident morphological changes). These results might be explained by the fact that the microglial ship from physiological (ramified) to ameboid state can reduce the area occupied by these cells. In addition, in pathological conditions, microglia tend to move to the site of injury in an attempt to eliminate the cause of the damage and reestablish homeostasis (Fu et al., 2014; Zhan et al., 2017). Therefore, microglia could be moving to the main injury site, that is, the dopaminergic system.

Thus, the data presented suggest that astrocytes are more involved in the LC-related symptoms of PD than microglia. Altogether, these findings place the *O. degus* as a good candidate to explore the role of different brain areas beyond the dopaminergic system in PD.

Finally, blood glucose levels were also determined, since increasing evidence is highlighting the link between diabetes and PD (Camargo-Maluf et al., 2019). We found that MPTP produced an increase in systemic glucose levels in the intoxicated degus, compared with the control animals. In other words, MPTP seems to dysregulate glucose levels, either through dopaminergic denervation or by another mechanism. This finding adds a pathological characteristic to this model that can make a high translational impact. The *O. degus* naturally develops type II diabetes and since glucose levels were more dysregulated after MPTP intoxication, this species offers the possibility to study the co-occurrence of type II diabetes and induced experimental parkinsonism.

The relevance of these results is also supported by the fact that the *O. degus*, differently to rats and mice, is a diurnal rodent that has been classically considered as a natural model to study neurodegeneration, since it spontaneously develops cognitive decline, Alzheimer's disease-like histopathological hallmarks, retinal and macular degeneration (Cuenca-Bermejo et al., 2020).

Additionally, this animal shows some age-related traits such as spontaneous tumors, kidneys dysfunction or electrocardiographic alterations (unpublished data of our lab) (Cadillac et al., 2003; Švara et al., 2020). Therefore, the use of this model offers the possibility to set a more realistic scenario related to the complex process of aging and also to test therapeutical strategies that could slow down de neurodegenerative process.

Finally, despite the fact that MPTP has been well characterized to generate animal models that mimic human PD, most of the rodents show low susceptibility to MPTP even a complete resistance, such as golden hamsters, rats and some mouse strains (e.g., SWR/J and AKR/J) (**Figure IV. 67**) (Zuddas et al., 1994; Rodríguez et al., 2013; Meredith and Rademacher, 2016). In contrast, we have demonstrated that the rodent *O. degus* is sensitive to the neurotoxic effect exerted by MPTP.

SUMMARY OF RESULTS

After subchronic MPTP intoxication in *O. degus*, we have detected the following features: dysregulation of blood glucose levels, both motor and cognitive alterations, dopaminergic neuronal death and increase in the inflammatory processes in the nigrostriatal pathway and in the hippocampus. These novel results suggest that the *O. degus* could represent a new natural tool in the research of age-associated PD, although future in-depth characterization is needed. Therefore, this study offers a new alternative to study PD from the perspective of aging and co-morbidities, closer to the human situation.

CHAPTER V

CONCLUSIONS

CONCLUSIONS

INFLUENCE OF AGE AND SEX ON BLOOD BIOCHEMICAL PROFILE

1. The reference values for different biochemical parameters in the plasma of *O. degus* during aging and with a sex perspective have been determined.

2. The age of the animals was the most influential variable on the values of the biochemical profile in blood.

3. In general metabolism, total protein, cholesterol and calcium increased significantly with the age of the animals.

4. The analytes analyzed indicated that *O. degus* presented alterations in hepatic, renal and pancreatic functions.

5. Blood oxidation status and inflammation parameters increased significantly with the age of the animals.

6. The greatest inter-individual variations were found in the oldest animals, indicating the existence of subclinical pathological situations that do not affect the population homogeneously.

AGE AND SEX DETERMINE ELECTROCARDIOGRAM PARAMETERS

1. Electrocardiogram parameters have been determined in the species *O. degus* during aging and taking into account sex-associated differences.

2. Heart rate was found to be significantly decreased in *O. degus* during aging, being more accentuated in males than in females.

3. Heart rate showed a very positive negative correlation with the weight of the animal and with the duration of the PR and QT intervals.

4. The QRS complex appeared significantly elongated during aging in females, but not in males.

5. The duration of the QT interval showed significant differences between males and females at juvenile and senescent ages.

6. The electrical axis of the heart of males showed more deviations than that of females.

7. Heart size of degus increased significantly during aging and showed a very positive negative correlation with R-wave voltage.

AGE AND SEX EFFECT ON COGNITIVE DECLINE AND NEUROINFLAMMATION IN THE HIPPOCAMPUS

1. *O. degus* showed cognitive impairment associated with aging.
2. At senile age, females showed less cognitive impairment than males during the training period, but greater on the retention day.
3. A significant increase of glial markers Iba1 and GFAP was detected in the dorsal hippocampus of aged *O. degus*, which was more exacerbated in males than in females.
4. Increased levels of neuroinflammation were positively correlated with worse cognition.
5. Increased neuroinflammation in hippocampal areas CA1 and dentate gyrus showed a greater involvement in aging-associated changes.

DIFFERENTIAL BRAIN LIPID COMPOSITION, A MATTER OF AGE AND SEX

1. Lipid composition in the brain of *O. degus* showed a region-dependent profile, with differences in aging and when comparing males and females.
2. Lipid composition in lipid extracts from the prefrontal cortex, striatum and cortex was most influenced by the age of the animals, while in the cerebellum both age and sex significantly influenced.
3. Further characterization of the lipid profile in the prefrontal cortex revealed that, during aging, there is a significant increase in glycosphingolipids, sulfatides and sphingomyelin. Sex-associated differences were detected in glycerophospholipid species, sphingomyelin and glycosylsphingosine, which were significantly higher in males than in females.
4. Further characterization of the lipid profile in the cerebellum revealed that the levels of glycosphingolipids and sulfatides increased significantly with aging. Regarding sex differences, males presented significantly higher levels of phosphatidylinositol, sphingomyelin and glycosylsphingosine than females.
5. The levels of the different ganglioside species were significantly higher in males than in females, both in the prefrontal cortex and in the cerebellum, without changes associated with aging.
6. Changes in lipid composition in the prefrontal cortex showed no significant correlation with working memory errors.
7. Lipid peroxidation in the prefrontal cortex increased significantly during aging, being significantly higher in males than in females.

8. A highly significant positive correlation was found between lipid peroxidation levels in the prefrontal cortex and working memory errors.

A NEW TOOL TO STUDY PARKINSONISM IN THE CONTEXT OF AGING: MPTP INTOXICATION IN A NATURAL MODEL OF MULTIMORBIDITY

1. *O. degus* was sensitive to MPTP-induced neurotoxicity, showing in vivo alterations and involvement of the dopaminergic system and related areas.
2. Subchronic administration of MPTP caused dysregulation of glucose levels in *O. degus*.
3. Parkinsonized degus showed motor and cognitive alterations compared to the control group.
4. MPTP intoxication caused a dramatic decrease of dopaminergic neurons in the SNpc and VTA, although dopaminergic terminals were not affected.
5. MPTP-administered animals showed increased neuroinflammatory processes in the dorsal hippocampus, striatum and ventral midbrain.
6. Parkinsonized animals presented a significant reduction in the number of TH+ neurons in the LC, accompanied by a predominant astrocyte activation in rostral and medial levels of this nucleus, with no changes in microglia.

CONCLUSIONES

INFLUENCIA DE LA EDAD Y EL SEXO EN EL PERFIL BIOQUÍMICO EN PLASMA

1. Se han determinado los valores de referencia para diferentes parámetros bioquímicos en el plasma de *O. degus* durante el envejecimiento y con una perspectiva de sexo.

2. La edad de los animales fue la variable más influyente sobre los valores del perfil bioquímico en sangre.

3. En el metabolismo general, las proteínas totales, el colesterol y el calcio aumentan significativamente con la edad de los animales.

4. Los analitos analizados indicaron que el *O. degus* presentó alteraciones de las funciones hepática, renal y pancreática.

5. El estado de oxidación en sangre y los parámetros de inflamación aumentaron significativamente con la edad de los animales.

6. Las mayores variaciones inter-individuales se encontraron en los animales más envejecidos, indicando la existencia de situaciones patológicas subclínicas que no afectan de manera homogénea a la población.

LA EDAD Y EL SEXO DETERMINAN LOS PARÁMETROS ELECTROCARDIOGRÁFICOS

1. Los parámetros del electrocardiograma han sido determinados en la especie *O. degus* durante el envejecimiento y teniendo en cuenta diferencias asociadas al sexo.

2. La frecuencia cardíaca se encontró disminuida significativamente en el *O. degus* durante el envejecimiento, siendo ésta más acentuada en machos que en hembras.

3. La frecuencia cardíaca mostró una correlación negativa muy positiva con el peso del animal y con la duración de los intervalos PR y QT.

4. El complejo QRS apareció significativamente alargado durante el envejecimiento en las hembras, pero no en los machos.

5. La duración del intervalo QT mostró diferencias significativas entre machos y hembras en las edades juveniles y seniles.

6. El eje eléctrico del corazón de machos presentó más desviaciones que el de las hembras.

7. El tamaño del corazón de los degus aumentó significativamente durante el envejecimiento y mostró una correlación negativa muy positiva con el voltaje de la onda R.

EFECTO DE LA EDAD Y EL SEXO EN EL DETERIORO COGNITIVO Y NEUROINFLAMACIÓN EN EL HIPOCAMPO

1. Los *O. degus* mostraron deterioro cognitivo asociado al envejecimiento.

2. En la edad senil, las hembras presentaron un menor deterioro cognitivo que los machos durante el período de entrenamiento, pero mayor el día de retención.

3. Se detectó un aumento significativo de los marcadores gliales Iba1 y GFAP en el hipocampo dorsal de los degus ancianos, que fue más exacerbado en machos que en hembras.

4. El aumento de los niveles de neuroinflamación se correlacionaron positivamente con una peor cognición.

5. El aumento de la neuroinflamación en las áreas hipocampales CA1 y giro dentado mostró una mayor implicación en los cambios asociados al envejecimiento.

COMPOSICIÓN LIPÍDICA EN EL CEREBRO, UNA CUESTIÓN DE EDAD Y SEXO

1. La composición lipídica en el cerebro del *O. degus* mostró un perfil región-dependiente, con diferencias en el envejecimiento y al comparar machos y hembras.

2. La composición lipídica en los extractos lipídicos de la corteza prefrontal, en el estriado y en la corteza se vio más influida por la edad de los animales, mientras que en el cerebelo tanto la edad como el sexo influyeron significativamente.

3. La mayor caracterización del perfil lipídico en la corteza prefrontal reveló que, durante el envejecimiento, existe un aumento significativo en los glicoesfingolípidos, en las sulfatidas y en la esfingomielina. Las diferencias asociadas al sexo se detectaron en las especies de glicerofosfolípidos, esfingomielina y glicosilesfingosina, que fueron significativamente superiores en machos que en hembras.

4. La mayor caracterización del perfil lipídico en el cerebelo reveló que los niveles de glicoesfingolípidos y sulfatidas aumentaron significativamente con el envejecimiento. En relación a las diferencias de sexo, los machos presentaron niveles de fosfatidilinositol, de esfingomielina y de glicosilesfingosina significativamente superiores a hembras.

5. Los niveles de las diferentes especies gangliosídicas fueron significativamente superiores en machos que en hembras, tanto en la corteza prefrontal como en el cerebelo, sin cambios asociados al envejecimiento.

6. Los cambios en la composición lipídica en la corteza prefrontal no mostraron correlación significativa con los errores de memoria de trabajo.

7. La peroxidación lipídica en la corteza prefrontal aumentó significativamente durante el envejecimiento, siendo significativamente superior en machos que en hembras.

8. Se encontró una correlación positiva muy significativa entre los niveles de peroxidación lipídica en la corteza prefrontal y los errores de memoria de trabajo.

UNA NUEVA HERRAMIENTA PARA EL ESTUDIO DE PARKINSONISMO EN EL CONTEXTO DE ENVEJECIMIENTO: INTOXICACIÓN CON MPTP EN UN MODELO NATURAL DE MULTIMORBILIDAD.

1. El *O. degus* fue sensible a la neurotoxicidad inducida por MPTP, mostrando alteraciones *in vivo* y afectación del sistema dopaminérgico y áreas relacionadas.

2. La administración subcrónica de MPTP provocó la desregulación de los niveles de glucosa en el *O. degus.*

3. Los degus parkinsonizados mostraron alteraciones motoras y cognitivas, en comparación al grupo control.

4. La intoxicación con MPTP provocó una dramática disminución de neuronas dopaminérgicas en la SNpc y en el ATV, aunque las terminales dopaminérgicas no se vieron afectadas.

5. Los animales administrados con MPTP mostraron un aumento de los procesos neuroinflamatorios en el hipocampo dorsal, en el estriado y en el mesencéfalo ventral.

6. Lo animales parkinsonizados presentaron una reducción significativa del número de neuronas TH+ en el LC, acompañado de una activación astrocitaria predominante en niveles rostral y medial de este núcleo, sin cambios en la microglía.

CONCLUSIONI

INFLUENZA DELL'ETÀ E DEL SESSO SUL PROFILO BIOCHIMICO DEL PLASMA

1. Sono stati determinati i valori di riferimento per diversi parametri biochimici nel plasma di *O. degus* durante l'invecchiamento e in relazione al sesso.
2. L'età degli animali è stata la variabile più influente sui valori del profilo biochimico del sangue.
3. Per quanto riguarda il metabolismo generale, le proteine totali, il colesterolo e il calcio sono aumentati significativamente con l'età degli animali.
4. Gli analiti analizzati indicano che *O. degus* presenta alterazioni delle funzioni epatiche, renali e pancreatiche.
5. Lo stato di ossidazione del sangue e i parametri di infiammazione sono aumentati significativamente con l'età degli animali.
6. Le maggiori variazioni interindividuali sono state riscontrate negli animali più vecchi, indicando l'esistenza di situazioni patologiche subcliniche che non colpiscono la popolazione in modo omogeneo.

L'ETÀ E IL SESSO DETERMINANO I PARAMETRI ELETTROCARDIOGRAFICI

1. I parametri dell'elettrocardiogramma sono stati determinati in *O. degus* durante l'invecchiamento e tenendo conto delle differenze legate al sesso.
2. La frequenza cardiaca è risultata significativamente diminuita in *O. degus* durante l'invecchiamento, in modo più accentuato nei maschi rispetto alle femmine.
3. La frequenza cardiaca ha mostrato una correlazione negativa molto significativa con il peso dell'animale e con la durata degli intervalli PR e QT.
4. Il complesso QRS si è allungato significativamente durante l'invecchiamento nelle femmine, ma non nei maschi.
5. La durata dell'intervallo QT ha mostrato differenze significative tra maschi e femmine in età sia giovanile sia senile.
6. L'asse elettrico del cuore maschile ha mostrato maggiori deviazioni rispetto a quello del cuore femminile.
7. Le dimensioni del cuore di *O. degus* sono aumentate in modo significativo durante l'invecchiamento e hanno mostrato una forte correlazione negativa con il voltaggio dell'onda R.

EFFETTO DELL'ETÀ E DEL SESSO SUL DETERIORAMENTO COGNITIVO E SULLA NEUROINFIAMMAZIONE NELL'IPPOCAMPO

1. *O. degus* ha mostrato un declino cognitivo associato all'invecchiamento.
2. In età senile, le femmine, rispetto ai maschi, hanno mostrato un deterioramento cognitivo minore durante il periodo di allenamento, e maggiore nel giorno di memorizzazione.
3. Nell'ippocampo dorsale dei degus anziani è stato rilevato un aumento significativo dei marcatori gliali Iba1 e GFAP, accentuato più nei maschi che nelle femmine.
4. L'aumento dei livelli di neuroinfiammazione è risultato positivamente correlato con il peggioramento delle capacità cognitive.
5. L'aumento della neuroinfiammazione nelle aree ippocampali CA1 e del giro dentato ha mostrato un maggiore coinvolgimento nei cambiamenti associati all'invecchiamento.

COMPOSIZIONE LIPIDICA DEL CERVELLO, UNA QUESTIONE DI ETÀ E DI SESSO

1. La composizione lipidica del cervello di *O. degus* ha mostrato un profilo dipendente dalla regione, con differenze nell'invecchiamento e nel confronto tra maschi e femmine.
2. La composizione lipidica degli estratti lipidici della corteccia prefrontale, dello striato e della corteccia è stata influenzata soprattutto dall'età degli animali, mentre nel cervelletto c'è stata l'influenza significativa sia dell'età sia del sesso.
3. Un'ulteriore caratterizzazione del profilo lipidico nella corteccia prefrontale ha rivelato che, durante l'invecchiamento, si verifica un aumento significativo di glicosfingolipidi, solfatidi e sfingomielina. Sono state rilevate differenze legate al sesso per le specie di glicerofosfolipidi, sfingomielina e glicosilsfingosina, che erano significativamente più alte nei maschi che nelle femmine.
4. Un'ulteriore caratterizzazione del profilo lipidico del cervelletto ha rivelato che i livelli di glicosfingolipidi e solfatidi aumentano significativamente con l'invecchiamento. In relazione alle differenze legate al sesso, i maschi presentavano livelli significativamente più elevati di fosfatidilinositolo, sfingomielina e glicosilsfingosina rispetto alle femmine.
5. I livelli delle diverse specie di gangliosidi erano significativamente più alti nei maschi rispetto alle femmine, sia nella corteccia prefrontale sia nel cervelletto, senza cambiamenti associati all'invecchiamento.

6. I cambiamenti nella composizione lipidica della corteccia prefrontale non hanno mostrato alcuna correlazione significativa con gli errori della memoria di lavoro.

7. La perossidazione lipidica nella corteccia prefrontale è aumentata in modo significativo durante l'invecchiamento, essendo significativamente più alta nei maschi che nelle femmine.

8. È stata trovata una correlazione positiva altamente significativa tra i livelli di perossidazione lipidica nella corteccia prefrontale e gli errori della memoria di lavoro.

UN NUOVO STRUMENTO PER LO STUDIO DEL PARKINSONISMO NEL CONTESTO DELL'INVECCHIAMENTO: L'INTOSSICAZIONE DA MPTP IN UN MODELLO NATURALE DI MULTIMORBILITÀ.

1. *O. degus* è risultato sensibile alla neurotossicità indotta da MPTP, mostrando alterazioni *in vivo* e coinvolgimento del sistema dopaminergico e delle aree correlate.

2. La somministrazione subcronica di MPTP ha causato una disregolazione dei livelli di glucosio in *O. degus*.

3. Gli *O. degus* "parkinsonizzati" hanno mostrato un deterioramento sia motorio sia cognitivo rispetto al gruppo di controllo.

4. L'intossicazione da MPTP ha causato una drastica riduzione dei neuroni dopaminergici nella SNpc e nella VTA, anche se i terminali dopaminergici non sono stati colpiti.

5. Gli animali somministrati con MPTP hanno mostrato un aumento dei processi neuroinfiammatori nell'ippocampo dorsale, nello striato e nel mesencefalo ventrale.

6. Gli animali "parkinsonizzati" hanno mostrato una riduzione significativa del numero di neuroni TH+ nel LC, accompagnata da un'attivazione predominante degli astrociti a livello rostrale e mediale di questo nucleo, senza cambiamenti della microglia.

CHAPTER VI

CONCLUDING REMARKS AND FUTURE PERSPECTIVES

The results obtained along this thesis have provided a deeper characterization of the *O. degus* as an experimental model for physiological and pathological aging. The findings allowed to determine systemic and brain changes along aging and their interaction, including the sex perspective. Briefly, *in vivo* evaluation revealed changes in selected biochemical analytes in the plasma, altered cardiac function and marked cognitive decline, all of them with sex-specific differences. The *post mortem* analyses revealed increased neuroinflammatory processes in the dorsal hippocampus, changes in the brain lipid composition in a region-specific manner, and an increment in lipid peroxidation. Furthermore, it was demonstrated that the *O. degus* is sensitive to the MPTP-induced neurotoxicity, placing this species as a valuable tool for the studies of experimental Parkinsonism beyond the dopaminergic system.

Since each results' block has been deeply discussed in its corresponding section (including the discussion of the method), the present section is not intended to repeat the previous content. Conversely, this final chapter is focused on the integration of these results in a wider perspective. Therefore, at this point, our main question is: what is the overall contribution of this research?

The principal aim of aging research is to enlarge the healthy lifespan. An accurate approach for aging studies should take into account that age is the main risk factor for all the leading causes of morbidity and mortality, such as cardiovascular diseases, cancer and neurodegenerative disorders, including dementia and movement disorders (Kaeberlein et al., 2015). Therefore, it seems clear that the first step to achieve "healthy aging" is to understand the biological age-associated changes in order to reduce the incidence of chronic diseases along aging (Wahl et al., 2017). In this sense, appropriate pre-clinical models of aging are needed to understand both the physiological and pathological mechanisms of age-associated changes (Kane et al., 2016; Rivera et al., 2021). In the recent years, the *O. degus* has been claimed as a potential tool for biomedical research, since it is diurnal and shows several human-like biological features including the development of age-related pathological (Tarragon et al., 2014; Estrada et al., 2015b; Inestrosa et al., 2015; Szabadfi et al., 2015; Hurley et al., 2018; Chang et al., 2020; Cuenca-Bermejo et al., 2020; Švara et al., 2020). However, even if the first published works appeared nearly more than 50 years ago, several aspects of the biology of this species have not been fully characterized yet. Thus, a crucial step to make the most of this interesting and potential experimental model is to deepen in our basic knowledge about it. For example, it was needed that Inestrosa and collaborators had characterized the spontaneous appearance of β-amyloid deposits in aged *O. degus* (Inestrosa et al.,

2005), to inspire further research questions regarding the age-related proteins aggregation and toxicity.

On the one hand, we have evidenced in this thesis that the selected materials and methods are adequate to be used in the *O. degus*: detection of different plasmatic analytes, specificity of the antibodies, protocol to determine the brain lipid composition or the MPTP intoxication, among others. On the other hand, our results contribute to a better characterization of the *O. degus* as an experimental model, providing data related to the biochemical profile, cardiac function, cognitive decline and related hippocampal-neuroinflammation and brain lipid composition (by regions). In addition, data presented regarding the study of age-related changes, serve as a reference not only for further research projects, but they are also useful for routine maintenance. For example, the plasmatic biochemical profile can be used by the animal houses as guideline to monitor the health status of the colony.

Beyond this immediate application of the results, we believe that the data presented here can serve as a starting point to inspire further research. For example, it would be of interest to study correlations between the altered blood parameters and other features, such as histological analyses in kidneys, liver or pancreas. Also, we consider that the findings obtained from the MPTP intoxication are the basis for future investigations that could provide key insights into the pathology with the benefits that a natural model of multimorbidity offers. That is, it would be interesting to know if males and females of this species exert the same sensitivity to this neurotoxin, as well as animals of different ages. Also, further research might validate and characterize the effects of different MPTP administration regimens and how they might induce or exacerbate the proteins deposits.

Obvious sex differences are present during normal development and in the onset and progression of diseases (Nalvarte, 2020). In the last years, increasing efforts have been made to include the differences between males and females as a variable; however, sex is rarely taken into account at the clinical level for the diagnosis and treatment decisions (Pinares-Garcia et al., 2018). In part, this is due to the still lack of understanding of the molecular mechanisms that underlie the sex-associated outcome of health and disease. In our study, both males and females were considered. Importantly, sex-related differences found along aging studies performed in this thesis were detected both in the *in vivo* tests and in the *post mortem* analyses, being more exacerbated in the last ones. This situation suggests that even if males and females can behave similarly at the clinical level, subtle changes are found in their biological scenario, which might help to understand future diseased outcomes. That is, does the fact that males have a higher neuroinflammatory state than females mean a differential predisposition to pathological outcomes? Does the

particular brain lipid composition in males and females affect their aging process? In addition, our experimental design allows that future studies can continue this research line to explore the sex-biased comorbidities and how they contribute to the complex clinical picture in men and women.

Another fundamental issue evidenced in this work is the inter-individual variability of the data. It is clear that, depending on the purpose of the research, data variability can be beneficial or not for the emerging conclusions. In our case, we interpret the higher degree of variability among individuals as an opportunity to explore the underlying clues that configure a particular clinical picture, especially because the higher variability appeared in the aged animals. Data presented in this thesis is the result of the partial analysis of the information and samples collected in the last 10 years in our laboratory. Therefore, a huge number of possibilities to continue this research emerge, ranging from specific scientific questions in one topic (e.g., genetic changes along aging that predispose to protein deposits) to multi-variable analysis. For example, the application of machine learning techniques can be useful to identify potential changes that might lead to pathological situations and the posterior development of early diagnostic tools and effective therapies.

Altogether, results compiled in this thesis are relevant to characterize the *O. degus* as a natural model for aging and multi-morbidity as well as to understand diseases that affect elderly people and their interactions. Therefore, we consider that this research is a reasonable contribution for the scientific community that, hopefully, may inspire further studies focused not only on the characterization of this model but also on the biological meaning of its features for the development of preventive strategies, early diagnose and treatments.

REFERENCES

Akita, M., Kuwahara, M., Tsubone, H., & Sugano, S. (1998). ECG changes during furosemide-induced hypokalemia in the rat. Journal of Electrocardiology, 31(1). https://doi.org/10.1016/S0022-0736(98)90006-1

Al-Awar, A., Kupai, K., Veszelka, M., Szucs, G., Attieh, Z., Murlasits, Z., Török, S., Pósa, A., & Varga, C. (2016). Experimental Diabetes Mellitus in Different Animal Models. Journal of Diabetes Research. https://doi.org/10.1155/2016/9051426

Allen Reference Atlas – Mouse Brain [brain atlas]. Available from atlas.brain-map.org.

Amarya, S., Singh, K., & Sabharwal, M. (2018). Ageing Process and Physiological Changes. In Gerontology. https://doi.org/10.5772/intechopen.76249

Anderson, J. R. (2013). Language, Memory, and Thought. Language, Memory, and Thought. https://doi.org/10.4324/9780203780954

Angelopoulou, E., Paudel, Y. N., & Piperi, C. (2020). Emerging role of S100B protein implication in Parkinson's disease pathogenesis. Cellular and Molecular Life Sciences. https://doi.org/10.1007/s00018-020-03673-x

Annese, V., Barcia, C., Ros-Bernal, F., Gómez, A., Ros, C. M., De Pablos, V., Fernández-Villalba, E., De Stefano, M. E., & Herrero, M. T. (2013). Evidence of oligodendrogliosis in 1-methyl-4-phenyl-1,2,3,6-tetrahydropyridine (MPTP)-induced Parkinsonism. Neuropathology and Applied Neurobiology, 39(2), 132–143. https://doi.org/10.1111/j.1365-2990.2012.01271.x

Araki, T., Ikegaya, Y., & Koyama, R. (2021). The effects of microglia- and astrocyte-derived factors on neurogenesis in health and disease. European Journal of Neuroscience, 54(5), 5880–5901. https://doi.org/10.1111/ejn.14969

Ardiles, A. O., Tapia-Rojas, C. C., Mandal, M., Alexandre, F., Kirkwood, A., Inestrosa, N. C., & Palacios, A. G. (2012). Postsynaptic dysfunction is associated with spatial and object recognition memory loss in a natural model of Alzheimer's disease. Proceedings of the National Academy of Sciences, 109(34), 13835–13840. https://doi.org/10.1073/pnas.1201209109

Ardiles, A., Ewer, J., Acosta, M. L., Kirkwood, A., Martinez, A., Ebensperger, L., Bozinovic, F., Lee, T. M., & Palacios, A. G. (2013). *Octodon degus* (Molina 1782): A model in comparative biology and biomedicine. Cold Spring Harbor Protocols, 8(4), 312–318. https://doi.org/10.1101/pdb.emo071357

Area-Gomez, E., & Schon, E. A. (2017). On the pathogenesis of Alzheimer's Disease: The MAM hypothesis. FASEB Journal, 31(3), 864–867. https://doi.org/10.1096/fj.201601309

Arques, S. (2018). Human serum albumin in cardiovascular diseases. European Journal of Internal Medicine. https://doi.org/10.1016/j.ejim.2018.04.014

Astur, R. S., Taylor, L. B., Mamelak, A. N., Philpott, L., & Sutherland, R. J. (2002). Humans with hippocampus damage display severe spatial memory impairments in a virtual Morris water task. Behavioural Brain Research, 132(1). https://doi.org/10.1016/S0166-4328(01)00399-0

Aureli, M., Grassi, S., Prioni, S., Sonnino, S., & Prinetti, A. (2015). Lipid membrane domains in the brain. Biochimica et Biophysica Acta (BBA) - Molecular and Cell Biology of Lipids, 1851(8), 1006–1016. https://doi.org/10.1016/j.bbalip.2015.02.001

Azam, S., Haque, M. E., Balakrishnan, R., Kim, I. S., & Choi, D. K. (2021). The Ageing Brain: Molecular and Cellular Basis of Neurodegeneration. Frontiers in Cell and Developmental Biology, 9(August), 1–22. https://doi.org/10.3389/fcell.2021.683459

Azizi, Z., Gisinger, T., Bender, U., Deischinger, C., Raparelli, V., Norris, C. M., Kublickiene, K., Herrero, M. T., Emam, K. E., Kautzky-Willer, A., Pilote, L., & GOING-FWD Investigators (2021). Sex, Gender, and Cardiovascular Health in Canadian and Austrian Populations. The Canadian journal of cardiology, 37(8), 1240–1247. https://doi.org/10.1016/j.cjca.2021.03.019

Babbar, M., & Saeed Sheikh, M. (2013). Metabolic stress and disorders related to alterations in mitochondrial fission or fusion. Molecular and Cellular Pharmacology. https://doi.org/10.4255/mcpharmacol.13.11

Balaban, R. S., Nemoto, S., & Finkel, T. (2005). Mitochondria, oxidants, and aging. Cell. https://doi.org/10.1016/j.cell.2005.02.001

Bandhyopadhyay, U., & Cuervo, A. M. (2007). Chaperone-mediated autophagy in aging and neurodegeneration: Lessons from α-synuclein. Experimental Gerontology, 42(1–2), 120–128. https://doi.org/10.1016/j.exger.2006.05.019

Barcia, C., Sánchez Bahillo, A., Fernández-Villalba, E., Bautista, V., Poza Y Poza, M., Fernández-Barreiro, A., Hirsch, E. C., & Herrero, M. T. (2004). Evidence of active microglia in substantia nigra pars compacta of parkinsonian monkeys 1 year after MPTP exposure. Glia, 46(4), 402–409. https://doi.org/10.1002/glia.20015

Bari, B. A., Chokshi, V., & Schmidt, K. (2020). Locus coeruleus-norepinephrine: Basic functions and insights into Parkinson's disease. Neural Regeneration Research. https://doi.org/10.4103/1673-5374.270297

Barnes, C. A. (1979). Memory Deficits Associated With Senescence: A Neurophysiological and Behavioral Study in the Rat. Journal of Comparative and Physiological Psychology, 93(1), 74–104. https://doi.org/10.1037/h0077579

Barrett, G. L., Bennie, A., Trieu, J., Ping, S., & Tsafoulis, C. (2009). The Chronology of Age-Related Spatial Learning Impairment in Two Rat Strains, as Tested by the Barnes Maze. Behavioral Neuroscience, 123(3). https://doi.org/10.1037/a0015063

Barrientos, R. M., M. M. Kitt, L. R. W., & Maier, S. F. (2015). Neuroinflammation in the normal aging hippocampus. Neuroscience, 19(309), 84–99. https://doi.org/10.1016/j.neuroscience.2015.03.007

Bauer, C. M., Correa, L. A., Ebensperger, L. A., & Romero, L. M. (2019). Stress, sleep, and sex: A review of endocrinological research in *Octodon degus*. General and Comparative Endocrinology, 273, 11–19. https://doi.org/10.1016/j.ygcen.2018.03.014

Becerra-Calixto, A., & Cardona-Gómez, G. P. (2017). The role of astrocytes in neuroprotection after brain stroke: Potential in cell therapy. Frontiers in Molecular Neuroscience. https://doi.org/10.3389/FNMOL.2017.00088

Becker, D. E. (2015). Fundamentals of Electrocardiography Interpretation. Amino Acids, 47(8), 1559–1565. https://doi.org/10.1007/s00726-015-1997-y

Beinfield, W. H., & Lehr, D. (1968). P-R interval of the rat electrocardiogram. The American Journal of Physiology, 214(1). https://doi.org/10.1152/ajplegacy.1968.214.1.205

Benjamin Chun-Kit Tong. (2017). Energy Metabolism and Inflammation in Brain Aging and Alzheimer's. Physiology & Behavior, 176(5), 139–148. https://doi.org/10.1016/j.freeradbiomed.2016.04.200.Energy

Berridge, C. W., & Waterhouse, B. D. (2003). The locus coeruleus-noradrenergic system: Modulation of behavioral state and state-dependent cognitive processes. Brain Research Reviews. https://doi.org/10.1016/S0165-0173(03)00143-7

Berry F.J (2020) The physiology of Heart [Available in https://app.biorender.com].

Bettio, L. E. B., Rajendran, L., & Gil-Mohapel, J. (2017). The effects of aging in the hippocampus and cognitive decline. Neuroscience and Biobehavioral Reviews, 79(May), 66–86. https://doi.org/10.1016/j.neubiorev.2017.04.030

Bezard, E., Gross, C. E., & Brotchie, J. M. (2003). Presymptomatic compensation in Parkinson's disease is not dopamine-mediated. Trends in Neurosciences, 26(4), 215–221. https://doi.org/10.1016/S0166-2236(03)00038-9

Bjostad, L. B., Wolf, W. A., & Roelofs, W. L. (1987). Pheromone Biosynthesis in Lepidopterans: Desaturation and Chain Shortening. In Pheromone Biochemistry. https://doi.org/10.1016/b978-0-12-564485-3.50008-7

Blesa, J., & Vila, M. (2019). Parkinson disease, substantia nigra vulnerability, and calbindin expression: Enlightening the darkness? Movement Disorders, 34(2), 161–163.

https://doi.org/10.1002/mds.27618

Blesa, J., Trigo-Damas, I., Dileone, M., del Rey, N. L. G., Hernandez, L. F., & Obeso, J. A. (2017). Compensatory mechanisms in Parkinson's disease: Circuits adaptations and role in disease modification. Experimental Neurology, 298(August), 148–161. https://doi.org/10.1016/j.expneurol.2017.10.002

Braak, H., & Del Tredici, K. (2015). The preclinical phase of the pathological process underlying sporadic Alzheimer's disease. Brain, 138(10). https://doi.org/10.1093/brain/awv236

Braak, H., & Del Tredici, K. (2017). Neuropathological Staging of Brain Pathology in Sporadic Parkinson's disease: Separating the Wheat from the Chaff. Journal of Parkinson's Disease, 7(s1), S73–S87. https://doi.org/10.3233/JPD-179001

Braak, H., Alafuzoff, I., Arzberger, T., Kretzschmar, H., & Tredici, K. (2006). Staging of Alzheimer disease-associated neurofibrillary pathology using paraffin sections and immunocytochemistry. Acta Neuropathologica, 112(4). https://doi.org/10.1007/s00401-006-0127-z

Braak, H., Del Tredici, K., Rüb, U., De Vos, R. A. I., Jansen Steur, E. N. H., & Braak, E. (2003). Staging of brain pathology related to sporadic Parkinson's disease. Neurobiology of Aging, 24(2), 197–211. https://doi.org/10.1016/S0197-4580(02)00065-9

Braidy, N., Poljak, A., Marjo, C., Rutlidge, H., Rich, A., Jugder, B. E., Jayasena, T., Inestrosa, N. C., & Sachdev, P. S. (2017). Corrigendum: Identification of cerebral metal ion imbalance in the brain of ageing *Octodon degus*. Frontiers in Aging Neuroscience, 9 (66). https://doi.org/10.3389/fnagi.2017.00066.

Bray, F., Laversanne, M., Cao, B., Varghese, C., Mikkelsen, B., Weiderpass, E., & Soerjomataram, I. (2021). Comparing cancer and cardiovascular disease trends in 20 middle- or high-income countries 2000–19: A pointer to national trajectories towards achieving Sustainable Development goal target 3.4. Cancer Treatment Reviews. https://doi.org/10.1016/j.ctrv.2021.102290

Brodde, O. E., Konschak, U., Becker, K., Rüter, F., Poller, U., Jakubetz, J., Radke, J., & Zerkowski, H. R. (1998). Cardiac muscarinic receptors decrease with age: In vitro and in vivo studies. Journal of Clinical Investigation, 101(2). https://doi.org/10.1172/JCI1113

Burke, S. N., Wallace, J. L., Nematollahi, S., Uprety, A. R., & Barnes, C. A. (2010). Pattern separation deficits may contribute to age-associated recognition impairments. Behavioral Neuroscience, 124(5). https://doi.org/10.1037/a0020893

Cadillac, J. M., Rush, H. G., & Sigler, R. E. (2003). Polycystic and chronic kidney disease in a young degu (*Octodon degus*). Contemporary Topics in Laboratory Animal Science, 42(2), 43–45.

Calabrese, V., Butterfield, D. A., & Stella, A. M. G. (2008). Aging and Oxidative Stress Response in the CNS. In Handbook of Neurochemistry and Molecular Neurobiology. https://doi.org/10.1007/978-0-387-32671-9_6

Calabrese, V., Santoro, A., Monti, D., Crupi, R., Di Paola, R., Latteri, S., Cuzzocrea, S., Zappia, M., Giordano, J., Calabrese, E. J., & Franceschi, C. (2018). Aging and Parkinson's Disease: Inflammaging, neuroinflammation and biological remodeling as key factors in pathogenesis. Free Radical Biology and Medicine, 115(October 2017), 80–91. https://doi.org/10.1016/j.freeradbiomed.2017.10.379

Calder, P. C. (2017). Omega-3 fatty acids and inflammatory processes: from molecules to man. Biochemical Society Transactions, (July), 1–11. https://doi.org/10.1042/BST20160474

Camargo-Maluf, F., Feder, D., & De Siqueira-Carvalho, A. A. (2019). Analysis of the Relationship between Type II Diabetes Mellitus and Parkinson's Disease: A Systematic Review. Parkinson's Disease, 2019. https://doi.org/10.1155/2019/4951379

Campbell, B. A., & Campbell, E. H. (1962). Retention and extinction of learned fear in infant and adult rats. Journal of Comparative and Physiological Psychology, 55(1). https://doi.org/10.1037/h0049182

Cappaert, N.L.M & van Strien, Niels & Witter, Menno. (2015). Chapter 20. Hippocampal Formation. https://doi.org/10.1016/B978-0-12-374245-2.00020-6.

Cao, W., & Zheng, H. (2018). Peripheral immune system in aging and Alzheimer's disease. Molecular Neurodegeneration, 13(1), 1–17. https://doi.org/10.1186/s13024-018-0290-4

Carrì, M. T., Ferri, A., Cozzolino, M., Calabrese, L., & Rotilio, G. (2003). Neurodegeneration in amyotrophic lateral sclerosis: The role of oxidative stress and altered homeostasis of metals. Brain Research Bulletin. https://doi.org/10.1016/S0361-9230(03)00179-5

Cataldi, S., Arcuri, C., Hunot, S., Légeron, F. P., Mecca, C., Garcia-Gil, M., Lazzarini, A., Codini, M., Beccari, T., Tasegian, A., Fioretti, B., Traina, G., Ambesi-Impiombato, F. S., Curcio, F., & Albi, E. (2017). Neutral sphingomyelinase behaviour in hippocampus neuroinflammation of MPTP-induced mouse model of Parkinson's disease and in embryonic hippocampal cells. Mediators of Inflammation, 2017. https://doi.org/10.1155/2017/2470950

Ceron, J. J., Tecles, F., & Tvarijonaviciute, A. (2014). Serum paraoxonase 1 (PON1) measurement: An update. BMC Veterinary Research, 10(1), 1–11. https://doi.org/10.1186/1746-6148-10-74

Chabrun, F., Dieu, X., Rousseau, G., Chupin, S., Letournel, F., Procaccio, V., Bonneau, D., Lenaers, G., Simard, G., Mirebeau-Prunier, D., Chao de la Barca, J. M., & Reynier, P. (2020). Metabolomics reveals highly regional specificity of cerebral sexual dimorphism in

mice. Progress in neurobiology, 184, 101698. https://doi.org/10.1016/j.pneurobio.2019.101698

Chan-Palay, V., & Asan, E. (1989). Alterations in catecholamine neurons of the locus coeruleus in senile dementia of the Alzheimer type and in Parkinson's disease with and without dementia and depression. Journal of Comparative Neurology, 287(3). https://doi.org/10.1002/cne.902870308

Chandler, N. J., Greener, I. D., Tellez, J. O., Inada, S., Musa, H., Molenaar, P., Difrancesco, D., Baruscotti, M., Longhi, R., Anderson, R. H., Billeter, R., Sharma, V., Sigg, D. C., Boyett, M. R., & Dobrzynski, H. (2009). Molecular architecture of the human sinus node insights into the function of the cardiac pacemaker. Circulation, 119(12). https://doi.org/10.1161/CIRCULATIONAHA.108.804369

Chang, L. Y. L., Ardiles, A. O., Tapia-Rojas, C., Araya, J., Inestrosa, N. C., Palacios, A. G., & Acosta, M. L. (2020). Evidence of Synaptic and Neurochemical Remodeling in the Retina of Aging Degus. Frontiers in Neuroscience, 14(March), 1–16. https://doi.org/10.3389/fnins.2020.00161

Chao, O. Y., Silva, M. A. de S., Yanga, Y.-M., & Huston, J. P. (2020). The medial prefrontal cortex - hippocampus circuit that integrates information of object, place and time to construct episodic memory in rodents: behavioral, anatomical and neurochemical properties. Neurosci Biobehav Rev., 113, 373–407. https://doi.org/10.1016/j.neubiorev.2020.04.007

Chen, C. Y., Chen, K. S., Chang, K. M., Lee, W. M., Chang, S. C., & Wang, H. C. (2013). Dexmedetomidine related bradycardia leading to cardiac arrest in a dog. Pakistan Veterinary Journal, 33(1).

Chen, X. Q., & Mobley, W. C. (2019). Alzheimer disease pathogenesis: Insights from molecular and cellular biology studies of oligomeric Aβ and tau species. Frontiers in Neuroscience. https://doi.org/10.3389/fnins.2019.00659

Chevaleyre, V., & Piskorowski, R. A. (2016). Hippocampal Area CA2: An Overlooked but Promising Therapeutic Target. Trends in Molecular Medicine. https://doi.org/10.1016/j.molmed.2016.06.007

Chia, S. J., Tan, E. K., & Chao, Y. X. (2020). Historical perspective: Models of Parkinson's disease. International Journal of Molecular Sciences, 21(7), 1–14. https://doi.org/10.3390/ijms21072464

Chiurchiù, V., Tiberi, M., Matteocci, A., Fazio, F., Siffeti, H., Saracini, S., Mercuri, N. B., & Sancesario, G. (2022). Lipidomics of Bioactive Lipids in Alzheimer's and Parkinson's Diseases: Where Are We?. International journal of molecular sciences, 23(11), 6235.

https://doi.org/10.3390/ijms23116235

Choi, M. L., & Gandhi, S. (2018). Crucial role of protein oligomerization in the pathogenesis of Alzheimer's and Parkinson's diseases. The FEBS Journal. https://doi.org/10.1111/febs.14587

Chung, C. G., Lee, H., & Lee, S. B. (2018). Mechanisms of protein toxicity in neurodegenerative diseases. Cellular and Molecular Life Sciences, (0123456789), 1–22. https://doi.org/10.1007/s00018-018-2854-4

Cini, M., & Moretti, A. (1995). Studies on lipid peroxidation and protein oxidation in the aging brain. Neurobiology of Aging, 16(1). https://doi.org/10.1016/0197-4580(95)80007-E

Cisternas, P., Zolezzi, J. M., Lindsay, C., Rivera, D. S., Martinez, A., Bozinovic, F., & Inestrosa, N. C. (2018). New Insights into the Spontaneous Human Alzheimer's Disease-Like Model *Octodon degus*: Unraveling Amyloid-β Peptide Aggregation and Age-Related Amyloid Pathology. Journal of Alzheimer's Disease, 66(3), 1145–1163. https://doi.org/10.3233/JAD-180729

Colonnello, V., Iacobucci, P., Fuchs, T., Newberry, R. C., & Panksepp, J. (2011). *Octodon degus*. A useful animal model for social-affective neuroscience research: Basic description of separation distress, social attachments and play. Neuroscience and Biobehavioral Reviews, 35(9), 1854–1863. https://doi.org/10.1016/j.neubiorev.2011.03.014

Contreras-Aguilar, M. D., Vallejo-Mateo, P. J., Lamy, E., Escribano, D., Cerón, J. J., Tecles, F., & Rubio, C. P. (2021). Changes in saliva analytes in dairy cows during peripartum: A pilot study. Animals, 11(3), 1–10. https://doi.org/10.3390/ani11030749

Corkin, S. (2002). What's new with the amnesic patient H.M.? Nature Reviews Neuroscience, 3(2). https://doi.org/10.1038/nrn726

Corkin, S., Amaral, D. G., Gilberto González, R., Johnson, K. A., & Hyman, B. T. (1997). H. M.'s Medial temporal lobe lesion: Findings from magnetic resonance imaging. Journal of Neuroscience, 17(10). https://doi.org/10.1523/jneurosci.17-10-03964.1997

Crossman, A. R., Neary, D. (2007). Neuroanatomy: an Illustrated Colour Text. 3rd edition. ISBN: 0-443-10036-5.

Cruz-Sánchez, F. F., Moral, A., Tolosa, E., De Belleroche, J., & Rossi, M. L. (1998). Evaluation of neuronal loss, astrocytosis and abnormalities of cytoskeletal components of large motor neurons in the human anterior horn in aging. Journal of Neural Transmission, 105(6–7). https://doi.org/10.1007/s007020050088

Cuenca-Bermejo, L., Almela, P., Navarro-Zaragoza, J., Villalba, E. F., González-Cuello, A. M., Laorden, M. L., & Herrero, M. T. (2021a). Cardiac changes in Parkinson's disease:

Lessons from clinical and experimental evidence. International Journal of Molecular Sciences, 22(24). https://doi.org/10.3390/ijms222413488

Cuenca-Bermejo, L., Pizzichini, E., Gonçalves, V. C., Guillén-Díaz, M., Aguilar-Moñino, E., Sánchez-Rodrigo, C., González-Cuello, A. M., Fernández-Villalba, E., & Herrero, M. T. (2021b). A new tool to study parkinsonism in the context of aging: MPTP intoxication in a natural model of multimorbidity. International Journal of Molecular Sciences, 22(9), 1–20. https://doi.org/10.3390/ijms22094341

Cuenca-Bermejo, L., Pizzichini, E., Gonzalez-Cuello, A. M., De Stefano, M. E., Fernandez-Villalba, E., & Herrero, M. T. (2020). *Octodon degus*: a natural model of multimorbidity for ageing research. Ageing Research Reviews, 64(June), 101204. https://doi.org/10.1016/j.arr.2020.101204

Cuenca-Bermejo L, Prinetti A, Kublickiene K, Raparelli V, Kautzky-Willer A, Norris CM, Pilote L, Herrero MT and the GOING-FWD Consortium. Old brain stories: how do age and sex influence the neurodegeneration-associated lipid changes? *(Under Review).*

Cuenca, L., Gil-Martinez, A. L., Cano-Fernandez, L., Sanchez-Rodrigo, C., Estrada, C., Fernandez-Villalba, E., & Herrero Ezquerro, M. T. (2019). Parkinson's disease: A short story of 200 years. Histology and Histopathology, 34(6), 573–591. https://doi.org/10.14670/HH-18-073

Dahl, M. J., Mather, M., Düzel, S., Bodammer, N. C., Lindenberger, U., Kühn, S., & Werkle-Bergner, M. (2019). Rostral locus coeruleus integrity is associated with better memory performance in older adults. Nature Human Behaviour, 3(11). https://doi.org/10.1038/s41562-019-0715-2

David, J. P., Ghozali, F., Fallet-Bianco, C., Wattez, A., Delaine, S., Boniface, B., Di Menza, C., & Delacourte, A. (1997). Glial reaction in the hippocampal formation is highly correlated with aging in human brain. Neuroscience Letters, 235(1–2). https://doi.org/10.1016/S0304-3940(97)00708-8

Davidsson, P., Fredman, P., Månsson, J. E., & Svennerholm, L. (1991). Determination of gangliosides and sulfatide in human cerebrospinal fluid with a microimmunoaffinity technique. Clinica Chimica Acta, 197(2). https://doi.org/10.1016/0009-8981(91)90272-E

de Diego, I., Peleg, S., & Fuchs, B. (2019). The role of lipids in aging-related metabolic changes. Chemistry and Physics of Lipids, 222(May), 59–69. https://doi.org/10.1016/j.chemphyslip.2019.05.005

de Lange, A. M. G., Barth, C., Kaufmann, T., Maximov, I. I., van der Meer, D., Agartz, I., & Westlye, L. T. (2020). Women's brain aging: Effects of sex-hormone exposure, pregnancies, and genetic risk for Alzheimer's disease. Human Brain Mapping, 41(18),

5141–5150. https://doi.org/10.1002/hbm.25180

De Lima, M. N. M., Laranja, D. C., Caldana, F., Bromberg, E., Roesler, R., & Schröder, N. (2005). Reversal of age-related deficits in object recognition memory in rats with L-deprenyl. Experimental Gerontology, 40(6). https://doi.org/10.1016/j.exger.2005.03.004

Deacon, R. M., Altimiras, F. J., Bazan-Leon, E. A., Pyarasani, R. D., Nachtigall, F. M., Santos, L. S., Tsolaki, A. G., Pednekar, L., Kishore, U., Biekofsky, R. R., Vasquez, R. A., & Cogram, P. (2015). Natural AD-Like Neuropathology in *Octodon degus*: Impaired Burrowing and Neuroinflammation. Current Alzheimer Research, 12(4), 314–322. https://doi.org/10.2174/1567205012666150324181652

Deiana, S., Platt, B., & Riedel, G. (2011). The cholinergic system and spatial learning. Behavioural Brain Research. https://doi.org/10.1016/j.bbr.2010.11.036

Deng, H., Wang, P., & Jankovic, J. (2018). The genetics of Parkinson disease. Aging Reserach Reviews, 42(December 2017), 72–85. https://doi.org/10.1016/B978-0-444-63233-3.00014-2

Desai, M. K., Guercio, B. J., Narrow, W. C., & Bowers, W. J. (2011). An Alzheimer's disease-relevant presenilin-1 mutation augments amyloid-beta-induced oligodendrocyte dysfunction. GLIA, 59(4). https://doi.org/10.1002/glia.21131

Di Domenico, F., Tramutola, A., & Butterfield, D. A. (2017). Role of 4-hydroxy-2-nonenal (HNE) in the pathogenesis of Alzheimer's disease and other selected age-related neurodegenerative disorders. Free Radical Biology and Medicine. https://doi.org/10.1016/j.freeradbiomed.2016.10.490

Díaz, M., Fabelo, N., Ferrer, I., & Marín, R. (2018). "Lipid raft aging" in the human frontal cortex during nonpathological aging: gender influences and potential implications in Alzheimer's disease. Neurobiology of Aging, 67, 42–52. https://doi.org/10.1016/j.neurobiolaging.2018.02.022

DiSabato, D., Quan, N., & Godbout, J. P. (2016). Neuroinflammation: The Devil Is in the Details. Journal of Neurochemistry, 139(1), 136–153. https://doi.org/10.1111/jnc.13607.

Donato, R., Sorci, G., Riuzzi, F., Arcuri, C., Bianchi, R., Brozzi, F., Tubaro, C., & Giambanco, I. (2009). S100B's double life: Intracellular regulator and extracellular signal. Biochimica et Biophysica Acta - Molecular Cell Research, 1793(6), 1008–1022. https://doi.org/10.1016/j.bbamcr.2008.11.009

Dorninger, F., Forss-Petter, S., Wimmer, I., & Berger, J. (2020). Plasmalogens, platelet-activating factor and beyond – Ether lipids in signaling and neurodegeneration. Neurobiology of Disease, 145(May). https://doi.org/10.1016/j.nbd.2020.105061

Doyle, R., Sadlier, D. M., & Godson, C. (2018). Pro-resolving lipid mediators: Agents of anti-

ageing? Seminars in Immunology. https://doi.org/10.1016/j.smim.2018.09.002

Driscoll, I., Davatzikos, C., An, Y., Wu, X., Shen, D., Kraut, M., & Resnick, S. M. (2009). Longitudinal pattern of regional brain volume change differentiates normal aging from MCI. Neurology, 72(22). https://doi.org/10.1212/WNL.0b013e3181a82634

Driscoll, I., Howard, S. R., Stone, J. C., Monfils, M. H., Tomanek, B., Brooks, W. M., & Sutherland, R. J. (2006). The aging hippocampus: A multi-level analysis in the rat. Neuroscience, 139(4). https://doi.org/10.1016/j.neuroscience.2006.01.040

Driscoll, Ira, Hamilton, D. A., Petropoulos, H., Yeo, R. A., Brooks, W. M., Baumgartner, R. N., & Sutherland, R. J. (2003). The Aging Hippocampus: Cognitive, Biochemical and Structural Findings. Cerebral Cortex, 13(12). https://doi.org/10.1093/cercor/bhg081

Du, A. T., Schuff, N., Zhu, X. P., Jagust, W. J., Miller, B. L., Reed, B. R., Kramer, J. H., Mungas, D., Yaffe, K., Chui, H. C., & Weiner, M. W. (2003). Atrophy rates of entorhinal cortex in AD and normal aging. Neurology, 60(3), 481–486. https://doi.org/10.1212/01.wnl.0000044400.11317.ec Du, A. T., Schuff, N., Chao, L. L., Kornak, J., Jagust, W. J., Kramer, J. H., Reed, B. R., Miller, B. L., Norman, D., Chui, H. C., & Weiner, M. W. (2006). Age effects on atrophy rates of entorhinal cortex and hippocampus. Neurobiology of Aging, 27(5). https://doi.org/10.1016/j.neurobiolaging.2005.03.021

Du, L. Y., Chang, L. Y., Ardiles, A. O., Tapia-Rojas, C., Araya, J., Inestrosa, N. C., Palacios, A. G., & Acosta, M. L. (2015). Alzheimer's disease-related protein expression in the retina of *Octodon degus*. PLoS ONE, 10(8), 1–17. https://doi.org/10.1371/journal.pone.0135499

Edler, M. K., Mhatre-Winters, I., & Richardson, J. R. (2021). Microglia in aging and Alzheimer's disease: A comparative species review. Cells. https://doi.org/10.3390/cells10051138

Edwards, M. S. (2009). Nutrition and Behavior of Degus (*Octodon degus*). Veterinary Clinics of North America - Exotic Animal Practice, 12(2), 237–253. https://doi.org/10.1016/j.cvex.2009.01.003

Egawa, J., Pearn, M. L., Lemkuil, B. P., Patel, P. M., & Head, B. P. (2016). Membrane lipid rafts and neurobiology: age-related changes in membrane lipids and loss of neuronal function. The Journal of Physiology, 594(16), 4565–4579. https://doi.org/10.1113/JP270590

Eichenbaum, H. (2004). Hippocampus: Cognitive processes and neural representations that underlie declarative memory. Neuron. https://doi.org/10.1016/j.neuron.2004.08.028

El-Falougy, H., & Benuska, J. (2006). History, anatomical nomenclature, comparative anatomy and functions of the hippocampal formation. Bratislavské Lekárske Listy.

Enzinger, C., Fazekas, F., Matthews, P. M., Ropele, S., Schmidt, H., Smith, S., & Schmidt, R. (2005). Risk factors for progression of brain atrophy in aging: Six-year follow-up of normal subjects. Neurology, 64(10). https://doi.org/10.1212/01.WNL.0000161871.83614.BB

Escartin, C., Galea, E., Lakatos, A., O'Callaghan, J. P., Petzold, G. C., Serrano-Pozo, A., Steinhäuser, C., Volterra, A., Carmignoto, G., Agarwal, A., Allen, N. J., Araque, A., Barbeito, L., Barzilai, A., Bergles, D. E., Bonvento, G., Butt, A. M., Chen, W. T., Cohen-Salmon, M., Cunningham, C., … Verkhratsky, A. (2021). Reactive astrocyte nomenclature, definitions, and future directions. Nature Neuroscience, 24(March). https://doi.org/10.1038/s41593-020-00783-4

Estrada, C., Cuenca, L., Cano-Fernandez, L., Gil-Martinez, A. L., Sanchez-Rodrigo, C., González-Cuello, A. M., Fernandez-Villalba, E., & Herrero, M. T. (2019). Voluntary exercise reduces plasma cortisol levels and improves transitory memory impairment in young and aged Octodon degus. Behavioural Brain Research, 373(January), 112066. https://doi.org/10.1016/j.bbr.2019.112066

Estrada, C., Fernández-Gómez, F. J., López, D., Gonzalez-Cuello, A., Tunez, I., Toledo, F., Blin, O., Bordet, R., Richardson, J. C., Fernandez-Villalba, E., & Herrero, M. T. (2015a). Transcranial magnetic stimulation and aging: Effects on spatial learning and memory after sleep deprivation in *Octodon degus*. Neurobiology of Learning and Memory, 125, 274–281. https://doi.org/10.1016/j.nlm.2015.09.011

Estrada, C., López, D., Conesa, A., Fernández-Gómez, F. J., Gonzalez-Cuello, A., Toledo, F., Tunez, I., Blin, O., Bordet, R., Richardson, J. C., Fernandez-Villalba, E., & Herrero, M. T. (2015b). Cognitive Impairment After Sleep Deprivation Rescued by Transcranial Magnetic Stimulation Application in *Octodon degus*. Neurotoxicity Research, 28(4), 361–371. https://doi.org/10.1007/s12640-015-9544-x

Evans, M. A., Sano, S., & Walsh, K. (2020). Cardiovascular Disease, Aging, and Clonal Hematopoiesis. Annual Review of Pathology: Mechanisms of Disease, 15, 419–438. https://doi.org/10.1146/annurev-pathmechdis-012419-032544

Ezekiel, F., Chao, L., Kornak, J., Du, A. T., Cardenas, V., Truran, D., Jagust, W., Chui, H., Miller, B., Yaffe, K., Schuff, N., & Weiner, M. (2004). Comparisons between global and focal brain atrophy rates in normal aging and Alzheimer disease: Boundary shift integral versus tracing of the entorhinal cortex and hippocampus. Alzheimer Disease and Associated Disorders, 18(4).

Fabbri, E., Zoli, M., Gonzalez-Freire, M., Salive, M. E., Studenski, S. A., & Ferrucci, L. (2015). Aging and Multimorbidity: New Tasks, Priorities, and Frontiers for Integrated Gerontological and Clinical Research. Journal of the American Medical Directors Association, 16(8), 640–647. https://doi.org/10.1016/j.jamda.2015.03.013

Fahn, S., & Cohen, G. (1992). The oxidant stress hypothesis in Parkinson's disease: Evidence supporting it. Annals of Neurology, 32(6). https://doi.org/10.1002/ana.410320616

Fahy, E., Cotter, D., Sud, M., & Subramaniam, S. (2011). Biochimica et Biophysica Acta Lipid classification, structures and tools ☆. Biochimica et Biophysica Acta, 1811(11).

Fahy, E., Subramaniam, S., Murphy, R. C., Nishijima, M., Raetz, C. R. H., Shimizu, T., … Dennis, E. A. (2009). Update of the LIPID MAPS comprehensive classification system for lipids. Journal of Lipid Research. https://doi.org/10.1194/jlr.R800095-JLR200

Fan, X., Wheatley, E. G., & Villeda, S. A. (2017). Mechanisms of Hippocampal Aging and the Potential for Rejuvenation. Annual Review of Neuroscience, 40(April), 251–272. https://doi.org/10.1146/annurev-neuro-072116-031357

Fang, E. F., Lautrup, S., Hou, Y., Demarest, T. G., Croteau, D. L., Mattson, M. P., & Bohr, V. A. (2017). NAD+ in Aging: Molecular Mechanisms and Translational Implications. Trends in Molecular Medicine. https://doi.org/10.1016/j.molmed.2017.08.001

Fantini, J., & Yahi, N. (2015). Chemical Basis of Lipid Biochemistry. In Brain Lipids in Synaptic Function and Neurological Disease. https://doi.org/10.1016/b978-0-12-800111-0.00001-1

Farina, C., Aloisi, F., & Meinl, E. (2007). Astrocytes are active players in cerebral innate immunity. Trends in Immunology. https://doi.org/10.1016/j.it.2007.01.005

Farooqui, A. A. (2009). Lipid mediators in the neural cell nucleus: Their metabolism, signaling, and association with neurological disorders. Neuroscientist. https://doi.org/10.1177/1073858409337035

Farooqui, A. A., Liss, L., & Horrocks, L. A. (1988). Neurochemical aspects of Alzheimer's disease: Involvement of membrane phospholipids. Metabolic Brain Disease. https://doi.org/10.1007/BF01001351

Farraj, A. K., Hazari, M. S., & Cascio, W. E. (2011). The utility of the small rodent electrocardiogram in toxicology. Toxicological Sciences, 121(1), 11–30. https://doi.org/10.1093/toxsci/kfr021

Feigenbaum, J. D., Polkey, C. E., & Morris, R. G. (1996). Deficits in spatial working memory after unilateral temporal lobectomy in man. Neuropsychologia, 34(3). https://doi.org/10.1016/0028-3932(95)00107-7

Fernández, I., Peña, A., Del Teso, N., Pérez, V., & Rodríguez-Cuesta, J. (2010). Clinical biochemistry parameters in C57BL/6J mice after blood collection from the submandibular vein and retroorbital plexus. Journal of the American Association for Laboratory Animal Science, 49(2), 202–206.

Ferrucci, L., Gonzalez-Freire, M., Fabbri, E., Simonsick, E., Tanaka, T., Moore, Z., Salimi, S., Sierra, F., & de Cabo, R. (2020). Measuring biological aging in humans: A quest. Aging Cell, 19(2), 1–21. https://doi.org/10.1111/acel.13080

Fielder, E., Von Zglinicki, T., & Jurk, D. (2017). The DNA Damage Response in Neurons: Die by Apoptosis or Survive in a Senescence-Like State? Journal of Alzheimer's Disease. https://doi.org/10.3233/JAD-161221

Fitzner, D., Bader, J. M., Penkert, H., Bergner, C. G., Su, M., Weil, M. T., Surma, M. A., Mann, M., Klose, C., & Simons, M. (2020). Cell-Type- and Brain-Region-Resolved Mouse Brain Lipidome. Cell Reports, 32(11), 108132. https://doi.org/10.1016/j.celrep.2020.108132

Fjell, A. M., McEvoy, L., Holland, D., Dale, A. M., & Walhovd, K. B. (2014). What is normal in normal aging? Effects of Aging, Amyloid and Alzheimer's Disease on the Cerebral Cortex and the Hippocampus. Progress Neurobiology, 117, 20–40. https://doi.org/10.1016/j.pneurobio.2014.02.004.What

Fjell, A. M., Walhovd, K. B., Fennema-Notestine, C., McEvoy, L. K., Hagler, D. J., Holland, D., Brewer, J. B., & Dale, A. M. (2009a). One-year brain atrophy evident in healthy aging. Journal of Neuroscience, 29(48). https://doi.org/10.1523/JNEUROSCI.3252-09.2009

Fjell, A. M., Westlye, L. T., Amlien, I., Espeseth, T., Reinvang, I., Raz, N., Agartz, I., Salat, D. H., Greve, D. N., Fischl, B., Dale, A. M., & Walhovd, K. B. (2009b). High consistency of regional cortical thinning in aging across multiple samples. Cerebral Cortex, 19(9). https://doi.org/10.1093/cercor/bhn232

Forno, L. S., Langston, J. W., DeLanney, L. E., Irwin, I., & Ricaurte, G. A. (1986). Locus ceruleus lesions and eosinophilic inclusions in MPTP-treated monkeys. Annals of Neurology, 20(4), 449–455. https://doi.org/10.1002/ana.410200403

Fotenos, A. F., Snyder, A. Z., Girton, L. E., Morris, J. C., & Buckner, R. L. (2005). Normative estimates of cross-sectional and longitudinal brain volume decline in aging and AD. Neurology, 64(6). https://doi.org/10.1212/01.WNL.0000154530.72969.11

Franceschi, C., & Campisi, J. (2014). Chronic inflammation (Inflammaging) and its potential contribution to age-associated diseases. Journals of Gerontology - Series A Biological Sciences and Medical Sciences. https://doi.org/10.1093/gerona/glu057

Franklin, Keith and Paxinos, G. (2004). The Mouse Brain in Stereotaxic Coordinates (2nd Editio).

Frasca, D., & Blomberg, B. B. (2016). Inflammaging decreases adaptive and innate immune responses in mice and humans. Biogerontology. https://doi.org/10.1007/s10522-015-9578-8

From the American Association of Neurological Surgeons (AANS), American Society of

Neuroradiology (ASNR), Cardiovascular and Interventional Radiology Society of Europe (CIRSE), Canadian Interventional Radiology Association (CIRA), Congress of Neurological Surgeons (CNS), European Society of Minimally Invasive Neurological Therapy (ESMINT), European Society of Neuroradiology (ESNR), European Stroke Organization (ESO), Society for Cardiovascular Angiography and Interventions (SCAI), Society of Interventional Radiology (SIR), Society of NeuroInterventional Surgery (SNIS), and World Stroke Organization (WSO), Sacks, D., Baxter, B., Campbell, B., Carpenter, J. S., Cognard, C., Dippel, D., Eesa, M., Fischer, U., Hausegger, K., Hirsch, J. A., Shazam Hussain, M., Jansen, O., Jayaraman, M. V., Khalessi, A. A., Kluck, B. W., Lavine, S., Meyers, P. M., Ramee, S., Rüfenacht, D. A., … Vorwerk, D. (2016). Parkinson's disease: Autoimmunity and neuroinflammation. Autoimmunity Reviews. https://doi.org/10.1016/j.autrev.2016.07.022

Fu, R., Shen, Q., Xu, P., Luo, J. J., & Tang, Y. (2014). Phagocytosis of microglia in the central nervous system diseases. Molecular Neurobiology, 49(3). https://doi.org/10.1007/s12035-013-8620-6

Fuentes, P., Amador, S., Lucas-Ochoa, A. M., Cuenca-Bermejo, L., Fernández-Villalba, E., Raparelli, V., … Herrero, M. T. (2021). Sex, rurality and socioeconomical status in Spanish centennial population (2017). Aging, 13(18), 22059–22077. https://doi.org/10.18632/aging.203563

Fuzzati-Armentero, M. T., Cerri, S., & Blandini, F. (2019). Peripheral-central neuroimmune crosstalk in parkinson's disease: What do patients and animal models tell us? Frontiers in Neurology, 10(March), 1–19. https://doi.org/10.3389/fneur.2019.00232

Gagnon, D., Eid, L., Coudé, D., Whissel, C., Paolo, T. Di, Parent, A., & Parent, M. (2018). Evidence for sprouting of dopamine and serotonin axons in the pallidum of parkinsonian monkeys. Frontiers in Neuroanatomy, 12(May), 1–14. https://doi.org/10.3389/fnana.2018.00038

Gallea, C., Ewenczyk, C., Degos, B., Welter, M. L., Grabli, D., Leu-Semenescu, S., Valabregue, R., Berroir, P., Yahia-Cherif, L., Bertasi, E., Fernandez-Vidal, S., Bardinet, E., Roze, E., Benali, H., Poupon, C., François, C., Arnulf, I., Lehéricy, S., & Vidailhet, M. (2017). Pedunculopontine network dysfunction in Parkinson's disease with postural control and sleep disorders. Movement Disorders, 32(5), 693–704. https://doi.org/10.1002/mds.26923

Gawel, K., Gibula, E., Marszalek-Grabska, M., Filarowska, J., & Kotlinska, J. H. (2019). Assessment of spatial learning and memory in the Barnes maze task in rodents—methodological consideration. Naunyn-Schmiedeberg's Archives of Pharmacology, 392(1), 1–18. https://doi.org/10.1007/s00210-018-1589-y

Geneva: World Health Organization. (2020). The impact of the COVID-19 pandemic on noncommunicable disease resources and services: results of a rapid assessment. https://apps.who.int/iris/rest/bitstreams/1299882/retrieve (accessed 5 May 2022).

Gesi, M., Soldani, P., Giorgi, F. S., Santinami, A., Bonaccorsi, I., & Fornai, F. (2000). The role of the locus coeruleus in the development of Parkinson's disease. Neuroscience and Biobehavioral Reviews, 24(6), 655–668. https://doi.org/10.1016/S0149-7634(00)00028-2

Gil-Martínez, A. L., Cuenca, L., Estrada, C., Sánchez-Rodrigo, C., Fernández-Villalba, E., & Herrero, M. T. (2018). Unexpected Exacerbation of Neuroinflammatory Response After a Combined Therapy in Old Parkinsonian Mice. Frontiers in Cellular Neuroscience, 12. https://doi.org/10.3389/fncel.2018.00451

Gil-Martínez, A. L., Cuenca, L., Sánchez-Rodrigo, C., Estrada, C., Fernández-Villalba, E., & Herrero, M. T. (2018). Effect of NAC treatment and physical activity on neuroinflammation in subchronic Parkinsonism ; is physical activity essential ? Journal of Neuroinflammation, 4(15:328), 1–13.

Gil-Martínez, A. L., Estrada, C., Cuenca, L., Cano, J. A., Valiente, M., Martínez-Cáceres, C. M., Fernández-Villalba, E., & Herrero, M. T. (2019). Local Gastrointestinal Injury Exacerbates Inflammation and Dopaminergic Cell Death in Parkinsonian Mice. Neurotoxicity Research, 35(4), 918–930. https://doi.org/10.1007/s12640-019-0010-z

González-Barrio, D., Huertas-López, A., Diezma-Díaz, C., Ferre, I., Cerón, J. J., Ortega-Mora, L. M., & Álvarez-García, G. (2021). Changes in serum biomarkers of inflammation in bovine besnoitiosis. Parasites and Vectors, 14(1). https://doi.org/10.1186/s13071-021-04991-0

González-Ramírez, M. M., Velázquez-Zamora, D. A., Olvera-Cortés, M. E., & González-Burgos, I. (2014). Changes in the plastic properties of hippocampal dendritic spines underlie the attenuation of place learning in healthy aged rats. Neurobiology of Learning and Memory, 109. https://doi.org/10.1016/j.nlm.2013.11.017

Gordon, B. A., Blazey, T., Benzinger, T. L. S., & Head, D. (2013). Effects of aging and Alzheimer's disease along the longitudinal axis of the hippocampus. Journal of Alzheimer's Disease, 37(1). https://doi.org/10.3233/JAD-130011

Grandi, L. C., Di Giovanni, G., & Galati, S. (2018). Animal models of early-stage Parkinson's disease and acute dopamine deficiency to study compensatory neurodegenerative mechanisms. Journal of Neuroscience Methods, 308(August), 205–218. https://doi.org/10.1016/j.jneumeth.2018.08.012

Grassi, S., Giussani, P., Mauri, L., Prioni, S., Sonnino, S., & Prinetti, A. (2020). Lipid rafts and neurodegeneration: Structural and functional roles in physiologic aging and

neurodegenerative diseases. Journal of Lipid Research, 61(5), 636–654. https://doi.org/10.1194/jlr.TR119000427

Gray, D. T., & Barnes, C. A. (2015). Distinguishing adaptive plasticity from vulnerability in the aging hippocampus. Neuroscience, 309, 17–28. https://doi.org/10.1016/j.neuroscience.2015.08.001

Gray, J. A. & McNaughton, N. The Neuropsychology of Anxiety: An Enquiry into the Functions of the Septo- Hippocampal System (Oxford Univ. Press,1982).

Grimm, A., & Eckert, A. (2017). Brain aging and neurodegeneration: from a mitochondrial point of view. Journal of Neurochemistry. https://doi.org/10.1111/jnc.14037

Grootendorst, J., De Kloet, E. R., Vossen, C., Dalm, S., & Oitzl, M. S. (2001). Repeated exposure to rats has persistent genotype-dependent effects on learning and locomotor activity of apolipoprotein E knockout and C57Bl/6 mice. In Behavioural Brain Research (Vol. 125). https://doi.org/10.1016/S0166-4328(01)00294-7

Guzman-Martinez, L., Maccioni, R. B., Andrade, V., Navarrete, L. P., Pastor, M. G., & Ramos-Escobar, N. (2019). Neuroinflammation as a common feature of neurodegenerative disorders. Frontiers in Pharmacology, 10(SEP), 1–17. https://doi.org/10.3389/fphar.2019.01008

Hagen, K., Clauss, M., & Hatt, J. M. (2014). Drinking preferences in chinchillas (Chinchilla laniger), degus (Octodon degu) and guinea pigs (Cavia porcellus). Journal of Animal Physiology and Animal Nutrition, 98(5), 942–947. https://doi.org/10.1111/jpn.12164

Hallett, P. J., Engelender, S., & Isacson, O. (2019). Lipid and immune abnormalities causing age-dependent neurodegeneration and Parkinson's disease. Journal of neuroinflammation, 16(1), 153. https://doi.org/10.1186/s12974-019-1532-2

Halliday, G. M., & McCann, H. (2010). The progression of pathology in Parkinson ' s disease, 1184, 188–195.

Hamadjida, A., Frouni, I., Kwan, C., & Huot, P. (2019). Classic animal models of Parkinson's disease: A historical perspective. Behavioural Pharmacology, 30(4), 291–310. https://doi.org/10.1097/FBP.0000000000000441

Hammond C. 2015. The adult hippocampal network. In: Cellular and Molecular Neurophysiology: Fourth Edition. https://doi.org/10.1016/B978-0-12-397032-9.00019-4

Hammond, T. R., Dufort, C., Dissing-Olesen, L., Giera, S., Young, A., Wysoker, A., Walker, A. J., Gergits, F., Segel, M., Nemesh, J., Marsh, S. E., Saunders, A., Macosko, E., Ginhoux, F., Chen, J., Franklin, R., Piao, X., McCarroll, S. A., & Stevens, B. (2019). Single-Cell RNA Sequencing of Microglia throughout the Mouse Lifespan and in the Injured Brain Reveals Complex Cell-State Changes. Immunity, 50(1).

https://doi.org/10.1016/j.immuni.2018.11.004

Hanada, E., Ohtani, H., Kotaki, H., Sawada, Y., Sato, H., & Iga, T. (1999). Pharmacodynamic analysis of the electrocardiographic interaction between disopyramide and erythromycin in rats. Journal of Pharmaceutical Sciences, 88(2). https://doi.org/10.1021/js980256r

Hardy, J., & Allsop, D. (1991). Amyloid deposition as the central event in the aetiology of Alzheimer's disease. Trends in Pharmacological Sciences. https://doi.org/10.1016/0165-6147(91)90609-V

Harman, D. (1992). Free radical theory of aging. Mutation Research DNAging, 275(3–6). https://doi.org/10.1016/0921-8734(92)90030-S

Harrison, F. E., Reiserer, R. S., Tomarken, A. J., & McDonald, M. P. (2006). Spatial and nonspatial escape strategies in the Barnes maze. Learning and Memory, 13(6). https://doi.org/10.1101/lm.334306

Hart, N. J., Koronyo, Y., Black, K. L., & Koronyo-Hamaoui, M. (2016). Ocular indicators of Alzheimer's: exploring disease in the retina. Acta Neuropathologica, 132(6), 767–787. https://doi.org/10.1007/s00401-016-1613-6

Hayes, M. T. (2019). Parkinson's Disease and Parkinsonism. American Journal of Medicine, 132(7), 802–807. https://doi.org/10.1016/j.amjmed.2019.03.001

Hayne, H. (2004). Infant memory development: Implications for childhood amnesia. Developmental Review, 24(1). https://doi.org/10.1016/j.dr.2003.09.007

Hägg, S., & Jylhävä, J. (2021). Sex differences in biological aging with a focus on human studies. eLife, 10, e63425. https://doi.org/10.7554/eLife.63425

Heaton-Jones, T. G., Ko, J. C. H., & Heaton-Jones, D. L. (2002). Evaluation of medetomidine-ketamine anesthesia with atipamezole reversal in American alligators (Alligator mississippiensis). Journal of Zoo and Wildlife Medicine. https://doi.org/10.1638/1042-7260(2002)033[0036:EOMKAW]2.0.CO;2

Hedden, T., & Gabrieli, J. D. E. (2004). Insights into the ageing mind: A view from cognitive neuroscience. Nature Reviews Neuroscience. https://doi.org/10.1038/nrn1323

Hedman, A. M., van Haren, N. E. M., Schnack, H. G., Kahn, R. S., & Hulshoff Pol, H. E. (2012). Human brain changes across the life span: A review of 56 longitudinal magnetic resonance imaging studies. Human Brain Mapping, 33(8). https://doi.org/10.1002/hbm.21334

Heman, P., Barcia, C., Gómez, A., Ros, C. M., Ros-Bernal, F., Yuste, J. E., de Pablos, V., Fernandez-Villalba, E., Toledo-Cárdenas, M. R., & Herrero, M. T. (2012). Nigral degeneration correlates with persistent activation of cerebellar Purkinje cells in MPTP-

treated monkeys. Histology and Histopathology, 27(1), 89–94. https://doi.org/10.14670/HH-27.89

Heneka, M. T., Rodríguez, J. J., & Verkhratsky, A. (2010). Neuroglia in neurodegeneration. Brain Research Reviews. https://doi.org/10.1016/j.brainresrev.2009.11.004

Henry, C. J., Huang, Y., Wynne, A. M., & Godbout, J. P. (2009). Peripheral lipopolysaccharide (LPS) challenge promotes microglial hyperactivity in aged mice that is associated with exaggerated induction of both pro-inflammatory IL-1β and anti-inflammatory IL-10 cytokines. Brain, Behavior, and Immunity, 23(3). https://doi.org/10.1016/j.bbi.2008.09.002

Herrero, M. T., Hirsch, E. C., Kastner, A., Luquin, M. R., Javoy-Agid, F., Gonzalo, L. M., Obeso, J. A., & Agid, Y. (1993). Neuromelanin accumulation with age in catecholaminergic neurons from Macaca fascicularis brainstem. Developmental Neuroscience, 15(1), 37–48. https://doi.org/10.1159/000111315

Herrero, M. T., Hirsch, E. C., Kastner, A., Ruberg, M., Luquin, M. R., Laguna, J., Javoy-Agid, F., Obeso, J. A., & Agid, Y. (1993). Does neuromelanin contribute to the vulnerability of catecholaminergic neurons in monkeys intoxicated with MPTP?. Neuroscience, 56(2), 499–511. https://doi.org/10.1016/0306-4522(93)90349-kHoldhoff, M., Yovino, S. G., Boadu, O., & Grossman, S. A. (2013). Blood-based biomarkers for malignant gliomas. Journal of Neuro-Oncology. https://doi.org/10.1007/s11060-013-1144-0

Homan, R., Hanselman, J. C., Bak-Mueller, S., Washburn, M., Lester, P., Jensen, H. E., Pinkosky, S. L., Castle, C., & Taylor, B. (2010). Atherosclerosis in Octodon degus (degu) as a model for human disease. Atherosclerosis, 212(1), 48–54. https://doi.org/10.1016/j.atherosclerosis.2010.06.004

Honour, J. W. (2018). Biochemistry of the menopause. Annals of clinical biochemistry, 55(1), 18–33. https://doi.org/10.1177/0004563217739930

Horjus, D. L., Oudman, I., van Montfrans, G. A., & Brewster, L. M. (2011). Creatine and creatine analogues in hypertension and cardiovascular disease. Cochrane Database of Systematic Reviews. https://doi.org/10.1002/14651858.cd005184.pub2

Hou, Y., Dan, X., Babbar, M., Wei, Y., Hasselbalch, S. G., Croteau, D. L., & Bohr, V. A. (2019). Ageing as a risk factor for neurodegenerative disease. Nature Reviews Neurology. https://doi.org/10.1038/s41582-019-0244-7

Huang, D., Xu, J., Wang, J., Tong, J., Bai, X., Li, H., Wang, Z., Huang, Y., Wu, Y., Yu, M., & Huang, F. (2017). Dynamic Changes in the Nigrostriatal Pathway in the MPTP Mouse Model of Parkinson's Disease. Parkinson's Disease, 2017, 9349487. https://doi.org/10.1155/2017/9349487

Hurley, M. J., Deacon, R. M. J., Beyer, K., Ioannou, E., Ibáñez, A., Teeling, J. L., & Cogram, P. (2018). The long-lived *Octodon degus* as a rodent drug discovery model for Alzheimer's and other age-related diseases. Pharmacology and Therapeutics, 1–9. https://doi.org/10.1016/j.pharmthera.2018.03.001

Hurley, M. J., Urra, C., Garduno, B. M., Bruno, A., Kimbell, A., Wilkinson, B., Marino-Buslje, C., Ezquer, M., Ezquer, F., Aburto, P. F., Poulin, E., Vasquez, R. A., Deacon, R., Avila, A., Altimiras, F., Whitney Vanderklish, P., Zampieri, G., Angione, C., Constantino, G., Holmes, T. C., Coba, M.P., Xu, X. & Cogram, P. (2022). Genome Sequencing Variations in the Octodon degus, an Unconventional Natural Model of Aging and Alzheimer's Disease. Frontiers in aging neuroscience, 14, 894994. https://doi.org/10.3389/fnagi.2022.894994

Hutter-Saunders, J. A. L., Gendelman, H. E., & Mosley, R. L. (2012). Murine motor and behavior functional evaluations for acute 1-methyl-4-phenyl-1,2,3,6-tetrahydropyridine (MPTP) intoxication. Journal of Neuroimmune Pharmacology, 7(1), 279–288. https://doi.org/10.1007/s11481-011-9269-4

Hwang, J. Y., Aromolaran, K. A., & Zukin, R. S. (2017). The emerging field of epigenetics in neurodegeneration and neuroprotection. Nature Reviews Neuroscience. https://doi.org/10.1038/nrn.2017.46

Inestrosa, N. C., Reyes, A. E., Chacón, M. A., Cerpa, W., Villalón, A., Montiel, J., Merabachvili, G., Aldunate, R., Bozinovic, F., & Aboitiz, F. (2005). Human-like rodent amyloid-β-peptide determines Alzheimer pathology in aged wild-type *Octodon degus*. Neurobiology of Aging, 26(7), 1023–1028. https://doi.org/10.1016/j.neurobiolaging.2004.09.016

Inestrosa, N. C., Ríos, J. A., Cisternas, P., Tapia-Rojas, C., Rivera, D. S., Braidy, N., Zolezzi, J. M., Godoy, J. A., Carvajal, F. J., Ardiles, A. O., Bozinovic, F., Palacios, A. G., & Sachdev, P. S. (2015). Age Progression of Neuropathological Markers in the Brain of the Chilean Rodent *Octodon degus*, a Natural Model of Alzheimer's Disease. Brain Pathology, 25(6), 679–691. https://doi.org/10.1111/bpa.12226

Inman-Wood, S. L., Williams, M. T., Morford, L. L., & Vorhees, C. V. (2000). Effects of prenatal cocaine on Morris and Barnes maze tests of spatial learning and memory in the offspring of C57BL/6J mice. Neurotoxicology and Teratology, 22(4). https://doi.org/10.1016/S0892-0362(00)00084-2

Insausti, A.M. & Amaral, D.G. (2012). Hippocampal formation; in Mai JK, Paxinos G (eds): The Human Nervous System, ed 3. San Diego, Academic Press, pp 896–942.

Ionescu-Tucker, A., & Cotman, C. W. (2021). Emerging roles of oxidative stress in brain aging and Alzheimer's disease. Neurobiology of Aging, 107, 86–95. https://doi.org/10.1016/j.neurobiolaging.2021.07.014

Jackson-Lewis, V., & Przedborski, S. (2007). Protocol for the MPTP mouse model of Parkinson's disease. Nature Protocols, 2(1), 141–151. https://doi.org/10.1038/nprot.2006.342

Jackson, K. H., & Harris, W. S. (2018). Blood Fatty Acid Profiles: New Biomarkers for Cardiometabolic Disease Risk. Current Atherosclerosis Reports. https://doi.org/10.1007/s11883-018-0722-1

Jacobs, G. H., Calderone, J. B., Fenwick, J. A., Krogh, K., & Williams, G. A. (2003). Visual adaptations in a diurnal rodent, *Octodon degus*. Journal of Comparative Physiology A: Neuroethology, Sensory, Neural, and Behavioral Physiology, 189(5), 347–361. https://doi.org/10.1007/s00359-003-0408-0

James, R. W. (2006). A long and winding road: Defining the biological role and clinical importance of paraoxonases. Clinical Chemistry and Laboratory Medicine. https://doi.org/10.1515/CCLM.2006.207

Jantaratnotai, N., Ryu, J. K., Kim, S. U., & McLarnon, J. G. (2003). Amyloid β peptide-induced corpus callosum damage and glial activation in vivo. NeuroReport, 14(11). https://doi.org/10.1097/00001756-200308060-00005

Jechura, T. J., & Lee, T. M. (2004). Ovarian hormones influence olfactory cue effects on reentrainment in the diurnal rodent, *Octodon degus*. Hormones and Behavior, 46(3), 349–355. https://doi.org/10.1016/j.yhbeh.2004.06.001

Jekl, V., Hauptman, K., Jeklova, E., & Knotek, Z. (2011). Selected haematological and plasma chemistry parameters in juvenile and adult degus (*Octodon degus*). Veterinary Record, 169(3), 71. https://doi.org/10.1136/vr.d2360

Jenner Peter. (2003). Oxidative stress in Parkinson's disease. Anals of Neurology, 53, S26-38. https://doi.org/10.1002/ana.10483.uitination

Jensen, M. B., & Jasper, H. (2014). Mitochondrial proteostasis in the control of aging and longevity. Cell Metabolism. https://doi.org/10.1016/j.cmet.2014.05.006

Jomova, K., Vondrakova, D., Lawson, M., & Valko, M. (2010). Metals, oxidative stress and neurodegenerative disorders. Molecular and Cellular Biochemistry. https://doi.org/10.1007/s11010-010-0563-x

Jones, J., Srodulski, Z. M., & Romisher, S. (1990). The aging electrocardiogram. American Journal of Emergency Medicine, 8(3), 240–245. https://doi.org/10.1016/0735-6757(90)90331-S

Jové, M., Portero-Otín, M., Naudí, A., Ferrer, I., & Pamplona, R. (2014). Metabolomics of human brain aging and age-related neurodegenerative diseases. Journal of Neuropathology and Experimental Neurology.

https://doi.org/10.1097/NEN.0000000000000091

Jyothi, H. J., Vidyadhara, D. J., Mahadevan, A., Philip, M., Parmar, S. K., Manohari, S. G., Shankar, S. K., Raju, T. R., & Alladi, P. A (2015). Aging causes morphological alterations in astrocytes and microglia in human substantia nigra pars compacta. Neurobiology of Aging, 36(12), 3321–3333. https://doi.org/10.1016/j.neurobiolaging.2015.08.024

Kaeberlein, M., Rabinovitch, P. S., & Martin, G. M. (2015). Healthy aging: The ultimate preventative medicine. Science. https://doi.org/10.1126/science.aad3267

Kakoty, V., K C, S., Dubey, S. K., Yang, C. H., Kesharwani, P., & Taliyan, R. (2021). The gut-brain connection in the pathogenicity of Parkinson disease: Putative role of autophagy. Neuroscience Letters, 753(February), 135865. https://doi.org/10.1016/j.neulet.2021.135865

Kalia, L. V., & Lang, A. E. (2015). Parkinson's disease. The Lancet, 386(9996), 896–912. https://doi.org/10.1016/S0140-6736(14)61393-3

Kam, T. I., Hinkle, J. T., Dawson, T. M., & Dawson, V. L. (2020). Microglia and astrocyte dysfunction in parkinson's disease. Neurobiology of Disease, 144(July), 105028. https://doi.org/10.1016/j.nbd.2020.105028

Kametani, F., & Hasegawa, M. (2018). Reconsideration of amyloid hypothesis and tau hypothesis in Alzheimer's disease. Frontiers in Neuroscience. https://doi.org/10.3389/fnins.2018.00025

Kandel, E., Schwartz, J., Jessell, T., Siegelbaum, S., Hudspeth, A. J., Kandel, E. R., … Siegelbaum, S. A. (2012). Principles of Neural Science, Fifth Edition (Principles of Neural Science (Kandel)). In Principles of Neural Science.

Kane, A. E., & Howlett, S. E. (2018). Differences in cardiovascular aging in men and women. Advances in Experimental Medicine and Biology, 1065, 389–411. https://doi.org/10.1007/978-3-319-77932-4_25

Kane, A. E., Hilmer, S. N., Mach, J., Mitchell, S. J., de Cabo, R., & Howlett, S. E. (2016). Animal models of frailty: Current applications in clinical research. Clinical Interventions in Aging, 11, 1519–1529. https://doi.org/10.2147/CIA.S105714

Kao, Y. C., Ho, P. C., Tu, Y. K., Jou, I. M., & Tsai, K. J. (2020). Lipids and Alzheimer's Disease. International journal of molecular sciences, 21(4), 1505. https://doi.org/10.3390/ijms21041505

Karimi-Moghadam, A., Charsouei, S., Bell, B., & Jabalameli, M. R. (2018). Parkinson Disease from Mendelian Forms to Genetic Susceptibility: New Molecular Insights into the Neurodegeneration Process. Cellular and Molecular Neurobiology, 38(6), 1153–1178. https://doi.org/10.1007/s10571-018-0587-4

Kashou, A. H., & Kashou, H. E. (2018). Electrical Axis (Normal, Right Axis Deviation, and Left Axis Deviation). StatPearls.

Kennard, J. A., & Woodruff-Pak, D. S. (2011). Age sensitivity of behavioral tests and brain substrates of normal aging in mice. Frontiers in Aging Neuroscience, 3(MAY). https://doi.org/10.3389/fnagi.2011.00009

Kettenmann, H., Hanisch, U.-K., Noda, M., & Verkhratsky, A. (2011). Physiology of microglia. Physiological Reviews, 91(2), 461–553. https://doi.org/10.1152/physrev.00011.2010

Kim, G. H., Kim, J. E., Rhie, S. J., & Yoon, S. (2015). The Role of Oxidative Stress in Neurodegenerative Diseases. Experimental Neurobiology, 24(4), 325–340. https://doi.org/10.5607/en.2015.24.4.325

Kirkwood, T. B. L. (2008). A systematic look at an old problem. Nature. https://doi.org/10.1038/451644a

Klencklen, G., Després, O., & Dufour, A. (2012). What do we know about aging and spatial cognition? Reviews and perspectives. Ageing Research Reviews. https://doi.org/10.1016/j.arr.2011.10.001

Kloske, C. M., & Wilcock, D. M. (2020). The Important Interface Between Apolipoprotein E and Neuroinflammation in Alzheimer's Disease. Frontiers in Immunology, 11(April), 1–12. https://doi.org/10.3389/fimmu.2020.00754

Knierim, J. J. (2015). The hippocampus. Current Biology, 25(23), R1116–R1121. https://doi.org/10.1016/j.cub.2015.10.049

Knowlton, B. J., Mangels, J. A., & Squire, L. R. (1996). A neostriatal habit learning system in humans. Science, 273(5280). https://doi.org/10.1126/science.273.5280.1399

Konopelski, P., & Ufnal, M. (2016). Electrocardiography in rats: A comparison to human. Physiological Research, 65(5), 717–725. https://doi.org/10.33549/physiolres.933270

Kopin, I. J., & Markey, S. P. (1988). MPTP toxicity: implications for research in Parkinson's disease. Annual Review of Neuroscience, 11, 81–96. https://doi.org/10.1146/annurev.neuro.11.1.81

Kracun, I., Rosner, H., Drnovsek, V., Vukelic, Z., Cosovic, C., Trbojevic-Cepe, M., & Kubat, M. (1992). Gangliosides in the human brain development and aging. Neurochemistry International, 20(3). https://doi.org/10.1016/0197-0186(92)90057-X

Krishnaswami, A., Beavers, C., Dorsch, M. P., Dodson, J. A., Masterson Creber, R., Kitsiou, S., Goyal, P., Maurer, M. S., Wenger, N. K., Croy, D. S., Alexander, K. P., Batsis, J. A., Turakhia, M. P., Forman, D. E., Bernacki, G. M., Kirkpatrick, J. N., Orr, N. M., Peterson, E. D., Rich, M. W., Freeman, A. M., … Innovations, Cardiovascular Team and the

Geriatric Cardiology Councils, American College of Cardiology (. (2020). Gerotechnology for Older Adults With Cardiovascular Diseases: JACC State-of-the-Art Review. Journal of the American College of Cardiology, 76(22), 2650–2670. https://doi.org/10.1016/j.jacc.2020.09.606

Kumazawa-Manita, N., Hama, H., Miyawaki, A., & Iriki, A. (2013b). Tool Use Specific Adult Neurogenesis and Synaptogenesis in Rodent (*Octodon degus*) Hippocampus. PLoS ONE, 8(3), 1–9. https://doi.org/10.1371/journal.pone.0058649

Kumazawa-Manita, N., Katayama, M., Hashikawa, T., & Iriki, A. (2013a). Three-dimensional reconstruction of brain structures of the rodent *Octodon degus*: A brain atlas constructed by combining histological and magnetic resonance images. Experimental Brain Research, 231(1), 65–74. https://doi.org/10.1007/s00221-013-3667-1

Lakatta, E. G. (1993). Cardiovascular regulatory mechanisms in advanced age. Physiological Reviews. https://doi.org/10.1152/physrev.1993.73.2.413

Lakatta, E. G. (2016). So! What's aging? Is cardiovascular aging a disease? Physiology & Behavior, 176(1), 100–106. https://doi.org/10.1016/j.gde.2016.03.011

Lammert, E., Zeeb, M. (2014). Metabolism of Human Diseases, DOI 10.1007/978-3-7091-0715-7_35, © Springer-Verlag Wien 2014 ISBN 978-3-7091-0715-7 (eBook).

Lana, D., Ugolini, F., Nosi, D., Wenk, G. L., & Giovannini, M. G. (2021). The Emerging Role of the Interplay Among Astrocytes, Microglia, and Neurons in the Hippocampus in Health and Disease. Frontiers in Aging Neuroscience, 13(April). https://doi.org/10.3389/fnagi.2021.651973

Langston, J. W. (2017). The MPTP story. Journal of Parkinson's Disease, 7, S11–S19. https://doi.org/10.3233/JPD-179006

Lazarov, O., Mattson, M. P., Peterson, D. A., Pimplikar, S. W., & van Praag, H. (2010). When neurogenesis encounters aging and disease. Trends in Neurosciences. https://doi.org/10.1016/j.tins.2010.09.003

Lei, Y. M. K., Lekha, N., & Alegre, M.-L. (2015). Role of species-specific primary structure differences in Aβ42 assembly and neurotoxicity. Clinics and Research in Hepatology and Gastroenterology, 39(1), 9–19. https://doi.org/10.1111/mec.13536.Application

Leonard, E. A., & Marshall, R. J. (2018). Cardiovascular Disease in Women. Primary Care - Clinics in Office Practice, 45(1), 131–141. https://doi.org/10.1016/j.pop.2017.10.004

Li, S., Callaghan, B. L., & Richardson, R. (2014). Infantile amnesia: Forgotten but not gone. Learning and Memory. https://doi.org/10.1101/lm.031096.113

Li, Y., Zhao, T., Li, J., Xia, M., Li, Y., Wang, X., Liu, C., Zheng, T., Chen, R., Kan, D., Xie, Y.,

Song, J., Feng, Y., Yu, T., & Sun, P. (2022). Oxidative Stress and 4-hydroxy-2-nonenal (4-HNE): Implications in the Pathogenesis and Treatment of Aging-related Diseases. Journal of Immunology Research, 2022, 1–12. https://doi.org/10.1155/2022/2233906

Liochev S. I. (2013). Reactive oxygen species and the free radical theory of aging. Free radical biology & medicine, 60, 1–4. https://doi.org/10.1016/j.freeradbiomed.2013.02.011

Lisboa, B. P. (1964). Characterization of Δ4-3-OXO-C21-steroids on thin-layer chromatograms by "in situ" colour reactions. Journal of Chromatography A, 16(C). https://doi.org/10.1016/s0021-9673(01)82448-1

Litviňuková, M., Talavera-López, C., Maatz, H., Reichart, D., Worth, C. L., Lindberg, E. L., … Teichmann, S. A. (2020). Cells of the adult human heart. Nature, 588(7838), 466–472. https://doi.org/10.1038/s41586-020-2797-4

Liu, J., Sirenko, S., Juhaszova, M., Sollott, S. J., Shukla, S., Yaniv, Y., & Lakatta, E. G. (2014). Age-associated abnormalities of intrinsic automaticity of sinoatrial nodal cells are linked to deficient cAMP-PKA-Ca2+ signaling. American Journal of Physiology - Heart and Circulatory Physiology, 306(10). https://doi.org/10.1152/ajpheart.00088.2014

Liu, M., Zhang, P., Chen, M., Zhang, W., Yu, L., Yang, X. C., & Fan, Q. (2012). Aging might increase myocardial ischemia / reperfusion-induced apoptosis in humans and rats. Age, 34(3), 621–632. https://doi.org/10.1007/s11357-011-9259-8

Locati, E. T., Bagliani, G., Testoni, A., Lunati, M., & Padeletti, L. (2018). Role of Surface Electrocardiograms in Patients with Cardiac Implantable Electronic Devices. Cardiac Electrophysiology Clinics, 10(2), 233–255. https://doi.org/10.1016/j.ccep.2018.02.012

Locklear, M. N., & Kritzer, M. F. (2014). Assessment of the effects of sex and sex hormones on spatial cognition in adult rats using the Barnes maze. Hormones and Behavior, 66(2). https://doi.org/10.1016/j.yhbeh.2014.06.006

Lombard, D. B., Chua, K. F., Mostoslavsky, R., Franco, S., Gostissa, M., & Alt, F. W. (2005). DNA repair, genome stability, and aging. Cell. https://doi.org/10.1016/j.cell.2005.01.028

López-Otín, C., Blasco, M. A., Partridge, L., Serrano, M., & Kroemer, G. (2013). The hallmarks of aging. Cell. https://doi.org/10.1016/j.cell.2013.05.039

Lum, G., & Leal-Khouri, S. (1989). Significance of low serum urea nitrogen concentrations. Clinical Chemistry, 35(4). https://doi.org/10.1093/clinchem/35.4.639

Luppi, P. H., Aston-Jones, G., Akaoka, H., Chouvet, G., & Jouvet, M. (1995). Afferent projections to the rat locus coeruleus demonstrated by retrograde and anterograde tracing with cholera-toxin B subunit and Phaseolus vulgaris leucoagglutinin. Neuroscience, 65(1). https://doi.org/10.1016/0306-4522(94)00481-J

Macfarlane, P. W. (2018). The Influence of Age and Sex on the Electrocardiogram. Advances in Experimental Medicine and Biology, 9(1), 9–43. https://doi.org/10.1007/978-3-319-77932-4_6 93

Maguire, E. A., Frackowiak, R. S. J., & Frith, C. D. (1996). Learning to find your way a role for the human hippocampal formation. Proceedings of the Royal Society B: Biological Sciences, 263(1377). https://doi.org/10.1098/rspb.1996.0255

Maheswaran, S., Barjat, H., Rueckert, D., Bate, S. T., Howlett, D. R., Tilling, L., Smart, S. C., Pohlmann, A., Richardson, J. C., Hartkens, T., Hill, D. L., Upton, N., Hajnal, J. V., & James, M. F. (2009). Longitudinal regional brain volume changes quantified in normal aging and Alzheimer's APP × PS1 mice using MRI. Brain Research, 1270. https://doi.org/10.1016/j.brainres.2009.02.045

Maier, S. F., & Watkins, L. R. (1998). Cytokines for Psychologists: Implications of Bidirectional Immune-to-Brain Communication for Understanding Behavior, Mood, and Cognition. Psychological Review, 105(1). https://doi.org/10.1037/0033-295X.105.1.83

Mansour, S. G., Verma, G., Pata, R. W., Martin, T. G., Perazella, M. A., & Parikh, C. R. (2017). Kidney Injury and Repair Biomarkers in Marathon Runners. *American journal of kidney diseases : the official journal of the National Kidney Foundation*, 70(2), 252–261. https://doi.org/10.1053/j.ajkd.2017.01.045

Marquardt, N., Feja, M., Hünigen, H., Plendl, J., Menken, L., Fink, H., & Bert, B. (2018). Euthanasia of laboratory mice: Are isoflurane and sevoflurane real alternatives to carbon dioxide? PLoS ONE, 13(9). https://doi.org/10.1371/journal.pone.0203793

Martín Barrasa, J. L., Santana Rodríguez, N., Rodríguez-Pérez, J. C., Hidalgo, A. C., García, A. T., Camarillo, J. A., Santisteban, P. L., Mireles, M. B., González, M. P., & Chico, B. D. (2008). Electrocardiographic changes in rats undergoing thoracic surgery under combined parenteral anesthesia. Lab Animal, 37(10), 469–474. https://doi.org/10.1038/laban1008-469

Martin, S. J., & Clark, R. E. (2007). The rodent hippocampus and spatial memory: From synapses to systems. Cellular and Molecular Life Sciences, 64(4), 401–431. https://doi.org/10.1007/s00018-007-6336-3

Martinez, Z., Zhu, M., Han, S., & Fink, A. L. (2007). GM1 specifically interacts with α-synuclein and inhibits fibrillation. Biochemistry, 46(7). https://doi.org/10.1021/bi061749a

Mattson, M. P., & Magnus, T. (2006). Ageing and neuronal vulnerability. Nature Reviews Neuroscience. https://doi.org/10.1038/nrn1886

Mayne, K., White, J. A., McMurran, C. E., Rivera, F. J., & de la Fuente, A. G. (2020). Aging and Neurodegenerative Disease: Is the Adaptive Immune System a Friend or Foe?

Frontiers in Aging Neuroscience, 12(September). https://doi.org/10.3389/fnagi.2020.572090

Mayo, S. J., Kuruvilla, J., Laister, R. C., Ayala, A. P., Alm, M., Byker, W., Kelly, D. L., & Saligan, L. (2018). Blood-based biomarkers of cancer-related cognitive impairment in non-central nervous system cancer: Protocol for a scoping review. BMJ Open. https://doi.org/10.1136/bmjopen-2017-017578

McCann, H., Durand, B., & Shepherd, C. E. (2021). Aging-related tau astrogliopathy in aging and neurodegeneration. Brain Sciences. https://doi.org/10.3390/brainsci11070927

McFarlane, O., & Kędziora-Kornatowska, K. (2019). Cholesterol and Dementia: A Long and Complicated Relationship. Current Aging Science, 13(1), 42–51. https://doi.org/10.2174/1874609812666190917155400

McMullen, J. R., & Jennings, G. L. (2007). Differences between pathological and physiological cardiac hypertrophy: Novel therapeutic strategies to treat heart failure. Clinical and Experimental Pharmacology and Physiology, 34(4), 255–262. https://doi.org/10.1111/j.1440-1681.2007.04585.x

Meerson, F. Z., Javich, M. P., & Lerman, M. I. (1978). Decrease in the rate of RNA and protein synthesis and degradation in the myocardium under long-term compensatory hyperfunction and on aging. Journal of Molecular and Cellular Cardiology, 10(2). https://doi.org/10.1016/0022-2828(78)90039-1

Melo-Thomas, L., Gil-Martínez, A. L., Cuenca, L., Estrada, C., Gonzalez-Cuello, A., Schwarting, R. K., & Herrero, M. T. (2018). Electrical stimulation or MK-801 in the inferior colliculus improve motor deficits in MPTP-treated mice. NeuroToxicology, 65, 38–43. https://doi.org/10.1016/j.neuro.2018.01.004

Meredith, G. E., & Rademacher, D. J. (2016). MPTP Mouse Models of Parkinson's Disease: An Update. New Library World, 96(January), 16–20. https://doi.org/10.3233/JPD-2011-11023.MPTP

Merz, A. A., & Cheng, S. (2017). Sex differences in cardiovascular ageing. Physiology & Moll, T., Marshall, J. N. G., Soni, N., Zhang, S., Cooper-Knock, J., & Shaw, P. J. (2021). Membrane lipid raft homeostasis is directly linked to neurodegeneration. Essays in biochemistry, 65(7), 999–1011. https://doi.org/10.1042/EBC20210026

Moll, T., Shaw, P. J., & Cooper-Knock, J. (2020). Disrupted glycosylation of lipids and proteins is a cause of neurodegeneration. Brain : a journal of neurology, 143(5), 1332–1340. https://doi.org/10.1093/brain/awz358Behavior, 176(12), 139–148. https://doi.org/10.1016/j.physbeh.2017.03.040

Mesa-Herrera, F., Taoro-González, L., Valdés-Baizabal, C., Diaz, M., & Marín, R. (2019). Lipid

and lipid raft alteration in aging and neurodegenerative diseases: A window for the development of new biomarkers. International Journal of Molecular Sciences, 20(15). https://doi.org/10.3390/ijms20153810

Mikolka, P., Kosutova, P., Balentova, S., Cierny, D., Kopincova, J., Kolomaznik, M., Adamkov, M., Calkovska, A., & Mokra, D. (2020). Early cardiac injury in acute respiratory distress syndrome: comparison of two experimental models. Physiological research, 69(Suppl 3), S421–S432. https://doi.org/10.33549/physiolres.934591

Miller, D. B., & O'Callaghan, J. P. (2005). Aging, stress and the hippocampus. Ageing Research Reviews. https://doi.org/10.1016/j.arr.2005.03.002

Mladěnka, P., Applová, L., Patočka, J., Costa, V. M., Remiao, F., Pourová, J., Mladěnka, A., Karlíčková, J., Jahodář, L., Vopršalová, M., Varner, K. J., Štěrba, M., & TOX-OER and CARDIOTOX Hradec Králové Researchers and Collaborators (2018). Comprehensive review of cardiovascular toxicity of drugs and related agents. Medicinal Research Reviews. https://doi.org/10.1002/med.21476

Moll, T., Marshall, J. N. G., Soni, N., Zhang, S., Cooper-Knock, J., & Shaw, P. J. (2021). Membrane lipid raft homeostasis is directly linked to neurodegeneration. Essays in biochemistry, 65(7), 999–1011. https://doi.org/10.1042/EBC20210026

Moll, T., Shaw, P. J., & Cooper-Knock, J. (2020). Disrupted glycosylation of lipids and proteins is a cause of neurodegeneration. Brain : a journal of neurology, 143(5), 1332–1340. https://doi.org/10.1093/brain/awz358

Monje, M. H. G., Blesa, J., García-Cabezas, M. Á., Obeso, J. A., & Cavada, C. (2020). Changes in thalamic dopamine innervation in a progressive Parkinson's disease model in monkeys. Movement Disorders, 35(3), 419–430. https://doi.org/10.1002/mds.27921

Moor, E., Shohami, E., Kanevsky, E., Grigoriadis, N., Symeonidou, C., & Kohen, R. (2006). Impairment of the ability of the injured aged brain in elevating urate and ascorbate. Experimental Gerontology, 41(3). https://doi.org/10.1016/j.exger.2005.12.006

Moser, E., Moser, M. B., & Andersen, P. (1993). Spatial learning impairment parallels the magnitude of dorsal hippocampal lesions, but is hardly present following ventral lesions. Journal of Neuroscience, 13(9). https://doi.org/10.1523/jneurosci.13-09-03916.1993

Moser, M. B., Moser, E. I., Forrest, E., Andersen, P., & Morris, R. G. M. (1995). Spatial learning with a minislab in the dorsal hippocampus. Proceedings of the National Academy of Sciences of the United States of America, 92(21). https://doi.org/10.1073/pnas.92.21.9697

Mounayar, S., Boulet, S., Tandé, D., Jan, C., Pessiglione, M., Hirsch, E. C., Féger, J., Savasta, M., François, C., & Tremblay, L. (2007). A new model to study compensatory mechanisms

in MPTP-treated monkeys exhibiting recovery. Brain, 130(11), 2898–2914. https://doi.org/10.1093/brain/awm208

Muramatsu, Y., Kurosaki, R., Watanabe, H., Michimata, M., Matsubara, M., Imai, Y., & Araki, T. (2003). Expression of S-100 protein is related to neuronal damage in MPTP-treated mice. Glia, 42(3), 307–313. https://doi.org/10.1002/glia.10225

Nakamura, M., & Sadoshima, J. (2018). Mechanisms of physiological and pathological cardiac hypertrophy. Nature Reviews Cardiology, 15(7), 387–407. https://doi.org/10.1038/s41569-018-0007-y

Nalvarte, I. (2020). Sex stratified treatment of neurological disorders: Challenges and perspectives. Brain Sciences, 10(2). https://doi.org/10.3390/brainsci10020103

Naudí, A., Cabré, R., Jové, M., Ayala, V., Gonzalo, H., Portero-Otín, M., Ferrer, I., & Pamplona, R. (2015). Lipidomics of Human Brain Aging and Alzheimer's Disease Pathology. International Review of Neurobiology, 122, 133–189. https://doi.org/10.1016/bs.irn.2015.05.008

Negrón-Oyarzo, I., Neira, D., Espinosa, N., Fuentealba, P., & Aboitiz, F. (2015). Prenatal stress produces persistence of remote memory and disrupts functional connectivity in the hippocampal-prefrontal cortex axis. Cerebral Cortex, 25(9). https://doi.org/10.1093/cercor/bhu108

Nelson, D. L., and Cox, M. M. (2017). Lehninger principles of biochemistry (7th ed.). W.H. Freeman.

Nichols, N. R., Day, J. R., Laping, N. J., Johnson, S. A., & Finch, C. E. (1993). GFAP mRNA increases with age in rat and human brain. Neurobiology of Aging, 14(5). https://doi.org/10.1016/0197-4580(93)90100-P

Nicolle, M. M., Gonzalez, J., Sugaya, K., Baskerville, K. A., Bryan, D., Lund, K., Gallagher, M., & McKinney, M. (2001). Signatures of hippocampal oxidative stress in aged spatial learning-impaired rodents. Neuroscience, 107(3), 415–431. https://doi.org/10.1016/s0306-4522(01)00374-8Nikus, K., Pérez-Riera, A. R., Konttila, K., & Barbosa-Barros, R. (2018). Electrocardiographic recognition of right ventricular hypertrophy. Journal of Electrocardiology, 51(1), 46–49. https://doi.org/10.1016/j.jelectrocard.2017.09.004

Nimmerjahn, A., Kirchhoff, F., & Helmchen, F. (2005). Neuroscience: Resting microglial cells are highly dynamic surveillants of brain parenchyma in vivo. Science, 308(5726). https://doi.org/10.1126/science.1110647

Nishi, M., & Steiner, D. F. (1990). Cloning of Complementary DNAs Encoding Islet Amyloid Polypeptide , Insulin , and Glucagon Precursors from a New World Rodent , the Degu ,

Octodon degus. Molecular Endocrinology, 4(November), 1192–1198.

Norden, D. M., & Godbout, J. P. (2013). Review: Microglia of the aged brain: Primed to be activated and resistant to regulation. Neuropathology and Applied Neurobiology. https://doi.org/10.1111/j.1365-2990.2012.01306.x

O'Brien, J. S., & Sampson, E. L. (1965). Lipid composition of the normal human brain: gray matter, white matter, and myelin. Journal of Lipid Research, 6(4). https://doi.org/10.1016/s0022-2275(20)39619-x

O'Keefe, J., & Black, A. H. (1977). Single unit and lesion experiments on the sensory inputs to the hippocampal cognitive map. Ciba Foundation Symposium, (58). https://doi.org/10.1002/9780470720394.ch9

O'Leary, T. P., & Brown, R. E. (2013). Optimization of apparatus design and behavioral measures for the assessment of visuo-spatial learning and memory of mice on the Barnes maze. Learning and Memory, 20(2). https://doi.org/10.1101/lm.028076.112

Oberauer, K., Wendland, M., & Kliegl, R. (2003). Age differences in working memory - The roles of storage and selective access. Memory and Cognition, 31(4). https://doi.org/10.3758/BF03196097

Oberman R, Bhardwaj A. Physiology, Cardiac. [Updated 2021 Jul 21]. In: StatPearls [Internet]. Treasure Island (FL): StatPearls Publishing; 2022 Jan-. Available from: https://www.ncbi.nlm.nih.gov/books/NBK526089/?report=classic.

Obeso, J A, Stamelou, M., Goetz, C. G., Poewe, W., & Lang, A. E. (2017). Past, Present, and Future of Parkinson ' s Disease : A Special Essay on the 200th Anniversary of the Shaking Palsy Introduction I. The Past, 32(9), 1264–1310. https://doi.org/10.1002/mds.27115

Obeso, Jose A., Rodriguez-Oroz, M. C., Lanciego, J. L., Rodriguez Diaz, M., Bezard, E., Gross, C. E., & Brotchie, J. M. (2004). How does Parkinson's disease begin? The role of compensatory mechanisms (multiple letters). Trends in Neurosciences, 27(3), 125–127. https://doi.org/10.1016/j.tins.2003.12.006

Ochiai, Y., Iwano, H., Sakamoto, T., Hirabayashi, M., Kaneko, E., Watanabe, T., Yamashita, K., & Yokota, H. (2016). Blood biochemical changes in mice after administration of a mixture of three anesthetic agents. Journal of Veterinary Medical Science, 78(6), 951–956. https://doi.org/10.1292/jvms.15-0474

Oh, J., Lee, Y. D., & Wagers, A. J. (2014). Stem cell aging: Mechanisms, regulators and therapeutic opportunities. Nature Medicine. https://doi.org/10.1038/nm.3651

Ohsawa, T., & Shumiya, S. (1991). Age-related alteration of brain gangliosides in senescence-accelerated mouse (SAM)-P/8 9. Mechanisms of Ageing and Development, 59(3), 263–274. https://doi.org/10.1016/0047-6374(91)90137-O

Okanoya, K., Tokimoto, N., Kumazawa, N., Hihara, S., & Iriki, A. (2008). Tool-use training in a species of rodent: The emergence of an optimal motor strategy and functional understanding. PLoS ONE, 3(3). https://doi.org/10.1371/journal.pone.0001860

Oliva, C. A., Rivera, D. S., Mariqueo, T. A., Bozinovic, F., & Inestrosa, N. C. (2022). Differential Role of Sex and Age in the Synaptic Transmission of Degus (Octodon degus). Frontiers in integrative neuroscience, 16, 799147. https://doi.org/10.3389/fnint.2022.799147

Ooi, K. M., Vacy, K., & Boon, W. C. (2021). Fatty acids and beyond: Age and Alzheimer's disease related changes in lipids reveal the neuro-nutraceutical potential of lipids in cognition. *Neurochemistry international*, *149*, 105143. https://doi.org/10.1016/j.neuint.2021.105143

Opazo, J. C., Soto-Gamboa, M., & Bozinovic, F. (2004). Blood glucose concentration in caviomorph rodents. Comparative Biochemistry and Physiology - A Molecular and Integrative Physiology, 137(1), 57–64. https://doi.org/10.1016/j.cbpb.2003.09.007

Ostan, R., Bucci, L., Capri, M., Salvioli, S., Scurti, M., Pini, E., Monti, D., & Franceschi, C. (2008). Immunosenescence and immunogenetics of human longevity. NeuroImmunoModulation. https://doi.org/10.1159/000156466.

Otalora BB, Vivanco P, Madariaga AM, Madrid JA, Rol MÁ. 2010. Internal temporal order in the circadian system of a dual-phasing rodent, the octodon degus. Chronobiol Int 27:1564–1579.

Otoki, Y., Kato, S., Nakagawa, K., Harvey, D. J., Jin, L. W., Dugger, B. N., & Taha, A. Y. (2021). Lipidomic Analysis of Postmortem Prefrontal Cortex Phospholipids Reveals Changes in Choline Plasmalogen Containing Docosahexaenoic Acid and Stearic Acid Between Cases With and Without Alzheimer's Disease. NeuroMolecular Medicine, 23(1), 161–175. https://doi.org/10.1007/s12017-020-08636-w

Ownby, R. L. (2010). Neuroinflammation and cognitive aging. Current Psychiatry Reports, 12(1), 39–45. https://doi.org/10.1007/s11920-009-0082-1

Oxford Dictionary of Biochemistry and Molecular Biology. (2000). Reference Reviews, 14(8). https://doi.org/10.1108/rr.2000.14.8.26.404

De Pablos, V., Barcia, C., Yuste-Jiménez, J.E., Ros-Bernal, F., Carrillo-de Sauvage, M.A., Fernández-Villalba, E., & Herrero M.T. (2011). Acute Phase Protein's Levels as Potential Biomarkers for Early Diagnosis of Neurodegenerative Diseases. In (Ed.), Acute Phase Proteins as Early Non-Specific Biomarkers of Human and Veterinary Diseases. IntechOpen. https://doi.org/10.5772/22626

Paneni, F., Diaz Cañestro, C., Libby, P., Lüscher, T. F., & Camici, G. G. (2017). The Aging Cardiovascular System: Understanding It at the Cellular and Clinical Levels. Journal of

the American College of Cardiology, 69(15), 1952–1967. https://doi.org/10.1016/j.jacc.2017.01.064

Paradis, É., Clavel, S., Bouillaud, F., Ricquier, D., & Richard, D. (2003). Uncoupling protein 2: A novel player in neuroprotection. Trends in Molecular Medicine, 9(12), 522–525. https://doi.org/10.1016/j.molmed.2003.10.009

Park, D. C., Lautenschlager, G., Hedden, T., Davidson, N. S., Smith, A. D., & Smith, P. K. (2002). Models of visuospatial and verbal memory across the adult life span. Psychology and Aging, 17(2). https://doi.org/10.1037/0882-7974.17.2.299

Paz Gavilán, M., Vela, J., Castaño, A., Ramos, B., del Río, J. C., Vitorica, J., & Ruano, D. (2006). Cellular environment facilitates protein accumulation in aged rat hippocampus. Neurobiology of Aging, 27(7). https://doi.org/10.1016/j.neurobiolaging.2005.05.010

Peng, W., Huang, J., Zheng, Y., Ding, Y., Li, S., Zhang, J., Lyu, J., & Zeng, Q. (2019). UCP2 silencing aggravates mitochondrial dysfunction in astrocytes under septic conditions. Molecular Medicine Reports, 20(5), 4459–4466. https://doi.org/10.3892/mmr.2019.10721

Perkins, A. E., Varlinskaya, E. I., & Deak, T. (2020). From adolescence to late aging: a comprehensive review of social behavior, alcohol, and neuroinflammation across the lifespan, 1(607), 1–62. https://doi.org/10.1016/bs.irn.2019.08.001.From

Persson, J., Pudas, S., Lind, J., Kauppi, K., Nilsson, L. G., & Nyberg, L. (2012). Longitudinal structure-function correlates in elderly reveal MTL dysfunction with cognitive decline. Cerebral Cortex, 22(10). https://doi.org/10.1093/cercor/bhr306

Phillips, G. R., Hancock, S. E., Jenner, A. M., McLean, C., Newell, K. A., & Mitchell, T. W. (2022). Phospholipid Profiles Are Selectively Altered in the Putamen and White Frontal Cortex of Huntington's Disease. Nutrients, 14(10), 2086. https://doi.org/10.3390/nu14102086

Pigott, S., & Milner, B. (1993). Memory for different aspects of complex visual scenes after unilateral temporal- or frontal-lobe resection. Neuropsychologia, 31(1). https://doi.org/10.1016/0028-3932(93)90076-C

Pinares-Garcia, P., Stratikopoulos, M., Zagato, A., Loke, H., & Lee, J. (2018). Sex: A significant risk factor for neurodevelopmental and neurodegenerative disorders. Brain Sciences, 8(8), 1–27. https://doi.org/10.3390/brainsci8080154

Piomelli, D., Astarita, G., & Rapaka, R. (2007). A neuroscientist's guide to lipidomics. Nature Reviews Neuroscience. https://doi.org/10.1038/nrn2233

Pirman, N. L., Milshteyn, E., & Fanucci, G. E. (2011). Characterizing Induced-Conformational Changes in Intrinscially Disordered Proteins via Multi-Frequency EPR Spectroscopy. Biophysical Journal, 100(3). https://doi.org/10.1016/j.bpj.2010.12.536

Pitts, M. (2018). Barnes Maze Procedure for Spatial Learning and Memory in Mice. BIO-PROTOCOL, 8(5). https://doi.org/10.21769/bioprotoc.2744

Poewe, W., Seppi, K., Tanner, C. M., Halliday, G. M., Brundin, P., Volkmann, J., Schrag, A. E., & Lang, A. E (2017). Parkinson disease. Nature Reviews Disease Primers, 3, 1–21. https://doi.org/10.1038/nrdp.2017.13

Ponce-Ruiz, N., Murillo-González, F. E., Rojas-García, A. E., Bernal Hernández, Y. Y., Mackness, M., Ponce-Gallegos, J., Barrón-Vivanco, B. S., Hernández-Ochoa, I., González-Arias, C. A., Ortega Cervantes, L., Cardoso-Saldaña, G., & Medina-Díaz, I. M. (2020). Phenotypes and concentration of PON1 in cardiovascular disease: The role of nutrient intake. Nutrition, Metabolism and Cardiovascular Diseases, 30(1). https://doi.org/10.1016/j.numecd.2019.08.013

Popović, N., Madrid, J. A., Rol, M. Á., Caballero-Bleda, M., & Popović, M. (2010). Barnes maze performance of *Octodon degus* is gender dependent. Behavioural Brain Research, 212(2), 159–167. https://doi.org/10.1016/j.bbr.2010.04.005

Preston, A. R., & Eichenbaum, H. (2013). Interplay of hippocampus and prefrontal cortex in memory. Current Biology, 23(17), 1–21. https://doi.org/10.1016/j.cub.2013.05.041

Prinetti, A., Chigorno, V., Tettamanti, G., & Sonnino, S. (2000). Sphingolipid-enriched membrane domains from rat cerebellar granule cells differentiated in culture. A compositional study. Journal of Biological Chemistry, 275(16). https://doi.org/10.1074/jbc.275.16.11658

Rabbitt, P. (2005). Frontal brain changes and cognitive performance in old age. Cortex, 41(2). https://doi.org/10.1016/S0010-9452(08)70906-7

Raparelli, V., Norris, C. M., Bender, U., Herrero, M. T., Kautzky-Willer, A., Kublickiene, K., El Emam, K., Pilote, L., & GOING-FWD Collaborators (2021). Identification and inclusion of gender factors in retrospective cohort studies: The GOING-FWD framework. BMJ Global Health. https://doi.org/10.1136/bmjgh-2021-005413

Raz, N., Gunning-Dixon, F., Head, D., Rodrigue, K. M., Williamson, A., & Acker, J. D. (2004). Aging, sexual dimorphism, and hemispheric asymmetry of the cerebral cortex: Replicability of regional differences in volume. Neurobiology of Aging, 25(3). https://doi.org/10.1016/S0197-4580(03)00118-0

Raz, N., Lindenberger, U., Rodrigue, K. M., Kennedy, K. M., Head, D., Williamson, A., Dahle, C., Gerstorf, D., & Acker, J. D. (2005). Regional brain changes in aging healthy adults: General trends, individual differences and modifiers. Cerebral Cortex, 15(11). https://doi.org/10.1093/cercor/bhi044

Ríos, J. A., Cisternas, P., Arrese, M., Barja, S., & Inestrosa, N. C. (2014). Is Alzheimer's

disease related to metabolic syndrome? A Wnt signaling conundrum. Progress in Neurobiology, 121, 125–146. https://doi.org/10.1016/j.pneurobio.2014.07.004

Ritz, P., & Berrut, G. (2005). Mitochondrial function, energy expenditure, aging and insulin resistance. Diabetes and Metabolism. https://doi.org/10.1016/s1262-3636(05)73654-5

Rivera, D. S., Inestrosa, N. C., & Bozinovic, F. (2016). On cognitive ecology and the environmental factors that promote Alzheimer disease: Lessons from *Octodon degus* (Rodentia: Octodontidae). Biological Research, 1–10. https://doi.org/10.1186/s40659-016-0074-7

Rivera, D. S., Lindsay, C. B., Oliva, C. A., Bozinovic, F., & Inestrosa, N. C. (2021). A Multivariate Assessment of Age-Related Cognitive Impairment in *Octodon degus*. Frontiers in Integrative Neuroscience, 15(August), 1–13. https://doi.org/10.3389/fnint.2021.719076

Rivera, D. S., Lindsay, C. B., Oliva, C. A., Codocedo, J. F., Bozinovic, F., & Inestrosa, N. C. (2020). Effects of long-lasting social isolation and re-socialization on cognitive performance and brain activity: a longitudinal study in *Octodon degus*. Scientific Reports, 10(1), 1–21. https://doi.org/10.1038/s41598-020-75026-4

Roden, D. M. (2004). Drug-Induced Prolongation of the QT Interval. New England Journal of Medicine, 350(10). https://doi.org/10.1056/nejmra032426

Rodríguez-Arellano, J. J., Parpura, V., Zorec, R., & Verkhratsky, A. (2016). Astrocytes in physiological aging and Alzheimer's disease. Neuroscience, 323, 170–182. https://doi.org/10.1016/j.neuroscience.2015.01.007

Rodriguez, R. D., & Schocken, D. D. (1990). Update on sick sinus syndrome, a cardiac disorder of aging. Geriatrics.

Rodríguez, S., Ito, T., He, X. J., Uchida, K., & Nakayama, H. (2013). Resistance of the golden hamster to 1-methyl-4-phenyl-1,2,3,6-tetrahydropyridine (MPTP)-neurotoxicity is not only related with low levels of cerebral monoamine oxidase-B. Experimental and Toxicologic Pathology, 65(1–2), 127–133. https://doi.org/10.1016/j.etp.2011.06.010

Rolland, A. S., Herrero, M. T., Garcia-Martinez, V., Ruberg, M., Hirsch, E. C., & François, C. (2007). Metabolic activity of cerebellar and basal ganglia-thalamic neurons is reduced in parkinsonism. Brain, 130(1), 265–275. https://doi.org/10.1093/brain/awl337

Rossi, S., Fortunati, I., Carnevali, L., Baruffi, S., Mastorci, F., Trombini, M., Sgoifo, A., Corradi, D., Callegari, S., Miragoli, M., & Macchi, E. (2014). The effect of aging on the specialized conducting system: A telemetry ECG study in rats over a 6 month period. PLoS ONE, 9(11). https://doi.org/10.1371/journal.pone.0112697

Rothblat, D. S., & Schneider, J. S. (1994). Spontaneous functional recovery from parkinsonism

is not due to reinnervation of the dorsal striatum by residual dopaminergic neurons. Brain Research Bulletin, 34(3), 309–312. https://doi.org/10.1016/0361-9230(94)90068-X

Rouser, G., & Yamamoto, A. (1968). Curvilinear regression course of human brain lipid composition changes with age. Lipids, 3(3). https://doi.org/10.1007/BF02531202

Roux, C. M., Leger, M., & Freret, T. (2021). Memory Disorders Related to Hippocampal Function: The Interest of 5-HT4Rs Targeting. International journal of molecular sciences, 22(21), 12082. https://doi.org/10.3390/ijms222112082

Rubio, C. P., Martínez-Subiela, S., Hernández-Ruiz, J., Tvarijonaviciute, A., Cerón, J. J., & Allenspach, K. (2017). Serum biomarkers of oxidative stress in dogs with idiopathic inflammatory bowel disease. Veterinary Journal, 221. https://doi.org/10.1016/j.tvjl.2017.02.003

Rubio, C. P., Tvarijonaviciute, A., Martinez-Subiela, S., Hernández-Ruiz, J., & Cerón, J. J. (2016). Validation of an automated assay for the measurement of cupric reducing antioxidant capacity in serum of dogs. BMC Veterinary Research, 12(1). https://doi.org/10.1186/s12917-016-0760-2

Rudy, J. W., & Morledge, P. (1994). Ontogeny of contextual fear conditioning in rats: Implications for consolidation, infantile amnesia, and hippocampal system function. Behavioral Neuroscience, 108(2). https://doi.org/10.1037/0735-7044.108.2.227

Salmon, D. P., & Butters, N. (1995). Neurobiology of skill and habit learning. Current Opinion in Neurobiology, 5(2). https://doi.org/10.1016/0959-4388(95)80025-5

Sampedro-Piquero, P., De Bartolo, P., Petrosini, L., Zancada-Menendez, C., Arias, J. L., & Begega, A. (2014). Astrocytic plasticity as a possible mediator of the cognitive improvements after environmental enrichment in aged rats. Neurobiology of Learning and Memory, 114, 16–25. https://doi.org/10.1016/j.nlm.2014.04.002

Sanchez, J. N., Summa, N. M. E., Visser, L. C., Norvall, A., Sheley, M. F., & Sanchez-Migallon Guzman, D. (2019). Ventricular septal defect and congestive heart failure in a common degu (*Octodon degus*). Journal of Exotic Pet Medicine, 31, 32–35. https://doi.org/10.1053/j.jepm.2019.04.016

Sara, S. J. (2009). The locus coeruleus and noradrenergic modulation of cognition. Nature Reviews Neuroscience. https://doi.org/10.1038/nrn2573

Sastry, P. S. (1985). Lipids of nervous tissue: Composition and metabolism. Progress in Lipid Research. https://doi.org/10.1016/0163-7827(85)90011-6

Scahill, R. I., Frost, C., Jenkins, R., Whitwell, J. L., Rossor, M. N., & Fox, N. C. (2003). A longitudinal study of brain volume changes in normal aging using serial registered magnetic resonance imaging. Archives of Neurology, 60(7).

https://doi.org/10.1001/archneur.60.7.989

Scandroglio, F., Loberto, N., Valsecchi, M., Chigorno, V., Prinetti, A., & Sonnino, S. (2009). Thin layer chromatography of gangliosides. Glycoconjugate Journal, 26(8), 961–973. https://doi.org/10.1007/s10719-008-9145-5

Scandroglio, F., Venkata, J. K., Loberto, N., Prioni, S., Schuchman, E. H., Chigorno, V., Prinetti, A., & Sonnino, S. (2008). Lipid content of brain, brain membrane lipid domains, and neurons from acid sphingomyelinase deficient mice. Journal of Neurochemistry, 107(2), 329–338. https://doi.org/10.1111/j.1471-4159.2008.05591.x

Scheltens, P., Strooper, B. De, Kivipelto, M., Holstege, H., Chételat, G., Teunissen, C. E., Cummings, J., & Flier, W. M. Van Der. (2022). Alzheimer ' s disease, 397(10284), 1577–1590. https://doi.org/10.1016/S0140-6736(20)32205-4.

Schindelin, J., Arganda-Carreras, I., Frise, E., Kaynig, V., Longair, M., Pietzsch, T., Preibisch, S., Rueden, C., Saalfeld, S., Schmid, B., Tinevez, J. Y., White, D. J., Hartenstein, V., Eliceiri, K., Tomancak, P., & Cardona, A. (2012). Fiji: An open-source platform for biological-image analysis. Nature Methods, 9(7), 676–682. https://doi.org/10.1038/nmeth.2019

Schneider, J. S., Schroeder, J. A., & Rothblat, D. S. (1998). Differential recovery of sensorimotor function in GM1 ganglioside- treated vs. spontaneously recovered MPTP-treated cats: Partial striatal dopaminergic reinnervation vs. neurochemical compensation. Brain Research, 813(1), 82–87. https://doi.org/10.1016/S0006-8993(98)01007-5

Schultz, C., & Engelhardt, M. (2014). Anatomy of the hippocampal formation. The Hippocampus in Clinical Neuroscience, 34, 6–17. https://doi.org/10.1159/000360925

Schwimmer, S., & Bevenue, A. (1956). Reagent for differentiation of 1,4- and 1,6-linked glucosaccharides. Science, 123(3196). https://doi.org/10.1126/science.123.3196.543

Segatto, M., Di Giovanni, A., Marino, M., & Pallottini, V. (2013). Analysis of the protein network of cholesterol homeostasis in different brain regions: An age and sex dependent perspective. Journal of Cellular Physiology, 228(7), 1561–1567. https://doi.org/10.1002/jcp.24315

Seniuk, N. A., Tatton, W. G., & Greenwood, C. E. (1990). Dose-dependent destruction of the coeruleus-cortical and nigral-striatal projections by MPTP. Brain Research, 527(1), 7–20. https://doi.org/10.1016/0006-8993(90)91055-I

Sharma, S., Rakoczy, S., & Brown-Borg, H. (2010). Assessment of spatial memory in mice. Life Sciences, 87(17–18), 521–536. https://doi.org/10.1016/j.lfs.2010.09.004

Shibata, N., Kato, Y., Inose, Y., Hiroi, A., Yamamoto, T., Morikawa, S., Sawada, M., & Kobayashi, M. (2011). 4-hydroxy-2-nonenal upregulates and phosphorylates cytosolic

phospholipase A2 in cultured Ra2 microglial cells via MAPK pathways. Neuropathology, 31(2). https://doi.org/10.1111/j.1440-1789.2010.01139.x

Siah, C. W., Ombiga, J., Adams, L. A., Trinder, D., & Olynyk, J. K. (2006). Normal iron metabolism and the pathophysiology of iron overload disorders. The Clinical biochemist. Reviews, 27(1), 5–16.

Sierra, A., Beccari, S., Diaz-Aparicio, I., Encinas, J. M., Comeau, S., & Tremblay, M. È. (2014). Surveillance, phagocytosis, and inflammation: How never-resting microglia influence adult hippocampal neurogenesis. Neural Plasticity, 2014. https://doi.org/10.1155/2014/610343

Silva-Santana, G., Bax, J. C., Fernandes, D. C. S., Bacellar, D. T. L., Hooper, C., Dias, A. A. S. O., Silva, C. B., de Souza, A. M., Ramos, S., Santos, R. A., Pinto, T. R., Ramão, M. A., & Mattos-Guaraldi, A. L. (2020). Clinical hematological and biochemical parameters in Swiss, BALB/c, C57BL/6 and B6D2F1 *Mus musculus*. Animal models and experimental medicine, 3(4), 304–315. https://doi.org/10.1002/ame2.12139

Singh, D. K., & Peter, C. T. (2016). Use of the Surface Electrocardiogram to Define the Nature of Challenging Arrhythmias. Cardiac Electrophysiology Clinics, 8(1), 1–24. https://doi.org/10.1016/j.ccep.2015.10.021

Singh, S., Mishra, A., Tiwari, V., & Shukla, S. (2019). Enhanced neuroinflammation and oxidative stress are associated with altered hippocampal neurogenesis in 1-methyl-4-phenyl-1,2,3,6-tetrahydropyridine treated mice. Behavioural Pharmacology, 30(8), 688–698. https://doi.org/10.1097/FBP.0000000000000516

Singletary, G. E., Saunders, A. B., Saunders, W. B., Suchodolski, J. S., Steiner, J. M., Fosgate, G. T., & Hartsfield, S. M. (2010). Cardiac troponin I concentrations following medetomidine-butorphanol sedation in dogs. Veterinary Anaesthesia and Analgesia, 37(4). https://doi.org/10.1111/j.1467-2995.2010.00540.x

Sipione, S., Monyror, J., Galleguillos, D., Steinberg, N., & Kadam, V. (2020). Gangliosides in the Brain: Physiology, Pathophysiology and Therapeutic Applications. Frontiers in Neuroscience, 14(October), 1–24. https://doi.org/10.3389/fnins.2020.572965

Skowronska-Krawczyk, Dorota & Budin, I. (2020). Aging membranes: unexplored functions for lipids in the lifespan of the central nervous system. Experimental Geron, 131, 110817. https://doi.org/10.1016/j.exger.2019.110817.Aging

Smith, T. D., Calhoun, M. E., & Rapp, P. R. (1999). Circuit and morphological specificity of synaptic change in the aged hippocampal formation. Neurobiology of Aging. https://doi.org/10.1016/S0197-4580(99)00073-1

Sobočanec, S., Balog, T., Šverko, V., & Marotti, T. (2003). Sex-dependent antioxidant enzyme

activities and lipid peroxidation in ageing mouse brain. Free Radical Research, 37(7), 743–748. https://doi.org/10.1080/1071576031000102178

Sobrero, R., Fernández-Aburto, P., Ly-Prieto, Á., Delgado, S. E., Mpodozis, J., & Ebensperger, L. A. (2016). Effects of Habitat and Social Complexity on Brain Size, Brain Asymmetry and Dentate Gyrus Morphology in Two Octodontid Rodents. Brain, Behavior and Evolution, 87(1), 51–64. https://doi.org/10.1159/000444741

Söderberg, M., Edlund, C., Kristensson, K., & Dallner, G. (1990). Lipid Compositions of Different Regions of the Human Brain During Aging. Journal of Neurochemistry, 54(2). https://doi.org/10.1111/j.1471-4159.1990.tb01889.x

Solari, N., & Hangya, B. (2018). Cholinergic modulation of spatial learning, memory and navigation. European Journal of Neuroscience. https://doi.org/10.1111/ejn.14089

Soltesz, I., Losonczy, A., & Author, N. N. (2018). CA1 pyramidal cell diversity enabling parallel information processing in the hippocampus HHS Public Access Author manuscript. Nat Neurosci, 21(4), 484–493. https://doi.org/10.1038/s41593-018-0118-0

Sonnino, S, & Prinetti, A. (2012). Membrane Domains and the Lipid Raft Concept. Current Medicinal Chemistry, 20(1), 4–21. https://doi.org/10.2174/0929867311320010003

Sonnino, Sandro, Aureli, M., Grassi, S., Mauri, L., Prioni, S., & Prinetti, A. (2014). Lipid Rafts in Neurodegeneration and Neuroprotection. Molecular Neurobiology, 50(1), 130–148. https://doi.org/10.1007/s12035-013-8614-4

Soreghan, B., Thomas, S. N., & Yang, A. J. (2003). Aberrant sphingomyelin/ceramide metabolic-induced neuronal endosomal/lysosomal dysfunction: Potential pathological consequences in age-related neurodegeneration. Advanced Drug Delivery Reviews, 55(11). https://doi.org/10.1016/j.addr.2003.07.007

Soria Lopez, J. A., González, H. M., & Léger, G. C. (2019). Alzheimer's disease. Handbook of Clinical Neurology, 167, 231–255. https://doi.org/10.1016/B978-0-12-804766-8.00013-3

Sottero, B., Rossin, D., Poli, G., & Biasi, F. (2017). Lipid Oxidation Products in the Pathogenesis of Inflammation-related Gut Diseases. Current Medicinal Chemistry, 25(11). https://doi.org/10.2174/0929867324666170619104105

Speerschneider, T., & Thomsen, M. B. (2013). Physiology and analysis of the electrocardiographic T wave in mice. Acta Physiologica, 209(4), 262–271. https://doi.org/10.1111/apha.12172

Spiteller, G. (2002). Are changes of the cell membrane structure causally involved in the aging process? In Annals of the New York Academy of Sciences (Vol. 959). https://doi.org/10.1111/j.1749-6632.2002.tb02080.x

Stefanacci, L., Buffalo, E. A., Schmolck, H., & Squire, L. R. (2000). Profound amnesia after damage to the medial temporal lobe: A neuroanatomical and neuropsychological profile of patient E. P. Journal of Neuroscience, 20(18). https://doi.org/10.1523/jneurosci.20-18-07024.2000

Stojanov, M., Stefanović, A., Džingalašević, G., Mandić-Radić, S., & Prostran, M. (2011). Butyrylcholinesterase activity in young men and women: Association with cardiovascular risk factors. Clinical Biochemistry, 44(8–9). https://doi.org/10.1016/j.clinbiochem.2011.03.028

Strange, B. A., Witter, M. P., Lein, E. S., & Moser, E. I. (2014). Functional organization of the hippocampal longitudinal axis. Nature Reviews Neuroscience, 15(10), 655–669. https://doi.org/10.1038/nrn3785

Sullivan, E. V., Marsh, L., Mathalon, D. H., Lim, K. O., & Pfefferbaum, A. (1995). Age-related decline in MRI volumes of temporal lobe gray matter but not hippocampus. Neurobiology of Aging, 16(4). https://doi.org/10.1016/0197-4580(95)00074-O

Surmeier, D. J. (2018). Determinants of dopaminergic neuron loss in Parkinson's disease. The FEBS Journal. https://doi.org/10.1111/febs.14607

Švara, T., Gomba, M., Poli, A., Ra, J., & Zadravec, M. (2020). Spontaneous Tumors and Non - Neoplastic Proliferative Lesions in Pet Degus (*Octodon degus*). https://doi.org/10.3390/vetsci7010032

Svennerholm, L., Boström, K., Jungbjer, B., & Olsson, L. (1994). Membrane lipids of adult human brain: lipid composition of frontal and temporal lobe in subjects of age 20 to 100 years. *Journal of neurochemistry*, *63*(5), 1802–1811. https://doi.org/10.1046/j.1471-4159.1994.63051802.x

Svennerholm, L., Boström, K., Helander, C. G., & Jungbjer, B. (1991). Membrane lipids in the aging human brain. *Journal of neurochemistry*, *56*(6), 2051–2059. https://doi.org/10.1111/j.1471-4159.1991.tb03466.x

Svennerholm, L., Boström, K., Fredman, P., Månsson, J. E., Rosengren, B., & Rynmark, B. M. (1989). Human brain gangliosides: developmental changes from early fetal stage to advanced age. *Biochimica et biophysica acta*, *1005*(2), 109–117. https://doi.org/10.1016/0005-2760(89)90175-6

Szabadfi, K., Estrada, C., Fernandez-Villalba, E., Tarragon, E., Setalo, G., Jr, Izura, V., Reglodi, D., Tamas, A., Gabriel, R., & Herrero, M. T. (2015). Retinal aging in the diurnal Chilean rodent (*Octodon degus*): histological, ultrastructural and neurochemical alterations of the vertical information processing pathway. Frontiers in Cellular Neuroscience, 9. https://doi.org/10.3389/fncel.2015.00126

Talavera, J., Guzmán, M. J., del Palacio, M. J., Albert, A. P., & Bayón, A. (2008). The normal electrocardiogram of four species of conscious raptors. Research in veterinary science, 84(1), 119–125. https://doi.org/10.1016/j.rvsc.2007.03.001

Tan, Z., Garduño, B. M., Aburto, P. F., Chen, L., Ha, N., Cogram, P., Holmes, T. C., & Xu, X. (2022). Cognitively impaired aged Octodon degus recapitulate major neuropathological features of sporadic Alzheimer's disease. Acta neuropathologica communications, 10(1), 182. https://doi.org/10.1186/s40478-022-01481-x

Tarragon, E., Lopez, D., Estrada, C., Ana, G. C., Schenker, E., Pifferi, F., Bordet, R., Richardson, J. C., & Herrero, M. T. (2013). *Octodon degus* : A Model for the Cognitive Impairment Associated with Alzheimer ' s Disease Basic Research in Alzheimer ' s Disease, 1–6. https://doi.org/10.1111/cns.12125

Tarragon, E., Lopez, D., Estrada, C., Gonzalez-Cuello, A., Ros, C. M., Lamberty, Y., Pifferi, F., Cella, M., Canovi, M., Guiso, G., Gobbi, M., Fernández-Villalba, E., Blin, O., Bordet, R., Richardson, J. C., & Herrero, M. T. (2014). Memantine prevents reference and working memory impairment caused by sleep deprivation in both young and aged *Octodon degus*. Neuropharmacology, 85, 206–214. https://doi.org/10.1016/j.neuropharm.2014.05.023

Teissier, T., Boulanger, E., & Deramecourt, V. (2020). Normal ageing of the brain: Histological and biological aspects. Revue Neurologique, 176(9), 649–660. https://doi.org/10.1016/j.neurol.2020.03.017

Tettamanti, G., Bonali, F., Marchesini, S., & Zambotti, V. (1973). A new procedure for the extraction, purification and fractionation of brain gangliosides. Biochimica et Biophysica Acta (BBA)/Lipids and Lipid Metabolism, 296(1). https://doi.org/10.1016/0005-2760(73)90055-6

Tia, B., Viaro, R., & Fadiga, L. (2018). Tool-use training temporarily enhances cognitive performance in long-tailed macaques (Macaca fascicularis). Animal Cognition, 21(3), 365–378. https://doi.org/10.1007/s10071-018-1173-3

Tu, J., Yin, Y., Xu, M., Wang, R., & Zhu, Z. J. (2018). Absolute quantitative lipidomics reveals lipidome-wide alterations in aging brain. Metabolomics, 14(1), 0. https://doi.org/10.1007/s11306-017-1304-x

Tulving, E. (1972). Chapter 10: Episodic and sematic memory. In Organisation of memory.

Turrin, N. P., Gayle, D., Ilyin, S. E., Flynn, M. C., Langhans, W., Schwartz, G. J., & Plata-Salamán, C. R. (2001). Pro-inflammatory and anti-inflammatory cytokine mRNA induction in the periphery and brain following intraperitoneal administration of bacterial lipopolysaccharide. Brain Research Bulletin, 54(4). https://doi.org/10.1016/S0361-9230(01)00445-2

Valero, J., Bernardino, L., Cardoso, F. L., Silva, A. P., Fontes-Ribeiro, C., Ambrósio, A. F., & Malva, J. O. (2017). Impact of Neuroinflammation on Hippocampal Neurogenesis: Relevance to Aging and Alzheimer's Disease. Journal of Alzheimer's Disease, 60(s1), S161–S168. https://doi.org/10.3233/JAD-170239

Van Den Akker, M., Buntinx, F., & Knottnerus, J. A. (1996). Comorbidity or multimorbidity: What's in a name? A review of literature. European Journal of General Practice. https://doi.org/10.3109/13814789609162146

van Groen, T., Kadish, I., Popović, N., Popović, M., Caballero-Bleda, M., Baño-Otálora, B., Vivanco, P., Rol, M. Á., & Madrid, J. A. (2011). Age-related brain pathology in Octodon degu: Blood vessel, white matter and Alzheimer-like pathology. Neurobiology of Aging, 32(9), 1651–1661. https://doi.org/10.1016/j.neurobiolaging.2009.10.008

Van Muiswinkel, F. L., De Vos, R. A. I., Bol, J. G. J. M., Andringa, G., Jansen Steur, E. N. H., Ross, D., … Drukarch, B. (2004). Expression of NAD(P)H:quinone oxidoreductase in the normal and Parkinsonian substantia nigra. Neurobiology of Aging, 25(9). https://doi.org/10.1016/j.neurobiolaging.2003.12.010

Vaskovsky, V. E., & Kostetsky, E. Y. (1968). Modified spray for the detection of phospholipids on thin-layer chromatograms. Journal of Lipid Research, 9(3). https://doi.org/10.1016/s0022-2275(20)43111-6

Venkateshappa, C., Harish, G., Mahadevan, A., Srinivas Bharath, M. M., & Shankar, S. K. (2012). Elevated oxidative stress and decreased antioxidant function in the human hippocampus and frontal cortex with increasing age: Implications for neurodegeneration in Alzheimer's disease. Neurochemical Research, 37(8). https://doi.org/10.1007/s11064-012-0755-8

Verkerke, M., Hol, E. M., & Middeldorp, J. (2021). Physiological and Pathological Ageing of Astrocytes in the Human Brain. Neurochemical Research, 46(10), 2662–2675. https://doi.org/10.1007/s11064-021-03256-7

Verra, D. M., Sajdak, B. S., Merriman, D. K., & Hicks, D. (2019). Diurnal rodents as pertinent animal models of human retinal physiology and pathology. Progress in Retinal and Eye Research, 100776. https://doi.org/10.1016/j.preteyeres.2019.100776

Vicent, L., & Martínez-Sellés, M. (2017). Electrocardiogeriatrics: ECG in advanced age. Journal of Electrocardiology, 50(5), 698–700. https://doi.org/10.1016/j.jelectrocard.2017.06.003

Von Bohlen und Halbach, O., & Unsicker, K. (2002). Morphological alterations in the amygdala and hippocampus of mice during ageing. European Journal of Neuroscience, 16(12). https://doi.org/10.1046/j.1460-9568.2002.02405.x

Vorhees, C. V., & Williams, M. T. (2014). Assessing spatial learning and memory in rodents. ILAR Journal, 55(2), 310–332. https://doi.org/10.1093/ilar/ilu013

Wagner, G. S., Macfarlane, P., Wellens, H., Josephson, M., Gorgels, A., Mirvis, D. M., Pahlm, O., Surawicz, B., Kligfield, P., Childers, R., Gettes, L. S., Bailey, J. J., Deal, B. J., Gorgels, A., Hancock, E. W., Kors, J. A., Mason, J. W., Okin, P., Rautaharju, P. M., van Herpen, G., … Heart Rhythm Society (2009). AHA/ACCF/HRS Recommendations for the Standardization and Interpretation of the Electrocardiogram. Part VI: Acute Ischemia/Infarction A Scientific Statement From the American Heart Association Electrocardiography and Arrhythmias Committee, Council on Clinical Cardiology; the American College of Cardiology Foundation. Journal of the American College of Cardiology. https://doi.org/10.1016/j.jacc.2008.12.016

Wagner, J. U. G., & Dimmeler, S. (2020). Cellular cross-talks in the diseased and aging heart. Journal of Molecular and Cellular Cardiology, 138, 136–146. https://doi.org/10.1016/j.yjmcc.2019.11.152

Wahl, D., Coogan, S. C., Solon-Biet, S. M., de Cabo, R., Haran, J. B., Raubenheimer, D., Cogger, V. C., Mattson, M. P., Simpson, S. J., & Le Couteur, D. G. (2017). Cognitive and behavioral evaluation of nutritional interventions in rodent models of brain aging and dementia. Clinical Interventions in Aging, 12, 1419–1428. https://doi.org/10.2147/CIA.S145247

Wang, T., Ruan, B., Wang, J., Zhou, Z., Zhang, X., Zhang, C., H., & Yuan, D. (2022). Activation of NLRP3-Caspase-1 pathway contributes to age-related impairments in cognitive function and synaptic plasticity. Neurochemistry International, 152, 105220. https://doi.org/10.1016/j.neuint.2021.105220

Wang, W., Nguyen, L. T., Burlak, C., Chegini, F., Guo, F., Chataway, T., Ju, S., Fisher, O. S., Miller, D. W., Datta, D., Wu, F., Wu, C. X., Landeru, A., Wells, J. A., Cookson, M. R., Boxer, M. B., Thomas, C. J., Gai, W. P., Ringe, D., Petsko, G. A., … Hoang, Q. Q. (2016). Caspase-1 causes truncation and aggregation of the Parkinson's disease-associated protein α-synuclein. Proceedings of the National Academy of Sciences of the United States of America, 113(34). https://doi.org/10.1073/pnas.1610099113

Wang, X., & Michaelis, E. K. (2010). Selective neuronal vulnerability to oxidative stress in the brain. Frontiers in Aging Neuroscience, 2(MAR), 1–13. https://doi.org/10.3389/fnagi.2010.00012

Wang, X., L. Michaelis, M., & K. Michaelis, E. (2010). Functional Genomics of Brain Aging and Alzheimers Disease: Focus on Selective Neuronal Vulnerability. Current Genomics, 11(8). https://doi.org/10.2174/138920210793360943

Wang, X., Pal, R., Chen, X. W., Limpeanchob, N., Kumar, K. N., & Michaelis, E. K. (2005).

High intrinsic oxidative stress may underlie selective vulnerability of the hippocampal CA1 region. Molecular Brain Research, 140(1–2). https://doi.org/10.1016/j.molbrainres.2005.07.018

Wang, X., Pal, R., Chen, X. wen, Kumar, K. N., Kim, O. J., & Michaelis, E. K. (2007). Genome-wide transcriptome profiling of region-specific vulnerability to oxidative stress in the hippocampus. Genomics, 90(2). https://doi.org/10.1016/j.ygeno.2007.03.007

Wang, X., Zaidi, A., Pal, R., Garrett, A. S., Braceras, R., Chen, X. W., Michaelis, M. L., & Michaelis, E. K. (2009). Genomic and biochemical approaches in the discovery of mechanisms for selective neuronal vulnerability to oxidative stress. BMC Neuroscience, 10. https://doi.org/10.1186/1471-2202-10-12

West, R. L. (1996). An application of prefrontal cortex function theory to cognitive aging. Psychological Bulletin, 120(2). https://doi.org/10.1037/0033-2909.120.2.272

WHO. (2022). World Health Statistics 2022. World Health Organization.

Wiedmeyer, C. E., Crossland, J. P., Veres, M., Dewey, M. J., Felder, M. R., Barlow, S. C., Vrana, P. B., & Szalai, G.. (2014). Hematologic and serum biochemical values of 4 species of Peromyscus mice and their hybrids. Journal of the American Association for Laboratory Animal Science, 53(4), 336–343.

Wilde, G. J. C., Pringle, A. K., Wright, P., & Iannotti, F. (1997). Differential vulnerability of the CA1 and CA3 subfields of the hippocampus to superoxide and hydroxyl radicals in vitro. Journal of Neurochemistry, 69(2). https://doi.org/10.1046/j.1471-4159.1997.69020883.x

Winner, B., Jappelli, R., Maji, S. K., Desplats, P. A., Boyer, L., Aigner, S., Hetzer, C., Loher, T., Vilar, M., Campioni, S., Tzitzilonis, C., Soragni, A., Jessberger, S., Mira, H., Consiglio, A., Pham, E., Masliah, E., Gage, F. H., & Riek, R. (2011). In vivo demonstration that alpha-synuclein oligomers are toxic. Proceedings of the National Academy of Sciences of the United States of America, 108(10), 4194–4199. https://doi.org/10.1073/pnas.1100976108

Wong, M. W., Braidy, N., Poljak, A., Pickford, R., Thambisetty, M., & Sachdev, P. S. (2017). Dysregulation of lipids in Alzheimer's disease and their role as potential biomarkers. Alzheimer's & dementia : the journal of the Alzheimer's Association, 13(7), 810–827. https://doi.org/10.1016/j.jalz.2017.01.008

Wood, P. L., Barnette, B. L., Kaye, J. A., Quinn, J. F., & Woltjer, R. L. (2015). Non-targeted lipidomics of CSF and frontal cortex grey and white matter in control, mild cognitive impairment, and Alzheimer's disease subjects. Acta Neuropsychiatrica, 27(5). https://doi.org/10.1017/neu.2015.18

World health statistics 2022: monitoring health for the SDGs, sustainable development goals.

Geneva: World Health Organization; 2022. Licence: CC BY-NC-SA 3.0 IGO.

Wright, J. W., & Kern, M. D. (1992). Stereotaxic atlas of the brain of *Octodon degus*. Journal of Morphology, 214(3), 299–320. https://doi.org/10.1002/jmor.1052140306

Xia, J., Song, P., Sun, Z., Sawakami, T., Jia, M., & Wang, Z. (2016). Advances of diagnostic and mechanistic studies of γ-glutamyl transpeptidase in hepatocellular carcinoma. Drug Discoveries & Therapeutics. https://doi.org/10.5582/ddt.2016.01052

Xing, S., Tsaih, S. W., Yuan, R., Svenson, K. L., Jorgenson, L. M., So, M., Paigen, B. J., & Korstanje, R. (2009). Genetic influence on electrocardiogram time intervals and heart rate in aging mice. American Journal of Physiology - Heart and Circulatory Physiology, 296(6). https://doi.org/10.1152/ajpheart.00681.2008

Yamamoto, N., Matsubara, T., Sato, T., & Yanagisawa, K. (2008). Age-dependent high-density clustering of GM1 ganglioside at presynaptic neuritic terminals promotes amyloid β-protein fibrillogenesis. Biochimica et Biophysica Acta - Biomembranes, 1778(12). https://doi.org/10.1016/j.bbamem.2008.07.028

Yancik, R., Ershler, W., Satariano, W., Hazzard, W., Cohen, H. J., & Ferrucci, L. (2007). Report of the National Institute on Aging Task Force on Comorbidity. Journals of Gerontology - Series A Biological Sciences and Medical Sciences. https://doi.org/10.1093/gerona/62.3.275

Yang, S., Liu, T., Li, S., Zhang, X., Ding, Q., Que, H., Yan, X., Wei, K., & Liu, S. (2008). Comparative proteomic analysis of brains of naturally aging mice. Neuroscience, 154(3). https://doi.org/10.1016/j.neuroscience.2008.04.012

Yang, X. L., Liu, G. Z., Tong, Y. H., Yan, H., Xu, Z., Chen, Q., Liu, X., Zhang, H. H., Wang, H. B., & Tan, S. H. (2015). The history, hotspots, and trends of electrocardiogram. Journal of Geriatric Cardiology, 12(4), 448–456. https://doi.org/10.11909/j.issn.1671-5411.2015.04.018

Yarnoz, M. J., & Curtis, A. B. (2008). More Reasons Why Men and Women Are Not the Same (Gender Differences in Electrophysiology and Arrhythmias). American Journal of Cardiology. https://doi.org/10.1016/j.amjcard.2007.12.027

Yoon, J. H., Seo, Y., Jo, Y. S., Lee, S., Cho, E., Cazenave-Gassiot, A., Shin, Y. S., Moon, M. H., An, H. J., Wenk, M. R., & Suh, P. G. (2022). Brain lipidomics: From functional landscape to clinical significance. Science advances, 8(37), eadc9317. https://doi.org/10.1126/sciadv.adc9317

Zampino, M., Polidori, M. C., Ferrucci, L., Neill, D. O., Pilotto, A., Gogol, M., & Rubenstein, L. (2022). Biomarkers of aging in real life: three questions on aging and the comprehensive geriatric assessment. GeroScience, (0123456789). https://doi.org/10.1007/s11357-022-

00613-4

Zarrouk, A., Vejux, A., Mackrill, J., O'Callaghan, Y., Hammami, M., O'Brien, N., & Lizard, G. (2014). Involvement of oxysterols in age-related diseases and ageing processes. Ageing Research Reviews. https://doi.org/10.1016/j.arr.2014.09.006

Zeng, X.-S., Geng, W.-S., Jia, J.-J., Chen, L., & Zhang, P.-P. (2018). Cellular and Molecular Basis of Neurodegeneration in Parkinson Disease. Frontiers in Aging Neuroscience, 10(April), 1–16. https://doi.org/10.3389/fnagi.2018.00109

Zhan, J. S., Gao, K., Chai, R. C., Jia, X. H., Luo, D. P., Ge, G., Jiang, Y. W., Fung, Y. W., Li, L., & Yu, A. C. (2017). Astrocytes in Migration. Neurochemical Research, 42(1). https://doi.org/10.1007/s11064-016-2089-4

Zhou, X., & Hansson, G. K. (2004). Effect of Sex and Age on Serum Biochemical Reference Ranges in C57BL/6J Mice. Comparative Medicine, 54(2), 176–178.

Zhu, G., Huang, Y., Chen, Y., Zhuang, Y., & Behnisch, T. (2012). MPTP modulates hippocampal synaptic transmission and activity-dependent synaptic plasticity via dopamine receptors. Journal of Neurochemistry, 122(3), 582–593. https://doi.org/10.1111/j.1471-4159.2012.07815.x

Zhu, X., Raina, A. K., Lee, H. G., Casadesus, G., Smith, M. A., & Perry, G. (2004). Oxidative stress signalling in Alzheimer's disease. Brain Research. https://doi.org/10.1016/j.brainres.2004.01.012

Zucker, I., Prendergast, B. J., & Beery, A. K. (2021). Pervasive Neglect of Sex Differences in Biomedical Research. Cold Spring Harbor Perspectives in Biology. https://doi.org/10.1101/cshperspect.a039156

Zuddas, A., Fascetti, F., Corsini, G. U., & Piccardi, M. P. (1994). In brown Norway rats, MPP+ is accumulated in the nigrostriatal dopaminergic terminals but it is not neurotoxic: A model of natural resistance to MPTP toxicity. Experimental Neurology. https://doi.org/10.1006/exnr.1994.1079

SUPPLEMENTARY MATERIAL

Supplementary Table IV.1. Values by age of the different biomarkers of general metabolism. Parametric data are presented as Mean ± SD, while the mean and quartiles (1 and 3) are provided for non-parametric data. Q1=first quartile; Q2=second quartile; SD=standard deviation; PROT = proteins; GLUC = glucose; CHOL = cholesterol; TRIGL = triglycerides; CA = calcium; CK = creatine kinase; ALBU = albumin; ALP = alkaline phosphatase; ALT = alanine aminotransferase; AST = aspartate aminotransferase; gGT = gamma-glutamyl transferase; UIBC= unsaturated iron-binding capacity; IU = international units.

PARAMETER	YOUNG	OLD	SENILE
PROT (g/dl)			
Mean ± SD or Median	5.66	6.17 ± 0.97	5.94 ± 1.09
Q1 | Q3	4.86 | 6.00		
Min - Max	3.57 - 6.50	4.24 - 7.92	3.28 - 7.16
GLUC (mg/dl)			
Mean ± SD or Median	186.00 ± 32.80	150.00	200.00 ± 144.00
Q1 | Q3		111.00 | 270.00	
Min - Max	108.00 - 243.00	47.20 - 345.00	12.80 - 468.00
COLES (mg/dl)			
Mean ± SD or Median	99.90 ± 19.00	94.70 ± 29.70	122.00 ± 40.10
Q1 | Q3			
Min - Max	56.40 - 140.00	43.70 - 177.00	62.70 - 219.00
TRIGL (mg/dl)			
Mean ± SD or Median	173.00	178.00 ± 84.20	178.00 ± 44.80
Q1 | Q3	87.90 | 272.00		
Min - Max	45.40 - 570.00	62.90 - 325.00	103.00 - 276.00
Amylase (IU/L)			
Mean ± SD or Median	1024.00 ± 187.00	1405.00 ± 363.00	1876.00 ± 657.00
Q1 | Q3			
Min - Max	639.00 - 1546.00	793.00 - 2060.00	868.00 - 2969.00
CA (mg/dl)			
Mean ± SD or Median	11.30 ± 0.40	17.20 ± 4.21	16.50 ± 3.69
Q1 | Q3			
Min - Max	10.30 - 12.20	8.84 - 24.50	9.32 - 22.40
CK (IU/L)			
Mean ± SD or Median	165.00	2716.00	4354.00
Q1 | Q3	102.00 | 193.00	1366.00 | 7773.00	2072.00 | 11134.00
Min - Max	59.00 - 435.00	821.00 - 12852.00	356.00 - 15958.00
ALBU (g/dl)			
Mean ± SD or Median	3.64 ± 0.23	3.30 ± 0.77	3.59 ± 0.71
Q1 | Q3			
Min - Max	3.21 - 4.16	2.00 - 4.68	2.16 - 4.72
ALP (IU/L)			
Mean ± SD or Median	117.00	109.00 ± 38.90	121.00 ± 54.10
Q1 | Q3	100.00 | 139.00		
Min - Max	64.80 - 205.00	47.60 - 176.00	56.80 - 221.00
ALT (IU/L)			
Mean ± SD or Median	10.60 ± 2.71	19.50 ± 13.50	17.70 ± 10.20
Q1 | Q3			
Min - Max	6.10 - 18.40	2.40 - 48.40	3.20 - 34.40
AST (IU/L)			
Mean ± SD or Median	31.30	105.00	132.00 ± 54.80
Q1 | Q3	25.90 | 44.00	73.00 | 165.00	
Min - Max	19.60 - 70.80	51.60 - 213.00	55.20 - 243.00

Supplementary Table IV.1 – continuation

PARAMETER	YOUNG	OLD	SENILE
Bilirubin(mg/dl)			
Mean ± SD or Median	0.08 ± 0.02	0.03	0.05 ± 0.03
Q1 | Q3		0.02 | 0.07	
Min - Max	0.06 - 0.12	0.02 - 0.12	0.02 - 0.10
gGT (IU/L)			
Mean ± SD or Median	3.80 ± 1.33	10.50 ± 4.20	16.20 ± 6.06
Q1 | Q3			
Min - Max	0.90 - 6.60	0.40 - 20.40	6.80 - 26.80
Creatinine (mg/dl)			
Mean ± SD or Median	0.44 ± 0.06	0.48 ± 0.06	0.54 ± 0.05
Q1 | Q3			
Min - Max	0.32 - 0.54	0.39 - 0.59	0.45 - 0.62
Iron (µg/dl)			
Mean ± SD or Median	222.00 ± 38.60	169.00 ± 44.60	219.00 ± 52.30
Q1 | Q3			
Min - Max	151.00 - 294.00	68.80 - 245.00	101.00 - 298.00
Ferritin (µg/l)			
Mean ± SD or Median	488.00 ± 210.00	405.00 ± 235.00	314.00 ± 137.00
Q1 | Q3			
Min - Max	86.00 - 788.00	112.00 - 936.00	32.00 - 532.00
UIBC (µg/dl)			
Mean ± SD or Median	145.00	260.00	207.00 ± 49.10
Q1 | Q3	126.00 | 202.00	209.00 | 280.00	
Min - Max	87.90 - 242.00	94.50 - 352.00	122.00- 315.00
Phosphorus (mg/dl)			
Mean ± SD or Median	4.32 ± 0.95	9.81 ± 2.51	13.30 ± 3.62
Q1 | Q3			
Min - Max	2.54 - 6.26	5.56 - 15.20	8.44 - 21.20
Urea (mg/dl)			
Mean ± SD or Median	73.30	56.50 ± 11.70	60.60 ± 10.10
Q1 | Q3	65.80 | 97.00		
Min - Max	54.20 - 115.00	30.00 - 84.00	39.60 - 76.00

Supplementary Table IV.2. Values of oxidative status, stress and inflammation in the *O. degus* by age. Parametric data are presented as Mean ± SD, while the mean and quartiles (1 and 3) are provided for non-parametric data. Q1=first quartile; Q2=second quartile; SD=standard deviation; CUPRAC = cupric ion reducing antioxidant capacity; FRAP = ferric reducing ability of the plasma; TEAC = trolox equivalent antioxidant capacity; THIOL = total thiol concentrations; TOS = total oxidant status; SAA = serum A-amyloid; BchE = butyrylcholinesterase; PON1 = paraoxonase-1; IU = international units.

PARAMETER	YOUNG	OLD	SENILE
CUPRAC (mmol/L)			
Mean ± SD or median	0.44 ± 0.02	0.51	0.53 ± 0.07
Q1 | Q3		0.49 | 0.56	
Min - Max	0.39 - 0.48	0.47 - 0.66	0.43 - 0.65
FRAP (mmol/L)			
Mean ± SD or median	0.43	1.09 ± 0.21	1.13 ± 0.28
Q1 | Q3	0.38 | 0.49		
Min - Max	0.34 - 0.52	0.67 - 1.47	0.75 - 1.69
TEAC (mmol/L)			
Mean ± SD or median	0.89 ± 0.05	1.17 ± 0.10	1.23 ± 0.21
Q1 | Q3			
Min - Max	0.83 - 0.99	0.97 - 1.32	0.95 - 1.63
THIOL (µmol/L)			
Mean ± SD or median	159.00 ± 28.40	76.30 ± 53.40	59.50 ± 39.30
Q1 | Q3			
Min - Max	83.20 - 217.00	0.30 - 183.00	4.00 - 137.00
TOS (µmol/L)			
Mean ± SD or median	5.70	13.10 ± 6.56	12.70 ± 5.66
Q1 | Q3	4.30 | 8.50		
Min - Max	3.00 - 14.20	4.50 - 25.00	4.70 - 23.90
SAA (µg/ml)			
Mean ± SD or median	0.10	10.50	15.00
Q1 | Q3	0.10 | 0.10	1.95 | 28.20	0.18 | 32.00
Min - Max	0.10 - 0.10	0.10 - 41.00	0.10 - 43.40
BChE (µmol/ml·min)			
Mean ± SD or median	3.21 ± 0.47	3.60	3.40 ± 0.39
Q1 | Q3		2.80 | 4.00	
Min - Max	2.60 - 4.30	2.00 - 4.40	2.80 - 4.00
PON1 (IU/ml)			
Mean ± SD or median	8.02 ± 2.01	13.00 ± 3.24	14.60 ± 4.69
Q1 | Q3			
Min - Max	4.36 - 11.10	5.32 - 18.90	7.20 - 24.20

Supplementary Table IV.3. **Reference values for the voltage of the ECG waves, heart rate (HR) and mean electrical axis (MEA). T**he data presented corresponds to: (A) the values of all the animals analyzed (no subdivisions), and divided either by sex (B) or age (C). Mean ± standard deviation (SD), median, first and third quartiles (Q1, Q3) and minimum - maximum values are reported. bpm = beats per minute.

Groups	HR (bpm)	P (mV)	R (mV)	S (mV)	T (mV)	MEA (º)
A. ALL ANIMALS TOGETHER						
Mean ± SD	207.2 ± 41.3	0.023 ± 0.007	0.168 ± 0.112	0.065 ± 0.063	0.053 ± 0.029	21.4 ± 61.7
Median	200.0	0.025	0.150	0.044	0.050	19.3
Q1 | Q3	180.0 | 230.0	0.019 | 0.032	0.090 | 0.217	0.025 | 0.075	0.038 | 0.063	-17.3 | 60.0
Min – Max	110.0 – 340.0	0.006 - 0.083	0.013 – 0.525	0.002 - 0.363	0.006 - 0.200	-138.0 – 180.0
B. BY SEX						
Males						
Mean ± SD	209.0 ± 47.0	0.026 ± 0.010	0.150 ± 0.078	0.057 ± 0.039	0.053 ± 0.026	8.3 ± 61.4
Median	200.0	0.025	0.146	0.044	0.051	0.0
Q1 | Q3	180.0 | 240.0	0.019 | 0.032	0.088 | 0.210	0.023 | 0.085	0.036 | 0.075	-29.0 | 39.0
Min – Max	110.0 – 320.0	0.013 - 0.050	0.019 - 0.525	0.013 - 0.363	0.006 - 0.129	-138.0 – 169.0
Females						
Mean ± SD	203.0 ± 28.3	0.027 ± 0.010	0.165 ± 0.100	0.043 ± 0.032	0.050 ± 0.021	35.6 ± 59.5
Median	200.0	0.025	0.152	0.032	0.050	39.0
Q1 | Q3	180.0 | 220.0	0.020 | 0.032	0.095 | 0.230	0.025 | 0.058	0.038 | 0.061	2.63 | 66.9
Min – Max	160.0 – 270.0	0.006 - 0.050	0.013 - 0.504	0.002 - 0.125	0.013 - 0.117	-128.0 – 180.0
BY AGE						
Juvenile						
Mean ± SD	216.0 ± 40.5	0.025 ± 0.009	0.183 ± 0.133	0.067 ± 0.058	0.071 ± 0.047	8.5 ± 79.4
Median	200.0	0.025	0.168	0.044	0.072	-5.75
Q1 | Q3	200.0 | 235.0	0.019 | 0.0303	0.085 | 0.231	0.025 | 0.103	0.032 | 0.087	-46.9 | 70.5
Min – Max	140.0 – 300.0	0.013 - 0.050	0.025 - 0.525	0.015 - 0.363	0.008 - 0.200	-138.0 – 169.0
Young						
Mean ± SD	244.0 ± 31.0	0.030 ± 0.011	0.157 ± 0.087	0.049 ± 0.044	0.046 ± 0.075	-10.7 ± 41.3
Median	240.0	0.025	0.138	0.029	0.050	-1.25
Q1 | Q3	220.0 | 260.0	0.025 | 0.038	0.087 | 0.198	0.019 | 0.053	0.035 | 0.063	-45.5 | 21.0
Min – Max	200.0 – 320.0	0.013 - 0.050	0.063 - 0.363	0.013 - 0.163	0.006 - 0.019	-90.0 – 46.0
Old						
Mean ± SD	187.0 ± 30.2	0.025 ± 0.010	0.148 ± 0.078	0.049 ± 0.035	0.049 ± 0.023	28.8 ± 58.1
Median	185.0	0.025	0.138	0.044	0.044	23.3
Q1 | Q3	170.0 | 210.0	0.015 | 0.031	0.091 | 0.198	0.019 | 0.077	0.038 | 0.062	-11.0 | 63.5
Min – Max	110.0 – 270.0	0.006 - 0.044	0.013 - 0.313	0.002 - 0.138	0.007 - 0.113	-128.0 – 163.0
Senile						
Mean ± SD	198.0 ± 31.5	0.027 ± 0.011	0.019 ± 0.504	0.051 ± 0.033	0.051 ± 0.018	34.4 ± 59.6
Median	193.0	0.026	0.163	0.040	0.050	27.3
Q1 | Q3	180.0 | 200.0	0.020 | 0.037	0.085 | 0.226	0.029 | 0.065	0.038 | 0.057	-2.88 | 70.5
Min – Max	160.0 – 300.0	0.012 - 0.083	0.182 - 0.116	0.001 - 0.125	0.019 - 0.100	-67.0 – 180.0

Supplementary Table IV.3 – **continuation.** Reference values for the amplitude of the ECG waves and intervals. The data presented corresponds to: (A) the values of all the animals analyzed (no subdivisions), and divided either by sex (B) or age (C). Mean ± standard deviation (SD), median, first and third quartiles (Q1, Q3) and minimum - maximum values are reported. Asterisks indicate statistical differences: *p < 0.05; **p<0.01.

Groups	P (ms)	PR interval (ms)	QRS (ms)	QT (ms)
A. ALL ANIMALS TOGETHER				
Mean ± SD	0.023 ± 0.007	0.055 ± 0.013	0.044 ± 0.010	0.155 ± 0.029
Median	0.022	0.055	0.043	0.151
Q1 | Q3	0.005 - 0.040	0.047 | 0.063	0.038 | 0.050	0.137 | 0.169
Min – Max	0.005 - 0.040	0.020 - 0.096	0.020 - 0.075	0.081 - 0.235
B. BY SEX				
Males				
Mean ± SD	0.024 ± 0.007	0.052 ± 0.012 *vs females*	0.044 ± 0.007	0.158 ± 0.029
Median	0.022	0.053	0.045	0.150
Q1 | Q3	0.018 | 0.030	0.047 | 0.060	0.040 | 0.050	0.140 | 0.174
Min – Max	0.013 - 0.040	0.020 - 0.073	0.025 - 0.056	0.116 - 0.230
Females				
Mean ± SD	0.022 ± 0.007	0.058 ± 0.013	0.043 ± 0.013	0.151 ± 0.026
Median	0.022	0.060	0.040	0.151
Q1 | Q3	0.018 | 0.026	0.048 | 0.063	0.035 | 0.049	0.135 | 0.168
Min – Max	0.005 - 0.040	0.034 - 0.096	0.020 - 0.075	0.081 - 0.235
C. BY AGE				
Juvenile				
Mean ± SD	0.025 ± 0.007	0.048 ± 0.012	0.040 ± 0.010	0.162 ± 0.032 *vs young*
Median	0.025	0.049	0.040	0.158
Q1 | Q3	0.019 | 0.030	0.036 | 0.060	0.040 | 0.047	0.140 | 0.186
Min – Max	0.015 - 0.040	0.030 - 0.065	0.020 - 0.056	0.120 - 0.230
Young				
Mean ± SD	0.022 ± 0.010	0.058 ± 0.008	0.036 ± 0.009	0.134 ± 0.022
Median	0.020	0.060	0.039	0.133
Q1 | Q3	0.014 | 0.030	0.050 | 0.060	0.030 | 0.040	0.120 | 0.146
Min – Max	0.005 - 0.035	0.045 - 0.075	0.020 - 0.053	0.085 - 0.175
Old				
Mean ± SD	0.023 ± 0.006	0.057 ± 0.012	0.044 ± 0.009	0.160 ± 0.026 *vs young*
Median	0.023	0.055	0.045	0.163
Q1 | Q3	0.020 | 0.028	0.049 | 0.065	0.036 | 0.050	0.138 | 0.173
Min – Max	0.013 - 0.035	0.035 - 0.090	0.025 - 0.058	0.121 - 0.220
Senile				
Mean ± SD	0.023 ± 0.007	0.056 ± 0.015	0.049 ± 0.012 ** *vs young*	0.157 ± 0.030 * *vs young*
Median	0.022	0.058	0.049	0.153
Q1 | Q3	0.017 | 0.027	0.048 | 0.064	0.041 | 0.053	0.140 | 0.168
Min – Max	0.013 - 0.040	0.020 - 0.096	0.026 - 0.075	0.081 - 0.235

Supplementary Table IV.4. Reference values for the voltage of the ECG waves, heart rate (HR) and mean electrical axis (MEA), of the animals divided by sex and age. Mean ± standard deviation (SD), median, first and third quartiles (Q1, Q3) and minimum - maximum values are reported. bpm = beats per minute.

Groups	HR (bpm)	P (mV)	R (mV)	S (mV)	T (mV)	MEA (º)
MALES						
Juvenile						
Mean ± SD	216.0 ± 46.2	0.023 ± 0.007	0.197 ± 0.149	0.109 ± 0.108	0.074 ± 0.052	-2.0 ± 86.9
Median	200.0	0.022	0.100	0.0438	0.069	-11.5
Q1 | Q3	193.0 | 235.0	0.019 | 0.030	0.031 | 0.225	0.017 | 0.116	0.031 | 0.088	-48.0 | 56.3
Min – Max	140-0 - 300.0	0.013 - 0.038	0.031 - 0.525	0.015 - 0.363	0.008 - 0.200	-138.0 - 169.0
Young						
Mean ± SD	250.0 ± 37.4	0.027 ± 0.012	0.120 ± 0.064	0.111 ± 0.098	0.050 ± 0.023	-25.6 ± 32.2
Median	240.0	0.025	0.075	0.0878	0.054	-38.0
Q1 | Q3	230.0 | 270.0	0.019 | 0.032	0.000 | 0.188	0.021 | 0.196	0.038 | 0.063	-47.0 | 9.0
Min – Max	200.0 - 320.0	0.013 - 0.050	0.063 - 0.192	0.013 - 0.263	0.006 - 0.075	-67.0 - 20.5
Old						
Mean ± SD	190.0 ± 43.8	0.026 ± 0.009	0.159 ± 0.070	0.062 ± 0.046	0.050 ± 0.026	25.7 ± 55.2
Median	180.0	0.025	0.144	0.0542	0.044	17.0
Q1 | Q3	163.0 | 200.0	0.022 | 0.033	0.100 | 0.189	0.019 | 0.081	0.042 | 0.063	-14.8 | 66.1
Min – Max	110.0 - 300.0	0.013 - 0.044	0.081 - 0.313	0.013 - 0.188	0.007 - 0.113	-76.0 - 163.0
Senile						
Mean ± SD	209.0 ± 45.0	0.032 ± 0.021	0.166 ± 0.125	0.053 ± 0.032	0.052 ± 0.018	9.4 ± 47.5
Median	200.0	0.022	0.122	0.044	0.044	9.0
Q1 | Q3	180.0 | 240.0	0.016 | 0.057	0.066 | 0.116	0.020 | 0.072	0.035 | 0.059	-11.5 | 37.0
Min – Max	160.0 – 300.0	0.013 - 0.083	0.019 - 0.442	0.013 - 0.117	0.035 - 0.082	-67.0 – 99.0
FEMALES						
Juvenile						
Mean ± SD	215.0 ± 19.1	0.025 ± 0.000	0.15 ± 0.086	0.025 ± 0.000	0.059 ± 0.024	39.8 ± 45.7
Median	210.0	0.025	0.168	0.030	0.069	52.0
Q1 | Q3	200.0 | 235.0	0.025 | 0.025	0.115 | 0.213	0.025 | 0.054	0.034 | 0.075	-8.3 | 75.5
Min – Max	200.0 - 240.0	0.025 - 0.025	0.025 - 0.225	0.025 - 0.025	0.025 - 0.0750	-21.0 - 76.0
Young						
Mean ± SD	200.0 ± 260.0	0.032 ± 0.010	0.184 ± 0.096	0.038 ± 0.019	0.041 ± 0.014	4.1 ± 46.3
Median	240.0	0.025	0.138	0.025	0.038	21.0
Q1 | Q3	220.0 | 260.0	0.025 | 0.038	0.100 | 0.213	0.013 | 0.05	0.025 | 0.050	-19.0 | 37.0
Min – Max	237.0 - 24.3	0.025 - 0.050	0.100 - 0.363	0.013 - 0.063	0.025 - 0.063	-90.0 - 46.0
Old						
Mean ± SD	197.0 ± 29.8	0.022 ± 0.010	0.134 ± 0.088	0.041 ± 0.035	0.047 ± 0.019	32.6 ± 63.2
Median	195.0	0.019	0.114	0.025	0.045	43.0
Q1 | Q3	173.0 | 210.0	0.016 | 0.029	0.065 | 0.225	0.013 | 0.055	0.038 | 0.056	-7.5 | 63.5
Min – Max	160.0 - 270.0	0.006 - 0.044	0.013 - 0.283	0.002- 0.119	0.013 - 0.083	-128.0 – 147.0
Senile						
Mean ± SD	191.0 ± 17.8	0.027 ± 0.010	0.212 ± 0.147	0.052 ± 0.034	0.050 ± 0.019	48.9 ± 62.1
Median	193.0	0.027	0.165	0.036	0.050	50.5
Q1 | Q3	180.0 | 200.0	0.021 | 0.033	0.113 | 0.272	0.027 | 0.068	0.039 | 0.056	3.5 | 102.0
Min – Max	160.0 - 230.0	0.012 - 0.044	0.033 - 0.033	0.007 - 0.125	0.019 - 0.100	-51.0 – 180.0

Supplementary Table IV.4– **continuation.** Reference values for the amplitude of the ECG waves and intervals, of the animals divided by sex and age. Mean ± standard deviation (SD), median, first and third quartiles (Q1, Q3) and minimum - maximum values are reported.

Groups	P (ms)	PR interval (ms)	QRS (ms)	QT (ms)
MALES				
Juvenile				
Mean ± SD	0.026 ± 0.008	0.047 ± 0.012	0.042 ± 0.008	0.172 ± 0.030
Median	0.023	0.049	0.041	0.164
Q1 | Q3	0.018 | 0.034	0.034 | 0.057	0.040 | 0.048	0.143 | 0.196
Min – Max	0.015 - 0.040	0.030 - 0.063	0.025 - 0.056	0.140 - 0.230
Young				
Mean ± SD	0.027 ± 0.008	0.053 ± 0.007	0.040 ± 0.007	0.133 ± 0.016
Median	0.030	0.050	0.040	0.130
Q1 | Q3	0.020 | 0.035	0.048 | 0.060	0.038 | 0.043	0.120 | 0.145
Min – Max	0.015 - 0.035	0.045 - 0.063	0.028 - 0.053	0.116 - 0.160
Old				
Mean ± SD	0.024 ± 0.006	0.057 ± 0.009	0.045 ± 0.008	0.160 ± 0.028
Median	0.021	0.055	0.048	0.161
Q1 | Q3	0.020 | 0.029	0.049 | 0.062	0.041 | 0.050	0.140 | 0.176
Min – Max	0.014 - 0.035	0.043 - 0.073	0.027 - 0.055	0.120 - 0.220
Senile				
Mean ± SD	0.019 ± 0.005	0.051 ± 0.017	0.045 ± 0.010	0.144 ± 0.020
Median	0.018	0.052	0.044	0.140
Q1 | Q3	0.016 | 0.022	0.038 | 0.068	0.040 | 0.051	0.131 | 0.148
Min – Max	0.013 - 0.028	0.020 - 0.071	0.038 - 0.052	0.128 - 0.193
FEMALES				
Juvenile				
Mean ± SD	0.020 ± 0.000	0.050 ± 0.015	0.040 ± 0.000	0.134 ± 0.017
Median	0.020	0.050	0.038	0.130
Q1 | Q3	0.020 | 0.020	0.036 | 0.064	0.020 | 0.040	0.120 | 0.151
Min – Max	0.020 - 0.020	0.035 - 0.065	0.015 – 0.040	0.120 - 0.155
Young				
Mean ± SD	0.016 ± 0.008	0.060 ± 0.000	0.031 ± 0.009	0.134 ± 0.028
Median	0.020	0.060	0.030	0.135
Q1 | Q3	0.010 | 0.020	0.060 | 0.060	0.020 | 0.040	0.120 | 0.150
Min – Max	0.005 - 0.030	0.040 - 0.040	0.020 - 0.040	0.085 - 0.175
Old				
Mean ± SD	0.022 ± 0.005	0.058 ± 0.015	0.042 ± 0.009	0.160 ± 0.024
Median	0.023	0.055	0.041	0.147
Q1 | Q3	0.018 | 0.025	0.046 | 0.063	0.035 | 0.048	0.136 | 0.171
Min – Max	0.013 - 0.032	0.035 - 0.090	0.025 - 0.058	0.133 - 0.202
Senile				
Mean ± SD	0.025 ± 0.008	0.059 ± 0.014	0.050 ± 0.012	0.158 ± 0.019
Median	0.023	0.059	0.049	0.157
Q1 | Q3	0.018 | 0.033	0.048 | 0.064	0.040 | 0.055	0.147 | 0.166
Min – Max	0.013 - 0.040	0.034 - 0.096	0.026 - 0.075	0.081 - 0.235

ANNEXES

ANNEX I

Agreement documents for the use of the published work Cuenca et al., 2019

UNIVERSIDAD DE
MURCIA

CONFORMIDAD, COMPROMISO Y DECLARACIÓN DE LOS COAUTORES DE LA PUBLICACIÓN

Doña Ana Luisa Gil Martínez, con DNI 48660949-X, como coautora del artículo:

Título: "Parkinson's disease: a short story of 200 years."

Año: 2019

Revista: Histology and Histopathology

Volumen, pág.: 34(6), 573-591

DOI/URL: https://doi.org/10.14670/HH-18-073

MANIFESTO:

La **conformidad** con la presentación del correspondiente artículo por parte de la doctoranda Lorena Cuenca Bermejo con el propósito de formular tesis como compendio de publicaciones.

El **compromiso** de no presentar el artículo de mi coautoría como parte de otra tesis doctoral.

La **declaración** de la relevancia de la contribución del mencionado doctorando en la investigación cuyos resultados quedan plasmados en el artículo de mi coautoría.

En Londres, a 20 de febrero de 2023.

Firma del coautor/a

UNIVERSIDAD DE
MURCIA

CONFORMIDAD, COMPROMISO Y DECLARACIÓN DE LOS COAUTORES DE LA PUBLICACIÓN

Doña Lorena Cano Fernández, con DNI 23304047X, como coautora del artículo:

Título: "Parkinson's disease: a short story of 200 years."

Año: 2019

Revista: Histology and Histopathology

Volumen, pág.: 34(6), 573-591

DOI/URL: https://doi.org/10.14670/HH-18-073

MANIFESTO:

La **conformidad** con la presentación del correspondiente artículo por parte de la doctoranda Lorena Cuenca Bermejo con el propósito de formular tesis como compendio de publicaciones.

El **compromiso** de no presentar el artículo de mi coautoría como parte de otra tesis doctoral.

La **declaración** de la relevancia de la contribución del mencionado doctorando en la investigación cuyos resultados quedan plasmados en el artículo de mi coautoría.

En Madrid, a 20 de febrero de 2023.

Firma de la coautora

CONFORMIDAD, COMPROMISO Y DECLARACIÓN DE LOS COAUTORES DE LA PUBLICACIÓN

Doña Consuelo Sánchez Rodrigo, con DNI 77578699K, como coautora del artículo:

Título: "Parkinson's disease: a short story of 200 years."

Año: 2019

Revista: Histology and Histopathology

Volumen, pág.: 34(6), 573-591

DOI/URL: https://doi.org/10.14670/HH-18-073

MANIFESTO:

La **conformidad** con la presentación del correspondiente artículo por parte de la doctoranda Lorena Cuenca Bermejo con el propósito de formular tesis como compendio de publicaciones.

El **compromiso** de no presentar el artículo de mi coautoría como parte de otra tesis doctoral.

La **declaración** de la relevancia de la contribución del mencionado doctorando en la investigación cuyos resultados quedan plasmados en el artículo de mi coautoría.

En Murcia, a 20 de febrero de 2023.

Firma de la coautora

CONFORMIDAD, COMPROMISO Y DECLARACIÓN DE LOS COAUTORES DE LA PUBLICACIÓN

Doña Cristina Estrada Esteban, con DNI 12396290A, como coautora del artículo:

Título: "Parkinson's disease: a short story of 200 years."

Año: 2019

Revista: Histology and Histopathology

Volumen, pág.: 34(6), 573-591

DOI/URL: https://doi.org/10.14670/HH-18-073

MANIFESTO:

La **conformidad** con la presentación del correspondiente artículo por parte de la doctoranda Lorena Cuenca Bermejo con el propósito de formular tesis como compendio de publicaciones.

El **compromiso** de no presentar el artículo de mi coautoría como parte de otra tesis doctoral.

La **declaración** de la relevancia de la contribución del mencionado doctorando en la investigación cuyos resultados quedan plasmados en el artículo de mi coautoría.

En Valladolid, a 20 de febrero de 2023.

Firma de la coautora

CONFORMIDAD, COMPROMISO Y DECLARACIÓN DE LOS COAUTORES DE LA PUBLICACIÓN

Don Emiliano Fernández Villalba, con DNI 27484607k, como coautor del artículo:

Título: "Parkinson's disease: a short story of 200 years."

Año: 2019

Revista: Histology and Histopathology

Volumen, pág.: 34(6), 573-591

DOI/URL: https://doi.org/10.14670/HH-18-073

MANIFESTO:

La **conformidad** con la presentación del correspondiente artículo por parte de la doctoranda Lorena Cuenca Bermejo con el propósito de formular tesis como compendio de publicaciones.

El **compromiso** de no presentar el artículo de mi coautoría como parte de otra tesis doctoral.

La **declaración** de la relevancia de la contribución del mencionado doctorando en la investigación cuyos resultados quedan plasmados en el artículo de mi coautoría.

En Murcia, a 20 de febrero de 2023.

Firma del coautor

CONFORMIDAD, COMPROMISO Y DECLARACIÓN DE LOS COAUTORES DE LA PUBLICACIÓN

Doña María Trinidad Herrero Ezquerro, con DNI 16529839S, como coautora del artículo:

Título: "Parkinson's disease: a short story of 200 years."

Año: 2019

Revista: Histology and Histopathology

Volumen, pág.: 34(6), 573-591

DOI/URL: https://doi.org/10.14670/HH-18-073

MANIFESTO:

La **conformidad** con la presentación del correspondiente artículo por parte de la doctoranda Lorena Cuenca Bermejo con el propósito de formular tesis como compendio de publicaciones.

El **compromiso** de no presentar el artículo de mi coautoría como parte de otra tesis doctoral.

La **declaración** de la relevancia de la contribución del mencionado doctorando en la investigación cuyos resultados quedan plasmados en el artículo de mi coautoría.

En Murcia, a 20 de febrero de 2023.

Firma de la coautora

Profs. J.F. Madrid, Editor
School of Medicine
University of Murcia
·0071 El Palmar – MURCIA
SPAIN   e-mail: jfmadrid@um.es

Histology and
Histopathology

http://www.hh.um.es

Dr. Lorena Cuenca
Clinical and Experimental Neuroscience Group (NiCE-IMIB)
Department of Human Anatomy and Psychobiology
Institute for Aging Research
School of Medicine
Biosanitary Research Institute of Murcia (IMIB-Arrixaca)
University of Murcia
Murcia, Spain
lorena.cuenca@um.es

August 11, 2022

Dear Dr. Cuenca,

You have our permission to include or reproduce any part of the article below indicated anywhere, including your PhD thesis:

Cuenca, L., Gil-Martinez, A. L., Cano-Fernandez, L., Sanchez-Rodrigo, C., Estrada, C., Fernandez-Villalba, E., & Herrero, M. T. (2019). Parkinson's disease: a short story of 200 years. *Histology and histopathology*, *34*(6), 573–591. https://doi.org/10.14670/HH-18-073

The article in *Histology and Histopathology* should be properly cited.

Yours sincerely,

Prof. Juan F. Madrid, Editor

ANNEX II

Agreement documents for the use of the published work Cuenca-Bermejo et al., 2020

UNIVERSIDAD DE
MURCIA

CONFORMIDAD, COMPROMISO Y DECLARACIÓN DE LOS COAUTORES DE LA PUBLICACIÓN

Doña Elisa Pizzichini, con pasaporte nº YC0321961, como coautora del artículo:

Título: "Octodon degus: a natural model of multimorbidity for ageing research."

Año: 2020

Revista: Ageing research reviews

Volumen, pág.: 64, 101204

DOI/URL: https://doi.org/10.1016/j.arr.2020.101204

MANIFESTO:

La **conformidad** con la presentación del correspondiente artículo por parte de la doctoranda Lorena Cuenca Bermejo con el propósito de formular tesis como compendio de publicaciones.

El **compromiso** de no presentar el artículo de mi coautoría como parte de otra tesis doctoral.

La **declaración** de la relevancia de la contribución del mencionado doctorando en la investigación cuyos resultados quedan plasmados en el artículo de mi coautoría.

En Roma, a 21 de febrero de 2023.

Firma de la coautora

292

CONFORMIDAD, COMPROMISO Y DECLARACIÓN DE LOS COAUTORES DE LA PUBLICACIÓN

Doña Ana María González Cuello, con DNI 34803324T, como coautora del artículo:

Título: "Octodon degus: a natural model of multimorbidity for ageing research."

Año: 2020

Revista: Ageing research reviews

Volumen, pág.: 64, 101204

DOI/URL: https://doi.org/10.1016/j.arr.2020.101204

MANIFESTO:

La **conformidad** con la presentación del correspondiente artículo por parte de la doctoranda Lorena Cuenca Bermejo con el propósito de formular tesis como compendio de publicaciones.

El **compromiso** de no presentar el artículo de mi coautoría como parte de otra tesis doctoral.

La **declaración** de la relevancia de la contribución del mencionado doctorando en la investigación cuyos resultados quedan plasmados en el artículo de mi coautoría.

En Murcia, a 20 de febrero de 2023.

Firma de la coautora

CONFORMIDAD, COMPROMISO Y DECLARACIÓN DE LOS COAUTORES DE LA PUBLICACIÓN

Doña Maria Egle De Stefano, con pasaporte nº YA6880348, como coautora del artículo:

Título: "Octodon degus: a natural model of multimorbidity for ageing research."

Año: 2020

Revista: Ageing research reviews

Volumen, pág.: 64, 101204

DOI/URL: https://doi.org/10.1016/j.arr.2020.101204

MANIFESTO:

La **conformidad** con la presentación del correspondiente artículo por parte de la doctoranda Lorena Cuenca Bermejo con el propósito de formular tesis como compendio de publicaciones.

El **compromiso** de no presentar el artículo de mi coautoría como parte de otra tesis doctoral.

La **declaración** de la relevancia de la contribución del mencionado doctorando en la investigación cuyos resultados quedan plasmados en el artículo de mi coautoría.

En Roma, a 20 de febrero de 2023.

Firma de la coautora

CONFORMIDAD, COMPROMISO Y DECLARACIÓN DE LOS COAUTORES DE LA PUBLICACIÓN

Don Emiliano Fernández Villalba, con DNI 27484607k, como coautor del artículo:

Título: "Octodon degus: a natural model of multimorbidity for ageing research."

Año: 2020

Revista: Ageing research reviews

Volumen, pág.: 64, 101204

DOI/URL: https://doi.org/10.1016/j.arr.2020.101204

MANIFESTO:

La **conformidad** con la presentación del correspondiente artículo por parte de la doctoranda Lorena Cuenca Bermejo con el propósito de formular tesis como compendio de publicaciones.

El **compromiso** de no presentar el artículo de mi coautoría como parte de otra tesis doctoral.

La **declaración** de la relevancia de la contribución del mencionado doctorando en la investigación cuyos resultados quedan plasmados en el artículo de mi coautoría.

En Murcia, a 20 de febrero de 2023.

Firma del coautor

CONFORMIDAD, COMPROMISO Y DECLARACIÓN DE LOS COAUTORES DE LA PUBLICACIÓN

Doña María Trinidad Herrero Ezquerro, con DNI 16529839S, como coautora del artículo:

Título: "Octodon degus: a natural model of multimorbidity for ageing research."

Año: 2020

Revista: Ageing research reviews

Volumen, pág.: 64, 101204

DOI/URL: https://doi.org/10.1016/j.arr.2020.101204

MANIFESTO:

La **conformidad** con la presentación del correspondiente artículo por parte de la doctoranda Lorena Cuenca Bermejo con el propósito de formular tesis como compendio de publicaciones.

El **compromiso** de no presentar el artículo de mi coautoría como parte de otra tesis doctoral.

La **declaración** de la relevancia de la contribución del mencionado doctorando en la investigación cuyos resultados quedan plasmados en el artículo de mi coautoría.

En Murcia, a 20 de febrero de 2023.

Firma de la coautora

ANNEX III

Agreement documents for the use of the published work Cuenca-Bermejo et al. 2021

UNIVERSIDAD DE
MURCIA

CONFORMIDAD, COMPROMISO Y DECLARACIÓN DE LOS COAUTORES DE LA PUBLICACIÓN

Doña Elisa Pizzichini, con pasaporte nº YC0321961, como coautora del artículo:

Título: "A New Tool to Study Parkinsonism in the Context of Aging: MPTP Intoxication in a Natural Model of Multimorbidity."

Año: 2021

Revista: International Journal of Molecular Sciences

Volumen, pág.: 22(9), 4341

DOI/URL: https://doi.org/10.3390/ijms22094341

MANIFESTO:

La **conformidad** con la presentación del correspondiente artículo por parte de la doctoranda Lorena Cuenca Bermejo con el propósito de formular tesis como compendio de publicaciones.

El **compromiso** de no presentar el artículo de mi coautoría como parte de otra tesis doctoral.

La **declaración** de la relevancia de la contribución del mencionado doctorando en la investigación cuyos resultados quedan plasmados en el artículo de mi coautoría.

En Roma, a 21 de febrero de 2023.

Firma de la coautora

UNIVERSIDAD DE
MURCIA

CONFORMIDAD, COMPROMISO Y DECLARACIÓN DE LOS COAUTORES DE LA PUBLICACIÓN

Doña Valeria de Cassia Gonçalves, con pasaporte nºGA702767, como coautora del artículo:

Título: "A New Tool to Study Parkinsonism in the Context of Aging: MPTP Intoxication in a Natural Model of Multimorbidity."

Año: 2021

Revista: International Journal of Molecular Sciences

Volumen, pág.: 22(9), 4341

DOI/URL: https://doi.org/10.3390/ijms22094341

MANIFESTO:

La **conformidad** con la presentación del correspondiente artículo por parte de la doctoranda Lorena Cuenca Bermejo con el propósito de formular tesis como compendio de publicaciones.

El **compromiso** de no presentar el artículo de mi coautoría como parte de otra tesis doctoral.

La **declaración** de la relevancia de la contribución del mencionado doctorando en la investigación cuyos resultados quedan plasmados en el artículo de mi coautoría.

En Murcia, a 20 de febrero de 2023.

Firma de la coautora

298

UNIVERSIDAD DE MURCIA

CONFORMIDAD, COMPROMISO Y DECLARACIÓN DE LOS COAUTORES DE LA PUBLICACIÓN

Doña MaríaGuillén Díaz, con DNI 48664366T, como coautora del artículo:

Título: "A New Tool to Study Parkinsonism in the Context of Aging: MPTP Intoxication in a Natural Model of Multimorbidity."

Año: 2021

Revista: International Journal of Molecular Sciences

Volumen, pág.: 22(9), 4341

DOI/URL: https://doi.org/10.3390/ijms22094341

MANIFESTO:

La **conformidad** con la presentación del correspondiente artículo por parte de la doctoranda Lorena Cuenca Bermejo con el propósito de formular tesis como compendio de publicaciones.

El **compromiso** de no presentar el artículo de mi coautoría como parte de otra tesis doctoral.

La **declaración** de la relevancia de la contribución del mencionado doctorando en la investigación cuyos resultados quedan plasmados en el artículo de mi coautoría.

En Murcia, a 20 de febrero de 2023.

Firma de la coautora

CONFORMIDAD, COMPROMISO Y DECLARACIÓN DE LOS COAUTORES DE LA PUBLICACIÓN

Doña Elena Aguilar Moñino, con DNI 48850591V, como coautora del artículo:

Título: A New Tool to Study Parkinsonism in the Context of Aging: MPTP Intoxication in a Natural Model of Multimorbidity.

Año: 2021

Revista: International Journal of Molecular Sciences

Volumen, pág.: 22(9), 4341

DOI/URL: https://doi.org/10.3390/ijms22094341

MANIFESTO:

La **conformidad** con la presentación del correspondiente artículo por parte de la doctoranda Lorena Cuenca Bermejo con el propósito de formular tesis como compendio de publicaciones.

El **compromiso** de no presentar el artículo de mi coautoría como parte de otra tesis doctoral.

La **declaración** de la relevancia de la contribución del mencionado doctorando en la investigación cuyos resultados quedan plasmados en el artículo de mi coautoría.

En Murcia, a 21 de febrero de 2023.

Firma de la coautora

CONFORMIDAD, COMPROMISO Y DECLARACIÓN DE LOS COAUTORES DE LA PUBLICACIÓN

Doña Consuelo Sánchez Rodrigo, con DNI 77578699K, como coautora del artículo:

Título: "A New Tool to Study Parkinsonism in the Context of Aging: MPTP Intoxication in a Natural Model of Multimorbidity."

Año: 2021

Revista: International Journal of Molecular Sciences

Volumen, pág.: 22(9), 4341

DOI/URL: https://doi.org/10.3390/ijms22094341

MANIFESTO:

La **conformidad** con la presentación del correspondiente artículo por parte de la doctoranda Lorena Cuenca Bermejo con el propósito de formular tesis como compendio de publicaciones.

El **compromiso** de no presentar el artículo de mi coautoría como parte de otra tesis doctoral.

La **declaración** de la relevancia de la contribución del mencionado doctorando en la investigación cuyos resultados quedan plasmados en el artículo de mi coautoría.

En Murcia, a 20 de febrero de 2023.

Firma de la coautora

CONFORMIDAD, COMPROMISO Y DECLARACIÓN DE LOS COAUTORES DE LA PUBLICACIÓN

Doña Ana María González Cuello, con DNI 34803324T, como coautora del artículo:

Título: "A New Tool to Study Parkinsonism in the Context of Aging: MPTP Intoxication in a Natural Model of Multimorbidity."

Año: 2021

Revista: International Journal of Molecular Sciences

Volumen, pág.: 22(9), 4341

DOI/URL: https://doi.org/10.3390/ijms22094341

MANIFESTO:

La **conformidad** con la presentación del correspondiente artículo por parte de la doctoranda Lorena Cuenca Bermejo con el propósito de formular tesis como compendio de publicaciones.

El **compromiso** de no presentar el artículo de mi coautoría como parte de otra tesis doctoral.

La **declaración** de la relevancia de la contribución del mencionado doctorando en la investigación cuyos resultados quedan plasmados en el artículo de mi coautoría.

En Murcia, a 20 de febrero de 2023.

Firma de la coautora

CONFORMIDAD, COMPROMISO Y DECLARACIÓN DE LOS COAUTORES DE LA PUBLICACIÓN

Don Emiliano Fernández Villalba, con DNI 27484607K, como coautor del artículo:

Título: "A New Tool to Study Parkinsonism in the Context of Aging: MPTP Intoxication in a Natural Model of Multimorbidity."

Año: 2021

Revista: International Journal of Molecular Sciences

Volumen, pág.: 22(9), 4341

DOI/URL: https://doi.org/10.3390/ijms22094341

MANIFESTO:

La **conformidad** con la presentación del correspondiente artículo por parte de la doctoranda Lorena Cuenca Bermejo con el propósito de formular tesis como compendio de publicaciones.

El **compromiso** de no presentar el artículo de mi coautoría como parte de otra tesis doctoral.

La **declaración** de la relevancia de la contribución del mencionado doctorando en la investigación cuyos resultados quedan plasmados en el artículo de mi coautoría.

En Murcia, a 20 de febrero de 2023.

Firma del coautor

UNIVERSIDAD DE MURCIA

CONFORMIDAD, COMPROMISO Y DECLARACIÓN DE LOS COAUTORES DE LA PUBLICACIÓN

Doña María Trinidad Herrero Ezquerro, con DNI 16529839S, como coautora del artículo:

Título: "A New Tool to Study Parkinsonism in the Context of Aging: MPTP Intoxication in a Natural Model of Multimorbidity."

Año: 2021

Revista: International Journal of Molecular Sciences

Volumen, pág.: 22(9), 4341

DOI/URL: https://doi.org/10.3390/ijms22094341

MANIFESTO:

La **conformidad** con la presentación del correspondiente artículo por parte de la doctoranda Lorena Cuenca Bermejo con el propósito de formular tesis como compendio de publicaciones.

El **compromiso** de no presentar el artículo de mi coautoría como parte de otra tesis doctoral.

La **declaración** de la relevancia de la contribución del mencionado doctorando en la investigación cuyos resultados quedan plasmados en el artículo de mi coautoría.

En Murcia, a 20 de febrero de 2023.

Firma de la coautora